Validation of the Canadian Precipitation Analysis (CaPA)

for Hydrological Modelling in the Canadian Prairies

by

KuangYin Zhao

A Thesis submitted to the Faculty of Graduate Studies of

The University of Manitoba

In partial fulfillment of the requirements of the degree of

MASTER OF SCIENCE

Department of Civil Engineering

University of Manitoba

Winnipeg

Declaration

I hereby declare that I am the author of this thesis. This is a true copy of the thesis, including any required final revisions, as accepted by my examiners.

I understand that my thesis may be made electronically available to the public. I authorize University of Manitoba to lend this thesis to other institutions or individuals for the purpose of scholarly research.

Abstract

Traditional hydrological model inputs are often deemed inadequate in areas where stations are sparse, such as the northern extents of the Canadian Prairie basins. The Canadian Precipitation Analysis (CaPA) combines GEM (Global Environmental Multi-scale model) data and available observation data to provide enhanced precipitation estimates. The CaPA analysis has recently been extended to produce high-resolution precipitation data over the Canadian Prairies, encompassing the Nelson-Churchill River Basin. Manitoba Hydro and other water practitioners in Manitoba have expressed interest in potentially using CaPA precipitation as hydrological model forcing for Prairie watersheds. A three step validation approach was designed and applied to assess CaPA for hydrologic modelling applications in the Nelson-Churchill River basin. Results of validation show that the quality of CaPA data varies among regions and seasons, with CaPA proving beneficial in both data-sparse regions and winter seasons most prominently. Overall, CaPA shows promise for water resource application in the Canadian Prairies.

Acknowledgements

I would like to thank my advisor Dr. Trish Stadnyk for the support of my M.Sc. study and research. Her knowledge and encouragement guided me throughout my program. This thesis will not be completed without her guidance.

I would like to thank my thesis committee members: Dr. Peter Rasmussen, and Dr. John Hanesiak for their time of reading my thesis and providing insightful comments.

My sincere thanks go to Dr. Vincent Fortin, Dr. Frank Lespinas and Mr. Bruce Davidson for providing and processing CaPA data as needed for this research.

Furthermore, I would like to express my sincere gratitude to former undergraduate students, now M.Sc Candidates, Mr. David Newsom and Mr. Gregory Schellenberg; and current undergraduate students Miss Chelsea Nguyen, and Miss Heather Stefaniuk for their hard work and contributions to this thesis.

Last but not the least; I thank my parents and grandmother for giving up everything in their life in order to support my study and life here in Canada for eight years.

Table of Contents

List of Tables

List of Figures

Chapter 1. Introduction

1.1. Motivation

Manitoba Hydro is concerned with the potential impacts that changes in temperature and precipitation patterns may have on energy production and/or the demand for energy, and the possibility of increases in the frequency and severity of extreme weather events. To better understand these possible impacts, the hydrological model WATFLOOD™ was set-up to simulate future flows under various climate change scenarios for the Manitoba Hydro system (i.e., the Nelson-Churchill River Basin, NCRB). These simulated flows will be used for both short- and long-term power generation capacity studies, both for present-day and future predictions.

A hydrological model provides a simplified representation of real world systems, created for different purposes, and hence having different modeling approaches. No matter what type of approach is used, precipitation is always necessitated as a forcing variable for computation of land-surface hydrological processes. Complete spatial coverage of forcing data over watershed domains is required for distributed classification of hydrological models (as opposed to lumped), which compute varying hydrological responses across the watershed (in units or grids) as opposed to one aggregated response.

The traditional method of obtaining the precipitation information is by gauge record from observation stations within or around the watershed domain. The scarcity of gauge coverage in the northern Canadian domain has, however, always been an issue for hydrological modeling purposes. The well-known Thiessen Polygon Method (Thiessen, 1911) was one of the few early attempts to interpolate precipitation among climate

stations in order to fill spatial gaps. With the development of computer technology, more advanced precipitation products and distribution methodologies were introduced such as gridded climate data that is produced from iterative interpolations using computers. Simple interpolation of station records, however, does not hold any physical basis (i.e., in response to weather systems, wind directionality, topography, etc.) until the introduction of Numerical Weather Prediction (NWP) models.

A NWP model utilizes prognostic three-dimensional differential atmospheric equations to predict future states of the atmosphere that requires initial conditions. These initial conditions come from a variety of observed data in combination with previous NWP predictions through data assimilation techniques. Many such modeled outputs are, however, not applicable for hydrological modeling purposes because of either differing temporal or spatial scales. Results of these NWP models can be adjusted or downscaled using bias adjustments or reanalysis processes by assimilating observation records. The outcome of the reanalysis process is called reanalysis data, such as the Canadian Precipitation Analysis (CaPA).

Without the appropriate precipitation forcing, efforts in developing a sophisticated hydrological model go astray. It is therefore important to conduct rigorous, additional validation processes to evaluate the reanalysis data's quality and its usefulness as an input to a hydrological model, within the domain of interest.

1.2. Scope

The scope of this study consists of the validation and evaluation of the Canadian Precipitation Analysis (CaPA) for hydrological modeling forcing of watershed models in the Manitoba Hydro domain. The validation process can be broken down into three steps:

(1) Point-to-point (P2P) comparisons where station observations at point locations are compared with the closest grid value from CaPA; (2) Map-to-map (M2M) comparisons where different interpolation methods are applied to station observation data to produce a distributed precipitation map that is compared with the CaPA field; and (3) Proxy validation where both distributed observations and CaPA data are used to force the hydrological model WATFLOOD^{TM} to simulate hydrographs and compare to observed streamflow at basin outlets. The observation data used for validation are from Environment Canada's CDCD precipitation records (Environment Canada, 2013), as well as United States Historical Climatology Network (USHCN) (NOAA, 2012). The domain of interest is the Manitoba Hydro system lying within the Nelson-Churchill River basin (~1.3 million km^2), with validation period from 2002 to 2005. In this thesis, the full three-step validation approach, including proxy validation is applied to three select watersheds within the domain of interest: Lake Winnipeg (196,000 km^2), Winnipeg River (135,000 km^2), and the headwater region of the Churchill River (119,000 km^2) watersheds. Meanwhile, the first two of three validation steps (P2P and M2M) are conducted on the entire Nelson-Churchill study domain. Using the methodology developed in this thesis, potential deficiencies in CaPAs methodology and performance, or potential bugs that have not yet been detected in CaPAs internal QA/QC processes are sought. The goal is to inform developers on the results from these analyses so potential improvements can be incorporated in the next operational version of CaPA. The validation approach is applied to four versions of CaPA: CaPA2.2, CaPA2.3, CaPA2.3a and CaPA 2.30; with no significant differences being detected among the results of these

four versions therefore results presented will pertain only to the latest operational version (CaPA version 2.30).

1.3. Objectives/Long Term Goals

This study has three main objectives. The first objective is to assess the quality of CaPA as a reanalysis precipitation product by comparing it with station observed precipitation. The second objective is to assess CaPAs ability to represent spatial weather features and whether or not it's an improvement over conventional WATFLOOD-interpolated climate input. The third objective is then to evaluate CaPAs ability as a hydrological modeling input by comparing the hydrological simulation of CaPA with the hydrological simulation of CDCD.

Overall, the long-term goal of this study is to establish a method that allows for rigorous, systematic evaluation of CaPA for use as forcing data to improve hydrological simulation in watersheds within the Manitoba Hydro domain. This methodology should be flexible enough to be applied to different time periods, new versions of CaPA as they are developed, and new watersheds of interest outside the current domain of interest.

Chapter 2. Background Information

In a NWP model, the domain of interest is divided into three dimensional grids where the microphysics processes described by coupled differential equations are solved numerically for each grid. The domain for such models can be either global or regional, and the temporal scale short- or long-term. Global models cover the entire earth atmosphere, but they often have much coarser resolutions. Regional models on the other hand allow a finer resolution of output, but have smaller domains. Due to the scale of formation and boundary conditions of weather-forming processes, the atmospheric modeling domain is significantly larger than that of hydrological models.

The Canadian Global Environmental Multi-scale (GEM) model is a NWP model developed by Meteorological Research Branch (MRB) in partnership with the Canadian Meteorological Centre (CMC) (Côté *et al*, 1998). It is an integrated forecasting and data assimilation system designed for operation weather forecasting, air quality and climate modeling and research purposes. In order to produce precipitation, GEM's data assimilation system first combines current weather observations with a short range forecast from a previous time step through statistical interpolation and balancing to create an initial condition. This initial condition is then used to simulate operational weather predictions as well as short range forecasts for the initial condition of next time step (Lackman, 2011). In its regional configuration, GEM has horizontal central core resolution of 10km to 15km (figure 1) and 58 vertical layers (Mailhot *et al.*, 2005, Jean *et al.*, 1998). Pietroniro *et al.* (2007) used 15km resolution and regionally configured GEM climate variables as atmospheric forcing for Environment Canada's Community Environmental Modeling system (Modelisation Environmentale Communautaire – MEC)

in a coupled land-surface and hydrological model configuration called MESH. Pietroniro *et al.* (2007) noted that GEM precipitation forcing could be improved if it was merged with a quality controlled and spatially interpolated synoptic station observations and remote sensing observations in a precipitation analysis (CaPA). Quality controlled station records can not only be used directly as hydrological model input but also be able to help improve the results of NWP predictions through assimilation schemes.

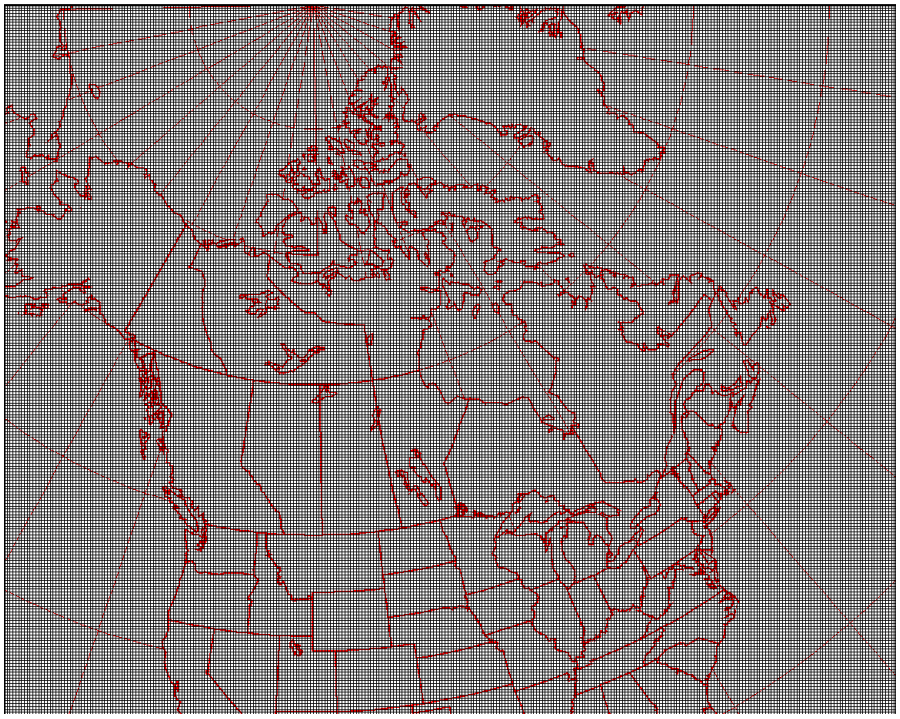

Figure 1: GEM in its 15km regional configuration with the coordinate of the first grid at 32.549° N, 134.62° W

2.1. Data Assimilation

Data assimilation is the process of passing down observation information to the forecast cycles. Observations are used either in the model's initial condition or to provide a restriction of the model's error growth. Assimilated observations are not taken directly to substitute model forecast but rather to provide small adjustments to initial model

forecasts. Different models utilize different assimilation schemes, but they all share some basic components and common traits.

Before assimilation, a 'background' field is first provided using model analysis of a short range forecast. This background field is assumed to not deviate significantly from the true representation of current weather conditions. Prior to assimilation, observation data under-go quality checks to eliminate any known instrument error and extreme anomaly readings. Some instrument errors are not well understood for example, solid precipitation is prone to under-catch due to wind, snow sublimation and blowing snow transportation loss (Goodison *et al.*, 1998). Fassnacht (2004) examined the wind under-catch effect of Alter-Shielded^{TM} gauged stations in relation with wind speed. It was found that at sites under low (1.3m/s), average (2.4 to 4.3 m/s) and high wind speed, 90%, 70% and 5.6% of the snow that fell was caught, respectively. Several methods have been developed to correct wind under-catch in the literature (Goodison *et al.*, 1998), but validation of the methods is often inadequate and so far no one method has proven robust. Therefore care should be taken when assimilating solid precipitation measurements.

An observation increment, also called innovation, is calculated at the location of each observation. Innovations are calculated by first obtaining a pseudo-observation from the background field at the nearest location and time increment to each observation occurrence. The innovation is then taken as the difference between observation and pseudo-observation. Rigorous quality control will then be conducted on the innovations.

Objective analysis, also called statistical interpolation, is then used to interpolate the innovations at each point to the analysis grid. Various statistical interpolations and

analyses can be performed at this stage to help with interpolation and in determining the observation increment at each grid point. Through statistical interpolation, the background values are inferred to the observation increment field. A model analysis is obtained by adding this observation increment field to the background field. Finally, the model analysis is then used as the initial state for the next time step.

Optimal interpolation is one of the common types of objective analysis. It weights the observation error and model analysis error to choose the combination with the least amount of total error (Hildebrand, 1956). The spatial pattern of error in the background is, however, predetermined and does not change with time and hence restricts the variety of weather features that can be represented. In order for an optimal interpolation method to accommodate smaller, regional features, the background error usually needs to be stretched along the terrain to produce a more realistic error distribution, requiring extra information that is not always available.

Many errors can occur during assimilation processes. Since innovations are interpolated to the resolution of the background field, any features smaller than the resolution of the model will not be assimilated properly. On the other hand, if the feature is larger, it is likely to be smoothed as well. Spatial interpolation of the observation data introduces errors if the coverage of observation information is non-uniform or sparse. Representativeness error also exists when a point measurement is used to represent a whole grid. Furthermore, the frequency of observations taken, instrument (measurement) error, and assumptions in the derivation of direct measurement to any meaningful data field contribute to combined sources of error during assimilation. These errors will be

present at any precipitation products that utilize the assimilation processes (i.e. reanalysis data). These errors needs to be considered, in order to assess the quality of the data,

2.2. Description of Reanalysis Data

Reanalysis models are sometimes called diagnostic atmospheric models. The main difference between NWP model and a reanalysis model is that the reanalysis models adjust and provide best estimates of historical data while NWP model focus on future weather predictions. Reanalysis data utilizes an assimilation scheme to assimilate observation data and produce climate variables, such as precipitation, at improved accuracies. The assimilated data in a reanalysis model is used to continuously adjust its background value rather than the initial conditions in a NWP model (which contains observation plus background at a previous time step). Reanalysis models are sometimes called diagnostic atmospheric models. A 'background field' usually consists of climate model simulations adjusted to assimilated observations. Assimilation systems can differ in their variational methods such as 2D-Var, 3D-Var and 4D-Var. Different variational methods use different cost functions to control the growth of analysis errors. The difference between 3D and a 4D is that 4D extends from the 3D spatial dimension to the fourth dimension of time (Lackmann, 2011). However, due to the simplicity, 3D-Var is the most commonly used in NWP models such as GEM. Quality of the reanalysis model output is influenced heavily by the observations assimilated to the reanalysis. Some notable examples of such reanalysis data products include NCEP-DOE R2, NCEP-NCAR R1, ERA-40, and North American Regional Reanalysis (NARR) (Kanamitsu *et al.*, 2002, Kållberg *et al.*, 2004, Mesinger *et al.*, 2006, Uppala *et al.*, 2005). However, a fully distributed hydrological model (e.g., WATFLOOD) requires input data to have roughly

the same spatial resolution (~10-15km) as the model discretization. Furthermore, hydrological routing equations require flow with time steps no larger than daily inputs. Therefore few reanalysis data are suitable, with NARR and ANUSPLIN being the most common in hydrological modelling applications due to spatial and temporal requirements.

NARR is developed by the National Centers for Environmental Prediction (NCEP). It is a long-term, dynamically consistent, high-resolution, high-frequency, atmospheric and land-surface hydrology dataset for the North American domain (Mesinger *et al.*, 2006,). The major components of the model include: the lateral boundaries from, and data used for the NCEP–DOE Global Reanalysis; the NCEP Eta Model and its Data Assimilation System; a recent version of the Noah land-surface model; and the use of numerous datasets for improving results (Mesinger *et al.*, 2006).

Precipitation is first generated within NARR as a first guess, and the generated first guess is then corrected against assimilated observed precipitation data to ensure the modeled precipitation during assimilation is close to the observed data (Mesinger *et al.*, 2006). The observation data is assimilated as latent heat instead of direct precipitation to the physically-based atmospheric model and used to adjust precipitation (Lin *et al.*, 1999). Precipitation data used for assimilation in NARR comes from the United States (US), Mexico, and Canada, however, Canadian observations have not been assimilated into NARR since 2003. US and non-US precipitation stations are analyzed and interpolated differently: in the US, a 1/8° resolution is used, while over non-US regions a 1° resolution is used (Mesinger *et al.*, 2006).

ANUSPLIN utilizes specific interpolation schemes on observation data and assimilate a second field (such as elevation) as an independent variable, or independent covariate to the observation, to produce the reanalysis data (Hutchinson, 1991). Reanalysis data produced by this method has improved the accuracy of interpolated background fields when compared with conventional spatial interpolation methods. Agriculture Canada developed daily 10km gridded climate data using ANUSPLIN V4.3 over Canada for the period of 1961 to 2003.

Mahfouf et al. (2007) listed several factors contributing to the difficulties in producing real-time precipitation analysis over Canada including 1) poor density of the climate gauges (especially in the north) and reduced coverage of radar networks, 2) orographic effects over the western part of the country, and 3) solid precipitation measurement. Very few stations over Canada were originally assimilated into the NARR analysis. In US the mount of stations and grid resolution are suitable for parameter-elevation regressions on independent slopes model (PRISM) procedure while in Canada, fewer stations are available and courser resolutions are used without the PRISM procedure. This often causes errors around the border area as detailed in Mo *et al.* (2005). Application of NARR as a hydrological input outside of the US is limited due to a lack of assimilated stations (Bukovsky *et al.,* 2007). ANUSPLIN has improved station coverage over NARR, but its results are solely based on interpolation of observations. ANUSLPIN therefore will also suffer in location where station density is poor (i.e., high latitudes in Canada) or under the presence of solid precipitation. Current reanalysis products available therefore for Canadian hydrological modelling lack either sufficient amounts of assimilated

observations stations (i.e. NARR) or a physically-based NWP model as background (i.e. ANUSLPIN).

2.3. Hydrological Modeling

Hydrologic models are useful representations of the hydrologic cycle, defining processes using both physics and conceptualizations within a simplified set of assumptions and constraints. They are primarily used for hydrological prediction like flood forecasting, and for research purposes to achieve better understanding of the hydrologic cycle and changes in/to hydrologic processes as a result of some stimulus (e.g., climate change). Pechlivanidis *et al.* (2011) classified models systematically based on their structure: metric, conceptual, physics based, and hybrid; spatial representation: lumped, semi-distributed and distributed; process: deterministic and stochastic; time-scale and space-scale.

A metric model utilizes characteristics of the hydrological response to available data (Wheater *et al.*, 1993). The equations describing these characteristics hold no physical basis, and they are used to predict outcome but not to represent the hydrological process inherently responsible for the result. This could be problematic when it is used for studies focus on the physical hydrological processes such as the climate change studies. The most well-known example of such a model is the unit hydrograph method (Dooge, 1959). Recent approaches in metric modeling are Data Based Mechanistic (DBM) modeling (Young, Jakeman and Post., 1997; Young, 2003; Ratto *et al.*, 2007) and Artificial Neural Networks (ANN) (Lange, 1999; Jain, Sudheer and Srinivasulu, 2004; Dawson *et al.*, 2006). Although the simplicity of these models sometimes allows them to be easily setup

and used for ungauged watersheds, results from such models usually lack quantifiable confidence limits (Wheater, 2002).

Conceptual models utilize a model structure that is not based on the actual physics but characteristic responses for specific situations. Conceptualized storages are commonly used in conceptual models, and the number of storages varies with the complexity of the model. For example, when describing groundwater flow a storage release function can be used instead of using the complete diffusivity equation, effectively simulating expected behaviour instead of model physics. Due to its conceptual nature, many of the model parameters do not hold direct physical interpretation, and therefore cannot be independently measured or verified; calibration is required to estimate these parameters. Using the groundwater flow example, a storage size and the release parameters need to be assigned yet these parameters cannot be measured since they are only conceptualizations of real groundwater storage. They are often left to be optimized during calibration. Increasing model complexity allows for a more comprehensive representation of the rainfall runoff relationship; however, it also requires more (complete and detailed) input data that may not be available to modellers over the entire watershed domain. Therefore, a balance between model complexity and data availability is needed to achieve success in data sparse (or large domain) regions.

Physically-based models attempt to describe hydrological processes by solving equations of motion and system continuity using finite difference or finite element spatial discretization methods. The most distinct characteristic of a truly and completely physically-based model is that calibration is not required to obtain model parameters, but rather parameters are defined by measureable variables. The physics behind the equations

are usually established from laboratory or site-specific experiments, therefore necessitating smaller-domain applications of these types of models. Using such models on larger, watershed-scale (>100 km^2) studies often lead to significant uncertainty resulting from model inputs (Beven and Robert, 2004). Theoretically, parameters in a physically-based model should be measureable, which is not possible at a watershed-scale due to spatial heterogeneity and feasibility over longer time scales (or future time periods) so aerially averaged estimations of these parameters are often used instead. Uncertainties in these averaged parameters can be significant and affect a wide range of hydrological processes (Stephenson and Freeze, 1974; Beven, 1995).

Hybrid models are the classification of models that utilize the strength of one type of model while compromising on the limitations of another. They could be metric-conceptual models, which alleviate the problems of equifinality in a metric model by reducing the dimensionality of the parameters in a conceptual model. A hybrid physical–conceptual model can also reduce the complexity in a physically-based model by conceptualising some of the physical processes to mathematical relationships. These models are often times the most practical for watershed-scale studies where physically-based simulations are desired, but limitations of parameter measurement and uncertainty necessitate some conceptual relationships.

Besides classifying the model by its structure and modeling approach, hydrological models can also be classified as lumped or distributed, deterministic or stochastic models etc. A lumped model treats an entire watershed as a single unit with one aggregated response (e.g. HMETS for simulated streamflow), while the distributed model discretizes the catchment into number of grids or elements and simulates processes at the grid-scale

(e.g., VIC, MIKE-SHE, WATFLOOD^{TM}). In principle, a distributed model can effectively simulate the spatial variability and heterogeneity of any hydrological process contributing to total runoff generation providing data is measureable and visible (in terms of model output) at each element. Parameters or inputs at each grid or element are sometimes taken as an averaged value over several grids due to availability of data. One such example is precipitation: in a distributed hydrological model, observed station precipitation must be interpolated across the modeling domain to yield one input per grid. This becomes problematic at the watershed-scale (>1000 km^2) in locations where observation stations are sparse, or in mountainous areas with significant topographic relief that results in orographic banding of precipitation (Ashiq et al., 2010). Simple interpolation methods lead to averaged or smoothed areal precipitation estimates in sparsely gauged watersheds. Therefore alternative sources of precipitation forcing, such as downscaled climate data or reanalysis data, are sometimes used to represent the precipitation field (Choi et al., 2009).

2.4. Reanalysis Data as Hydrological Forcing & Proxy Validation

Reanalysis data along with downscaled climate models and interpolated station observations can be applied for distributed hydrological modeling to simulate past (or future) runoff. Reanalysis data, when combined with climate model and station observation information, can alleviate the shortcomings of one dataset by incorporating another's advantages. This can resolve issues of spatial gaps among observation stations, yet extend the historic climate observation records to future scenarios for hydrologic simulation purposes.

Syewoon *et al.* (2013) tested the capability of the 10km downscaled Florida State University Center for Ocean-Atmospheric Prediction Studies CLARReS10 data (NCEP DOE 2 reanalysis data (R2) for hydrological simulation in the Tampa Bay region. The hydrological model was previously calibrated with observed precipitation and temperature, and it was found that downscaled reanalysis forcing data did not improve results and needed to be corrected for bias before being used as input to a hydrological model. This study suggests that although reanalysis data has the advantage of better areal coverage, worse results are potentially still expected if bias is not first removed from reanalysis data.

Haberlandt and Kite (1998) similarly applied reanalysis data to the Mackenzie River Basin using the hydrological model SLURP. Improvements in hydrological simulations were realized using better interpolation techniques and combined precipitation data sources. Enhancements were found to be related to the relative size of the watershed; with simulation errors decreasing with increasing drainage area. Furthermore, the smaller the watershed, the more sensitive it was to improvements in the precipitation forcing, therefore, the relationship between the drainage area size and model performance were also examined in this study.

Choi *et al.* (2009) used temperature and precipitation data from NARR in the SLURP model for hydrological modeling in northern Manitoba (i.e., Burntwood, Taylor, and Sapochi Rivers). SLURP is a semi-distributed land use-based runoff processes model (Kite, 1995). SLURP was initially calibrated with metrological data from observation stations, and without further calibration, the model underestimated runoff when NARR forcing was used instead of observed station forcing. At all three tested basins

(Burntwood, Taylor and Sapochi river basins) NARR scored -20.6%, -21.7% and -28.2% in comparison with scores from station simulated runs: 0.1%, 1.1% and 4.3%. This negative bias however was not found in precipitation input comparisons. NARR-forced simulations were later improved to 9.4%, 5.0% and 3.3% by re-calibrating the model using NARR temperature and precipitation as input. Although the results were seen to be improved; the re-calibration approach is not generally favored in the literature because it introduces model uncertainty into the precipitation data assessment process. Instead, further calibration can be performed after first gaining confidence in the quality of the forcing. Reanalysis data products are prone to errors from various sources as discussed in Section 2.2. Reanalysis data therefore needs to therefore be carefully evaluated before using it for hydrological modeling and other water resource engineering applications.

Several studies in the past decade have evaluated the performance of reanalysis data in the literature. One common validation approach is to compare reanalysis data with observation data, and/or other (independent) reanalysis data. For example, the widely used NCEP-NCAR model has been compared with numerous other reanalysis datasets and observations since its inception (Nieto *et al.*, 2004; Ruiz-Barradas and Nigam, 2006; Tolika *et al.*, 2006). This method is proven to be effective in diagnosing the general biases of annual or seasonal precipitation, and provides first insight on the quality of the reanalysis data as a precipitation product.

Mesinger *et al.*, (2006) compared NARR with other reanalysis products and demonstrated NARR's improvement in the accuracy of precipitation simulation (and other climate variables) over the entire North American continent. Becker *et al.* (2009) examined the precipitation characteristic in NARR and compared it with the observed

station data in the US, and NARR's annual precipitation was found to be close to the observed precipitation with a slight underestimation during summer across the US. Bukovsky *et al.* (2007) compared NARR with NCEP R1, NCEP R2 and ERA-40 reanalysis data and demonstrated that NARR is superior in depicting precipitation over the continental US. Analysis of NARR on other part of the North American continent, including trans-boundary regions with Canada and Mexico suggest that care should be taken when using NARR over these regions (Bukovsky *et al.*, 2007). Mo *et al.* (2005) detailed the discontinuity over the border regions and suggested that the decrease in model (and observation) resolution and the difference in data interpolation schemes is the cause of the spatial discontinuity.

Newlands *et al.* (2009) evaluated the Agriculture Canada's ANUSPLIN (AC-ANUSPLIN) dataset; known errors in the dataset calculated using 50 independent reference stations. Calculations showed that the Mean Bias (MB) in daily winter precipitation was 0.07 mm versus MB in spring and summer of -0.11mm. Furthermore, comparison of the ANUSPLIN data and reference sites shows that AC-ANUSPLIN has a superior precipitation field in Canadian Prairie region than BC-Alberta mountain region, which suggests such data in Manitoba could potentially be useful for hydrological modeling during periods where the data are available.

Many of the above studies evaluate reanalysis data products against station observations with the implied assumption of observations being representative of the 'truth', or real weather features over an entire spatial domain. This assumption is questionable in northern Canadian basins where observation stations are sparse (much coarser resolution of observations than in southern regions), and hydrographic features are more complex.

Figure 2 shows the basin extents of the Nelson-Churchill River Basin (NCRB) and location of climate observations stations (inactive and active) located within the basin. Northern regions have notably fewer climate stations than southern areas.

Representativeness error can also be significant when areas are sparsely gauged and/or stations are non-uniformly distributed. Interpolating observation stations within a sparsely-gauged watershed will yield misleading conclusions when comparing to reanalysis data products because the station interpolation itself holds little truth if the stations are sparse. Conversely, hydrometric data represents an aggregated hydrological response of an entire domain (basin or sub-basin), hence the representativeness effect is minimized. Reanalysis data products can be verified through proxy validation which uses a hydrological model forced with the reanalysis data to generate a hydrologic simulation and compares the outcome to observed stream flow data at a basin outlet.

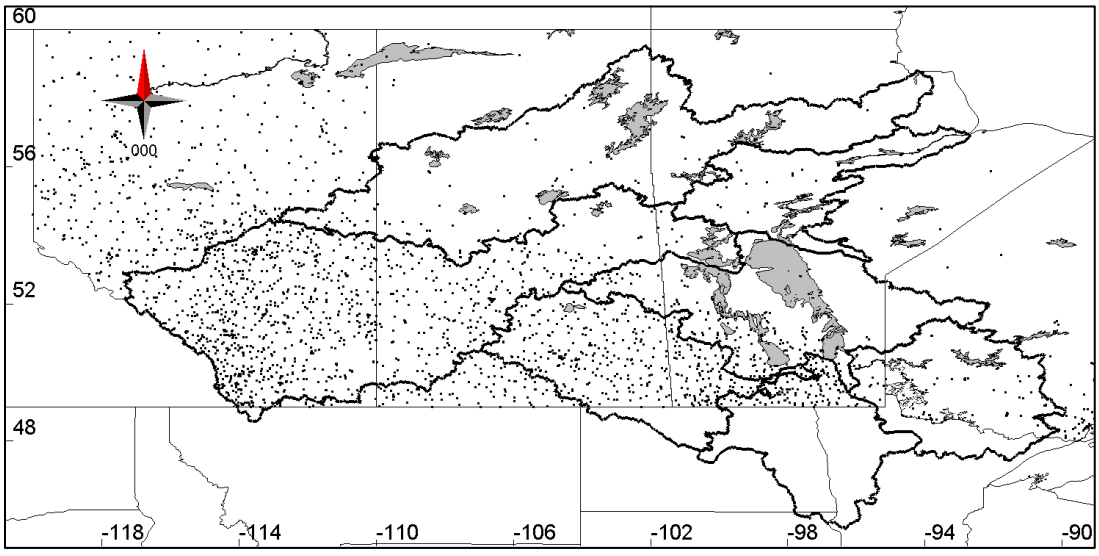

Figure 2: Nelson-Churchill River basin extent showing both active and inactive Environment Canada CDCD precipitation observation stations with precipitation data.

Comparing hydrological model simulations using different precipitation forcing (both observed and numerical) tests the quality of various areal precipitation products while avoiding representativeness errors since the hydrometric information is cumulative over drainage area (Heistermann and Kneis, 2011). On the other hand, proxy validation is also prone to other sources of errors like model setup, calibration, streamflow measurement error, and error in the up/downscaling of precipitation forcing.

There are several studies in recent literature that have used proxy validation for data verification (Heistermann and Kneis, 2011; Stisen and Sandholt, 2010; Klyszejko, 2007). Stisen and Sandholt (2010) compared outputs from a distributed hydrological model with different satellite-based rainfall estimations (SRFE) to evaluate the quality of these SRFEs. Overall, proxy validation inferred the superiority of precipitation products relative to other model forcing under the assumption that the model is a true representation of the physical system. It was found that there is significant influence of model calibration on proxy validation studies, which was addressed in Stisen and Sandholt's (2010) study through the difference among outputs even when SRFEs are adjusted to the same mean rainfall amounts. Heistermann and Kneis (2011) evaluated the proxy validation method at a small catchment scale with a simple rainfall-runoff model. Synthetic precipitation data sets were fed into the rainfall-runoff model, and simulation results then compared based on goodness-of-fit scores. Model parameters were not calibrated to any of the datasets, but rather kept random to avoid calibration bias. Large numbers of simulations were computed using different datasets with the same random parameter under a Monte Carlo framework. Comparisons of different simulations showed that the proxy validation method was useful in determining the superior input

among other precipitation inputs, even with errors in streamflow records and model setup/calibration (discussed in Chapter 4).

2.5. Summary

Reanalysis data utilizes the NWP models as background for assimilation processes with observations then assimilated to adjust the background. These data sets are potentially useful for hydrological forcing after their quality has been evaluated and any potential biases corrected. Hydrological simulations using reanalysis data as forcing are prone to bias intruded from observations and background, as well as assimilation procedures. Reanalysis data therefore needs to be carefully evaluated prior to use for hydrological modeling purposes.

Many studies have evaluated the quality of reanalysis data by directly comparing them with observation or other reanalysis data; or by indirect comparison through forcing of hydrological models and using hydrometric station records for verification. Hydrometric gauges can help to infer local precipitation and water balance information and are especially important in areas with sparse precipitation gauge networks, such as in high latitude regions. Moreover, proxy validation is end-goal oriented, and since the goal of this study is to validate the application of CaPA as hydrological forcing it is a useful tool for validation. In this study, both direct comparison with observations and proxy validations are used, furthermore, due to the limitations in both methods of comparison, the results from both types of comparison are evaluated side-by-side rather than independently. Although many studies use the proxy validation method, models are calibrated (or re-calibrated) in only a few of those studies. Re-calibration introduces uncertainties into the validation and questions surrounding parameter equifinality, and

therefore is not adopted in this study. Hydrological modeling is a numerical representation of the hydrological processes and can be classified in many different ways; each type of model has its merits and short comings. The choice of hydrological model in this study, WATFLOOD^{TM}, suits the gridded nature of CaPA data, and is suitable for the computational demand required for watersheds in this studies domain. Moreover, it is one of the hydrological models used by Manitoba Hydro for modeling studies, the same studies they are interested in using CaPA as forcing.

Chapter 3. Study Area

The study domain encompasses the entire Churchill-Nelson River basin, which includes seven sub-watersheds (each assigned a short code): Assiniboine River (ASI), Churchill River (CHU), Nelson River (NEL), Saskatchewan River (SAS), Red River (RED), Lake Winnipeg (WPL), and Winnipeg River (WPR). The total drainage area of these seven watersheds is about 1.3 million square kilometers. Figure 3 shows the boundary of the watersheds and their names; major lakes and water bodies are also highlighted in gray. Solid arrows represent the natural flow directions and dashed arrows represent directions of manmade diversions.

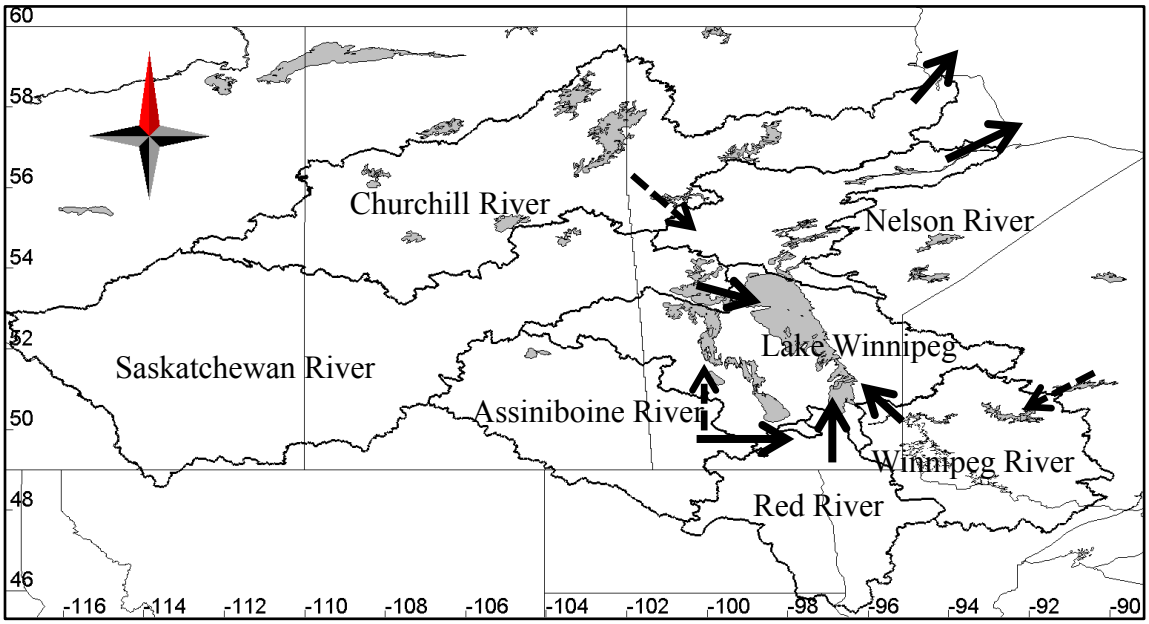

Figure 3: Seven Nelson-Churchill River sub-watersheds and their drainage directions

3.1. Ecological frame work

Environment Canada divided the Canadian land mass according to ecological frameworks. Each framework is characterised by its unique geological, hydrological and ecological features. The following figure indicates the ecological zones within the frame work with different colors (Figure 4).

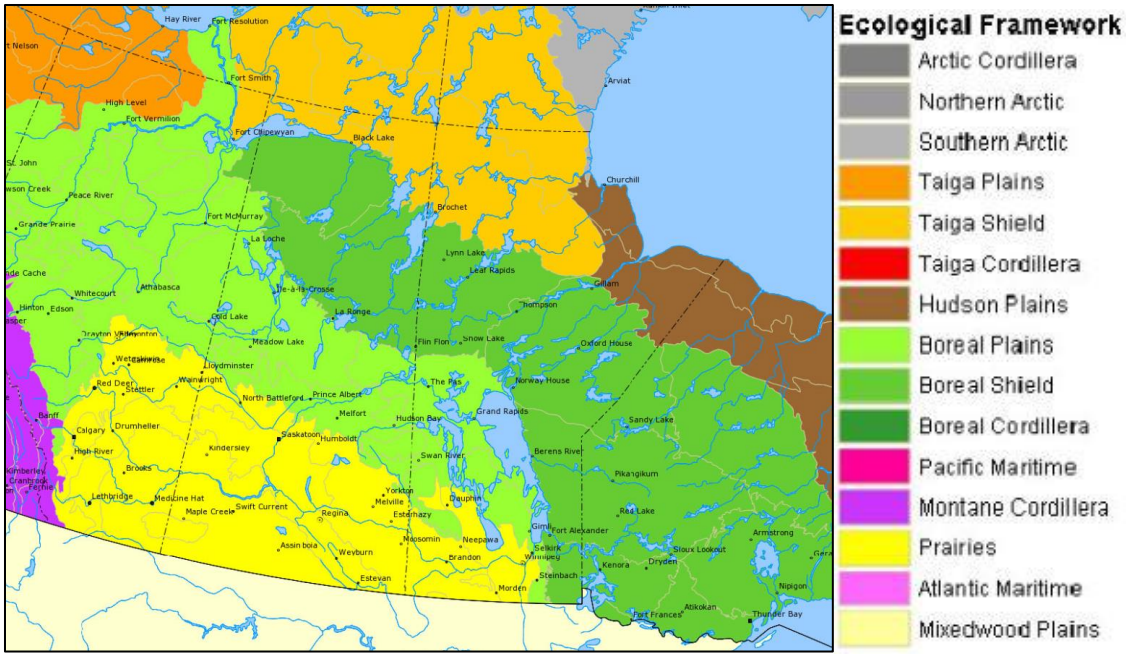

Figure 4: Canadian Ecological framework, adopted from Natural Recourse Canada (2009)

The study area comprises three different Canadian ecological frameworks: Boreal plain, Boreal shield, and prairie (Agriculture and Agri-Food Canada, 2013). Table 1 indicates the total drainage area and the ecological framework to which each watershed pertains. A brief description of each ecological framework pertaining to the study area is provided after the table.

Table 1: Seven sub-watersheds and the ecological framework they reside in.

Watershed Name	Total Drainage Area km^2	Ecological Frame work
Assiniboine River	182,000	Prairie
Churchill River	259,000	Boreal shield
		Boreal plain
Nelson River	68,000	Boreal shield
Red River	105,000	Prairie
Saskatchewan River	335,000	Prairie
		Boreal plain
Lake Winnipeg	196,000	Boreal plain
		Boreal shield
Winnipeg River	135,000	Boreal shield

Boreal Shield is located within the geological regions of Canadian Shield. It stretches from northern Alberta to eastern coast of Newfoundland. Canadian Shield is one of rudimentary geological structures in North America formed around the Precambrian era, a relatively earlier geological period. During the last ice age, the exposed bedrock was continuously scoured by the advance and subsequent retreat of glaciers. This left many surface depressions on the bedrock and many glacial deposits such as gravel and sand. These surface depressions, being inadequately drained, eventually transformed into lakes and wetlands with a thin layer of soil formed from the glacial deposits left behind. Much of the vegetation within the Boreal Shield is ever green; species like spruce and fir form dense forest covering the thin layer of soil with impermeable bedrock underneath. Many wetlands form around the lake and ponds due to poor or inadequate drainage conditions. (Agriculture and Agri-Food Canada, 2013)

The implication of these unique characteristics on hydrological processes and runoff generation is significant. If wetlands are not present, the shallow soil layer and impermeable bedrock cause an immediate rainfall-runoff response. The response will be attenuated where wetlands or lakes exists. Some wetlands are disconnected during dry seasons, and become connected only once upstream storage is filled. Regulation of lake levels are often in place to maintain adequate water levels downstream, which imposes more challenges when depicting and determining natural hydrological response characteristics. Such challenges are more acute in the Winnipeg River and Lower Nelson River basins.

Prairie and Boreal Plain ecological frameworks make up the central plain area. Unlike the bareness of Canadian Shield subsurface strata, the central plain is under laid with rich

soils and deposits. The fertile land causes agriculture development, which marks the most distinguished characteristics of the Prairie portion of the central plane area. Prairie and Boreal Plain differ based on landcover type. Prairie is agriculture land dominated while boreal plain is dominated with natural forest (Agriculture and Agri-Food Canada, 2013). Change in landcover from natural to developed agriculture land imposes changes on hydrological responses. This change is most significant at the Prairie portion of the central plain rather than the Boreal Plain portion. Hydrographs tend to be 'flashier' in agriculture zones as the land is well drainage by trenches or man-made channels. Furthermore, crop vegetation has a higher evaporation rate than vegetation with high canopies such as the mixed forest at the boreal plain.

3.2. Hydrography

The Red River, Assiniboine River, Winnipeg River and Saskatchewan River flow into the Lake Winnipeg Basin, which then drains into the lower Nelson River Basin. Within the lower Nelson, Notigi is a control structure located on the Rat River just below Southern Indian Lake (in the Churchill River basin), thorough which the majority of the Churchill River basin flows are diverted into Burntwood River and subsequently the lower Nelson River and eventually reaches Hudson Bay and the Arctic Ocean. There are a few major lakes located within the study area, including: Lakes Winnipeg and Manitoba in the Lake Winnipeg basin; Reindeer Lake in the Churchill River basin and Lake of the Woods in the Winnipeg River basin. Watersheds within the Canadian Shield portion of Canada have drastically different hydrography than those in the Central Plain areas. Due to the erosion of the exposed bedrock, watersheds inside the Shield region have abundant small lakes and wetlands. These watersheds include Winnipeg River basin, Eastern half of the

Lake Winnipeg basin, lower Nelson River basin and majority of Churchill River basin. River channels in these watersheds and regions are often interconnected with lakes and wetlands. Unlike channels in the Boreal Shield, rivers in the Central Plain region are typically highly erosive but have defined channel geometry with characteristic meandering and braided channels.

3.3. Climatology

Canada can be categorized into climate zones depending on local climatology. The majority of Canada's land mass, including the study domain, is within the subarctic climate zone, with a small portion of the Saskatchewan River and the entire Red and Assiniboine River basins lying in the Prairie climate zone. The subarctic climate zone is characterized by short, cool summers and long, cold winters with low winter precipitation. The prairie climate zone, on the other hand, is characterized by continental extremes of long, cold winters and hot, dry summers (Canadian Atlas Online, 2013).

There are five air masses that dominate the climate pattern of Canada and all of them affect the climate over the study domain: Continental Arctic (CA), Maritime Arctic (MA), Maritime Polar (MP), Maritime Tropical (MT), and Continent Polar (CP). (Canadian Atlas Online, 2013). When cold and dry CA air massed dominate the study area, this results in long and cold winters. West to east winds carry slightly warmer and moister MA and MP air masses from the Pacific Ocean on the west coast over the orographic features of the Rocky Mountains and onto the Prairies. During spring, warm air comes with MP, MT along the southern Canada, while cold air comes with the CA along the northern Canada. These air masses at different temperatures often collide and produce intense, late winter snow storms. During summer, the CA retreats to the north

and MP and CP dominates the study area. MP air is moister and warmer than CP, resulting in a very wet, west coast prior to the Rocky Mountain ridge. Beyond the Rockies however, moisture from the Pacific Ocean has already drastically decreased, meaning that precipitation rarely forms, causing drier climate conditions across the prairies around the upper to mid-portions of the Saskatchewan River basin (Canadian Atlas Online, 2013). Meanwhile, frequent and widely scattered convective storms occur over the entire Prairie region during summer mostly the result of local convection and intense heating. Raddatz and Hanesiak (2008) analysed about 1000 summer rain events that are considered as significant (≥10 mm in 24 h) occurred over Canadian Prairie from 2000 to 2004. It was found that over 79% of the events were associated with convective events. During fall, evaporation of large Canadian lakes is high as their exchange of latent heat flux reaches peak (Schertzer, 1997). The prevailing west to east wind carries the evaporated moisture, which condenses into rain and falls along lee shores of the larger lakes (Lackmann, 2011).

The El Niño/Southern Oscillation (ENSO) represents ocean-atmospheric oscillations over the tropical pacific. It has significant impact on Canadian climate as well as the study area. The years of 2002 to 2005 were under a prevalent El Niño episode, which is characterised by warmer Pacific Ocean temperatures. ENSO typically causes warmer winter temperatures within the NCRB study domain, with the warmest around Manitoba (Hoerling *et al.*, 1997; Shabbar and Khandekar, 1996). Moreover, the southern boundary of the study domain usually receives less winter precipitation during ENSO periods (Shabbar *et al.*, 1997).

3.4. Summary

The total area of study domain is about 1.3 million square kilometers and consists of seven sub-basins: Assiniboine River, Churchill River, Nelson River, Red River, Saskatchewan River, Lake Winnipeg and Winnipeg River basins. The outlet of the study domain is located at the downstream end of the Nelson River, draining into Hudson Bay. This study domain resides within three different types of ecological framework: Boreal Shield, Boreal Plain and Prairie. Each framework is differentiated with its distinctive geology and landcover classifications that will influence sub-basin hydrological responses within the domain. The Prairie region is characterized by agriculture landcover within the Boreal Plain; the Boreal Shield is covered by mix forests and wetlands. It is important to examine the ability of WATFLOOD^{TM} to simulate localized sub-basin responses landcover to ensure proper model setup prior to conducting the proxy validation, including the effect of large lakes that could influence both the shape of the hydrograph and rainfall-runoff relationship.

Chapter 4. Methodology

CaPA data and other data used to compare with CaPA, as well as the hydrological model WATFLOOD™ are described in Sections 4.1 and 4.2. A three step methodology is introduced for this research which includes: Point-to-Point (P2P), Map-to-Map (M2M) and proxy validation methods. P2P and M2M evaluate CaPA data as a precipitation product by comparing it directly to other precipitation data, while proxy validation indirectly compares CaPA to CDCD station data via use as hydrological model forcing in WATFLOOD™. Furthermore, the assumptions and limitations of each step of validation are also presented in this chapter.

4.1. Introduction to CaPA and Observation Data

4.1.1. Canadian Precipitation Analysis (CaPA)

CaPA utilizes statistical interpolation to produce estimates of six hourly gridded precipitations over North America (Mahfouf, *et al.*, 2007). It is developed by Meteorological Research Division of Environment Canada (EC) and the Meteorological Services of Canada (MSC). Optimal Interpolation (OI) technique is used to combine different sources of precipitation information in order to provide the best estimate. The current operational version of CaPA (version 2.3) was released April 2011 at the Canadian Meteorological Center. It produces precipitation analysis in near-real time with a horizontal resolution of 15km. CaPA outputs analyses exist at two time scales: 6 hourly, reported 4 times a day at synoptic hours; and 24 hourly reported once a day.

Four different types of observation networks are assimilated into CaPA as shown on Figure 5: synoptic network (SYNOP); aeronautics network (METAR); and two

cooperative networks, the American meteorological cooperative network (SHEF) and the Réseau Météorologique Coopératif du Québec (RMCQ). All stations before being assimilated into CaPA first under-go a quality control process to correct physically impossible/improbable readings and known instrumental bias. Furthermore, due to uncertainty in solid precipitation measurement, an algorithm checks wind speed and temperature and will remove solid precipitation observations during higher wind speeds and low temperatures.

The SYNOP network consists of surface synoptic weather observations from about 300 manned stations and about 750 automated stations manually maintained by Environment Canada. One measurement is recorded every fixed synoptic hour (00UTC, 06UTC, 12UTC and 18UTC). By taking measurements at fixed time intervals simultaneously with a wide spatial coverage, the network is designed to present a comprehensive and near real-time representation of current weather over a large domain.

METAR is one of the most commonly used formats for reporting and transmitting weather information. The majority of the METAR network observations come from weather stations at airports. The network was initially intended to be used by pilots in fulfillment of a pre-flight weather briefing, but meteorologists then began to aggregate the METAR information and use it to enhance weather prediction. METAR reports are generated on hourly basis for both automated and manual stations in the METAR network.

The SHEF network is a corporative network first initiated by U.S. National Weather Service (NOAA). It contains mainly cumulative precipitation reported at 24-hour time

steps, thus it is only used in the 24-hour CaPA analysis. It has wide spatial coverage and good gauge densities over the entire United States. The RMCQ network is a Canadian Provincial (Quebec) meteorological cooperative network and is available at synoptic hourly readings. It is therefore used in both the 6- and 24-hour CaPA analyses. The stations from RMCQ are installed and managed cooperatively by private agencies in conjunction with the Quebec provincial government, and data are shared in common format among the two.

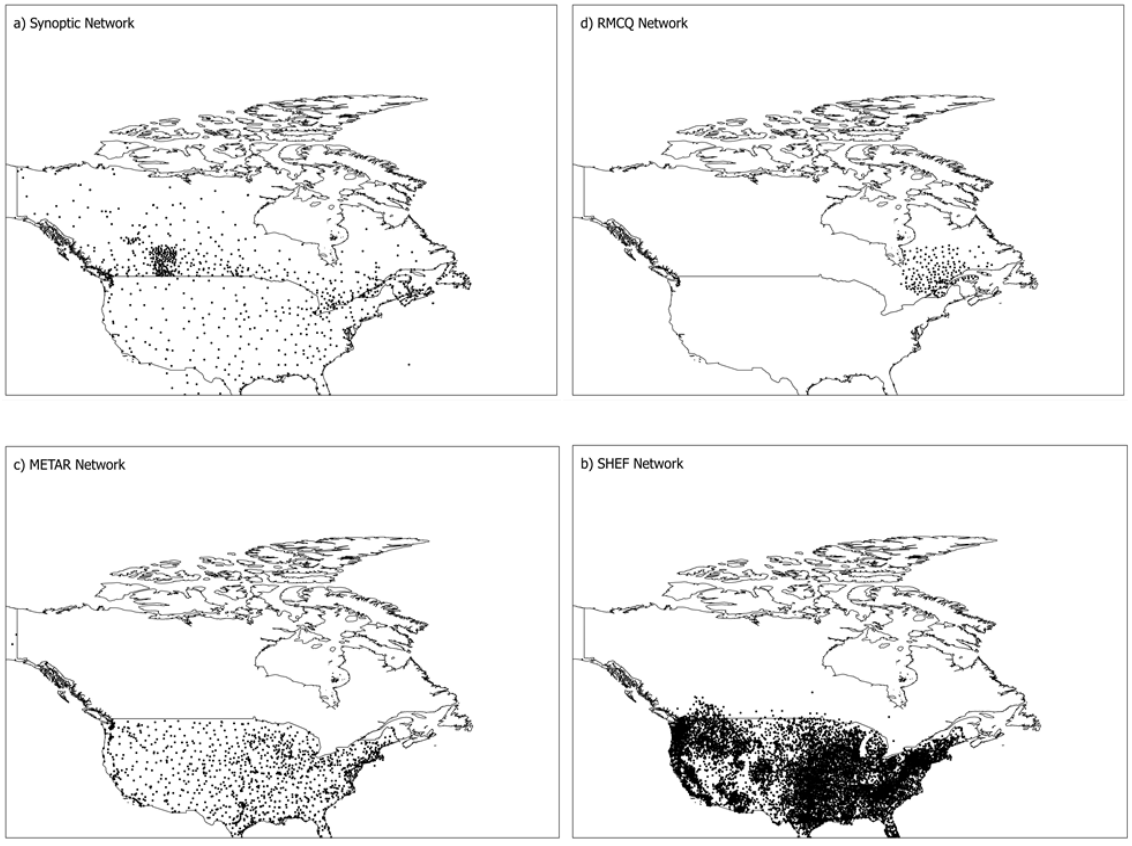

Figure 5: The precipitation networks used in CaPA from Davidson *et al.*, (in preparation).

Many gauges in the Canadian precipitation network are known to underestimate solid precipitation due to instrumentation errors and wind under-catch (Goodison, 1978). This issue is even more acute for automatic gauges than manual gauges. Nipher gauges can

underestimate approximately 20% of the real snow precipitation at a 5m/s wind speed, and under-estimation can be more severe when the wind speed is higher (Goodison *et al.*, 1998, Rasmussen *et al.*, 2012). CaPA's Quality Control (QC) procedure eliminates any precipitation record at an automated station when temperature is below threshold value while at the manual gauges CaPA discards the record only if both temperature and wind speed exceeds threshold (Lespinas *et al.*, in preparation).

In order to detect/adjust systematic errors in observations, CaPA's QC examines the observation in both temporal and spatial perspective (Lespinas *et al.*, In Preparation). A temporal error occurs when a station systematically repots false zeros or reports precipitation too frequently, and a spatial error occurs when one station deviates too significantly from nearby stations. Temporal errors in the observation data are detected by transforming the innovations over last 30 time step to normal distribution. The values associated with the tail of the distributions are then eliminated. On the other hand, spatial errors in the observations data are detected by comparing each station value with the average of all observations within a limited spatial boundary (Lespinas *et al.*, In Preparation).

To produce the 6-hour CaPA reanalysis, a short range 6-hour forecast from the GEM model and observation data are first obtained at the same time step. The forecast is calculated as the difference between GEM model output at T0+6h (T0 is the start of a model initialization) and T0+12h time step, given the first 6 hour for model initialization in order to avoid initialization errors. Four consecutive forecasts are used to produce reanalysis results at each synoptic hour. These four analyses are then summed together to create the 24-hour CaPA reanalysis field. Most of the assimilated observation networks

do not contain temperature recordings, thus CaPA analysis relies on GEM short-term temperature forecasts to provide "pseudo-analysis" of surface temperature to detect the occurrence of solid precipitation.

CaPA outputs two main data files. The first data file contains two fields: analysis results, and the confidence index. The confidence index, ranging from 0 to 1 is an indicator for the contribution of the observation to the analysis. Confidence index of 0 represents no contribution from the observation. For this thesis, analysis results were reformatted into r2c for direct input to WATDFLOOD™. The second field of CaPA contains various diagnostic variables, such as the cross validation analyses and the quality grades assigned by CaPA to each of the assimilated observations through statistical interpolation.

In theory, CaPA has advantages for hydrological simulation in station spare regions due to its physically driven background in comparison with ANUSPLIN, and increased assimilation of station data in comparison with NARR. Davison *et al.* (In Preparation) compared CaPA data with three other common reanalysis and NWP datasets (NARR, GEM and ANUSPLIN) that are used in North America for hydrological modelling purposes. Two observation datasets were used in this study: Alberta Agriculture and Rural Development (AARD) and Saskatchewan Environment and Resource Management (SERM). The analysis was carried out from June 1st to October 31st. Tests were broken down into three different sets: The first set considered two categories of data outcome (precipitation or no precipitation); the second set of tests considered multiple categories by breaking down the precipitation intensity; the third set of tests considered the products as deterministic estimates of continuous variables. They were carried out based on bias, accuracy and skill (GEM as reference) tests. Results of the tests showed that CaPA as

well as ANUSLPIN scored the highest for accuracy but worst in terms of bias. It suggested that CaPA is most suitable for short term weather related studies. The GEM and NARR data has lowest overall bias but were both lower in terms of accuracy, suggesting they are suitable for longer term climate related studies (Davison *et al.*, In Preparation). Furthermore, results from the two category tests showed that ANUSLPIN outperformed CaPA in term of bias due to ANSLPIN's superior ability of predicting "no-rain" conditions. However, results from the multiple category tests revealed that the test score was greatly skewed to the no-rain condition to favour ANUSPLIN data due to a high number of days with no-rain conditions. Over all, CaPA is more accurate than ANUSPLIN for the higher precipitation ranges (25 to 50mm), which are of greater concern for hydrologic modeling purposes. Furthermore, Davison *et al.* (In preparation) did not compare winter solid precipitation.

4.1.2. Canadian Daily Climate Data (CDCD)

Environment Canada provides archives of daily temperature, and precipitation including snow depth of over 7000 stations across Canada (Environment Canada, 2013) called Canadian Daily Climate Data (CDCD). Data are stored in the National Archive Format and can be retrieved from the website using an extraction utility that is provided by Environment Canada, or from purchased CDs. The CDCD data are available from early 20th century (varies depending on station) to December of 2007. Previously shown, Figure 2 shows the total number of precipitation gauges in the CDCD dataset, although many of these stations shown are no longer active or are only seasonally active. As such, the number of stations used for this research is significantly less than what the figure indicates.

Many different types of observation gauges are used in the CDCD network to obtain observation records. The types of precipitation gauges that are active during this study's time period are listed below (Table 2).

Table 2: Types of gauges used by Environment Canada, their resolution, and period of service.

Type	Model	Resolution(mm)	Time period
Manual	Type B plastic	0.1	1970 to present
Recording	MSC tipping bucket	0.2	1937 to present
	Hydrological Service TB3	0.2	2002 to present
All weather	F&P/Belfort	0.6	1967 to present
	Geonor T-200B	0.6	2002 to present

Instrument errors under different field conditions are widely documented among different type of instruments; however, little is understood regarding the physics pertaining to these errors. Problems are generally more acute for solid precipitation measurement under windy conditions. Knowledge is limited regarding solid precipitation aerodynamics properties under changing wind conditions. Moreover, corrections of solid precipitation require wind measurement at the location (and ideally height) where the measurement is taken, yet wind measurements are not always available. Therefore, without correction, validation of CaPA solid precipitation against CDCD solid precipitation needs to be done with caution.

The Red River and Assiniboine Rivers flow through both Canada and the United States. Observed precipitation is collected from the US cooperative networks and then homogenized by NOAA's NCDC in collaboration with the Department of Energy's Carbon Dioxide Information Analysis Center (CDIAC) to produce the United States Historical Climatology Network (USHCN) (Easterling, 1996). The USHCN data is used

in the study, and a comparison between US Cooperative Network and USHCN data made in Section 5.2.

The observation data are directly compared with CaPA in the P2P analysis as subsequently described in Section 4.3.1. They are then interpolated onto a precipitation map and compared with CaPA in the M2M analysis as subsequently described in Section 4.3.2. For the proxy validation analysis, the interpolated observation data are used to simulate hydrographs in WATFLOOD™ as subsequently described in Section 4.4.

It is important to understand the observation data including its spatial and temporal coverage, measurement accuracy, and known bias in order to properly conduct the validation analyses. It is also important to understand the hydrological model setup and calibration used for proxy validation as they both make significant contributions to the analysis uncertainties.

4.2. Hydrological Model WATFLOOD™

WATFLOOD™ is a fully distributed, semi-physically-based hydrological model; it simulates the hydrological budget of a watershed using an integrated set of programs (Kouwen, 2012).

To setup WATFLOOD™ for the entire NCRB, each sub-watershed was modeled separately. Watersheds were further discretized to Group Response Units (GRUs), with each GRU containing information on grid elevation and percentage of each landcover unit identified from harmonized landcover imagery (Geobase, 2003). In WATFLOOD™ hydrological responses are determined on a per landcover basis, with distinct landcover units (no matter their placement) each having distinct hydrological responses. The total

gridded runoff response is the sum of each individual landcover response; Figure 6 below demonstrates the concept of the GRU.

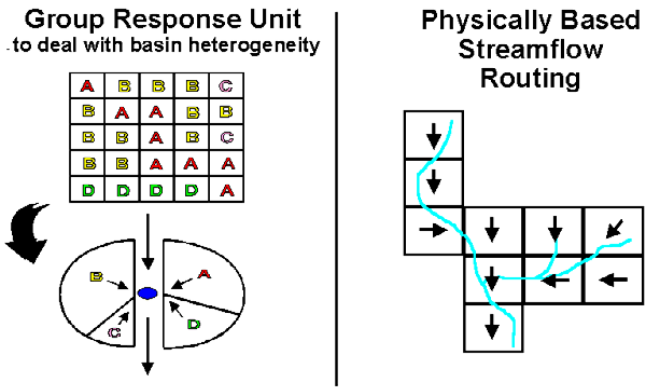

Figure 6: GRU concept in the WATFLOOD™ model (Adapted from Kouwen, 2012)

The GRU configuration allows WATFLOOD™ to capture the spatial variability in hydrological processes from distributed, non-homogenous forcing data without losing computational efficiency. Despite the computational advantage of GRU system though, to construct a model that is entirely physically-based at the mesoscale (>1000 km^2) is not yet an attainable goal. Therefore, WATFLOOD™ takes a physical-conceptual hybrid approach to achieve computational efficiency over large domains. Figure 7 illustrates the different hydrological processes represented within the WATFLOOD™ modeling package.

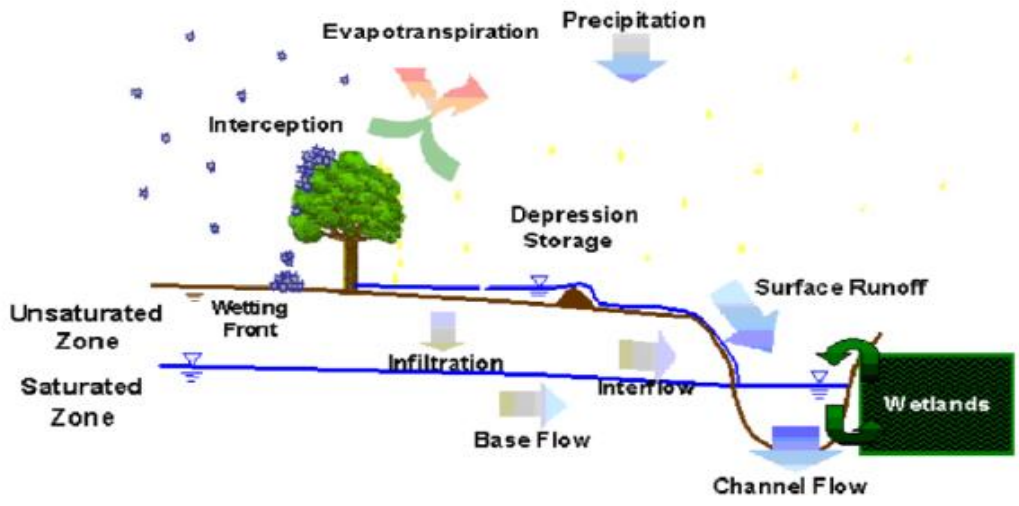

Figure 7: Hydrological processes simulated by the WATFLOOD™ model from Stadnyk-Falcone (2008).

Modeled processes include interception, infiltration, evaporation, snow accumulation and melt, snow ablation, interflow, recharge, base flow, overland flow, and channel routing (Kouwen, 2012). Each process occurs for every land class, and is controlled by separate parameters for each river and landcover classification.

Throughout the soil strata, storages are assigned to saturated zone (lower zone storage), unsaturated zone (upper zone storage), and at the soil top surface (depression and interception storage). The interaction between each zone is detailed in the user manual (Kouwen, 2012).

The main proponent of this study, Manitoba Hydro's Water Resource Engineering group, has previously setup WATFLOOD^{TM} models within the Nelson-Churchill domain for future use in both short-and long-term water resource studies. The models are at various stages of setup and calibration, with the Winnipeg River, Lake Winnipeg Basins and Saskatchewan river basins being the most complete; Churchill and Red River basins

among the second most complete (minor calibration still required); and the Assiniboine and Nelson River Basins setup but not yet calibrated. The development of CaPA over the study domain has brought forth the opportunity to test it as forcing data for the WATFLOOD™ model since it provides a finer resolution precipitation dataset than station data alone, and may help to improve hydrological modeling outcomes and calibration. The distributed nature of WATFLOOD™ is well-suited to forcing by CaPA output.

4.3. Direct Validation of CaPA Precipitation

The validation methodology established to test CaPA over the study domain for hydrological modeling purposes consists of three stages: the point to point validation (P2P), map to map validation (M2M) and proxy (WATFLOOD™) validation. Each step in the methodology has its own strengths, limitations and constraints; hence only by piecing all the validation results together can one comprehensively review the characteristics and quality of CaPA data. Despite CaPA analyses being available from 2002 to 2011 and CDCD data from the early 20th century up until 2007; the period of analysis in this thesis was from 2002 to 2005. This was due to a limited period of data overlap between CDCD and CaPA analyses with sufficient stations to be statistically relevant. For the P2P and M2M analyses, each of the years are further divided into four seasons: Spring (MAM: March, April, May), summer (JJA: June, July, August), Fall (SON, September, October, November) and Winter (DJF, December, January, February).

4.3.1. Point to Point (P2P)

P2P comparisons denote the process of comparing the nearest CaPA grid to a station observation (CDCD data). Since the comparison is done between a point and a grid area,

station representativeness errors are therefore introduced. No downscaling (or up scaling) method was used as any method would inherently introduce a new bias into the analysis. Comparisons are done through the use of empirical Quantile-to-Quantile plots on annual, seasonal, and averaged seasonal precipitation values from 2002 to 2005. Averaged seasonal plots are used to reduce or constrain station representativeness error. CDCD stations are not independent of the stations assimilated into CaPA: Figure 8 shows the overlap between CDCD and assimilated stations from 2002 to 2005. Churchill River basin has the highest percentage of overlapping stations. The coverage of assimilated stations is important to the quality of CaPA as discussed in Chapter 5.

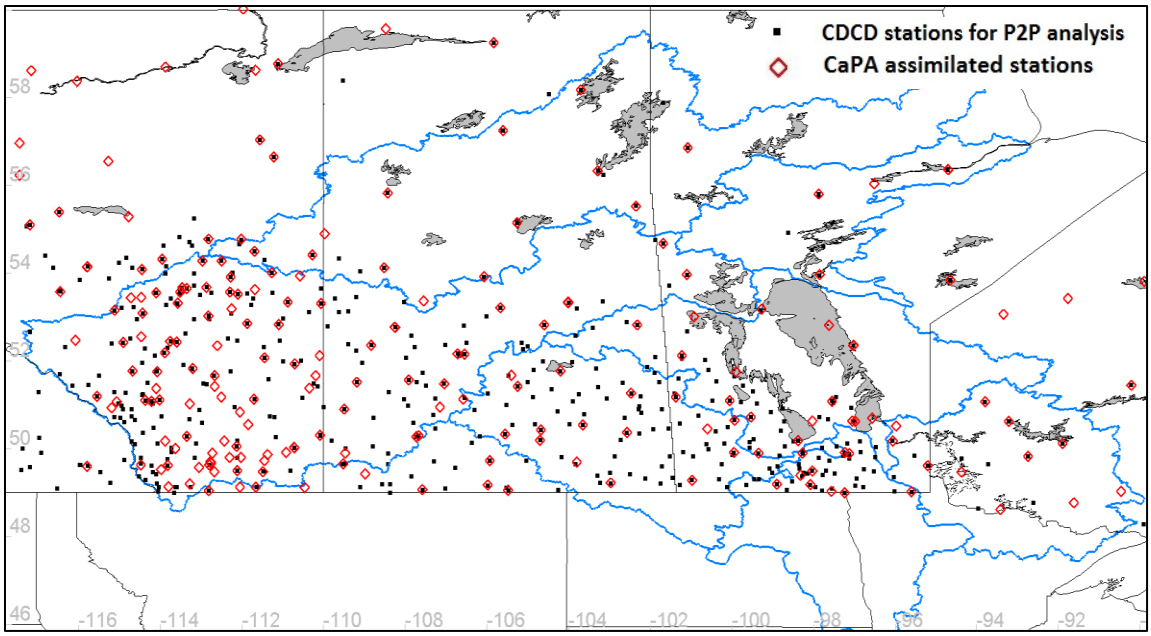

Figure 8: CDCD stations relative to CaPA assimilated stations from 2002-2005.

Empirical Quantile-to-Quantile (QQ) plots are used to compare the CDCD to CaPA precipitation data on a point-scale. The empirical QQ plots are formed by plotting the two sample datasets to determine whether they share the same statistical distribution. They are preferred over scatter or performance plots because they evaluate the difference between the two datasets at different range of magnitude over the entire distribution, yet

do not require the two datasets to share the same distribution. Both datasets are first ranked from smallest to largest based on distinct sub-basin regions, and plotted according to rank in the respective dataset, with CDCD on the x-axis and CaPA on y-axis. The degree of linearity of the QQ plot suggests the similarity in shape of two distributions; the more linear the QQ plot, the closer the distribution shapes are (along a 1:1 line is perfect fit). A relatively linear QQ plot that departs in a parallel fashion away from the 1:1 line suggests the two datasets share the same distribution, but the locations of percentiles are shifted and therefore they have different means. On the other hand, if a relatively liner QQ plot has a slope less than one and passes through the 1:1 line suggests that the spreads of the two datasets distributions are different. Furthermore, a QQ plot with a small sample size will usually appear more non-linear, particularly for precipitation data where seasonality is inherent; in which case, the results of the QQ plot analysis need to be interpolated with caution. Matlab™ provides a built-in function, *qqplot()* for generating QQ plots from two datasets and was used in this thesis.

The P2P analysis ground-truths CaPA data against available observations, assuming station observation data as truth. This assumption can be invalid under several circumstances, notably during months with solid precipitation recordings. Furthermore, distributed hydrological models such as WATFLOOD™ require spatially distributed precipitation input, rather than precipitation one (or single) points. P2P analyses alone cannot therefore adequately assess the quality of CaPA as hydrological model forcing.

Preparation of Observations

CDCD data are first downloaded from Environment Canada's website. Several python codes were adapted by the author to batch extract the CDCD data at each station. The data from CDCD datasets are transformed into Excel™ .CSV files with year, month, days and data (precipitation in mm) in each column, respectively.

Since QQ plot are generated for annual or seasonal averages, missing data are not permitted or included in the analyses. A Matlab™ script called '*creatavgsta.m'* was developed to filter out stations with missing precipitation and exclude them from the analysis, thereby discarding many data. The script '*creatavgsta.m'* calculates the percentage of missing days for each station in each year. Figure 9 shows the histogram generated for percentage of days with missing data from 2002 to 2006 over entire study domain, categorized by year. From this figure, the number of stations with 0-15% missing records has declined significantly from 2005 to 2006.

Since stations with missing records are excluded from the QQ plot and the QQ plot is sensitive to sample size, conducting the P2P analysis in a year with insufficient sample size will result in misleading conclusions. This is the primary reason that the period of analysis for CaPA validation is from 2002 to 2005. The remaining CDCD stations are called 'available and good stations' (avgsta), and CaPA precipitation is extracted at their locations using the stations spatial information.

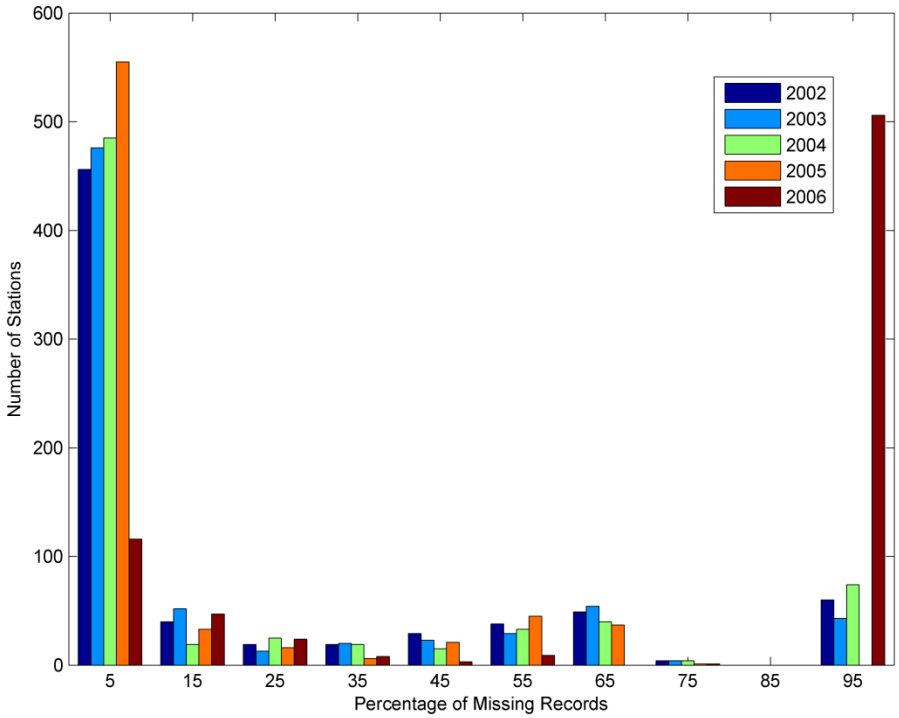

Figure 9: Histogram of percentage missing record for the years 2002 to 2006.

These stations are then classified by their respective sub-basin shown in Section 3.2 according to their latitude/longitude coordinates using customized Matlab™ scripts. Daily precipitation data from these stations are summed into seasonal cumulative precipitation. USHCN data are processed the same, with stations having missing data also being filtered out.

Preparation of CaPA data

CaPA analyses are downloaded directly from the Canadian Meteorological Centre RPN server, Pegasus in .fst format and transformed into .r2c format for individual sub-basins using an r2c convertor developed by CMC (fst2r2c). The r2c files contain 6 hourly precipitation fields over the entire analysis period (2002-2005). Matlab™ scripts are used to compute monthly and seasonal precipitation fields. The CaPA grid at the CDCD

station location is determined using latitude/longitude coordinates of the station, and the seasonal precipitation at that grid is extracted and averaged over entire study period.

4.3.2. Map to Map (M2M)

The M2M comparison is designed to directly analyze CaPA skills in representing spatial trends in precipitation, which is critical for use of CaPA as a hydrological forcing. M2M allows for the assessment of the distributed precipitation field by comparison to the standard WATFLOOD™ forcing (i.e., inverse distance weighted, IDW interpolations of CDCD station data). Traditional IDW methods do not include orographic effects on precipitation distribution, whereas CaPA does (through the GEM model background field). In order to conduct a fair comparison between CaPA and interpolated CDCD station data, lapse rate functions were incorporated to the IDW interpolation method for a secondary M2M analysis.

Interpolation of observation data

CDCD stations are interpolated using the ragmet.exe pre-processing utility program of WATFLOOD™. The IDW method assigns four quadrants per grid, centered at the midpoint of each grid. Closest climate gauges to each quadrant are weighted against the distance to the midpoint and precipitation is geometrically averaged among all four quadrants to produce the precipitation estimate for the grid. Observation stations are assigned a common radius of influence and smoothing coefficients. A radius of influence is used to determine how far a station's precipitation information spreads. For example, if a radius of influence of 50km is assigned to a station and the station receives 10mm of rainfall, this 10mm of rainfall will then be distributed across a 50km radius from the

station. The further the location is from the stations, the less precipitation it will receive. The IDW method is commonly known to smooth the resulting interpolated precipitation field, effectively dampening the magnitude of extreme events. Although the IDW method is a simple interpolation method that does not hold any physical-basis, it enables large amounts of data for long time periods to be effectively distributed for hydrological modeling purposes (Pietroniro *et al.*, 1996). For this study, a revised version of the IDW method was created by adapting the current method to incorporate orographic effects on precipitation via a lapse rate function for a more direct comparison to CaPA.

The lapse rate function utilizes the local maximum elevation and the given station elevation to interpolate and adjust gridded (interpolated) precipitation estimations. Observed precipitation is first interpolated back to sea level, according to a lapse rate (mm/m). Precipitation estimates at adjacent grids are then calculated using the same lapse rate, and the maximum grid elevation. Table 3 provides the lapse rate, radius of influence and smoothing distance used for each sub-basin in this study for reference. All radius of influence values and some of the lapse rate values (SAS, WPR, and WPL) are obtained through calibration outside of this study period. If the lapse rate is not obtained through calibration, a default value (0.001) representing the average of all lapse rate values is assigned. The difference in the lapse rate used for a basin introduces uncertainties into subsequent analyses using interpolations with lapse rate functionality. The interpolated precipitation is more sensitive to lapse rate if the orographic changes are significant (i.e. only the Saskatchewan River in this study), while for basins such as the Red River basin, the effect of the lapse rate parameter is not as significant due to its flatter surface.

The radiuses of influence values were obtained through calibration as well, however, the density of gauges also affect the radius of influence. For example, sparse station network in the Churchill River Basin, a higher value for the radius of influence is used to ensure that the entire watershed area is included in the interpolated station data field.

Table 3: RAGMET radius of influence and lapse rates used for each sub-basin.

	ASI	**CHU**	**NEL**	**RED**	**SAS**	**WPL**	**WPR**
Lapse rate (mm/1m)	0.001	0.001	0.001	0.001	0.0004	0.001504	0.002758
Radius of influence (km)	300	600	280	300	300	250	300
Smoothing distance (m)	35	50	55	50	35	53	35

For the M2M analysis, stations with missing data are incorporated: ragmet temporarily discards stations with missing data, and includes these stations when records are available. The interpolated precipitation field is therefore not entirely the same as that used in the P2P analysis, but includes more (all available) stations over the study period. Figure 10 shows the stations used in P2P versus M2M analyses, indicating that stations used in the M2M analysis significantly out-number the stations used in P2P.

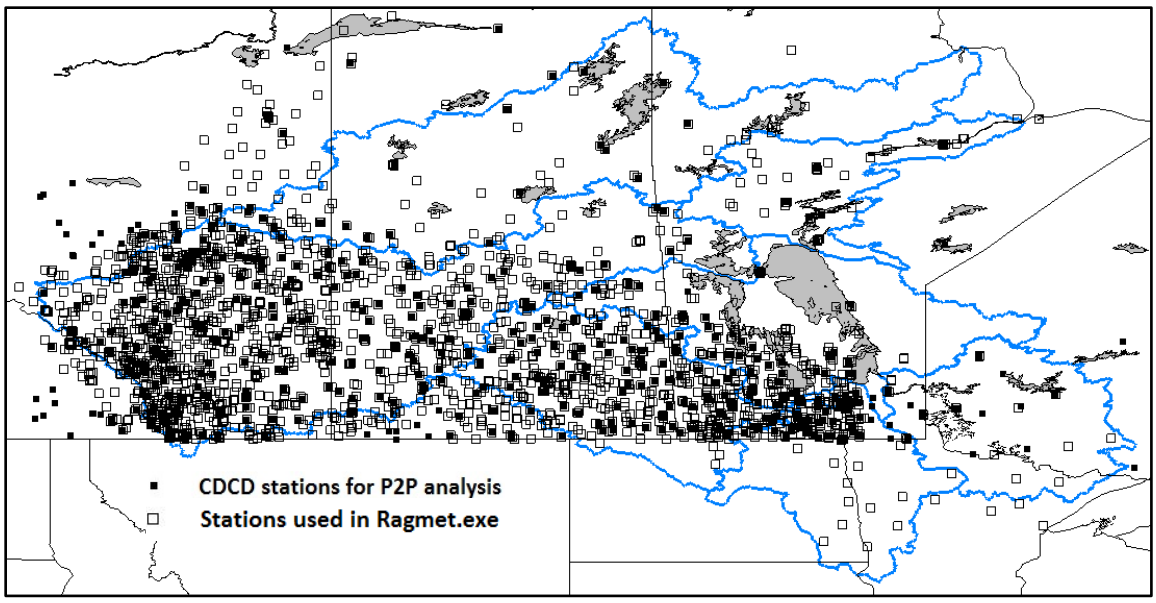

Figure 10 : Stations used by ragmet for the M2M comparison (all available stations) versus stations used in P2P analysis (containing no missing data).

In the US portion of the study area, the USHCN data are used instead of the denser Cooperative network due to discontinuity across the border, evident particularly winter after interpolation. Figure 11 shows average winter precipitation (in mm) across the Red River basin interpolated from the US Cooperative network station data. A clear divide is visible at the Canada-US border, where the transition from US Coop stations to CDCD stations occurs. The interpolated cooperative network data underestimates precipitation for the majority of the US portion of the Red River basin, which is likely caused by wind under-catch errors at the cooperative stations (i.e., uncorrected observations). The cooperative network data was therefore not used in this study.

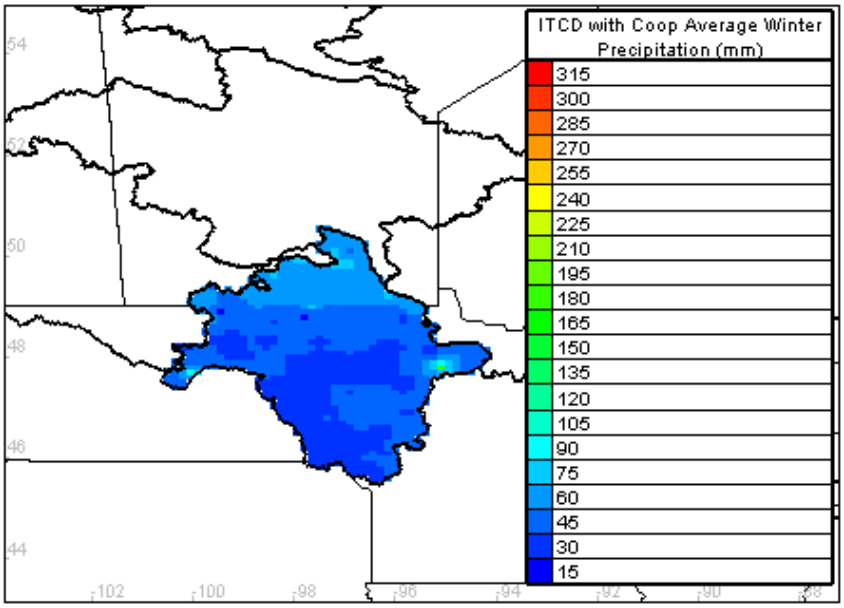

Figure 11: Average winter precipitation (mm) from ITCD interpolated Cooperative network stations

Anomaly calculation

For the M2M comparison, anomalies are calculated in the form of relative difference between each grid from the interpolated CDCD precipitation map and CaPA precipitation map. The equation for calculating the anomaly is shown below (Equation 1), assuming CDCD data to be "truth":

$$\textbf{Anomaly} = \frac{\textbf{CaPA}-\textbf{CDCD}}{\textbf{CDCD}} * \textbf{100} \qquad (1)$$

Daily CaPA and CDCD data are first accumulated to seasonal summations for every year, and are then further averaged over entire study period from 2002 to 2005.

M2M analyses evaluate CaPA data on an areal basis to quantify spatial differences between CaPA and interpolated CDCD precipitation. The precipitation map represented by the IDW interpolated CDCD precipitation field is assumed to be ground-truth because it represents the precipitation forcing used for model calibration (i.e., the standard input),

however it should be noted that it is not necessarily more accurate. Problems with the IDW method include smoothing of more extreme precipitation values and variable spatial distributions (i.e., convective storm cells), and decreased accuracy in watersheds where gauges are sparse or are un-evenly distributed (such as in the CHU and WPL watersheds). The objective of the M2M analysis is to examine the differences between CaPA and CDCD, rather than a true validation against a known, true value (as one does not exist for spatially distributed precipitation values). Since spatially interpolated precipitation is required for WATFLOOD™ forcing, the M2M analysis also provides a direct comparison of forcing data products prior to hydrological simulation and output analysis (Section 4.4).

4.4. Indirect Proxy Validation of CaPA

Owing to the fact that true (spatially distributed) precipitation fields are difficult (if not impossible) to obtain given poor climate station density in northern Canada, hydrometric station records can assist in the validation of precipitation products through proxy validation measures (Klyszejko, 2007).

Proxy validation is conducted by forcing WATFLOOD™ using both interpolated CDCD and CaPA precipitation fields to simulate streamflow response. Simulations using both precipitation forcing can then be quantified relative to observed flow, and the difference between CaPA and CDCD simulations quantified using statistical scores for hydrological model evaluation. As previously mentioned though, if CDCD station density is too sparse, this will result in erroneous interpolation of CDCD precipitation, hence the validation is meaningless. The ideal test basin for proxy validation therefore needs to have adequate density of precipitation observation stations, a gauged outflow

(representing cumulative runoff across the basin), and a fully calibrated hydrologic model. Both Lake Winnipeg Basin (WPL) and Winnipeg River Basin (WPR) meet these criteria, and are both of interest to Manitoba Hydro due to their significant influence on, or contribution to hydroelectric generation. Furthermore, as shown previously on Figure 8, the Lake Winnipeg Basin has significant differences in the density of assimilated stations to the west versus east sides of the watershed, as well as north and south sides of watershed. This makes for a good testing ground to observe the impact of assimilated stations on CaPA's quality. An analysis performed by Schellenberg (2013) and supervised by the author was also performed on the Churchill (CHU) basin, highlighting the need for improved hydrologic calibration, and is discussed in Section 5.5.

Three modeling statistics were used to evaluate proxy validation simulations. Percentage volume deviation (D_v) is used to evaluate the simulation in terms of volume. It is calculated from Equation 2 below (Stadnyk-Falcone, 2008):

$$D_v = \frac{\sum_{i=1}^{n}(S_i - O_i)}{\sum_{i=1}^{n} O_i} \qquad (2)$$

where O and S are observed and simulated values, respectively. D_v represents the percent difference in volume between simulated runoff and observed hydrograph. A score of 0 is perfect, representing no volume difference over the period of simulation. A positive value represents an over-estimation of volume, with a negative representing under-estimation. It does not, however, consider timing of the volume change or errors in timing of peak flow, thus in addition to the Dv score; both R^2 and Nash scores were also included.

R^2 is also called the coefficient of determination and it is calculated using Equation 3 shown below (Krause *et al.*, 2005):

$$R^2 = \left(\frac{\sum_{i=1}^{n}(O_i-\bar{O})(S_i-\bar{S})}{\sqrt{\sum_{i=1}^{n}(O_i-\bar{O})^2}\sqrt{\sum_{i=1}^{n}(S_i-\bar{S})^2}}\right)^2 \qquad (3)$$

It ranges from 0 to 1 with 0 being no correlation between timing and 1 meaning perfect timing match. R^2 can't be used alone because if a simulation systematically over- or under-estimates rising and falling limbs, it can still achieve very high R^2 value.

The Nash-Sutcliffe statistic (E), on the other hand, is a hydrological simulation score that evaluates both volume and timing of a simulation against the observed hydrograph. It is calculated using Equation 4 shown below:

$$E = 1 - \frac{\sum_{1=1}^{n}(O_i-S_i)^2}{\sum_{i=1}^{n}(O_i-\bar{O})^2} \qquad (4)$$

A score ranging from -1 to 1 is assigned to each simulation, with a score of one indicating the best fit between the simulation and observed hydrograph. Any score smaller than zero suggests that the simulation is an inferior representation of the observed hydrograph relative to the long-term observed mean. The Nash statistic places emphasis on peak flows, making it suitable for assessing extreme precipitation events.

4.4.1. Current WATFLOOD™ model setup

WATFLOOD™ models of the WPL and the WPR basins were previously established by Manitoba Hydro and calibrated from CDCD and Adjusted and Homogenized Canadian Climate Data (AHCCD) respectively for time periods outside of the 2002-2005 study periods. AHCCD is based on the climate data from the National Climate Data Archive. It has improved solid precipitation measurements as well as trace precipitation records that have been quality controlled and corrected (Mekis, 2011).

Both watersheds were setup using Digital Elevation Models (DEM) and landcover data obtained from varies sources such as GeoBase (Geobase, 2003) and Land Information Ontario (LIO). DEM and landcover data on the US side of the WPR was obtained from USGS (USGS, 2012). The spatial resolution of the DEM data used was 0.75 arc seconds, which is sufficient to generate accurate water pathways, drainage directions and delineations for hydrological modeling purposes (Charrier and Li, 2012). Both DEM and landcover data were processed using GreenKenue™ (National Research Council Canada, 2012) to create WATFLOOD™ watershed files (Kouwen, 2012). WPR and WPL basins both have complex, yet distinctive hydrographic features as discussed previously in Section 3.2. Figure 12a and Figure 12b show the delineated watershed boundaries (outlined in black), sub-basin delineations, hydrometric station locations, reservoir locations, and reservoir inflow observation locations for the WPL and WPR basins, respectively.

At the center of the WPL basin (Figure 12a) lay two of the largest lakes in Manitoba: Lake Manitoba to the west, and Lake Winnipeg to the east. The western portion of the watershed (Boreal Plain ecozone) flows eastward into Lake Manitoba, while the eastern portion (Boreal Forest ecozone) flows westward into Lake Winnipeg. The WPL basin receives direct inflow from several major river basins including the Red, Assiniboine, Saskatchewan, and Winnipeg Rivers.

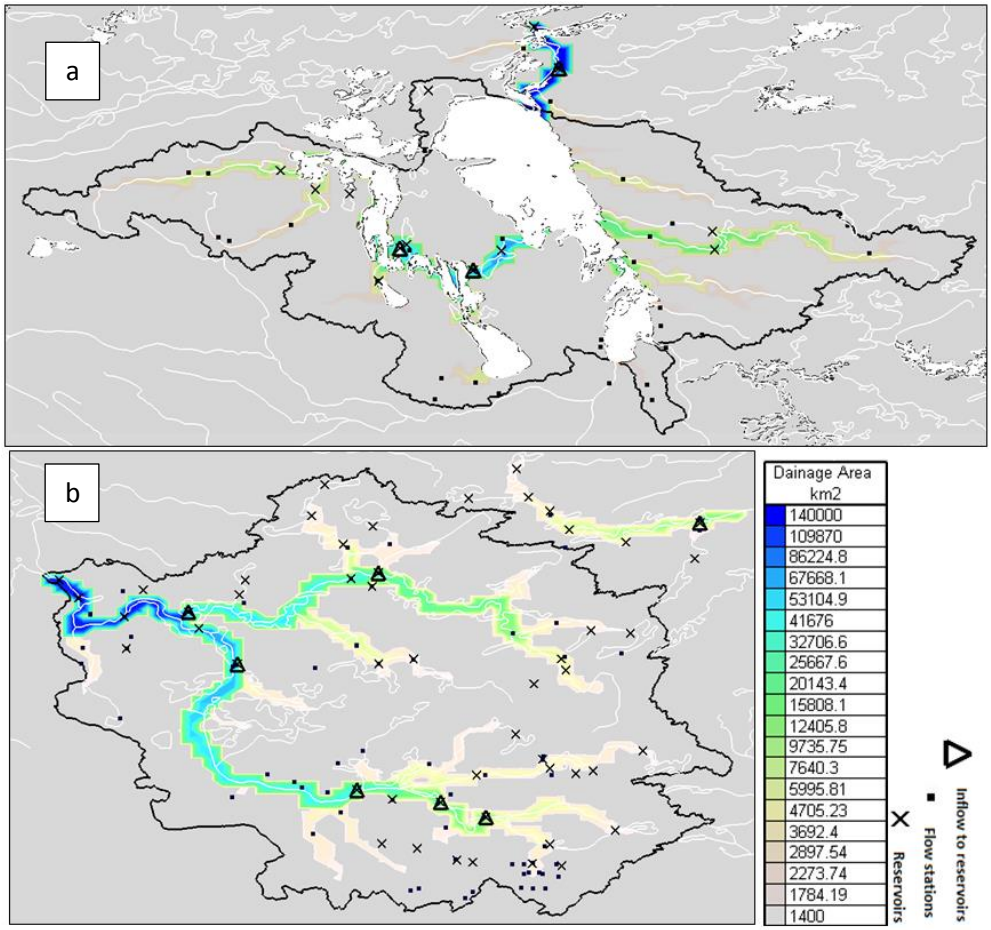

Figure 12: Current WATFLOOD™ watershed setups for the (a) Lake Winnipeg and (b) Winnipeg River basins showing main drainage network, reservoir locations, and hydrometric station locations

A portion of the Assiniboine River (typically during spring freshet) contributes to the WPL basin through the Portage la Prairie diversion (Province of Manitoba, 2013). The outlet of the WPL basin exists at the northern end of Lake Winnipeg, draining into the Nelson River and lower Nelson River Basin (LNRB). There are eight reservoirs in the existing model setup; each of the reservoirs is controlled by a programmed storage-release function based on current operating rules.

Due to large volume of inflow from adjacent watersheds and large storage capacity of Lake Winnipeg, runoff at the outlet of the WPL basin is heavily regulated and inflow

dominated; de-coupling the rainfall-runoff response. The WATFLOOD™ model nudges flow (to the observed record) at each upstream sub-basin inflow point, and the remaining contributing area of the WPL basin itself is much smaller than the sum of the upstream contributing areas. This results in little variation in the hydrograph within the basin itself.

The Winnipeg River is located in the Canadian Shield region and is covered with predominately by Boreal Forest. Surface depressions extruding from underlying geological formations form numerous lakes and rivers in different shapes and sizes, hence becoming impractical to simulate every single lake in this watershed. Fifty-one distinct lakes and reservoirs are setup in the existing watershed model, many of these having regulated outflows. If available, WATFLOOD™ uses initial lake levels as input to initialize lake storage. Using calibrated storage-discharge relationships that are specified for each reservoir, WATFLOOD™ then routes lake inflows downstream. The inflow is either taken as the summation of inflow from previous grids or as user-defined input. Simulated inflow and outflow were plotted against measured inflow and outflow for comparison at seven lakes where observations of lake level were available. Regulation has a significant impact on the model behavior as discussed in section 4.4.3. Furthermore, the Lake St. Joseph outside the natural boundary of Winnipeg River also diverts flow to Winnipeg River basin and this diversion is setup in WATFLOOD™ model.

4.4.2. Lake Winnipeg WATFLOOD™ Setup

Twenty landcover classes are included in the WPL basin WATFLOOD™ model, harmonized from over 100 classes in the original landcover dataset. The main land cover types are listed in Appendix A (Figure A-1). The eastern versus western portions of the

basin show very different dominate landcover types: *'Mixed forest'* being the most common on the western side, interspersed with some agriculture and grassland; and Boreal forest (i.e., '*Coniferous*') dominating the eastern half, along with significant wetland and shrub coverage in low-lying regions (Figure 13). Figure 13 summarizes the major landcovers dominating the WPL basin.

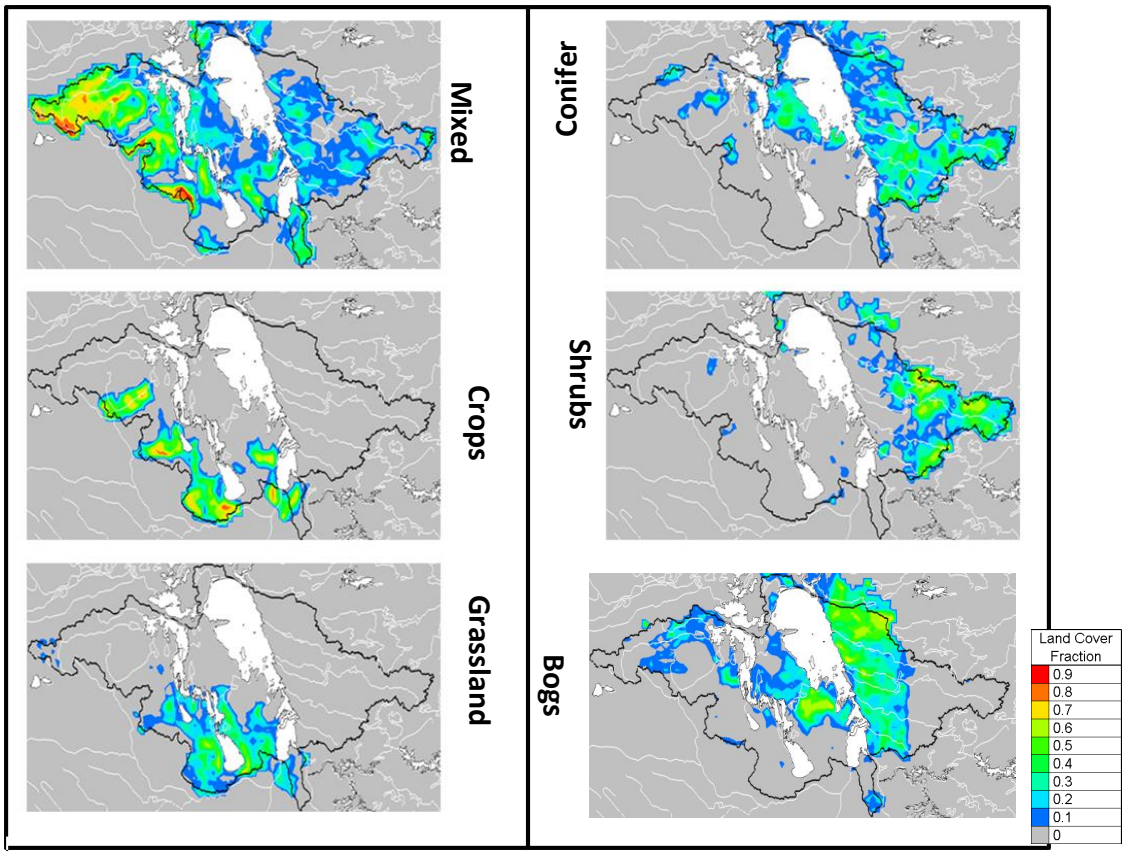

Figure 13: Landcover distribution for the WPL basin WATFLOOD™ model

Different hydrological responses from different land cover types will directly influence the shape of the hydrograph (and model calibration) generated by a hydrologic model. Sub-basins located along the south-western half of the Winnipeg Lake watershed generate more flashy hydrographs due to quick drainage in agriculture zones. One example of such a quick response is shown in Figure 14:

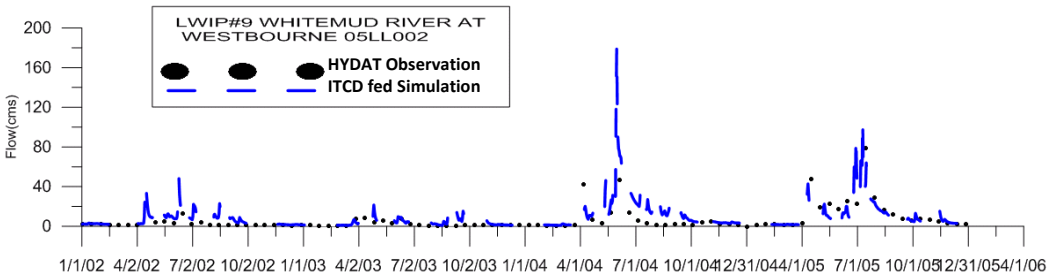

Figure 14: WATFLOOD simulated hydrograph using CDCD (dashed blue line) compared with observed streamflow (black dots) at station 05LL002: Whitemud River at Westbourne.

The black dots represent observed flow measured by Water Survey of Canada; with the blue line representing the hydrograph simulated using interpolated CDCD stations as model forcing. Contrast that to the eastern portion of the Lake Winnipeg basin however, where the hydrograph is less spiky and rainfall-runoff responses are more damped (Figure 15).

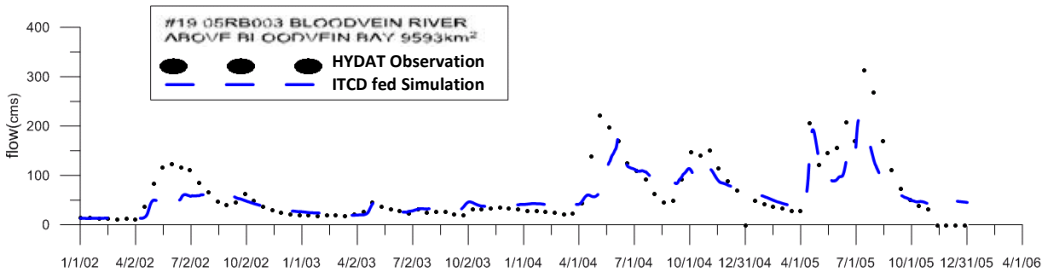

Figure 15: WATFLOOD simulated hydrograph using CDCD (dashed blue line) compared with observed streamflow (black dots) at station 05LE011: Maloneck Creek near Pelly.

One reason for the difference in the characteristic runoff responses is attributed to wetlands and baseflow. The ice-on winter low flows (i.e., baseflows) in the western part of the WPL basin is higher than those in the eastern portion of the watershed. This is likely due to higher percentage of wetlands in the western watersheds. Wetlands retain water during wet seasons, thus reducing the summer peak and gradually releasing water

during drier seasons, hence increasing sustained baseflow during winter months due to under-ice connectivity.

The above hydrographs offer an example of WATFLOOD^{TM} simulations in two WPL sub-basins with contrasting dominant landcover types. WATFLOOD^{TM} was calibrated from 1985 to 1995 and scored 0.89 in Nash , 0.91 in R^2 with a total volume difference with observed hydrograph of -5.1% at the Lake Winnipeg outlet. The above hydrograph analyses and calibration statistics suggest that WATFLOOD^{TM} is sufficiently calibrated for proxy validation of CaPA, and is able to capture different hydrological responses in different regions in response to different landcover typology.

4.4.3. Winnipeg River WATFLOOD^{TM} Setup

Landcover data at the Winnipeg River basin were collected from Canada as well as the United States, and harmonized to ensure similar landcover types via the two classification systems in Canada and the US. The main land cover types are listed in Appendix A, figure A-2. The majority of the forest canopy over the WPR basin consists of coniferous and deciduous mixed forest. A notable fraction of wetlands in the form of bogs around the many small lakes and ponds also exists (Figure 16).

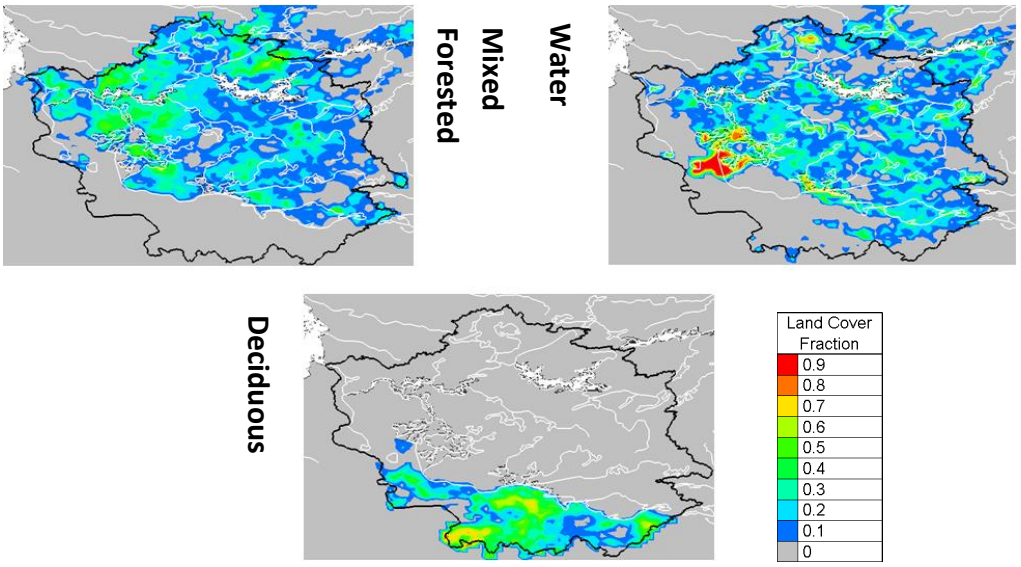

Figure 16: Dominant landcover distribution for the WPR basin WATFLOOD™ model.

The following two figures demonstrate the difference between natural, unregulated flows and regulated flow hydrographs in the Winnipeg River Basin (Figure 17 and Figure 18).

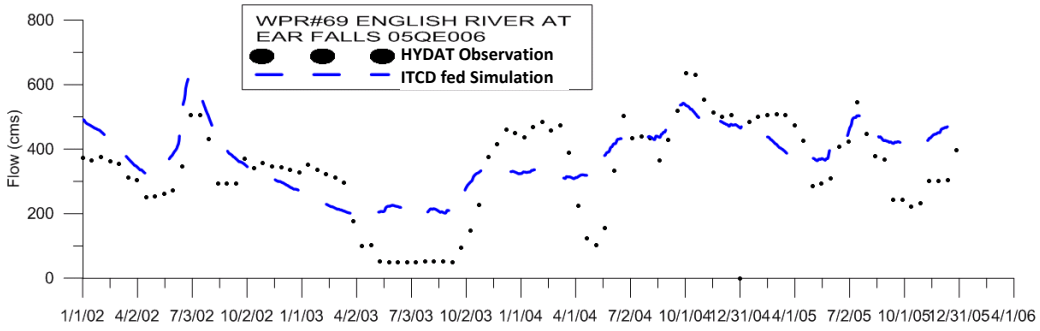

Figure 17: WATFLOOD simulated hydrograph using CDCD (dashed blue line) compared with observed, regulated streamflow (black dots) at station 05QE006: English river at Ear Fall.

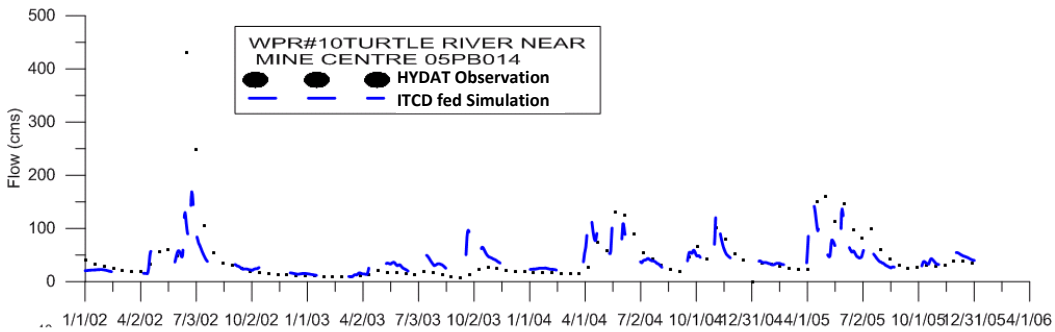

Figure 18: WATFLOOD simulated hydrograph using CDCD (dashed blue line) compared with observed, natural streamflow (black dots) at station 05PB014: Turtle River near Mine Center

Figure 17 shows the outflow from the regulated English River sub-basin of the WPR basin, while Figure 18 shows an example of a typical sub-basin that generates naturalized, unregulated flow. WATFLOOD™ simulations capture the observed streamflow relatively well without any calibration at the natural flow stations. However, the simulated hydrograph at the controlled outflow station (Figure 17) does not show a distinct rainfall-runoff response because runoff is regulated according to downstream needs. Modeling regulated river flows requires knowledge of the control structures rules of operation and inflow generated from the upstream watershed. It is not expected that CaPA will outperform CDCD (or any other precipitation forcing) at such regulated stations, yet the difference between CDCD and CaPA is still meaningful. It should be noted that all the initial lake levels and storage release functions are kept the same regardless of forcing data used to eliminate uncertainties in model setup. More implications on the effect of regulation on proxy analysis are discussed in Section 5.4.

The above comparison shows an example comparing WATFLOOD™ simulations for regulated versus natural outflows in the WPR basin. Calibration was performed from 1985 to 1995 and validated from 1960-2005, with WATFLOOD™ scoring 0.42 in Nash,

0.51 in R^2 and a total volume difference from the observed hydrograph of 2.2% at the outlet of the Winnipeg River basin for calibration. The calibration of WPR basin mainly focused on volume because the calibrated model was originally intended to use in a climate change study. The calibration statistic suggests that the model is sufficiently calibrated for proxy validation, and is capable of simulating both regulated and unregulated sub-basin flows.

4.5. Summary

In summary, the methodology used in this research, to assess the quality of CaPA for hydrological modeling applications, can be broken down into three main steps: 1) P2P where CaPA precipitation is directly compared to point observation data, assuming the observations are ground-truth, and using empirical QQ plots and K-S tests to compare the two data sets; 2) M2M compares CaPA precipitation fields with interpolated observed precipitation (ITCD) across an area domain by calculating anomalies, with the anomalies then being related to local basin characteristics; and 3) proxy validation via streamflow records where CaPA-fed WATFLOOD^{TM} simulations are compared with ITCD-fed WATFLOOD^{TM} simulations and assessed via three statistical scores: Nash, R^2 and D_v.

Chapter 5. Results and Discussions

This chapter discusses the results obtained by applying the validation methods discussed in Chapter 4. Results throughout the three step methodology are analyzed, through which the underlying significance of the results is then interpreted and supported with evidence. Limitations in the interpretations are also presented.

5.1. P2P Comparison

The P2P analysis compares observed station precipitation to the CaPA grid where the station is located. Observation stations are grouped into to sub-basins, and an empirical QQ plot is made for each sub-basin to form a summary plot, as shown on Figure 19. The seasonal QQ plots for each sub-basin are all shown in Appendix B. Average seasonal precipitation is indicated by cross-hairs in different colors: Spring (MAM) is blue; Summer (JJA) is green, Fall (SON) is red, and Winter (DJF) is cyan.

The majority of the sub-basins share a characteristic under-estimation of **summer** precipitation, with the exception of summer precipitation in the CHU basin which is relatively close to that of the CDCD observation records. This is in agreement with the bias under continuous test category from Davison et al. (In preparation) where CaPA was shown to have large negative bias during summer and early fall. It is interesting to note that, from Figure 8 the majority of the observation stations in the CHU basin were assimilated by CaPA (unlike many of the other basins) and could contribute to the similarity seen on Figure 19. However, Kochtubajda *et al.* (in preparation) conducted a study on the contributions of thunderstorm rainfall to warm season precipitation across the Prairies. It was found that the summer precipitation at Canadian Prairies could make up to 60 to 70% of total annual precipitation and the thunderstorm rain accounts for at

least 40% of the July precipitation over 50% of the area where agriculture landcover dominates. Therefore, summer precipitation in most of the sub-basins is convective storm-dominant; especially at higher magnitude events. Scattering of higher magnitude events also suggests differences between CaPA and CDCD records regarding the summer precipitation events. Furthermore, Davison et al. (In preparation) suggest the innovation back transformation leads to underestimation of higher intensity precipitations. Therefore it seems that CaPA appears to have difficulty in correctly simulating higher magnitude events such as convective storm precipitations. Although convective precipitation events are small-scale for each individual event, they are never-the-less widely scattered and prevalent over a large spatial domain. P2P comparison assesses CaPA at observation points alone; spatial characteristics of the anomalies will require further comparison via the M2M methodology.

During **winter**, CaPA precipitation exceeds CDCD observations in all sub-basins with the exception of the occasional outlier (Figure 19). CaPA shows more precipitation than CDCD during winter overall, which is expected since the CDCD observations are known to under-catch solid precipitation, particularly in windy conditions common to the Prairie watersheds (Goodison *et al.*, 1998). Meanwhile, moderate scattering of the QQ plot occurs around the lower bin precipitation range, common to winter precipitation events. Errors in solid precipitation measurement often increase the variation of precipitation records among stations due to widely varied amounts of under-catch and unknown correction factors.

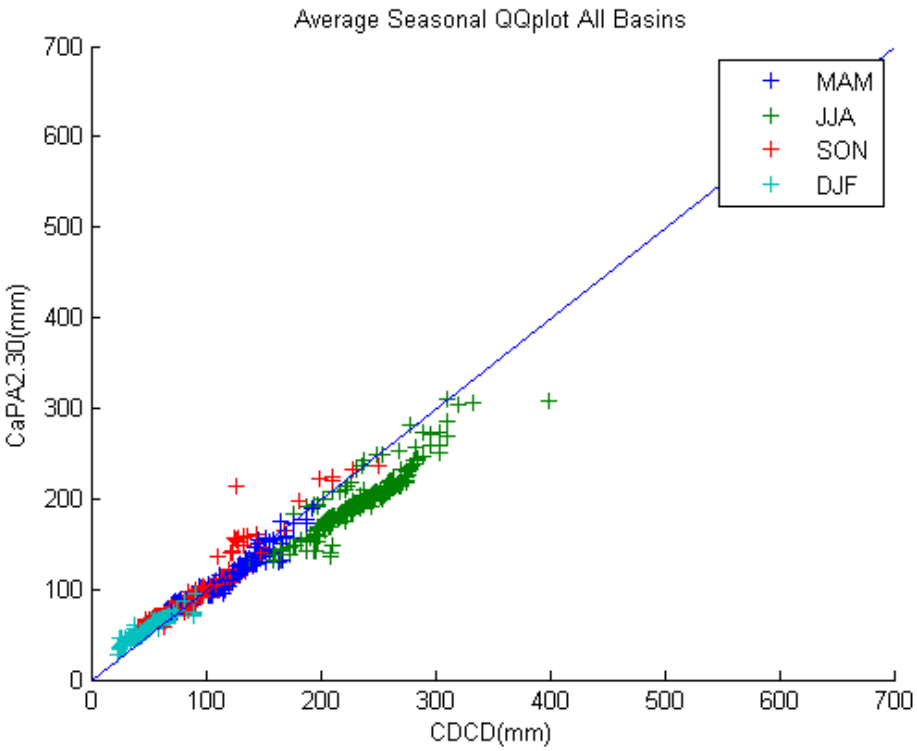

Figure 19: Average seasonal QQ plot for all seven sub-basins.

CaPA precipitation background (i.e., GEM) does not suffer from under-catch error, and the observations assimilated into CaPA that are potentially afflicted by wind under-catch are eliminated during the QC process. Therefore the agreement between CaPA and CDCD observations shown on Figure 19, along with decreased variability (scatter) in winter precipitation should be further investigated.

Fall precipitation covers the widest range of event magnitude (41mm to 250mm); with the QQ plot separating into three segments around the median (~150 mm). The first segment of the fall QQ plot includes the smaller magnitude events and starts above the 1:1 line, gradually sloping downward until it's below the 1:1 line; indicating different precipitation distributions between CaPA and CDCD. The second segment of the fall QQ plot appears to remain below the 1:1 line, but at a constant offset (parallel to 1:1 line); indicating similar distributions with different means. The third segment starts with a

rapid increase in CaPA precipitation (relative to CDCD), and gradually decreasing and undulating about the 1:1 line at notable magnitudes. The angulation and segmented distribution makes the fall precipitation QQ plot the most un-linear pattern among all seasons, suggesting that fall precipitation varies significantly relative to CDCD observed precipitation records; and that some of these differences are spatially correlated as shown on Figure 20. The difference between CDCD and CaPA precipitation, unlike the constant differences in summer and winter, are spatially localized hence the magnitude of difference varies greatly at different locations. In the Lake Winnipeg (WPL) basin, for example CaPA precipitation greatly exceeds CDCD compared to any other watershed, but this is the result of one particular 'anomalous' point. Figure 20 shows that some basins follow the s-shaped patterning about the 1:1 line (RED, ASI, SAS, WPR), whereas others do not (CHU, NEL, WPL). The increased spatial variability between CaPA and CDCD precipitation during the fall is not surprising given the size of the study domain and that fall marks the transition from a summer to winter climate. Possible causes of these localized events include large frontal precipitation events caused by the collision of cold and warm air masses, widely varied fall convective storms and possibly, the lake affected precipitation events initiated by intense periods of evaporation. It appears that the more northern the basin, the more agreement there is between CaPA and CDCD.

During **spring**, precipitation lies from the small to middle range on QQ plot. Spring precipitation at the lower range lays above the 1:1 line, similar to that of the winter precipitation. From the middle range; spring precipitation follows the 1:1 line more closely (Figure 19).

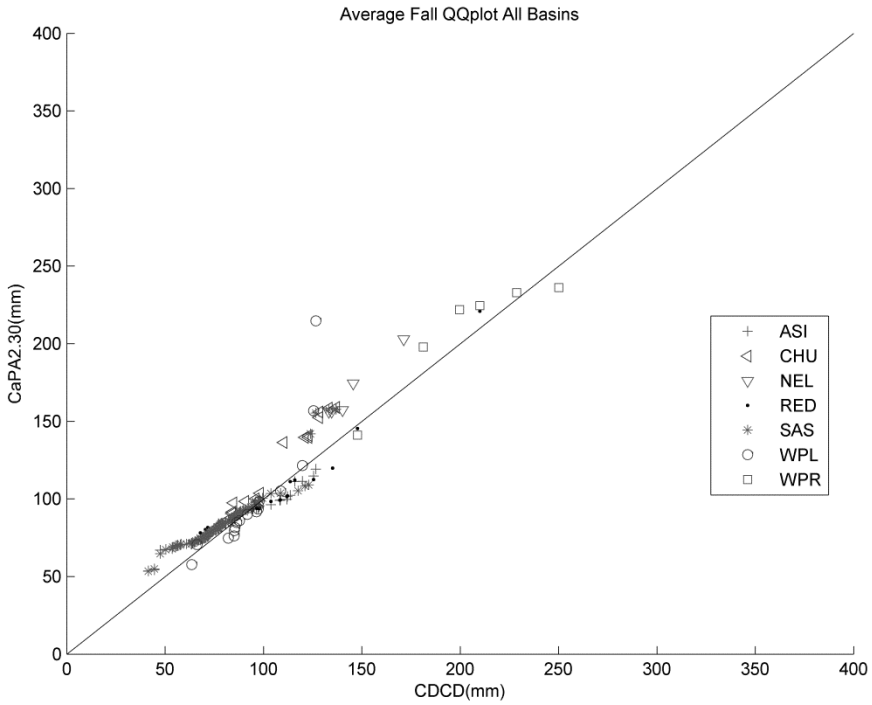

Figure 20: Average QQ plot for the fall season (SON) across all basins.

The difference between the lower and middle range spring precipitation could be due to the wind under-catch errors noted for solid precipitation events that carry over into spring. Mid-spring marks the end of solid precipitation events, and therefore more continuity between CDCD and CaPA, for middle to higher magnitude (i.e., likely liquid) precipitation events.

These findings regarding CaPA and CDCD are not valid across the entire study domain, but rather only at the points where stations exist for comparison. Comparison of precipitation on an aerial basis will be conducted in the M2M analysis, summarized in Sections 5.2 and 5.3. Furthermore, QQ plots do not quantify the exact differences between the two precipitation products; conclusions are drawn from visual inspections, and statistical methods like the Kolmogorov–Smirnov (K-S) tests that can be deployed to determine whether the difference between CDCD and CaPA precipitation distributions are significant.

Kolmogorov–Smirnov (K-S) tests determine the statistical significance of spatial and temporal distribution differences between CaPA and CDCD seasonally-averaged precipitation for each sub-basin (Justel, 1997). The test does not require an assumed distribution of the dataset and emphasizes the similarity of the two datasets distributions. The overall distribution of seasonally averaged precipitation is considered to be more important for hydrological modeling purposes than whether or not the exact amount of precipitation is simulated by CaPA relative to observations at any one time. Verifying distributions and seasonal averages also reduces the effects of station representativeness errors. The maximum difference between two sample cumulative distribution curves is used to compute the p-value. KS tests used here quantify the differences between CDCD and CaPA data from the QQ plots, with tests based on three hypotheses with 95% confidence level. The three null hypotheses are: 'unequal', which hypothesizes CaPA and CDCD are unequal; 'smaller' that hypothesizes CaPA is smaller than CDCD; and 'larger' that hypothesizes CaPA is larger than CDCD. If the alternative null hypothesis is rejected at 95% confidence, test scores equal '1' (versus '0' if it is not rejected). Furthermore, a paired Wilson-Cox test is also conducted due to the nature of the two datasets. The following table (Table 4) summarizes the K-S test scores for all sub-basins under the three hypotheses and WC test scores.

Table 4: K-S test results based on the 95% confidence level and three null hypotheses: unequal, smaller and larger and paired Wilson-Cox test results based on the 95% confidence

K-S-test 95% confidence				
	MAM	**JJA**	**SON**	**DJF**
UNEQUAL				
ASI	0	1	0	1
CHU	1	0	0	0
NEL	0	0	1	0
RED	0	1	0	1
SAS	1	1	1	1
WPL	0	1	0	1
WPR	0	0	0	0
SMALLER				
ASI	0	1	0	0
CHU	0	0	0	0
NEL	0	0	0	0
RED	0	1	0	0
SAS	1	1	0	0
WPL	1	1	0	0
WPR	0	1	0	0
LARGER				
ASI	0	0	0	1
CHU	1	0	1	0
NEL	0	0	1	0
RED	0	0	0	1
SAS	0	0	1	1
WPL	0	0	0	1
WPR	0	0	0	1
Wilson-cox test 95% confidence (Unequal)				
ASI	0	1	0	1
CHU	0	0	0	0
NEL	0	0	1	0
RED	0	1	0	1
SAS	0	1	1	1
WPL	0	1	0	1
WPR	0	0	0	0

During both summer and winter, most of the basins score 1 under the 'unequal' hypothesis suggesting that CDCD and CaPA have more significant differences during summer and winter than during other seasons. The only exceptions are the CHU, WPR, and NEL basins where the number of stations assimilated by CaPA is most equal to the observation stations used in the P2P analysis (as CDCD). Scores of 'smaller' and 'larger'

hypothesis tests further reveal that CaPA estimates less precipitation than CDCD in summer and more than CDCD in winter for sub-basins where CaPA and CDCD are different. Being a paired test, the Wilson-Cox test is expected to be more sensitive than K-S tests for distributions that are similar. However, only two test results differ (during winter when annual minimum precipitation occurs) and otherwise the results are the same as the K-S test results during other seasons. The CHU and SAS basins in winter (MAM) are not significantly different according to the Wilson-Cox test, and any differences detected by the K-S test are attributed to the paired nature of the distributions. The test scores confirm the QQ plot results shown in Figure 19 in terms of statistical significance.

Breaking the entire domain into sub-basins during the P2P analysis provides insights to the spatial patterning of differences between CDCD and CaPA precipitation. In order to evaluate the entire domain, simple statistics are calculated for stations for each season to assess trends and inter-annual variability over entire domain. Table 5 below shows statistics of precipitation averaged over all sub-basins for each season. Six simple statistics are presented: average, maximum, minimum, standard deviation, the coefficient of variance (COV) and Root Mean Square Error (RMSE) for both CDCD stations and the corresponding CaPA grid. Average precipitation is calculated as the average among all stations or CaPA grids during each season. Average precipitation in Table 5 provides an overall assessment of the magnitude of precipitation for each season. Similar to average precipitation, the minimum, maximum, standard deviation and COV are computed among all stations for each season, or CaPA grids. Unlike the P2P QQ plot where variations are depicted within each sub-basin, the standard deviation and COV calculated in Table 5 represent the spatial variation of precipitation over entire domain.

Furthermore, summer shows the highest RMSE, indicating that accuracy between the two estimates of precipitation is the worst in summer, reflecting CaPA's limited ability to accurately simulate high magnitude events.

Table 5: Seasonal statistics averaged over the entire study domain.

	MAM		**JJA**		**SON**		**DJF**	
	CDCD	CaPA	CDCD	CaPA	CDCD	CaPA	CDCD	CaPA
Mean (mm)	112	108	235	197	89.5	94.8	51.8	60
Max (mm)	193	189	400.0	310	250	236	91.6	95.1
Min (mm)	54.0	65.1	139	132	41.5	53.3	23	26.9
Std. Dev. (mm)	29.1	24.0	34.3	31.9	29.9	31.6	13.5	9.8
Coefficient of Variance (COV)	0.26	0.22	0.14	0.16	0.33	0.33	0.26	0.16
RMSE(mm)	16.8		52.2		13.4		12.3	

The statistics show that spring freshet (MAM) generally consists of medium precipitation magnitudes with moderate variation. Summer displays the highest average, maximum and minimum precipitation. Summer also has the largest standard deviation, yet the smallest coefficient of variance (COV). Since COV is calculated as normalized standard deviation against the average, the higher average precipitation of summer causes the COV to be smaller than other seasons despite the larger standard deviation. Furthermore, although at a smaller-scale, summer precipitation is highly variable due to prevalence of convective storms, thus across the entire study domain a smaller COV would be expected (although falsely representing the sub-basin scale). Meanwhile, fall shows a notably higher COV and standard deviation indicating the presence of localized precipitation variability, which will be further examined in Section 5.2.2.

Winter has the lowest mean, minimum and maximum precipitation, with CaPA exceeding CDCD observed precipitation. As previously mentioned, this is more than

likely the result of gauge under-catch errors in recordings of solid precipitation. Although the magnitude of gauge under-catch of winter solid precipitation is yet unknown, the higher precipitation in CaPA suggests that CaPA may be superior to CDCD during winter months. Furthermore, the effect of wind under-catch increases as wind speed increases thus, the poorest CDCD observations would be during the most severe winter snow storms when maximum snowfall is more likely to occur. The largest reduction in standard deviation also occurs during the winter, with the different variance of CaPA and CDCD explaining the scatter in winter precipitation from Figure 19. The high COV in CDCD winter measurement is due to the variance introduced by wind under-catch and measurement correction algorithms.

5.2. M2M comparison without lapse rate

P2P comparisons assess CaPA precipitation at selected observation station locations alone. It is important to understand the difference between interpolated CDCD (i.e., ITCD) and CaPA on an aerial basis to assess spatial formation and patterning of precipitation, and because WATFLOOD^{TM} requires distributed precipitation forcing (and therefore validation of the forcing data).

CDCD stations are distributed using a conventional method provided as a pre-processing module for WATFLOOD, called Ragmet. CDCD data are distributed across each watershed separately using the Inverse Distance Weighting (IDW) method both with and without the incorporation of a precipitation lapse rate function which mimics the effect of topography on precipitation formation (i.e., orographic effects). The seasonal average distributed CDCD (i.e., ITCD) with and without lapse rate, as well as the CaPA average seasonal precipitation are shown in Appendix C, Figures C-1 to C-3. The M2M analysis

then compares CaPA precipitation with the ITCD precipitation field. Anomalies between CaPA and CDCD are calculated at each grid using Equation 1. Figure 21 shows the anomaly map produced between CaPA and the ITCD precipitation field interpolated without a lapse rate function. Positive anomalies indicate that CaPA precipitation is greater than ITCD, and negative that CaPA is lower than ITCD.

The anomaly maps are discussed in Sections 5.2.1, 5.2.2 and 5.2.3 in order of seasons, consistent with the analyses from the P2P section. Furthermore, CDCD station observations are used for comparison to grids from the ITCD precipitation field where the station resides. QQ plots similar to those made for the previous P2P analyses are produced for each sub-basin in each season and are provided in Appendix B (Figure B-2). Figure 22 shows the summarized results across all basins, categorized by season.

Figure 22 provides insight on how much the interpolation procedure contributes to the anomaly shown on Figure 21. The QQ plot scatters around the 1:1 line during all the seasons, with no consistent under- or over-estimation found. This indicates that the interpolation procedure does not add any direct bias into the ITCD precipitation field, and that the anomaly map (Figure 21) is likely a representative comparison between CaPA and ITCD.

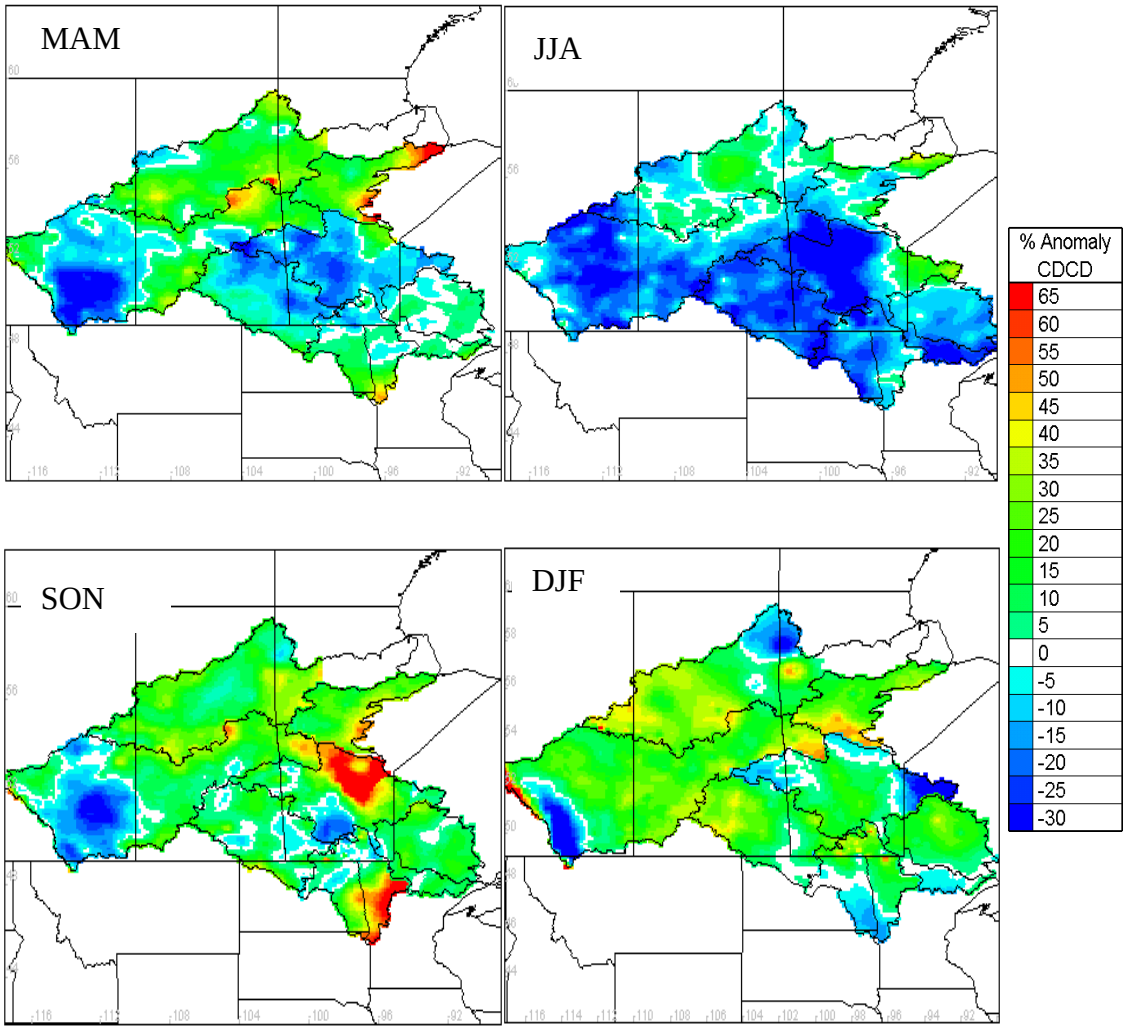

Figure 21: Seasonal anomaly maps computed between CaPA and interpolated CDCD without lapse rate.

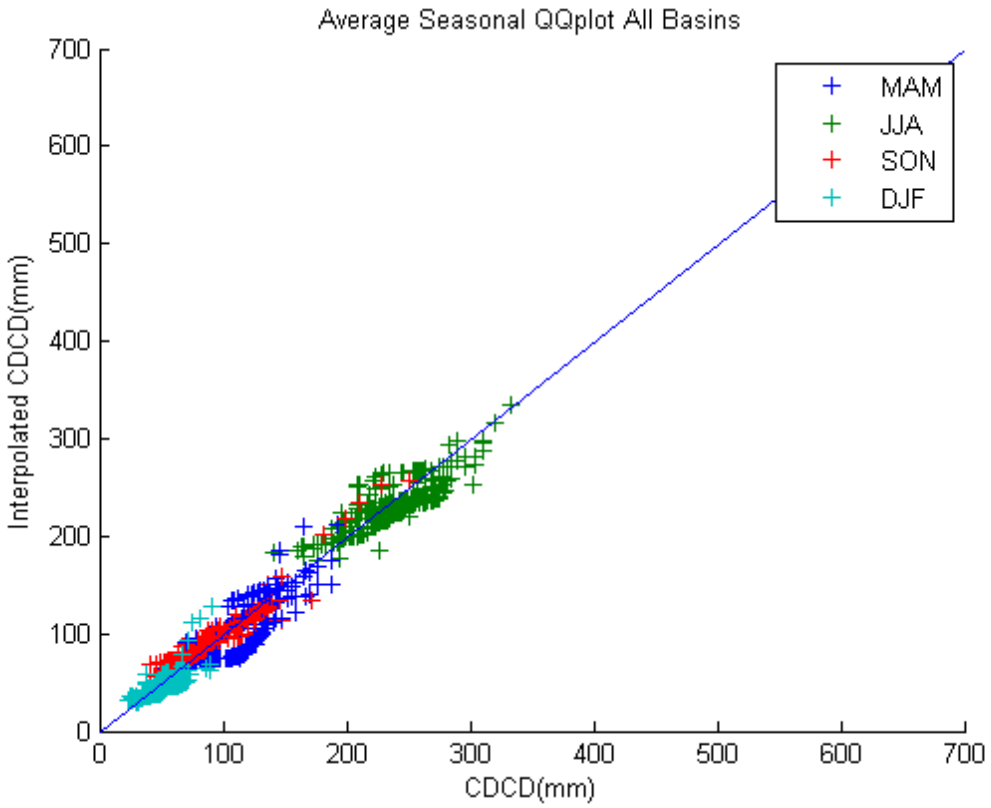

Figure 22: Average seasonal QQ plot for interpolated CDCD (ITCD) relative to CDCD observations across the study domain.

5.2.1. Summer Precipitation Anomaly

In summer (JJA), the anomaly map (Figure 21) shows that most of the study domain exhibits negative anomalies except for CHU and NEL basins, which were previously identified and attributed to (1) assimilation of the majority of observation stations into CaPA, and (2) convective storm precipitation. The eastern portion of the WPL basin shows an opposite trend in anomalies with the rest of the basins, which the P2P analysis failed to identify. P2P analysis relies on the number of observation stations, and Figure 8 shows few (to no) stations along the eastern portion of the WPL basin; thus the over-estimation was not previously captured. Although WPR basin's under-estimation is less acute than in other basins, interestingly the CHU, NEL, WPR and eastern side of the WPL basins all belong to the Boreal Forest ecological frame work as previously

discussed, thus connecting the spatial formation and distribution of summer precipitation directly to the ecological framework.

To further investigate the cause of the differences in summer precipitation anomaly, a study focused on relating the differences with the nature of the type of precipitation in summer was performed. One dominant precipitation feature during summer is thunderstorms, often occurring at a very high intensities but much more localized scales (usually less than 10km; Lackmann, 2011). Despite their smaller-scale, they are important since they comprise the majority of large precipitation events, and a significant portion of summer and annual total rainfall which results in late summer/early fall runoff across the study domain (Kochtubajda et al, 2012). Convective storms in summer are often hard to simulate in NWP models due to their small spatial size and dynamic mechanics (Lackmann, 2011). CaPAs background field, GEM, has a 15km horizontal resolution, therefore convective weather features are often not effectively simulated by GEM and hence not within CaPA either. This results in a lower total annual (and summer) precipitation in CaPA analyses than is recorded by CDCD station observations (assuming the observations captured the localized convective events to some degree as well); hence could be the reason for the negative anomaly during P2P and M2M analyses. The resulting negative bias will inevitably contribute to an under-estimation of streamflow simulated by WATFLOOD^{TM} (or other hydrological models) if CaPA is used as model forcing.

It therefore seems that the negative bias is, at least in part, related to the occurrence of convective storms, and that the bias should vary with the amount of convective storm activity in different regions. Kochtubajda et al. (in preparation) conducted a study on the

contributions of thunderstorm rainfall to warm season precipitation across the Prairies. The three Prairie Provinces in Canada (i.e., Alberta, Saskatchewan and Manitoba) are divided into two eco zones by land use: agriculture and Boreal as shown in Figure 23. Lightening hour data are also collected over the entire Canadian Prairies and is shown on Figure 24.

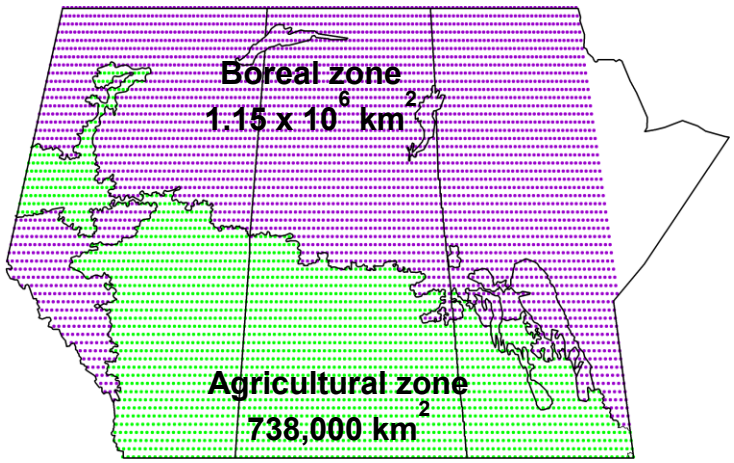

Figure 23: The agriculture and the boreal eco-zones defined by Kochtubajda *et al.* (in preparation).

A clear divide resides along the border of the boreal and agriculture eco-zones, with the agricultural zone having a higher occurrence of convective storm activity (i.e., higher number of lightning strikes) than the boreal zone. Numerous factors such as climatology and/or landcover type would lead to the differences between agriculture and boreal forest zones, with the actual dominant cause yet unknown.

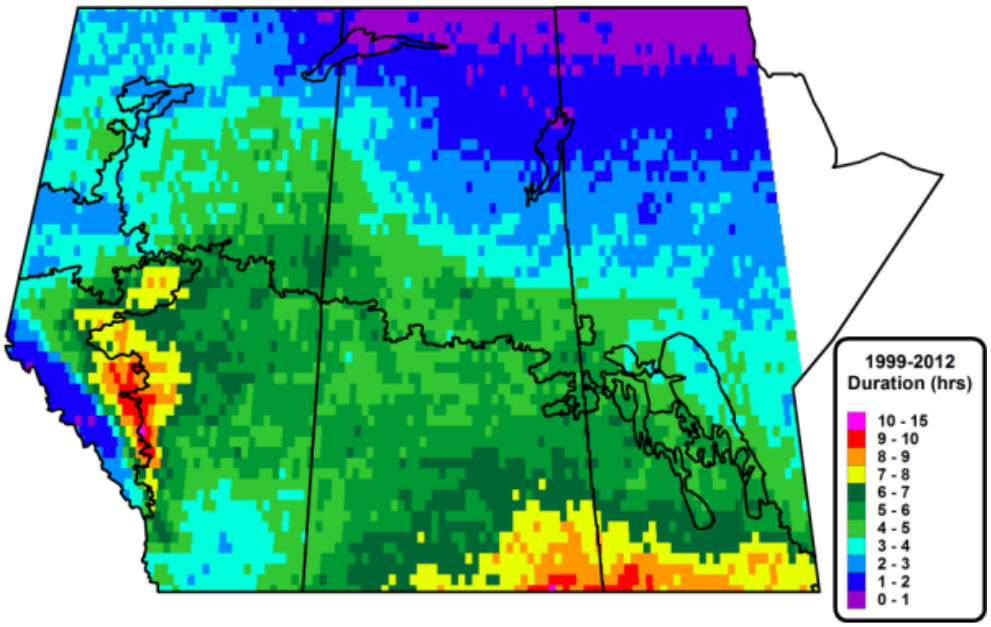

Figure 24: Lightning duration over the three Prairie Provinces adapted from Kochtubajda *et al.* (In Preparation).

Watersheds within the study domain that are located in the Boreal eco-zone are the CHU and NEL basins, and the eastern part of WPL basin; the same three regions where positive summer precipitation anomaly occur. The Boreal ecozone receive significantly less convective storm precipitation, as do the three basins residing within this eco-zone; therefore experiencing positive rather than negative summer anomalies. The positive anomaly can be observed throughout both P2P and M2M analysis: K-S and Wilson-Cox tests from the P2P analyses using 'smaller' null hypothesis (Table 4) concluded that CaPA simulates less precipitation than CDCD in all sub-basins except for CHU and NEL basins. The M2M anomaly map also indicates that the difference between CaPA and ITCD is closer to zero percent over these two basins, while other basins were more negatively biased (Figure 21). It appears that CaPA has difficulties simulating the summer convective storm events relative to observation data, while its performance is improved in regions with less convective storm activities.

5.2.2. Fall Precipitation Anomaly

Fall (SON) precipitation anomaly demonstrates the greatest spatial variation, which is also suggested by the P2P results. Although the P2P analysis is not able to spatially locate the anomaly, it is clear from the M2M analysis that the most notable spatial differences lie along the north-eastern portion of the WPL watershed. This observation, further verifies the hypothesis proposed in Section 5.1 that the occurrence of localized lake evaporation may contribute to spatial variability in fall. The RED basin also displays strong spatial anomaly between North Dakota and Minnesota, which could be caused by the sparse observation station network there failing to capture fall storm events.

Large water bodies can significantly influence the formation of precipitation patterns, particularly during and immediately following periods of strong lake evaporation (Miner and Fritsch, 1997; Spence *et al*., 2011). Water vapour generated by lake evaporation along the windward shore of a lake condenses into liquid as it rises and cools (at higher elevations), then falling as localized precipitation along the lee shore (Miner and Fritsch, 1997). Evaporation from large lakes is controlled by many factors including incoming solar radiation, surface roughness, and heat storage. The timing of strong evaporation over large lakes is usually delayed compared to the cycle of annual maximum temperature as a result of lake heat storage capacities (Spence *et al*., 2011). Over Lakes Winnipeg and Manitoba, lake heat storage gradually reaches its maximum capacity in early and late fall, marking the onset of maximum evaporation occurrence (Manitoba Water Stewardship, 2011).

The figure below (Figure 25) published by Environment Canada shows total mean precipitation in October over the WPL basin. Direct comparison to CaPA fall

precipitation from the WPL basin (Figure 26), assuming that October precipitation in is representative of fall (SON) seasonal precipitation shows the same patterns and about three times the precipitation from Figure 25 (which represents only October).

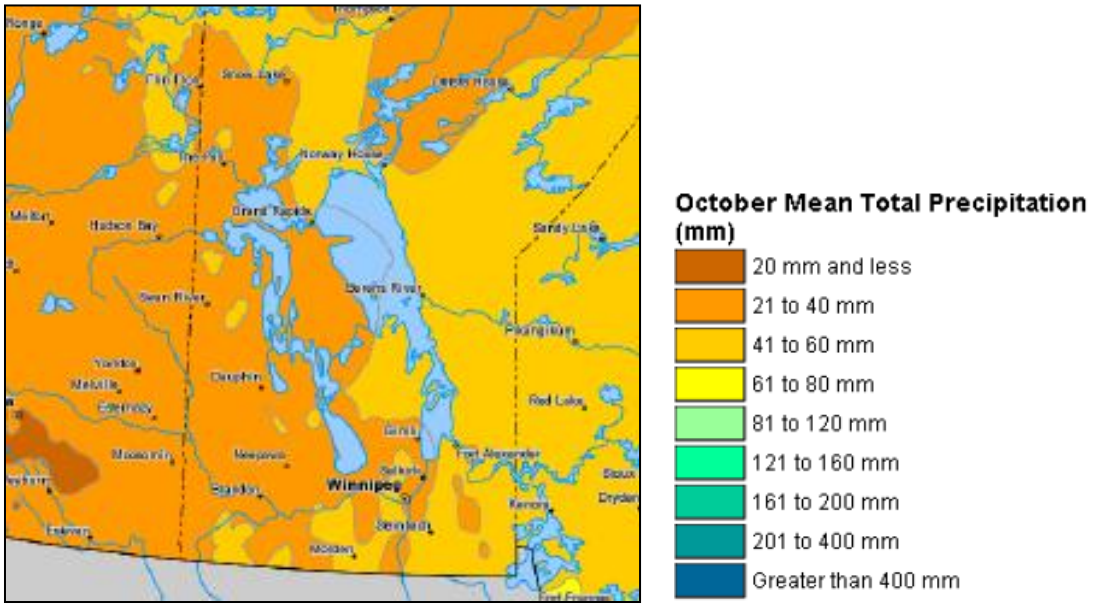

Figure 25: October mean total precipitation (Natural Resource Canada, 2013)

A significant precipitation divide is noted denoting high precipitation to the east, and lower precipitation to the west on both maps, which is most obvious across the large lakes in Manitoba. This pattern exists is general based on moisture transport processes from west to east in Canada (Pacific moisture sources), but is also likely exaggerated by lake effect moisture. Water evaporates from the lake surfaces with a strong west to east transport mechanism via the prevailing wind patterns and dominant jet stream (Manitoba Water Stewardship, 2011), falling as higher precipitation on the lee side of the lake (Eastern shoreline). The triangles on Figure 26 represent stations assimilated by CaPA, with clearly fewer stations on the east relative to the west shoreline. The presence of the divided precipitation pattern infers the skill of the CaPA analysis when simulating long

term, large scale precipitation patterns in this region of the Canadian Prairies where complex climate dynamics exist.

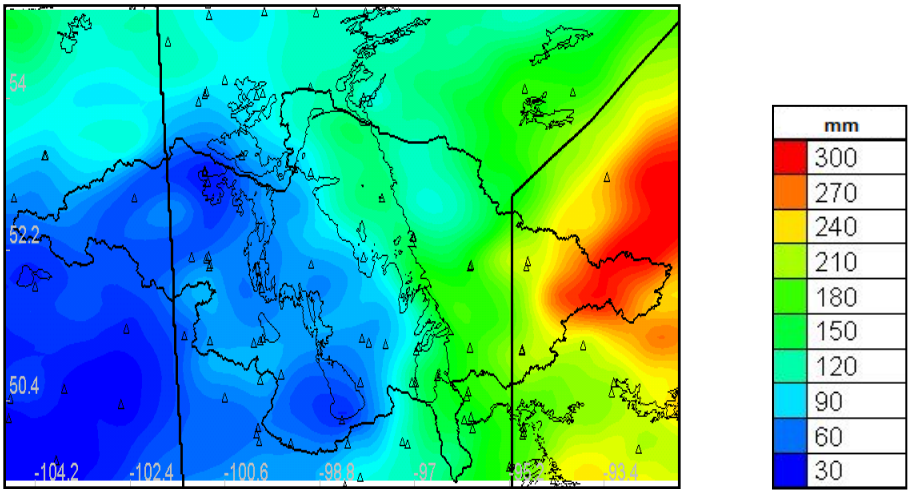

Figure 26: Average fall (SON) precipitation from CaPA for the WPL basin.

5.2.3. Winter and Spring Precipitation Anomaly

Winter (DJF) precipitation shows an overall positive anomaly (i.e., CaPA predicts higher precipitation) across the majority of the study domain, except for the northern part of the WPR basin, western part of WPL basin, north and south end of CHU and RED basins and finally, the western tip of the SAS basin. Positive winter anomalies are generally expected since observations used to interpolate CDCD data onto the ITCD map do not adjust for wind under-catch effects, yet this does not guarantee the quality of observations at locations where negative anomalies occur.

Firstly, clear differences in density between the northern portion of the WPR and western tip of the SAS basins can be found on Figure 10. Denser observation networks help to improve the interpolated precipitation field, thus the negative anomaly (i.e., under-estimation of CaPA relative to ITCD) at the western tip of the SAS basin is not likely

caused by interpolation error given the dense observation network. Other areas experiencing negative anomalies on the other hand, have virtually no observation stations, and therefore the negative anomalies can be caused by interpolation error. Secondly, topographic relief is prominent at the western end of SAS basin where significant elevation changes occur at the edge of the Rocky Mountain range, whilst other basins in the study domain are relatively flat. Orographic effects are likely the cause of the negative anomaly at the western part of SAS basin, which is verified by the presence of a negative anomaly here during all seasons (Figure 21).

Along the mountainous regions of the Nelson-Churchill River Basin, orographic effects play an important role in the formation of seasonal precipitation and spatial patterning. Maps published by Environment Canada show average maximum snow depth obtained over 18 winter seasons from 1979 to 1999 (Figure 27 shows the average snow depth was deepest in the late 70s through to the late 90s along the border of Saskatchewan and Alberta where the mountains begin, decreasing drastically onto the flatter Prairie terrain to form a band that divides high and low snow depth. Although climate records have notably changed from 1970 to 2005 (Figure 28), spatial patterning caused by the orographic effects are assumed to be persistent and consistent throughout this period.

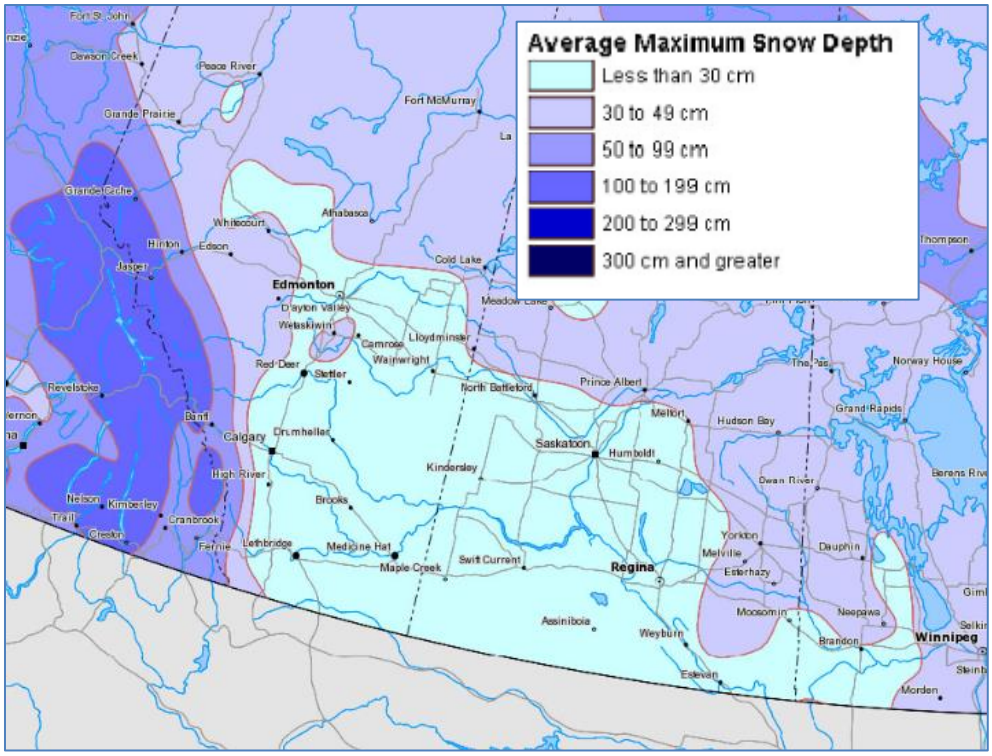

Figure 27: Average maximum snow depth (Natural Recourse Canada 2012)

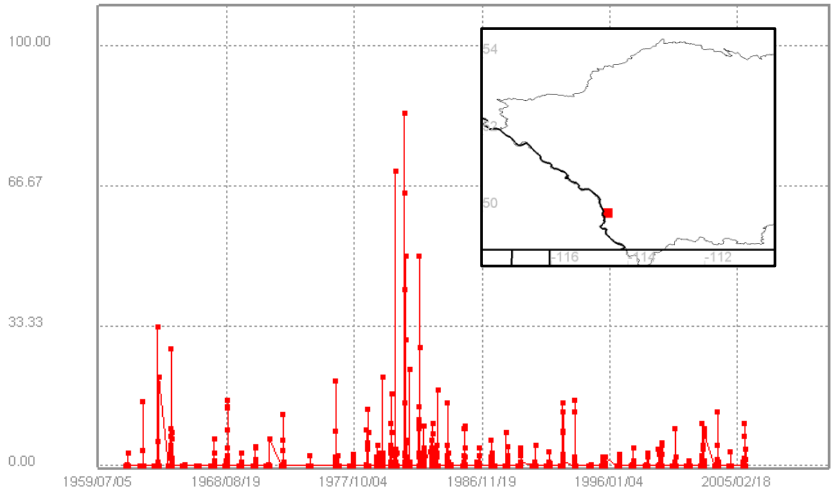

Figure 28: Snow depth precipitation record at SUGARLOAF, located in the SAS basin as indicated in the inset (top right) from 1959 to the end of 2005.

The band of high solid precipitation in the Rocky Mountain range is also visible from 2002 to 2005 in CaPA seasonal plots as shown on Figure 29, with stations assimilated into CaPA plotted on the figure as triangles.

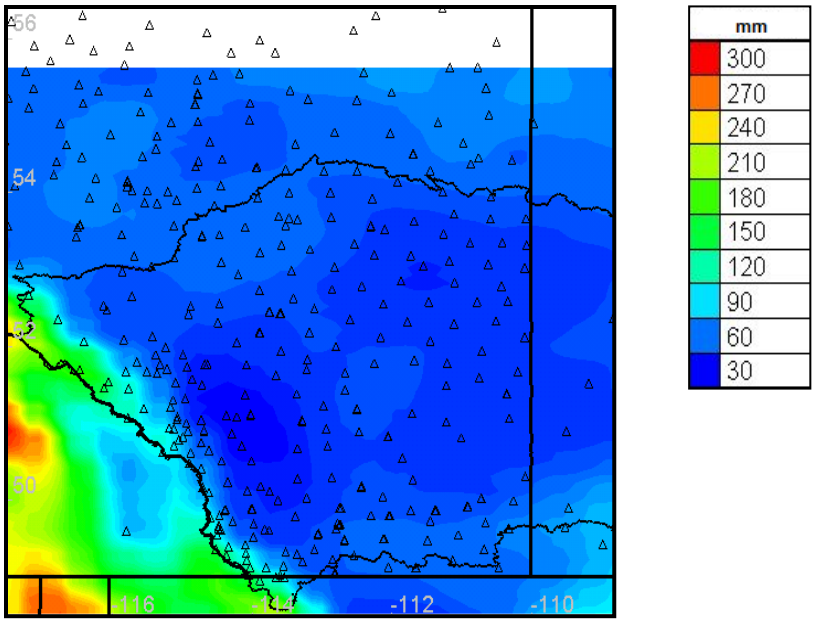

Figure 29: Average winter precipitation simulated by CaPA at the western edge of the SAS basin along the Rocky Mountain range.

Despite the lack of observation stations in the Rocky Mountains, CaPA solid precipitation amounts are in agreement with long-term published amounts from snow depth measurements (Figure 27). This agreement infers that the orographic effects are included (and appear to be realistic) within CaPA. CaPAs orographic effects are passed down from the GEM background field more-so than from the assimilated stations given the scarcity of the station density in the mountains, suggesting that GEM provides an accurate background for the CaPA analysis.

There is one station located within the mountain area that does, however, seem to improve CaPAs output as the reduced precipitation around this station matches well with the band of reduced snow depth indicated on the Environment Canada published map (Figure 27). This improvement implies that improving the density of the assimilated stations likely also leads to more reasonable precipitation analysis.

After examining the anomaly maps, the advantage of using M2M analysis clearly lies in the ability of this analysis to reveal spatial correlation in anomalies, and relate the anomalies to specific types of precipitation formation or landform features.

5.3. M2M Comparison with Lapse rate

M2M analysis with lapse rate functions incorporated into the ITCD precipitation field are used to further assess orographically-driven precipitation between CaPA and station observations. Increasing elevation causes air parcels to be more rapidly lifted and cooled (as a result of decreased temperatures at higher elevations), condense more easily, thus generating more precipitation rain-out. Lapse rates are important for watersheds with significant elevation difference across their domain for example, the SAS basin. CDCD stations are re-interpolated using a modified IDW function with a built-in lapse rate and M2M anomaly maps are re-generated (Figure 30).

In general, M2M results for the CaPA/ITCD comparison with lapse rate agree well with the results without lapse rates, with only slight differences. This result was anticipated given the generally low-relief of the study domain, and the fact that precipitation is generally not orographically-driven within the domain. It is anticipated, however, that in regions of higher relief and significant topographic change (i.e., the headwaters of the SAS basin) that the use of a lapse rate function should improve anomalies between CaPA and the ITCD precipitation fields.

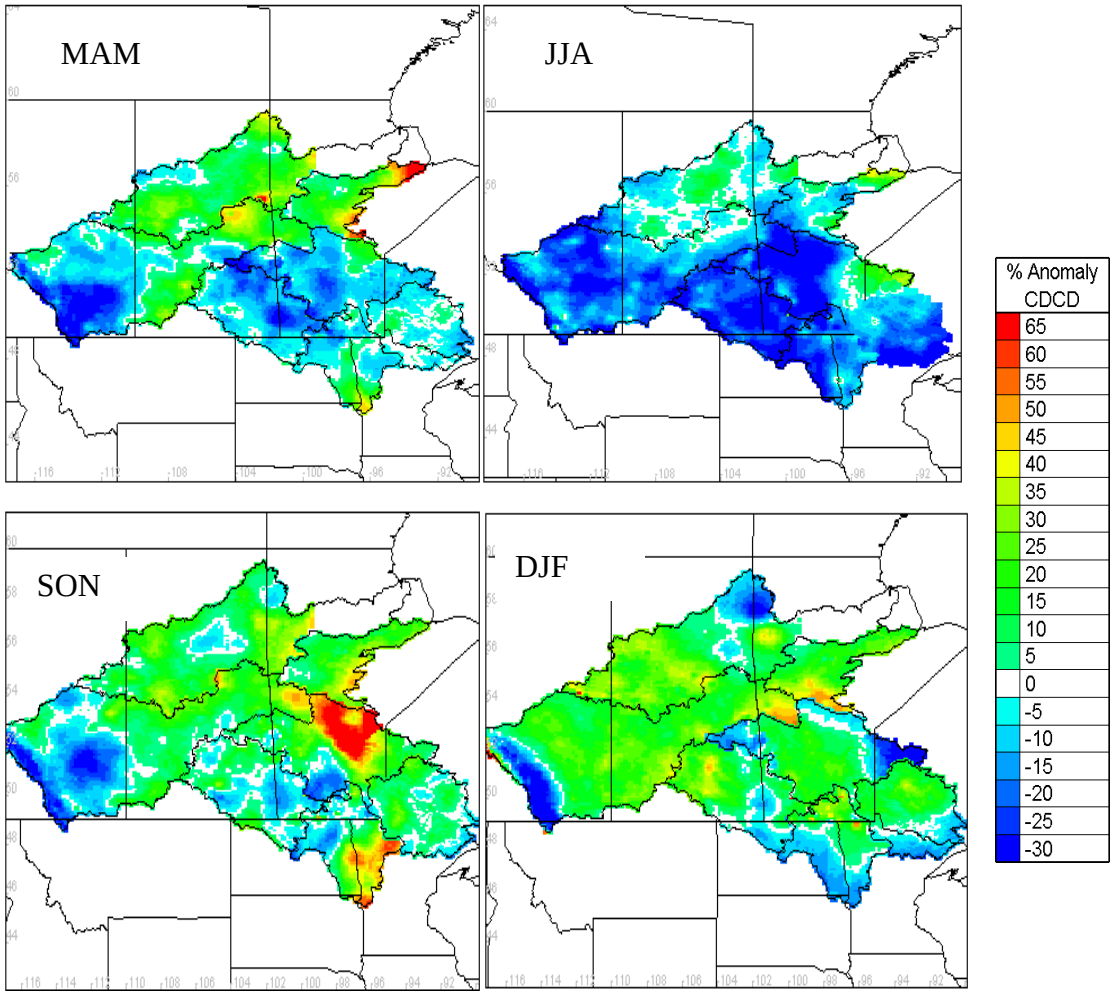

Figure 30: Seasonal anomaly maps computed between CaPA and interpolated CDCD observations with lapse rate.

In fact, there is a slight increase in the negative anomaly across the study domain, suggesting there is a decrease in interpolated CDCD precipitation overall by using a lapse rate. The decrease in the overal ITCD precipitation is discussed in Section 5.3.1. A supplimentary histrogram analysis is conducted to futher investigate these anomalies, as well as the differences between ITCD interpolated with and without lapse rate functions.

Anomalies obtained from the M2M analysis are examined using histograms. The magnitudes of anomalies are grouped into several bins on the x-axis and the number of grids whose anomaly fall within each bracket are counted and plotted on the y-axis.

Histograms for all sub-basins and seasons are provided in Appendix C (Figures C-4 to C-10), with two examples given below (Figure 31 and Figure 32) showing summer anomalies in CHU and NEL basins. The blue bars represent the histogram for anomaly maps computed without a lapse rate, while the red bars represent the histogram computed for anomaly maps with lapse rate.

The distribution of anomalies without lapse rate in the NEL basin (169m relief) is positively skewed, with an arithmetic mean of -3% suggesting that CaPA simulates 3% less precipitation than ITCD without lapse rate. On the other hand, the distribution of summer anomalies without lapse rate in the CHU basin is closer to a normal distribution with an arithmetic average that is close to 0%, indicating that CaPA and ITCD are roughly the same. Furthermore, in line with the P2P results, the CHU basin is the only sub-basin that does not show a significant underestimation of precipitation during the summer.

Direct comparison of interpolation with and without lapse rate can be performed by comparing the red and blue bars on these histogram plots. In the NEL basin (Figure 31), use of a lapse rate decreases the peak of the probability distribution function (PDF), while the negative bias is increased (and subsequently positive bias decreased). These two distributions infer that interpolating CDCD with lapse rate in the NEL basin causes the interpolated precipitation field (ITCD) to differ more from that of CaPA. The distribution of anomalies when using a lapse rate in the CHU basin (~300m relief) on the other hand is closer to zero, suggesting that interpolating station data using a lapse rate improves the similarity of the precipitation field relative to CaPA.

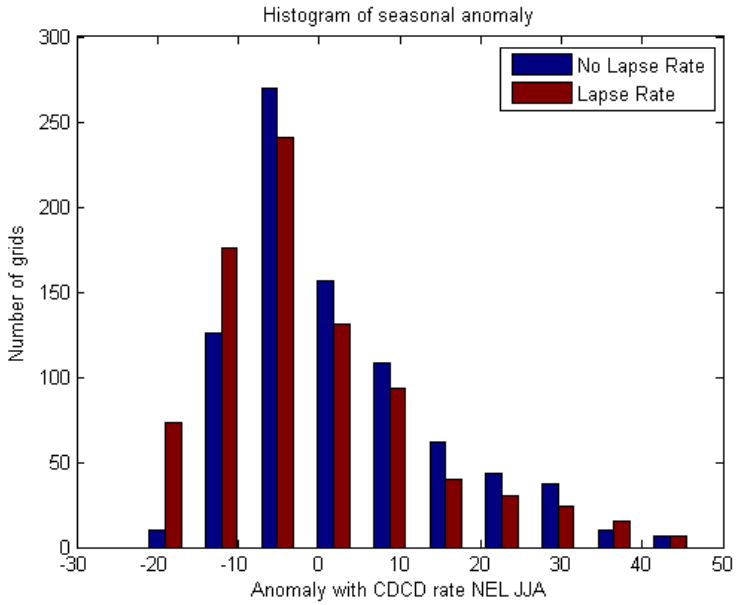

Figure 31: Histograms of anomalies in the NEL basin during summer (JJA).

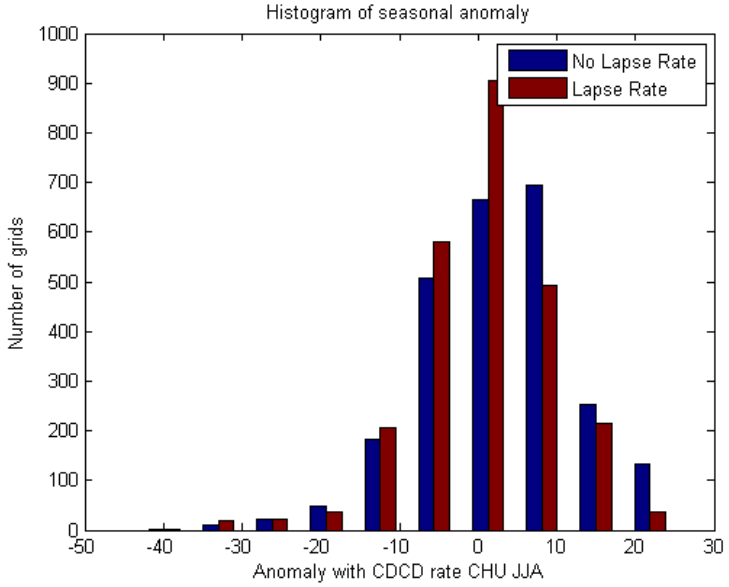

Figure 32: Histograms of anomalies in the CHU basin during summer (JJA)

A categorical score is assigned to each of the sub-basins during each season. If one anomaly distribution is closer to zero after using a lapse rate, a score of '1' is assigned; if the distribution is not closer to zero, a score of '0' is assigned. Table 6 summaries the scores for every sub-basin during different seasons. A spatial score is given to each sub-

watershed by summing all the seasonal scores, and the temporal score is assigned to each season by summing scores among all basins during the same season. The higher the spatial score means that the ITCD is closer to CaPA after using lapse rate for that watershed, hence validating the presence of orographic effects.

Table 6: Categorical score for histogram analyses in each sub-watershed for each season

Basin	**Estimated Relief (m)**	**MAM**	**JJA**	**SON**	**DJF**	**Spatial Score**
ASI	150	**0**	**0**	**1**	**1**	**2/4**
CHU	450	**1**	**1**	**1**	**1**	**4/4**
NEL	245	**1**	**0**	**1**	**1**	**3/4**
RED	130	**1**	**0**	**0**	**0**	**1/4**
SAS	1600	**1**	**0**	**1**	**0**	**2/4**
WPL	500	**1**	**1**	**0**	**0**	**2/4**
WPR	200	**0**	**1**	**0**	**1**	**2/4**
Temporal Score	-	**5/7**	**3/7**	**4/7**	**4/7**	**57.1%**

Table 6 indicates that the scores vary among basins and seasons. Overall, summer scores are the lowest among all the seasons, and the CHU and NEL basins score the highest among all the basins. There are a few main factors contributing to the different scores among watersheds and seasons.

The first factor is the elevation change across the domain: the larger the elevation change, the more significant the orographic effects and thus the changes introduced by lapse rate function in the ITCD field. For example, comparing the WPR basin and the CHU basin, which have 200m and 450m of elevation change respectively and the CHU basin is more affected by the lapse rate than the ASI basin.

Although elevation change is an important factor, it does not always guarantee a more pronounced difference before and after using lapse rate. The second factor deals with the density of stations used to create the ITCD field: the denser the station network, the less

improvement lapse rate will contribute since interpolation using high density stations networks inherently capture orographic effects. The SAS basin, for example, has a very high station density as seen on Figure 10 as well as high overall elevation difference (~1600m). Adding the lapse rate function does not bring ITCD closer to the CaPA as we would expect for a watershed with high relief changes in this basin, likely because orographic effect is already captured within the station interpolations. Moreover, stations in the SAS basin are less dense in the eastern portion of the basin but denser to the west where greater elevation changes and more orographic effect occur. This uneven distribution of stations would contribute to increasing overall differences before and after using lapse rate.

The third factor that impacts changes observed with and without lapse rate is seasonality. Some precipitation events during specific seasons, like winter (solid) precipitation for example, are more affected by orographic features than summer convective storms. Summer therefore scores the lowest in Table 6, highlighting the importance of examining seasonal statistics in this analysis.

Despite these preliminary findings, it is important to further evaluate the application of lapse rate on the generation of the ITCD preciptation field because ITCD is used to validate CaPA on a areal basis, with CaPA using a physically-based backgound field which contains orographic effects on precipitaiton. Using ITCD without a lapse rate introduces bias into any comparison, hence failing to examine the quality of CaPA alone. Second, as metioned in Chapter 4, ITCD is used to calibrate WATFLOOD. If parameters in WATFLOOD are optimized using an inferior ITCD field, uncertainties in any kind of proxy validation exercise will be increased.

Further analyses are therefore conducted to investigate the effect of a lapse rate on interpolated station observations by comparing the ITCD precipitation field to the CDCD observations. This comparison, similar to a P2P analysis, asumes the CDCD observations as ground-truth. Hypsometric curves of observation station elevation and DEM elevation are also used in Section 5.3.1 to further investigate the importance of incorporating a lapse rate function.

5.3.1. Hypsometric Curve Analysis

The difference between point CDCD measurements and interpolated CDCD (ITCD) is computed, simple statistics are calculated by season, averaged over entire domain as shown in Table 7.

Table 7: Simple statistics of CDCD observations and ITCD grids with and without lapse rate.

	MAM		JJA		SON		DJF	
ITCD	**No lapse rate**	**With Lapse Rate**	**No lapse rate**	**With Lapse Rate**	**No lapse rate**	**With Lapse Rate**	**No lapse rate**	**With Lapse Rate**
Mean(mm)	105	100	232	219	91.4	86.2	49.1	46.8
Max(mm)	212	207	342	335	257	247	127	124
Min(mm)	64.4	32.9	176	87.7	50.6	33.5	28.9	14.8

Table 7 shows an overall decrease in mean seasonal precipitation, maximum precipitation and minimum precipitation. Decreased ITCD precipitation may cause CaPA to appear to perform better or worse when using a lapse rate during specific seasons, for example, CaPA might appear to perform better after using a lapse rate in summer since CaPA was under-estimating precipitation relative to ITCD without a lapse rate. It is therefore essential to ensure the changes after using a lapse rate are inferred for the right reasons. The lapse rate function relies on the difference between the station elevations and DEM

elevations to create the orographic effect. To properly distribute the lapse rate effect and avoid biases, a statistical distribution of the station elevations needs to be a fair representation of the DEM elevations over entire study domain.

Figure 33 shows the hypsometric curve for the entire Nelson-Churchill study domain derived from the DEM data and stations used by ragmet.exe to create the ITCD field, and CaPA stations.

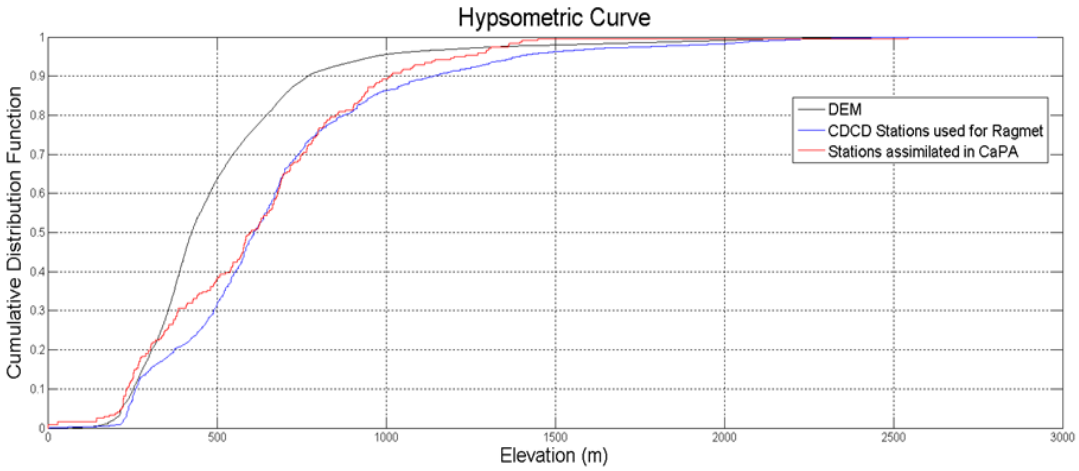

Figure 33: Hypsometric curve showing the distribution of DEM, CDCD stations, and stations assimilated into the CaPA analysis.

The hypsometric curve derived from both CaPA assimilated stations (red line), and CDCD stations used in the interpolated precipitation field (ITCD; blue line) suggests that DEM elevations are consistently lower (and smoothed) relative to actual station elevations. Lapse rate adjustments to the interpolated precipitation field are made according to the relative difference between station and grid elevation. Therefore, if the stations are generally located at higher elevations relative to the maximum DEM elevation, incorporating a lapse rate will result in less precipitation. This in turn causes a reduced ITCD mean precipitation (with lapse rate), hence the reduced difference between ITCD and CaPA (with lapse rate) (Table 7). Therefore, it is not necessarily true that

using a lapse rate function will always improve the interpolated precipitation field since part of the current improvement is contributed through existing negative bias. To achieve better interpolated precipitation fields that represent larger-scale weather patterns, distributions of elevations at precipitation stations need to be representative of the overall watershed relief, or at least the watershed relief as represented by the DEM used to develop the watershed model.

So far, the P2P and M2M analysis have examined the CaPA analysis with CDCD observation and ITCD precipitation fields. Through these two analyses, CaPA has demonstrated its ability in representing orographic effects and improving overall fall precipitation and winter solid precipitation prediction. However, due to the analysis scale, size, and simulation physics, the CaPA analysis experiences difficulty in simulation of more localized convective storm events, hence causing negative bias when compare to CDCD. A watershed or region that does not have frequent convective storm activities, however, is less affected by this fault. Furthermore, using lapse rate can improve the quality of ITCD, hence improving WATFLOOD^{TM} calibration comparison with CaPA; however not universally and the result is highly dependent on the representativeness of station elevation relative to the DEM. To assess CaPAs ability as forcing for a hydrological model, proxy validations will be conducted on select sub-basins of the study domain.

5.4. Proxy Validation

The purpose of proxy validation is to assess the suitability of CaPA for hydrological simulation relative to the traditional interpolated station forcing (i.e., ITCD). In the proxy validation analysis, simulated hydrographs for the WPR and WPL basins are

generated using WATFLOOD™ forced by interpolated CDCD (ITCD) and CaPA precipitation fields. Observed streamflow is used for comparison and to validate the suitability of each forcing for hydrological simulation purposes. The analysis period used for proxy validation is consistent with the study period: 2002 to 2005. WATFLOOD™ was previously setup for the two basins and calibrated based on ITCD forcing (WPL) and AHCCD forcing (WPR) during a different time period. Three statistical scores are used to describe the simulations forced by ITCD and CaPA, relative to observed flows. Hydrographs of each simulation can be found in Appendix D. The legend of each hydrograph plot indicates its station number whose location can be found in Appendix E. Table 8 summarizes the statistical scores (D_v, Nash, and R^2) for the two basins.

Table 8: WATFLOOD™ simulation scores based on ITCD and CaPA forcing, and net change in scores after using CaPA for the WPR and WPL basin outlets.

	WPL basin			WPR basin		
Evaluation Stats	**ITCD**	**CaPA**	**Δ**	**AHCCD**	**CaPA**	**Δ**
D_v (%)	-6.81	-8.30	-1.50	0.36	-10.8	-11.16
Nash	0.91	0.90	-0.10	0.63	0.60	-0.03
R^2	0.93	0.93	0.00	0.65	0.70	0.05

Table 8 shows that regardless of the forcing data used, simulation statistics for the WPR and WPL basins are reasonable, and that in most cases, there is little change observed at the basin outlets from one forcing dataset to the next. Note that the results in Table 8 represent statistics at the outlet of the basins and therefore cumulative error from the headwaters downstream. Based on the results of the M2M analysis, spatial differences in error within sub-basins of the WPR and WPL would be expected, with local differences possibly being more significant. Using CaPA as forcing for WATFLOOD™ results in an under-estimation of simulated runoff in both basins (negative D_v statistics), as did

AHCCD for the WPR. The WPL basin experienced a lower magnitude of change in D_v than the WPR (-1.5% verses 18.7 %); mainly because the basin is inflow controlled. Unlike D_v, the R^2 and Nash values do not change significantly, suggesting that most of the changes in hydrological simulation are volume-derived. This makes sense given timing of the hydrograph would not be heavily influenced by precipitation forcing given one product is observation-based (ITCD), and one assimilates observations (CaPA). The subsequent section discusses the results for each basin in more detail.

5.4.1. Winnipeg River Basin

Figure 34 below presents the results of the proxy validation for the outlet of the WPR basin. Hydrographs using CaPA and ITCD forcing for all sub-basins of the WPR are provided in Appendix D (Figures D-1). During calibration, Lake of the Woods outflow is forced by observation to aid the calibration of English River; this however, will not remain in the operational model. Hydrographs show varying degrees of difference between CaPA- and ITCD-forced streamflow simulations, however, at the outlet, CaPA is consistently under-estimating runoff compared to both observed and ITCD-simulated streamflow.

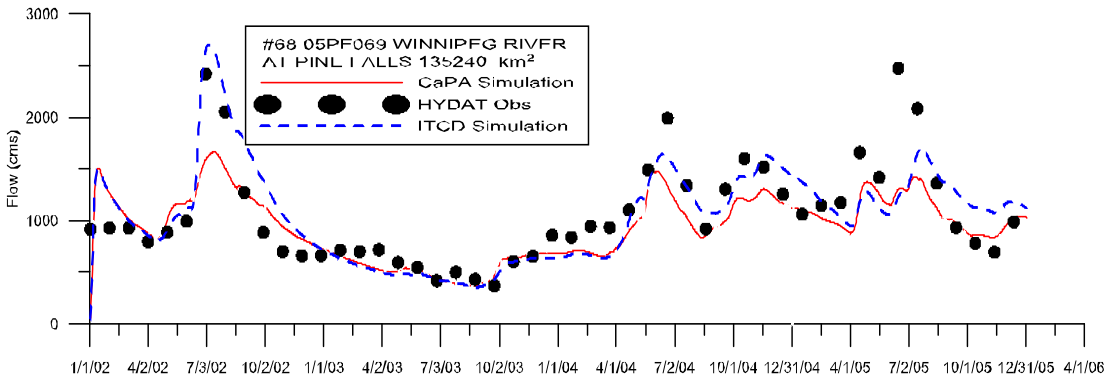

Figure 34: Proxy validation for the WPR basin outlet at Pie Falls (05PF069).

WATFLOOD™ appears to underestimate peak freshet runoff relative to the observed hydrograph (dotted black line), regardless of model forcing used. No significant natural peaks occur in 2003; however, indicating upstream regulation heavily influences hydrograph shape. In the case of the upstream reaches having reservoir storage capacity like the Lake of the Woods, the reservoir will store water during a wet season (i.e., spring or summer) that will later be drawn down during drier seasons (i.e., winter) to meet demand. Furthermore, the timing of peak streamflow will be different than that of natural stream channel.

WPR basin is set up to utilize any available lake inflow and outflow record as input. WATFLOOD™ uses the station record at station 19: Lake of the Woods Outlet at Boat Lift Channel (05PE003) as input to a previously calibrated storage release function to compute the hydrographs at station 20: Winnipeg River below Lake of the Woods Outlet (05PE020). Due to this specific watershed setup, comparing runoff solely at the outlet cannot provide meaningful results since runoff simulated by half of the total upstream contributing area is nudged by an observed record and essentially independent of climate forcing. Therefore it was decided to divide the watershed domain into two regions according to station's characteristic rainfall-runoff response. Regions are distinguished as Region A (Lake of the Woods system) and Region B (English River system) respectively. These two regions are outlined in red on Figure 35 below.

Region A consists of two major drainage systems: Lake of the Woods and a small tributary that joins to the English River, both of which flow from southeast to northwest. Region A represents about 60% of the total drainage area (~101,000 km^2) of the WPR

basin. Region B consists mostly of the English River system (~67,000 km^2) and drains from east to west.

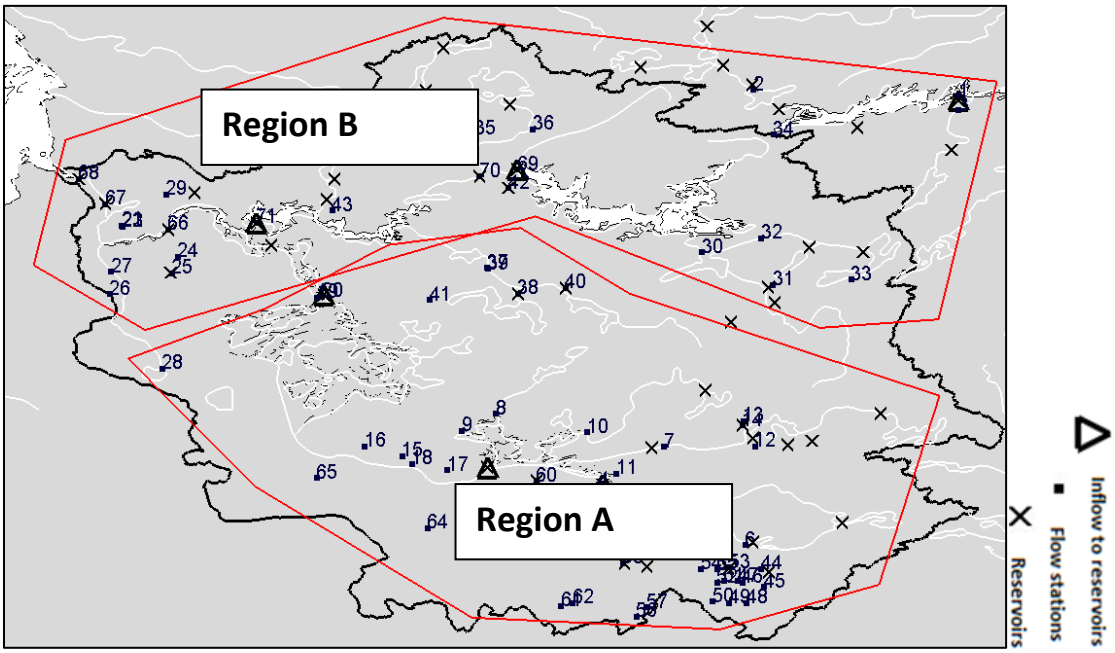

Figure 35: Division of Region A (Lake of the Woods drainage system) and Region B (the English River drainage system) in the WPR basin.

Flow regulations play an important role on the main stream of both regions. The difference between regulated and natural flow simulations are explained in Section 4.4.3 and an example comparing the two was shown in Figure 17 and Figure 18. In Region A, most flow stations are located on smaller-unregulated tributaries rather than main stem rivers, while most flow stations in Region B are located along on the main stem and more heavily influenced by flow regulations. Region B gauges therefore generally have larger drainage areas than those in Region A. The natural rainfall-runoff relationship dominates in the smaller tributaries (Region A), while flow regulation dominates along the main stem of the English River. Last but not least, landcover differences exist between Regions A and B within sub-basin areas as shown in Appendix A (Figure A-2). In the

lower portion of Region A, where most of stations are located, wetland is a dominant feature (Figure A-2, o.), while the majority of Region B is dominated by mixed forest or coniferous (figure A-2, j). Tributary size, flow regulation, and land cover will significantly impact the rainfall-runoff response relationship.

The D_v evaluation criteria for simulations from both ITCD and CaPA forcing for both regions are plotted on Figure 36.

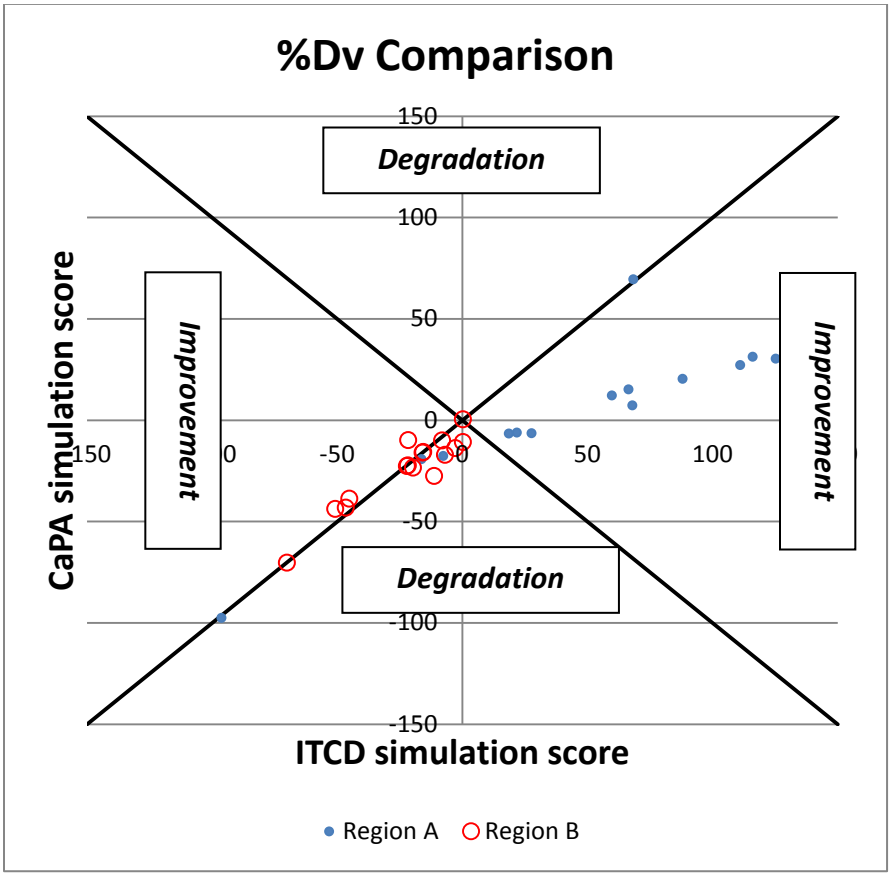

Figure 36: WATFLOOD™ D_v scores for simulations in Regions A and B of the WPR basin using CaPA versus ITCD forcing.

Firstly, the x-axis in Figure 36 represents the D_v score obtained using ITCD as climate forcing for WATFLOOD™, and the y-axis the D_v score obtained by using CaPA as a climate forcing. The plot is divided into four quadrants: the upper and lower quadrants

represent the degradation zone, wherein the simulations D_v statistical score worsens when CaPA is used for forcing over ITCD; left and right quadrants represent the improvement zones, where simulations using CaPA improve the D_v score relative to simulations using ITCD. Stations for Region A are represented by blue filled circles, while stations for Region B are represented with red open circles. For example, a red circle located at coordinates (-60,-70) lies in the degradation zone because the D_v statistic "degrades" from -60% to -70% by using CaPA instead of ITCD.

The majority of the stations in Region B fall along the 1:1 line indicating no significant changes (in D_v score). Most of the stations in Region A fall within the improvement zone of the far right quadrant. Stations falling in that zone have positive D_v scores (i.e., overestimation of runoff volume) from ITCD simulations, with their D_v statistics becoming reduced (i.e., closer to zero) using CaPA forcing. Results from the D_v statistical comparison suggest that stations over-estimating runoff volume (positive D_v) using ITCD are improved using CaPA (i.e., brought closer to zero) in Region A. Conversely, simulations remain relatively unchanged in Region B as most of the points on Figure 36 lie close to 1:1 line. This result indicates that, overall, using CaPA decreases runoff more significantly in Region A but has no obvious effect for Region B. Results from the M2M analysis are consistent with indicating more difference between CaPA and ITCD-derived precipitation over Region A, where generally Region A has negative anomalies indicating CaPA simulates reduced precipitation for the southern portion of the WPR basin.

The R^2 plot (Figure 37) is divided into two sections by a black line depending on whether the simulation is improved (or not) when using CaPA. The improvement zone is to the left, and to the right is the degradation zone.

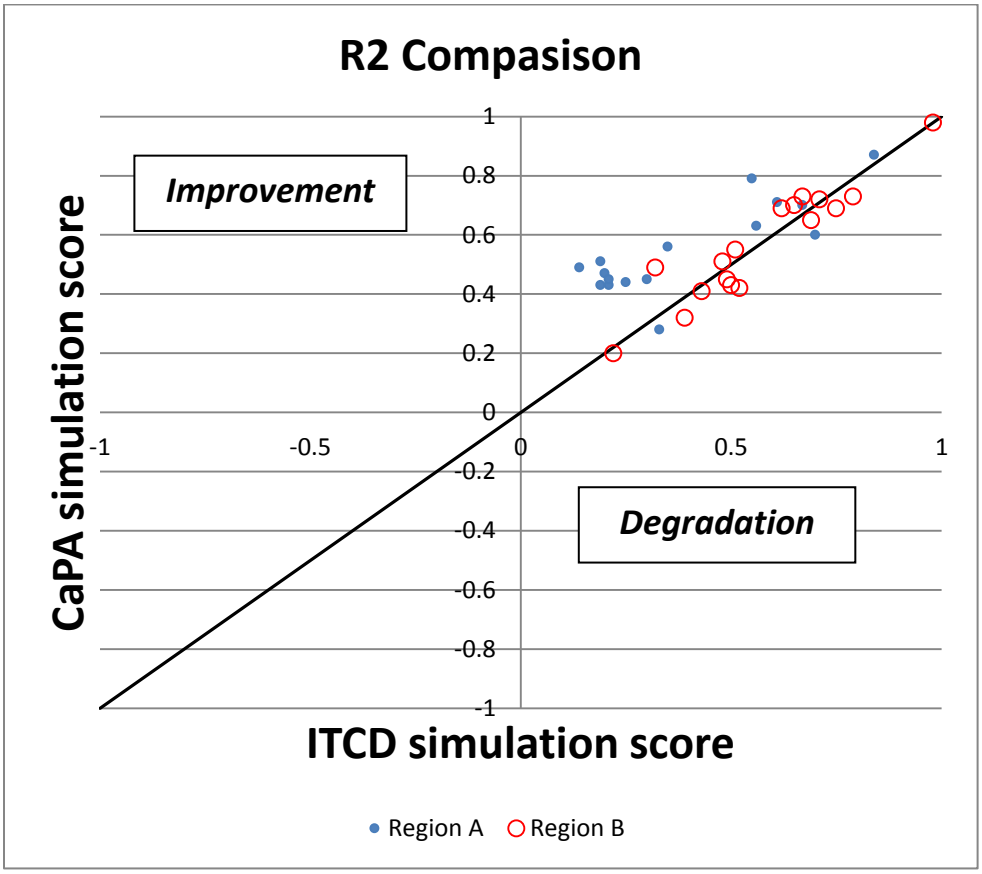

Figure 37: WATFLOOD™ R^2 scores for simulations in Regions A and B of the WPR using CaPA and ITCD forcing.

The R^2 statistic examines the timing of the simulated hydrograph against the observed hydrograph using Equation 3. R^2 statistical scores should be used with caution since a high R^2 score does not guarantee a better fit because a simulated hydrographs R^2 can appear to be high while the simulated runoff volume is erroneous.

The R^2 comparison plot suggests that the timing of simulations at most stations in Region A when using CaPA forcing is improved. Region B, on the other hand appears to have

little change in timing using CaPA as climate forcing. Little to no influence of precipitation forcing on hydrograph timing in a region that is regulated is anticipated, given it is the storage-release function and not the onset of precipitation that determines the timing of flow in such regions. Although parts of Region A is also regulated, the majority of flow stations lie along unregulated tributaries and therefore hydrograph timing at these stations is mainly determined by the onset of precipitation. Furthermore, the size of the sub-basins also affects climate-induced changes in runoff timing. Timing improvements in Region A therefore can be attributed to improvements in CaPA as a model forcing where interpolation of observations fails to as accurately depict the onset of precipitation fronts due to limited nearby stations. Meanwhile, if the interpolation is properly executed with enough observations, improvements in timing would infer improper model calibration because timing of observations would not likely be erroneous. An answer to whether the improved timing in Region A reflects better CaPA precipitation quality is not yet substantiated.

Figure 38 shows the Nash score plot for ITCD versus CaPA forcing in WATFLOOD^{TM}. Similar to that of R^2 plot, this plot is also divided into two zones: degradation and improvement. Nash statistical scores are improved in Region A since almost all the stations from this region fall within the improvement zone; yet Region B shows the no obvious changes. It is expected that the Nash scores would be comparable to those of the D_v analysis since the Nash score also considers volume differences, emphasizing peak volume differences. Furthermore Region A shows little to no change in timing yet significant degradation in volume after using CaPA, therefore, it seems that the cause of the degraded Nash score is mainly the result of volume errors or changes. Model

calibration is kept constant thought out the proxy validation, thus it does not directly contribute to difference in volume changes between the simulations, and hence the volumes of precipitation input between ITCD and CaPA are the main cause of any differences.

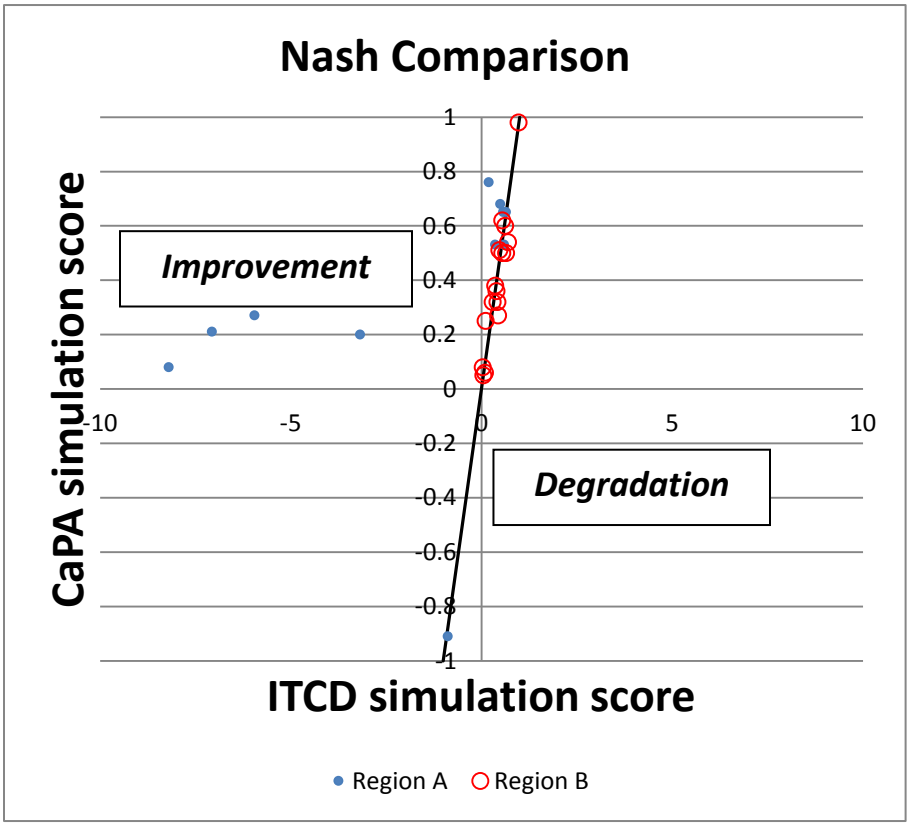

Figure 38: WATFLOOD™ Nash scores for simulations in Regions A and B of the WPR basin using CaPA and ITCD forcing.

In order to further investigate the change in simulated volume, runoff and climate inputs are divided into seasons, and a seasonal analysis of rainfall-runoff is conducted in both Regions A and B. Relative differences between ITCD-simulated and CaPA-simulated runoff are separated seasonally from 2002 to 2005, and averaged over all streamflow stations within their respective region. Meanwhile, the relative differences between CaPA and CDCD seasonal precipitation at each grid point are averaged across each

region. These averaged seasonal runoff and precipitation estimates are represented in the box whisker plots below (Figure 39). The x-axis on these plots represents the four seasons and the y-axis represents the relative difference between CaPA-simulated and ITCD-simulated runoff, or between CaPA seasonal precipitation and ITCD seasonal precipitation. Relative differences in runoff are represented in blue, while precipitation is in red. The top two figures are for Region B, while the bottom two are for Region A.

Lag effects between precipitation and runoff occur between winter and spring on account of accumulation of solid precipitation; therefore runoff during spring is mainly controlled by the winter precipitation and runoff is snowmelt dominated. Meanwhile, winter runoff is mainly controlled by late summer or fall precipitation (prior to ice-on) since any precipitation that falls when the river is frozen will simply accumulate until spring. This lag effect, however, is not expected during summer and fall seasons.

During spring (MAM) CaPA-forced runoff is higher than ITCD-forced runoff in Region B. Figure 21 in M2M analysis shows that during winter, CaPA simulates more precipitation than ITCD at the Winnipeg River basin. The over estimation of runoff is therefore due to the increased precipitation and is well captured in M2M analysis. While in Region A average CaPA-forced simulations are lower than ITCD-forced runoff and more widely varied, which is likely due to similar precipitation patterns and amounts during both spring and winter seasons, and the smaller (more responsive) basin sizes in Region A.

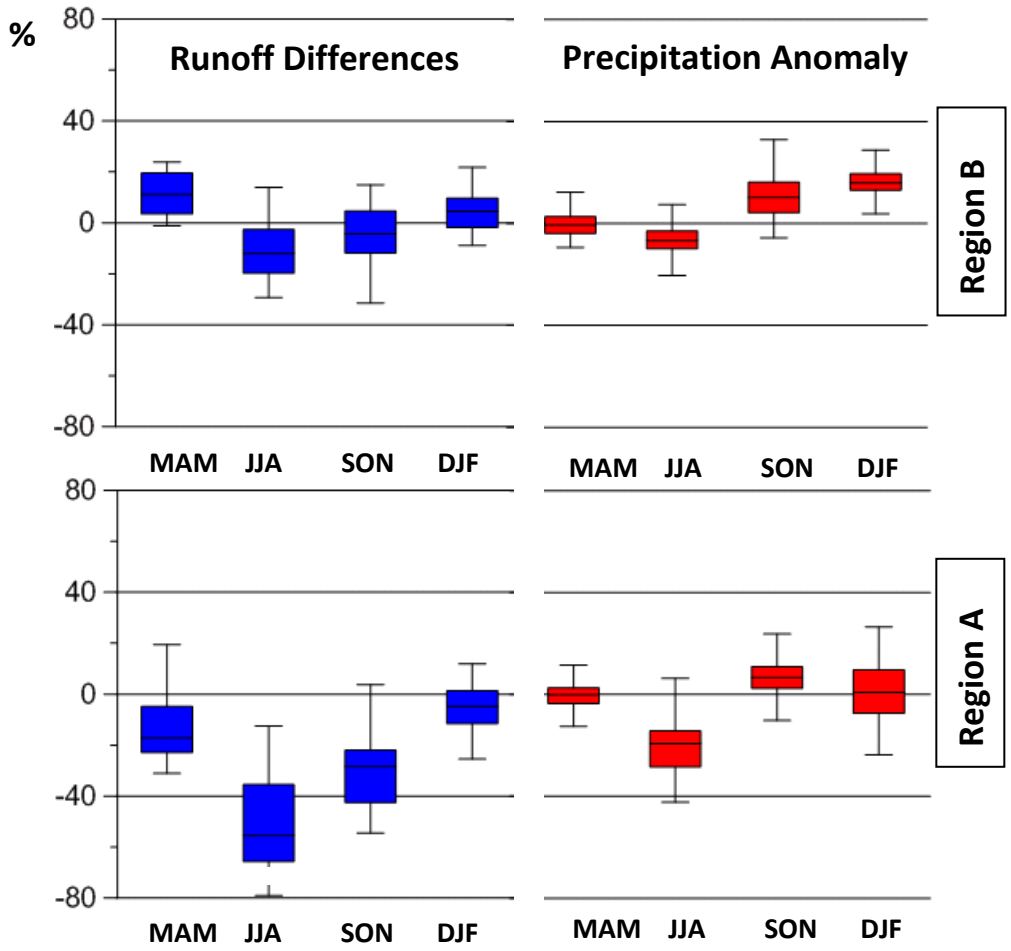

Figure 39: Comparison of runoff and precipitation differences between ITCD- and CaPA-forced WATFLOOD™ simulations in Regions A and B.

During summer and fall, differences between CaPA-fed and ITCD-fed simulations are similar between both Region A and B. Region B stations have overall less runoff variability than stations in Region A, which is likely due to more flow regulation in Region B. Overall, Region A shows reduced runoff in CaPA-fed simulations compare to ITCD-fed simulations, which is coupled with reduced precipitation in CaPA versus ITCD for Region A.

The inconsistent correlation between precipitation and runoff can be partially explained using the relationship of basin size/regulation with volume errors in simulated runoff. To demonstrate the effect of basin size on the rainfall-runoff response, the deviation of

runoff volume statistic (D_v) is plotted for Region A (Figure 40a, average basin size ~8000km^2) and Region B (Figure 40b, average basin size ~20000km^2) separately.

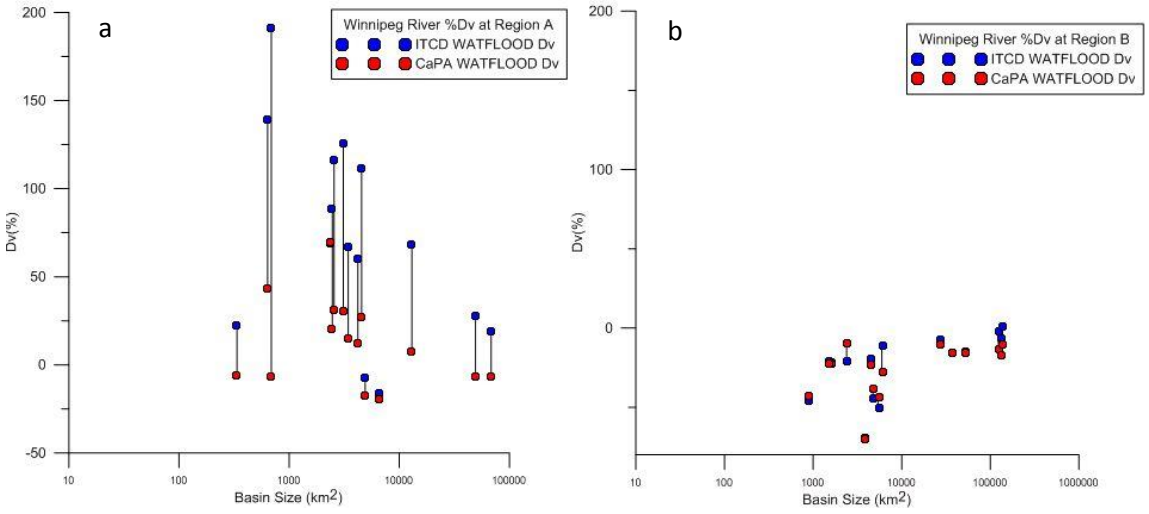

Figure 40: Relationship between sub-basin size and simulation D_v error statistic at a) Region A b) Region B

The x-axis represents the basin size in km^2 and is in log scale. The y-axis represents the D_v statistic for simulations forced by ITCD (blue dots) and CaPA (red dots). There is a clear difference between Region A and Region B changes in runoff volume from one precipitation forcing to the next, with fewer impacts to the D_v for Region B (average drainage area >20000km^2) being evident. This result is attributed to the regulation and streamflow nudging inherent in Region B simulations, resulting in precipitation forcing having little impact on the overall simulation. For smaller, un-regulated basins in Region A (average drainage area 8000km^2), the differences in simulation error between CaPA- and ITCD-forced simulations are much more highly variable, and so are relative improvements or degradations. This variability is at least partially related to the non-uniform spatial distribution of the precipitation field. For example, a CaPA precipitation field over a larger domain could show an overall negative bias against ITCD, however, at

the smaller sub-basin scale, it could show local positive biases against ITCD (less error averaging). The above plot, and statistical comparisons represent points at the sub-basin scale, whereas hydrographs plotted at the basin outlet represent cumulative basin errors (and biases).

Previous analyses of the simulations suggest that the improvement in simulation for Region A are due to decreased runoff volume induced by decreased precipitation volume. Flow regulation in Region B however, hinders the diagnosis of changes in precipitation forcing from runoff, hence the simulation scores did not change significantly. Proxy validation in the WPR basin shows that CaPA is capable of simulating hydrological response in natural channels; however, regulation hinders the assessment of the skill of CaPA from proxy validation.

5.4.2. Lake Winnipeg Basin

Figure 41 below shows the results of the proxy validation at WPL basin outlet. The black dotted line indicates the observed hydrograph (gauge number 31); red line represents the WATFLOOD™ simulated streamflow using CaPA forcing; and the blue line represents the WATFLOOD™ simulated streamflow using interpolated CDCD (ITCD) forcing. Hydrographs for sub-basins of the WPL basin are provided in Appendix D (Figure D-2).

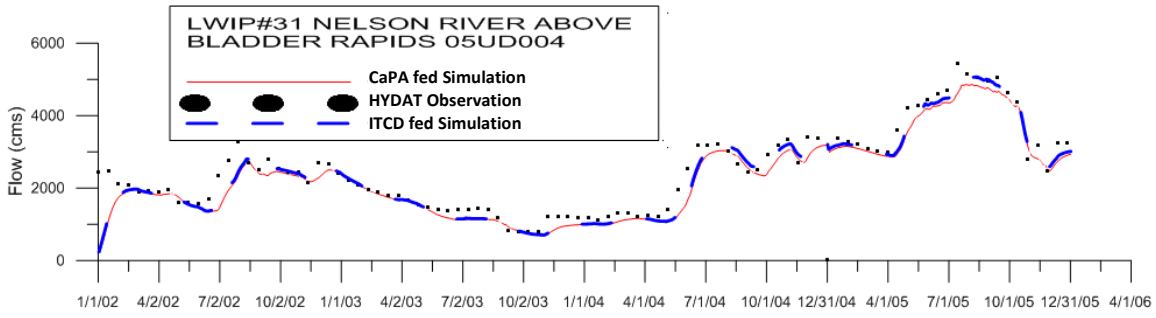

Figure 41: Proxy validation for WPL basin outlet (05UD004).

The WPL (246,000 km^2) is an inflow dominated watershed, with over 90% of the flow at the outlet being generated within upstream basins (i.e., ASI, RED, WPR and SAS). Very little runoff is generated and added within the basin itself, as the majority of the basin is open water surface area (Lake Winnipeg, ~24,500 km^2). Therefore, the difference between runoff simulations and the observed hydrograph is always relatively small, with very little hydrologic variation in the hydrographs (Figure 41). CaPA-forced simulations are shown to slightly under-estimate the hydrograph relative to ITCD-forced simulations. This however, could be more directly related to stations within the WPL that are assimilated into CaPA and have been shown to report false zeros (Personal communication with V. Fortin, 2013). Assimilating the stations with false zeros to adjust the GEM background causes the final CaPA output to under-estimate precipitation. Two such stations were detected by the M2M analysis in CaPA versions 2.2, 2.3 and 2.3a. They were fixed in CaPA2.30, yet another station was found in the M2M analysis for version 2.30 that reports false zeros. The analyses in this thesis are based upon version 2.30, and another operational version was not available for testing at the time of writing. This station will be removed in future CaPA releases.

Comparison of CaPA- and ITCD-forced simulations over the entire WPL basin indicates that CaPA-forced simulations consistently underperform ITCD-forced simulations. The lower precipitation field simulated by CaPA (relative to ITCD) is a main contributor to this under-estimation of runoff; with model calibration also being a factor. A statistical analysis comparing the two simulations is conducted in the same manner as for the WPR basinby comparison of the Dv, R^2 and Nash statistical scores from simulations forced by ITCD and CaPA. Figure 42 shows the outcome for the D_v statistic in the WPL basin.

Further inspection of Figure 42 revels the grouping of runoff at three different categories of stations: solid triangles representing runoff generated at stations within the mixed forest land type; solid orange dots representing runoff generated at flow stations close to the "false zero" reporting climate stations; and black stars representing runoff generated at stations located within the crop landcover region. Furthermore, the amount of flow stations that are available for comparison are limited, not all flow stations setup in WATFLOOD^{TM} are records flow during 2002 to 2005, especially in the eastern portion of the watershed.

Simulations of runoff within these three classifications behave uniquely for differing reasons. Runoff generated over the crop landcover region shows significant improvement in terms of volume, while the runoff within the mixed forest region does not change significantly from one forcing product to the next. The difference between these two categories of stations is likely not attributable to landcover type directly, but more so to differences in precipitation fields resulting from dominant forms of precipitation or other regional differences. Similar to that of WPR basin, comparison for the R^2 score is also carried out as shown in Figure 43.

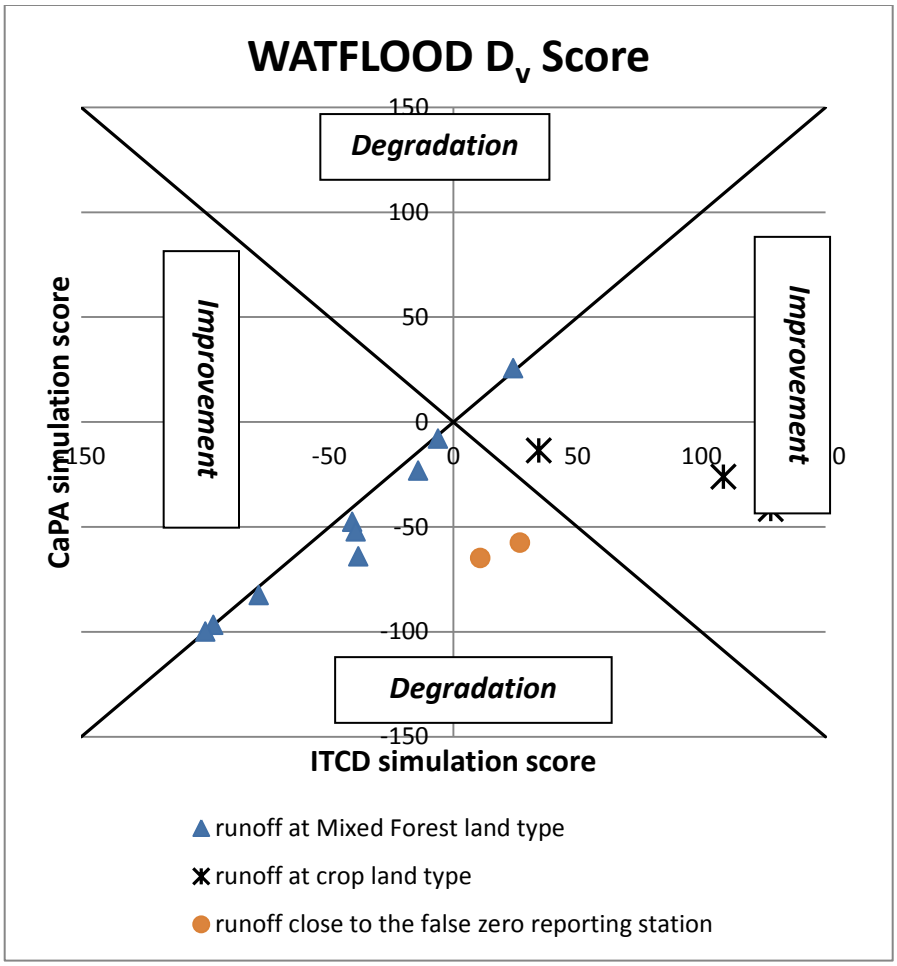

Figure 42: WATFLOOD™ D_v scores for simulations at WPL basin outlet using CaPA and ITCD forcing.

At most of the stations, there is not much change in timing resulting from the two precipitation fields. At the flow stations near the false zero reporting stations, however, CaPA-forced simulations consistently score 0; which is a direct result of the false reporting. These stations reported false zeros during periods where the stations were not in service (and therefore not recording actual precipitation events). The CaPA background was then adjusted to 'zero' events; hence CaPA-forced simulations are erroneous. With respect to simulation timing, there were no significant differences

among the two landcover typologies, reinforcing that precipitation type is likely not the main factor as convective cells are difficult to predict in terms of both volume and timing.

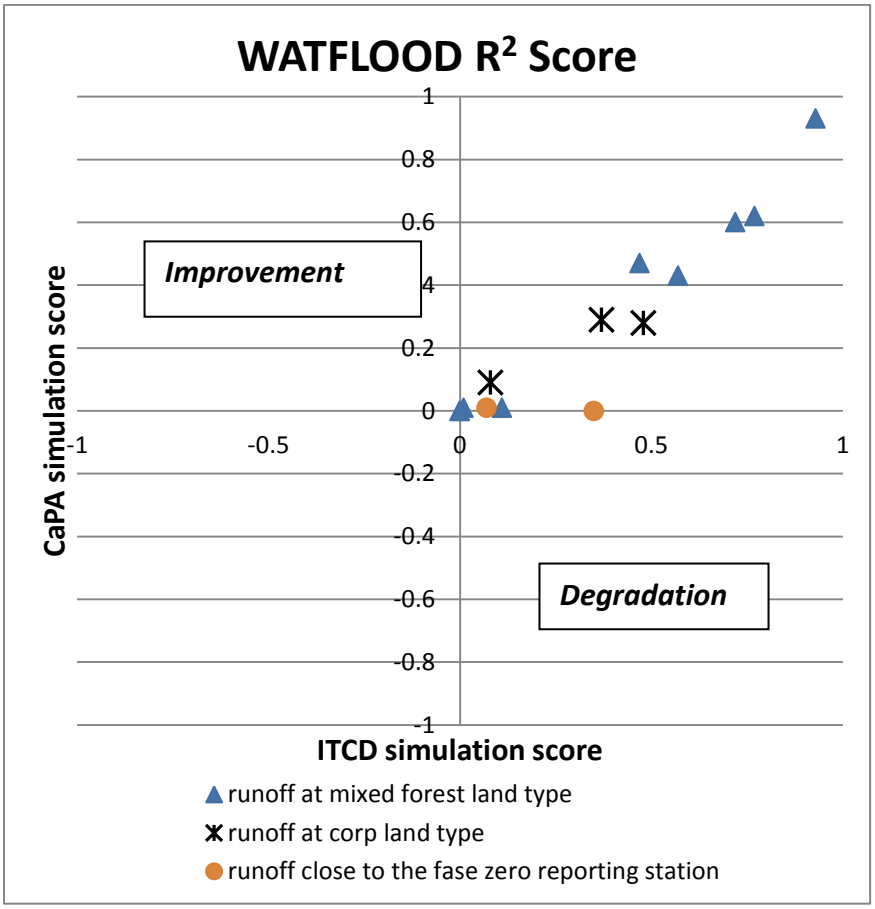

Figure 43: WATFLOOD™ R^2 scores for simulations at the WPL outlet using CaPA and ITCD forcing.

Figure 44 shows the Nash score comparison between ITCD and CaPA forced simulations. Stations in the crop region show significant improvements, and since there was no significant change in timing (Figure 43), volume differences are the main contributor to this improvement. It is unlikely that this improvement is landcover related, but more likely that landcover is a proxy for precipitation formation or regional differences such as station densities. Since the WPL basin shows improvement when

using CaPA as hydrologic forcing (not degradation), it is unlikely that precipitation type is the root cause.

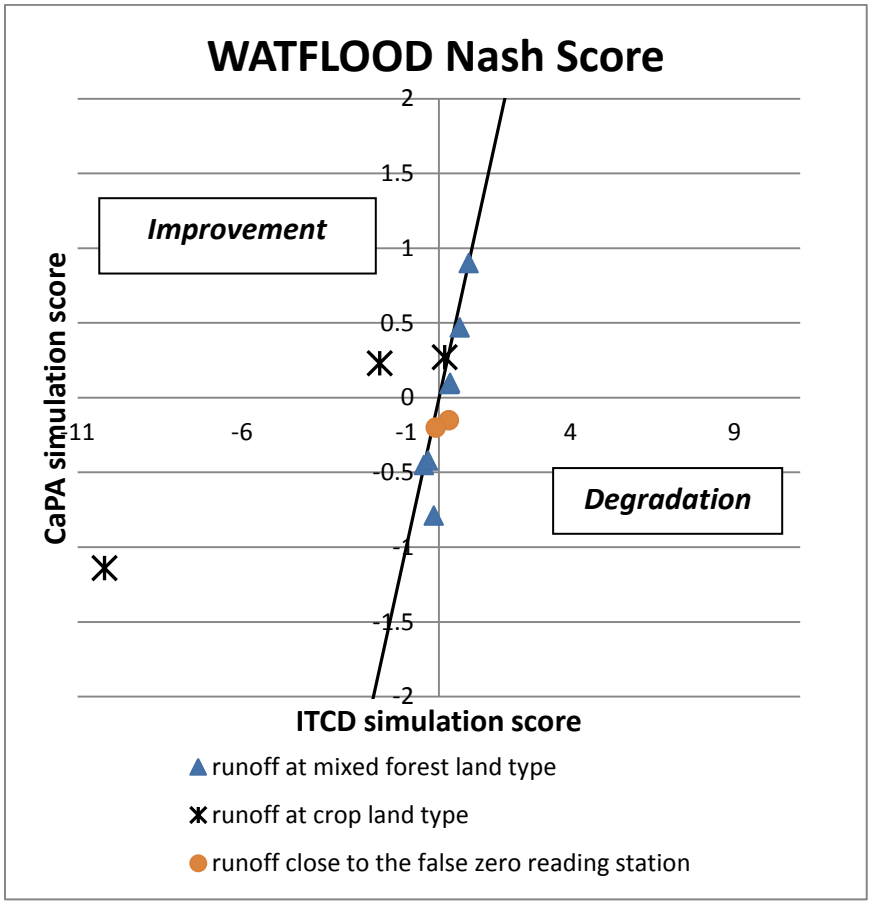

Figure 44: WATFLOOD™ Nash scores for simulations at the outlet of the WPL using CaPA and ITCD forcing.

Since model parameters are kept the same for both simulations, and WATFLOOD™ parameters pertain to specific landcover types, it is possible that model calibration contributes to the differences between landcover type and model performance.

Figure 8 showed the observations being assimilated into the model background, and around the crop land region of WPL basin (Figure A-1, a). There is a higher station density than anywhere else within the WPL basin. Crop land area also shows improvement after using CaPA, therefore one main reason for the difference in CaPA-

forced simulations in the different regions can be attributed to the density of assimilated stations. The effect of increasing the amount of assimilated stations is also apparent in the CHU basin, and is demonstrated in Section 5.5.1. In the CHU basin, assimilating observation stations is shown to decrease the over-estimation of precipitation inherent in the GEM background field (see Figure 45). Therefore it is likely the primary reason for improvements in hydrologic simulation over the crop land regions of the WPL as well. This finding demonstrates the importance of assimilated stations to the quality of CaPA data as a hydrological model input. Landcover on the other hand, serves as a surrogate to the difference in amount of assimilated stations since more useful stations at the agriculture zones are expected.

Using CaPA data appears to improve WATFLOOD^{TM} model simulations in some regions of the WPL (and WPR) basin; this, however, is not always the case. Two main factors so far hinder the performance of CaPA as hydrological forcing: 1) model setup plays an important role in how the model responds to changes in climate input. Regulated basins with storage have a tendency to decouple the rainfall-runoff relationship hence making the model less sensitive to climate input; and 2) sufficient assimilated stations are important to adjust the anomalies introduced by the GEM background field in the CaPA analysis.

5.5. GEM versus CaPA Comparison

CaPA uses a short range forecast from GEM as its background field, thus the quality of CaPA is closely tied to the quality of GEM. To further investigate the relationship between GEM and CaPA, analyses of CaPA and GEM using CDCD as a reference dataset were conducted over the CHU basin, using the three-step validation process

adopted for this thesis. The results for this analysis were performed by undergraduate research assistant (now Masters Candidate) Gregory Schellenberg under the supervision of KuangYin Zhao during winter 2013. The analyses are summarised below, with details included in Mr. Schellenberg's BSc thesis (Schellenberg, 2013)

5.5.1. P2P Analysis

Figure 45 shows the results from the seasonal P2P analysis comparing both CaPA and GEM relative to CDCD observations (Schellenberg, 2013). Percentage differences were calculated for each season during each year, and averaged over all stations in the CRB.

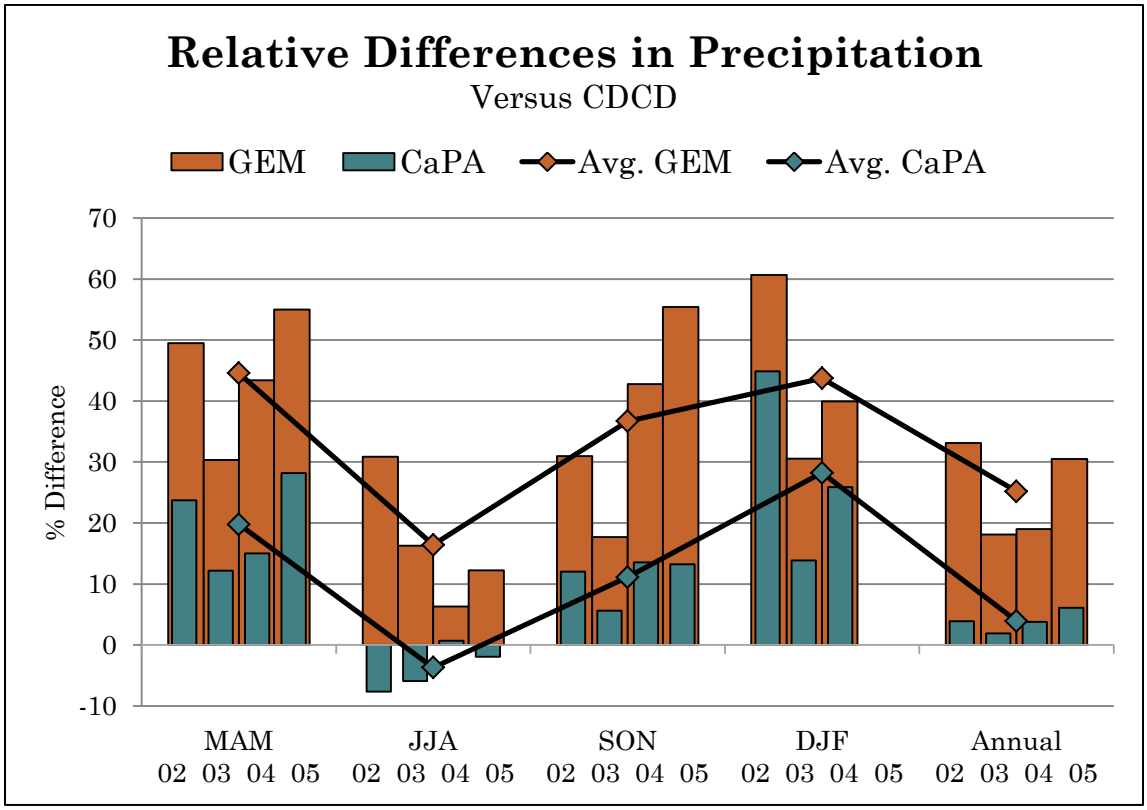

Figure 45: Seasonal P2P analysis in the CHU basin comparing GEM, CaPA and CDCD for all stations (reproduced with permission from Schellenberg, 2013)

This P2P analysis indicated that the inter-annual trend is consistent between both GEM and CaPA; however, GEM consistently over-estimates precipitation relative to CaPA and

CDCD. Therefore CaPAs general overestimation of precipitation appears to be passed down from the GEM background field, but is significantly reduced relative to GEM. This is expected since many of the CHU basins CDCD stations are assimilated into the CaPA analysis (Figure **8**), and would act to adjust the background field overestimation. Improvements in the precipitation field from GEM to CaPA thus directly reflect the added value of assimilated stations.

Similar to previous P2P analyses, the results obtained by Schellenberg (2013) also demonstrate that the difference between CaPA and CDCD during summer is insignificant relative to other seasons. Detailed discussions relating to the quality of summer precipitation in the CHU basin can be found in Section5.2.1.

5.5.2. M2M Analysis

An M2M analysis was also conducted by Schellenberg (2013) using both GEM and CaPA precipitation fields, with comparison to an interpolated CDCD (ITCD) field with lapse rate. Anomalies between GEM and ITCD were computed by Schellenberg (2013) and correlated to iso-lines extracted from the anomaly maps with the basin DEM underlain (e.g., Figure 46).

An example of the winter (DJF) precipitation M2M analysis is shown on Figure 46. Winter seems to be most heavily influenced by orographic effects, with anomaly iso-lines being most correlated with the underlain topography of the basin from the DEM. At locations where elevation and anomalies are correlated, iso-line patterns in CaPA are very similar to those in GEM. This finding seems to indicate that much of the correlation between CaPA anomalies and the DEM are directly inherited from the GEM background field, and that CaPAs orographically-influenced precipitation is inherited from GEM.

Overall, the M2M analysis revealed that assimilating stations into CaPA in the CHU basin applies an almost uniform adjustment to the GEM background; the GEM anomaly pattern does not appear to shift but rather only change in magnitude.

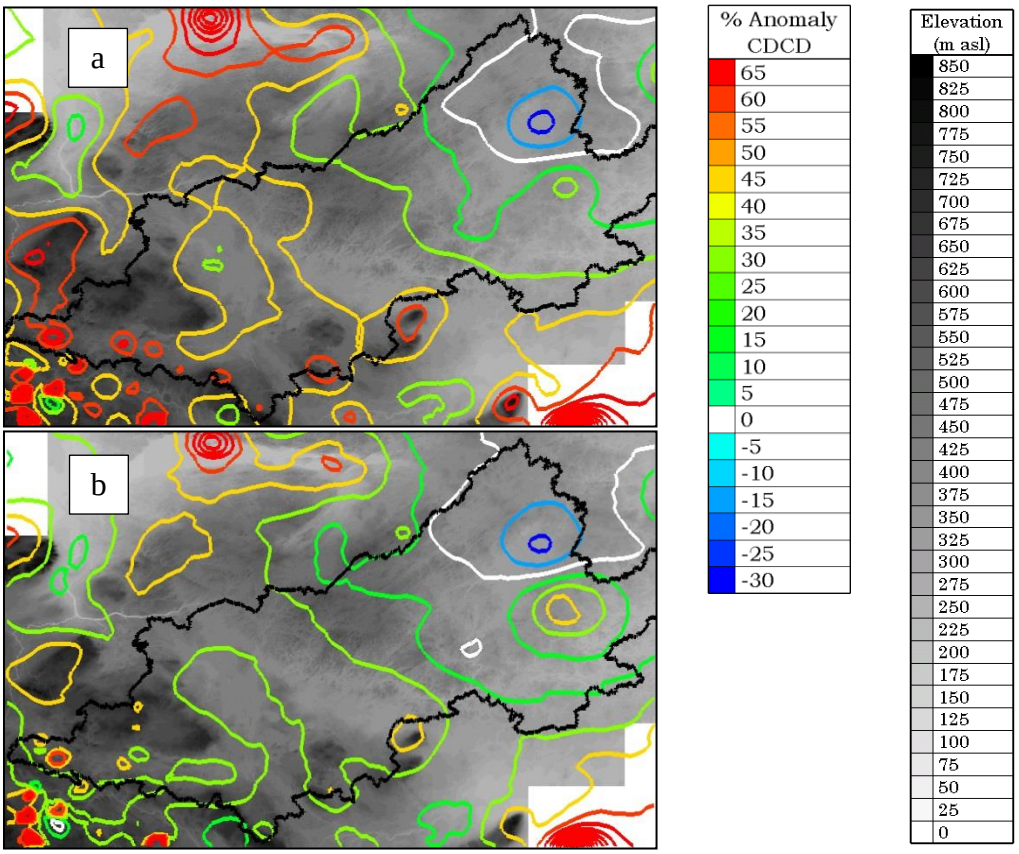

Figure 46: M2M analysis for winter in the CHU basin for anomalies in (a) GEM, and (b) CaPA relative to the ITCD precipitation field correlated with topography (reproduced with permission from Schellenberg, 2013)

5.5.3. Proxy Validation

Proxy validation using both GEM and CaPA as forcing for the CHU basin WATFLOOD™ model was also conducted, with the results compared by Schellenberg (2013) to observed flows at station 06CD002, Otter Rapids. The CHU basin WATFLOOD™ model for the Otter Rapids headwater gauge (119,000 km^2) was originally setup and calibrated (using ITCD forcing) by Bohrn (2012), and subsequently

used for this proxy validation exercise. Results of the proxy validation conducted by Schellenberg (2013) from 2002-2005 are presented in Figure 47.

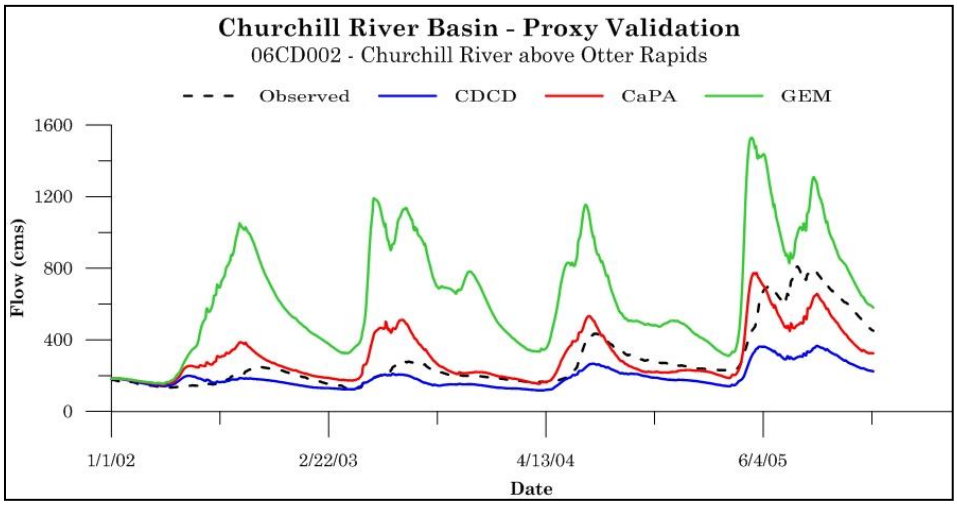

Figure 47: Proxy validation in the CHU basin at station 06CD002 (reproduced with permission from Schellenberg, 2013)

On Figure 47, the dashed black line represents the observed streamflow at Otter Rapids gauge (06CD002), the headwater (unregulated) region of the CHU basin; along with WATFLOOD™ simulations forced by ITCD (blue), CaPA (red), and GEM (green).

From Schellenberg's (2013) results, the ITCD-forced simulation is seen to under-estimate streamflow; while the GEM-forced simulation drastically over-estimates streamflow. Using CaPA as a WATFLOOD™ forcing, however, results in a significantly improved hydrologic simulation output and corresponding statistical scores (Table 9). From the P2P analysis, it was noted that assimilating stations reduced the over-estimation of precipitation inherited from GEM, so this result is not unexpected. What is perhaps interesting to note (that P2P could not diagnose), however, is that proxy analysis seems to indicate an under-estimation of precipitation from station (the ITCD precipitation field).

This finding is even more significant recognizing the model was calibrated using the ITCD fields.

Table 9: WATFLOOD™ simulation scores for the CHU basin using CDCD, GEM and CaPA as model forcing.

SIMULATION STATISTICS			
	CDCD	**GEM**	**CaPA**
Nash	0.24	-5.32	0.61
R^2	0.86	0.40	0.62
D_v %	-33.0	127	7.03

Schellenberg's (2013) results agree well with the P2P, M2M and proxy validation conducted in this study on the other watersheds in the Nelson-Churchill domain. In the CHU basin, CaPA decreased the positive errors of GEM-fed simulations as well as the negative errors in ITCD-fed simulations. CaPA fed simulations are able to improve both negative and positive errors, hence it appears that CaPA is more suitable for hydrological modeling than ITCD precipitation fields, and perhaps would perform even better should the model be re-calibrated using CaPA data.

5.6. Summary

The three-step validation procedure designed to assess CaPA included P2P, M2M and proxy (streamflow) analyses and was applied to CaPA version 2.30 to assess the suitability of CaPA for hydrological simulation in the Manitoba Hydro watershed domain (i.e., the Nelson-Churchill Basin).

From the P2P analyses; QQ plots, statistical analyses, and K-S tests demonstrate that CaPA is capable of simulating the recorded inter-annual precipitation variability; but

simulates reduced precipitation during summer at all basins except for CHU and NEL basins, which is likely due to fewer convective storms. Furthermore, CaPA shows increased precipitation in winter in all watersheds, likely the result of superior (relative to CDCD) winter solid precipitation prediction. Increased winter precipitation infers inferior solid precipitation observation records during winter months, making further winter precipitation validation impossible at this time. During fall, significant spatial variability in precipitation is observed among CDCD stations, and is well captured by CaPA.

Station observation records were interpolated both with and without lapse rates to produce spatially distributed station observation precipitation fields (ITCD). Anomalies between CaPA and the ITCD maps were calculated and histogram analyses performed. Results further support the conclusions from the P2P analyses regarding reduced estimates of summer precipitation and increased winter precipitation in CaPA. A supplementary analysis on storm-scale precipitation events alone suggests that the reduced summer precipitation in CaPA is caused by inadequate skill in simulating convective storm events owing to the CaPA analysis' resolution relative to the scale of such convective events. Meanwhile, the M2M analysis helped demonstrate CaPAs ability in simulation of large scale weather features, such as orographic precipitation effects over the Rocky Mountains in the headwater region of the SAS basin, and lake-effect precipitation over the WPL basin.

Histogram analyses emphasize the differences between ITCD precipitation with and without the use of a lapse rate to capture basin topographic detail. The analysis shows that the use of a lapse rate brings the distribution of ITCD precipitation closer to that of

CaPAs, yet the effect is weakest during summer when convective storms dominate. The two exceptions were noted in the CHU and NEL basins, which were shown to lie outside the extents of known summer convective storm regions. Overall, lapse rates effectively reduced the differences between CaPA and ITCD in 57% of the cases as shown in Table 6, keeping in mind that the Nelson-Churchill River basin is a relatively flat, low-relief basin overall and would not be expected to have significant orographic effects. Analysis of hypsometric curves indicates that the reduction in differences between CaPA and ITCD distributions are due to the distribution of observation stations at higher elevations rather than over the entire study domain. This finding indicates that incorporation of lapse rate functions should be used with caution in basins where the distribution of station elevations does not match the distribution of elevations in the model (i.e., from the DEM).

Proxy validation was conducted in the WPR and WPL basins, with a summary of the CHU basin analysis from Schellenberg (2013). In both the WPR and WPL basins, CaPA-forced WATFLOOD^{TM} simulations under-estimated streamflow more than ITCD-forced simulations. The WPR shows distinct spatial correlation among simulation scores, and was accordingly divided into two regions for further analyses. Comparison of precipitation and runoff in Regions A and B revels that the primary differences in average annual simulation scores is the result of differences between CaPA and ITCD precipitation for regions that are unregulated. Furthermore, basin size and regulation affected the net differences between runoff and precipitation change observed between CaPA and CDCD stations. Basin size was shown to have a significant impact on errors resulting from hydrologic simulation; due to smaller basin sizes in Region A, the

differences between CaPA-forced and ITCD-forced simulations are generally higher and more variable. Due to regulation in Region B, diagnosis of precipitation product error or differences was significantly masked. Similar to the WPR basin, spatial correlations were also found to exist in simulation scores in the WPL basin. The crop landcover region showed significant improvement in terms of volume using CaPA as model forcing; whereas the mixed forest region did not. The main cause of the improvement was found to be related to the number of assimilated observation stations within each region, with crop regions having more stations as a result of population density as well as model calibration. Schellenberg's work (2013) also showed that assimilated observation data decreases the positive bias inherited from GEM, hence reducing WATFLOOD^{TM} simulated runoff volume relative to GEM-derived runoff volumes.

The supplementary analyses done by Schellenberg (2013) in the CHU basin compared GEM directly to CaPA and highlighted the close relationship between the quality of CaPA and its background field. Assimilated precipitation data were shown to significantly improve background estimates from GEM. M2M analyses revealed that orographic precipitation effects in CaPA are inherited directly from GEM, resulting in anomalies as a result of GEMs coarser horizontal resolution. Proxy validation showed significant improvement in streamflow hydrographs in the CHU basin when CaPA is used as WATFLOOD^{TM} forcing, which is the direct result of under-estimated precipitation by the ITCD fields.

Chapter 6. Conclusions and Recommendations

6.1. CaPA Validation and Application Assessment

The analysis hitherto conducted is an attempt to assess CaPAs quality as a hydrological model forcing product over the Nelson-Churchill River Basin (NCRB). The study domain covers 1.3 million square kilometers of the Canadian Prairies and spans over three different ecological frameworks zones and two major Canadian climate zones. The analysis time period used was from 2002 to 2005, under which a three-step validation procedure is applied. CaPA data are compared directly to observations at point locations (P2P), and interpolated observations (M2M). Hydrograph simulations using CaPA and interpolated observation fields are also compared to observed streamflow.

Although it is expected that the performance of CaPA varies from basin to basin within the NCRB due to its large extent and physiographic variability, some common traits of the CaPA precipitation field can be derived from the validation process. The most notable of these traits, relative to observed data, include:

- reduced summer precipitation,
- increased winter precipitation,
- high spatial variability in fall precipitation, and
- Successful simulation of dominant weather patterns and orographic precipitation.

Although these traits are common among the NCRB sub-watersheds, they do not occur everywhere, and are specifically correlated with specific watershed characteristics. Decreased summer precipitation in CaPA is shown to be related to the occurrence and magnitude of convective storm events. Convective storms are prevalent in summer

across regions of the Prairie watersheds where landcover is dominated by the agricultural (crop) ecozone, with less frequent occurrence in watersheds within the Boreal forest region. This explains why summer precipitation is closer to CDCD and ITCD in the Nelson and Churchill River Basins, which reside within the Boreal forest region. CaPAs skill in simulating precipitation events other than convective storms is quite good; therefore overall the precipitation field represents an improvement over interpolated CDCD fields. Furthermore, CaPA shows improved skill when simulating large-scale weather features, with the GEM background field being shown to contribute the most to orographic precipitation prediction improvements. Application of CaPA as a hydrological input was demonstrated in the Winnipeg River, Lake Winnipeg and Churchill River Basins. Simulation results, and CaPAs performance as a hydrological forcing, vary from watershed-to-watershed and only the Churchill River basin showed consistent overall improvement. This is likely the result of poor quality station data generating errors in the interpolation CDCD precipitation field, which is attributed to the sparse climate data network in the Churchill basin.

Results from all three validation processes favor CaPA data for use as a precipitation field for hydrological investigation and modeling in the Churchill River Basin. Compared to the conventional WATFLOOD model input (ITCD) used in the CRB where density is sparse and suffers erroneous solid precipitation recordings, CaPA gains an advantage through its physically-based GEM background, and used of corrected observations from CDCD stations. Using CaPA in the Churchill River Basin, (and other watersheds like the Nelson River basin in a same ecological frame work) is recommended. The proxy validations for the Winnipeg River and Lake Winnipeg Basins

clearly show, however, that the universal application of CaPA as a hydrological input should not yet occur, and that CaPA should be used with caution. Proxy results in the Winnipeg River basin reveal that the difference between winter and spring precipitation between the English River system (Region B) and Lake of the Woods system (Region A) causes significant differences in hydrological simulation performance within the same watershed. Use of CaPA as hydrological forcing seems to improve simulations in Region A, but has little to no impact on Region B which is heavily regulated. Differences in model performance are due to seasonal (i.e., winter) differences in CaPAs performance over the two regions, and regulatory effects damping the rainfall-runoff relationship. This result highlights the importance of assessing hydrologic model performance in various sub-basins and not just at the outlet where error is averaged across the domain. CaPA does not however degrade model performance in the Winnipeg River Basin and therefore should continue to be explored as a hydrological forcing dataset.

Furthermore, proxy validation in the Lake Winnipeg basin shows that CaPA out performs ITCD in areas where more stations are assimilated into CaPA. More stations are therefore recommended to be assimilated into CaPA. Furthermore, Raddatz and Kern (1984) suggest that using radar or remote sensing data could be more cost effective than adding new stations while interpolating precipitation. Therefore radar and remote sensing data are also recommended to be assimilated or used during ITCD interpolation. On the other hand, the assimilation of falsely reported zero precipitation at stations within the basin causes worse results of CaPA-fed simulations; more simulations are required once the CaPA field has been corrected to verify this result. The validation procedure was robust enough to identify such station errors and provide meaningful feedback to CaPA

developers. The use of CaPA as hydrological forcing for simulations in the Saskatchewan, Assiniboine, and Red River basins should be approached with caution due to CaPAs difficulty in simulating convective storm (i.e., high precipitation) events that are significant sources of summer precipitation in these regions; contributing to up to 40% of summer precipitation across 50% of the study domain (Kochtubajda *et al.*, in preparation). Simulations during fall and winter, however, would be expected to improve, particularly in the headwater region of the Saskatchewan River due to the improved orographic effects and improved simulation of winter precipitation amounts.

Once an operational version of CaPA has shown adequate skill to be used as a universal hydrological input, it can be used for many different scientific applications such as climate change studies, hydrological model development and improve understanding of water balance and hydrological cycling.

6.2. Methodology Review

Analyses hitherto discussed include CaPA P2P, M2M and proxy validation. Each of the analyses is built upon its own assumptions, and hence the conclusions are restricted by these assumptions.

The P2P analysis assumes the CDCD observation data are 'truth', while in fact instrumental errors such as wind under-catch, station representativeness errors, and other uncertainties challenge this assumption. In addition, conclusions drawn from the P2P analysis are only valid at the location of the CDCD observation stations, and for the specific time period analysed (2002-2005). Station enhancements, upgrades to equipment, and/or failures in existing infrastructure and equipment all challenge the validity of the results outside the analysis time period. Future studies to investigate the

effects of known instrumental errors such as the wind under-catch on the outcome of the analysis are recommended; along with an extension of the period of analysis.

A hydrological model like WATFLOOD^{TM} utilizes distributed precipitation as input for weather data and hydrologic analyses. Therefore, for fair comparison of CaPA to pseudo-observed input data, the M2M analysis was performed by interpolating the observed precipitation at stations onto a distributed field covering the study spatial domain. Numerous factors such as the choice of distribution method, station density, station inclusion, and observation data quality introduce significant uncertainties to the ITCD map, and subsequent M2M analysis. Uncertainty introduced by interpolation method is very important in the M2M analysis, future studies are therefore recommended to incorporate evaluation scores that are independent of scale usually obtained as an averaged field of upscale and down scale field. Differences between CaPA and the interpolated CDCD precipitation field (ITCD) are calculated with and without lapse rate functions. Incorporating a lapse rate for interpolation of observed precipitation introduces uncertainties in terms of choice of lapse rate algorithm and assumptions made by the algorithm. Future studies with a better distribution of stations at different elevations are therefore recommended to test the lapse rate function, and M2M analysis with lapse rate.

Proxy validation utilizes CaPA and the interpolated CDCD precipitation fields as input to the hydrological model, and compares both simulated hydrographs to the observed hydrograph at a basin outlet. Model setup and calibration plays an important role during the proxy validation, and also contributes to uncertainties in the proxy analyses. Although model calibration is not altered from one forcing to the other, the calibration itself can dictate the hydrologic response to incoming precipitation (i.e., in the

distribution of water within the hydrologic cycle based on antecedent conditions). The more accurate the model calibration, the more accurately changes in streamflow response can be associated to changes in precipitation fields. To minimize model calibration uncertainties, the model is setup and calibrated during a different time period than this study period. The differences between streamflow simulated using ITCD and CaPA data are directly compared, and associated directly to changes in the forcing data (and not to model performance). The observed hydrograph is used solely as a reference point for model performance and statistical computation. Nevertheless, model parameters still heavily influence the outcome of the simulation by choosing how water (precipitation) is distributed internally in the model, and how much streamflow is generated from that input. Further calibration using CaPA data (for both Winnipeg River and Lake Winnipeg basins) compared to calibrations from ITCD data (for Winnipeg River basins) are recommended to investigate the effect of calibration on analysis results. More sophisticated analyses are recommended to further examine the uncertainties in model parameterization on proxy validation outcome. One such analysis could utilize a coupled climate–hydrological model such as MESH so that the erroneous hydrological parameter can be detected though climate- land surface feedbacks as it simulates both land and atmospheric process physically and simultaneously.

References

Agriculture and Agri-Food Canada. (2013 October). National Ecological Framework. In *Agriculture and Agri-Food Canada*. Retrieved 2013 October 20th, from http://sis.agr.gc.ca/cansis/nsdb/ecostrat/index.html.

Ashiq, M. W. , Zhao, C. Y. , Ni, J. and Akhtar, M. (2010): GIS based high-resolution spatial interpolation of precipitation in mountain-plain areas of Upper Pakistan for regional climate change impact studies, *Theoretical and Applied Climatology*, 99: 239-253 .

Becker E. J., Berbery E. Hugo, Wayne R. H. (2009). Understanding the Characteristics of Daily Precipitation over the United States Using the North American Regional Reanalysis. *Journal of Climate*, 22:23, 6268-6286.

Beven K., Robert E. (2004). Horton's perceptual model of infiltration processes. *Hydrological processes*, 18: 3447-3460.

Beven K.J. (1995). Linking parameters across scales: subgrid parameterizations and scale dependent hydrological models. *Hydrological Processes*, 9: 507–525.

Bohrn S. (2012). Multi-Model uncertainty Assessment under Climate Change in the Churchill River Basin. M.Sc. thesis, Department of Civil Engineering, University of Manitoba.

Bukovsky, Melissa S., Karoly David J. (2007). A Brief Evaluation of Precipitation from the North American Regional Reanalysis. *J. Hydrometeor*, 8: 837–846.

Canadian Atlas Online (2013). Extreams of weather. In Canadian Atlas Online. Retrieved September, 2013, from http://www.canadiangeographic.ca/atlas/themes.aspx?id=weather&lang=En.

Charrier, R., Li, Y. (2012). Assessing resolution and source effects of digital elevation models on automated floodplain delineation: A case study from the Camp Creek Watershed, Missouri. *Applied Geography*, 34: 38-46.

Choi, W, Kim, S. J, Rasmussen, P. F., Moore, A. R. (2009). Use of the North American Regional Reanalysis for Hydrological Modeling in Manitoba. *Canadian Water Resources Journal*, 34(1): 17-36.

Côté, J., Sylvie G., André M., Alain P., Michel R., and Andrew S. (1998): The Operational CMC–MRB Global Environmental Multiscale (GEM) Model. Part I: Design Considerations and Formulation. *Monthly Weather Review (American Meteorological Society)* 126 (6): 1373–1374. Bibcode:1998MWRv..126.1373C

Davison B., Fortin V., Lespinas F. Mekonnen M., Zhao K., Stadnyk T., Chun S., and Newsom D., (In Preparation). Direct Verification of Gridded Precipitation

Products over Selected Areas. Manuscript in preparation for submission to *Monthly Weather Review* (late 2013).

Dawson C.W., Abrahart R.J., Shamseldin A.Y. and Wilby R.L. (2006). Flood estimation at ungauged sites using artificial neural networks. *Journal of Hydrology*, 319 (1-4): 391-409.

Dooge, J. C. I. (1959). A General Theory of the Unit Hydrograph. *Journal of Geophysical Research*, 64 (2): 241-256.

Easterling, D. R., Karl T. R., Mason E.H., Hughes P. Y., and Bowman D. P. (1996). United States Historical Climatology Network (U.S. HCN) Monthly Temperature and Precipitation Data. ORNL/CDIAC-87, NDP-019/R3. Carbon Dioxide Information Analysis Center, Oak Ridge National Laboratory, U.S. Department of Energy, Oak Ridge, Tennessee.

Environment Canada, (2013). Historical Climate Data. In Environment Canada Weather. Retrieved 2013, Aug, from http://climate.weather.gc.ca/.

Fassnacht, S.R. (2004). Estimating alter-shielded gauge snowfall under catch, snowpack sublimation, and blowing snow transport at six sites in the coterminous United States. *Hydrological Processes*, 18(18): 3481-3492.

Geobase. (2013). Data. In *Geobase*. Retrieved September, 2013, from http://www.geobase.ca/geobase/en/data/index.html.

Goodison, B. E., P. Y. T. Louie, and D. Yang, (1998). WMO solid precipitation measurement intercomparison. WMO Instruments and Observing Methods Report 67, WMO/TD-872, 212 p.

Goodison, B. E. (1978). Accuracy of Canadian snow gage measurements. *J. Appl. Meteor.*, 17: 1542–1548.

Haberlandt, U. and Kite G. W. (1998). Estimation of daily space-time precipitation series for macroscale hydrological modeling. *Hydrological Processes*, 12: 1419-1432.

Heistermann, M. and Kneis, D. (2011). Benchmarking quantitative precipitation estimation by conceptual rainfall-runoff modeling. *Water Resource. Res.*, 47: W06514.

Hildebrand, F.B. (1956) *Introduction to numerical analysis*, New York, McGraw-Hill Inc.

Hoerling, M.P., Kumar, A. and Zhong, M. (1997). El Niño, La Niña and the nonlinearity of their teleconnections. *Journal of Climate*, 10: 1769-1786.

Hutchinson M. F. (1991). The application of thin plate smoothing splines to continent-wide data assimilation. In:. Jasper JD (ed.) *BMRC Research Report No.27, Data Assimilation Systems*. Melbourne: Bureau of Meteorology: 104-113.

Jain A., Sudheer K.P. and Srinivasulu S. (2004). Identification of physical processes inherent in artificial neural network rainfall runoff models, *Hydrological Processes*, 18: 571–583.

Justel, A., Peña, D. and Zamar, R. (1997) A multivariate Kolmogorov-Smirnov test of goodness of fit, *Statistics & Probability Letters*, 35(3), 251-259.

Kållberg, P., A. Simmons, S. Uppala, and M. Fuentes (2004). The ERA-40 Archive. *ERA-40 Project Report Series*, Vol. 17, ECMWF, 31p.

Kanamitsu, M., Ebisuzaki W., Woollen J., Yang S.-K., Hnilo J.J., Fiorino M., Potter G.L. (2002). NCEP-DOE AMIP-II Reanalysis (R-2). *Bull. Amer. Meteor. Soc.*, 83: 1631-1643.

Kite, G.W. (1995). The SLURP Model, Chapter 15 in: *Computer Models of Watershed Hydrology*, V.P. singh (ed.) Water Resource Publications, Colorado, 521-562.

Klyszejko, E.S. (2007). Hydrologic Validation of Real-Time Weather Radar VPR Correction Methods. Master's thesis, Department of Civil and Environmental Engineering, University of Waterloo, Waterloo, ON: 276p. http://uwspace.uwaterloo.ca/handle/10012/2635

Kochtubajda B., Brimelow J., Hanesiak J., Stewart R. and Burrows W. (2013). Contributions of thunderstorm rainfall to warm season precipitation across the Prairies from 2009 to 2011. Manuscript in preparation.

Kouwen, N. (2012). WATFLOOD/WATROUTE Hydrological model routing and flood forecasting system. Waterloo, ON: Unpublished manuscript. 264p.

Krause P, Boyle DP, Base, F. (2005). Comparison of different efficiency criteria for hydrological model assessment. *Advances in Geosciences* 5: 89–97.

Lackmann, G. (2011), Midlatitude Synoptic Meteorology: Dynamics, Analysis, and Forecasting, Boston, MA: American Metrological Society.

Lange N. (1999). New mathematical approaches in hydrological modelling. An application of Artificial Neural Networks. *Physics and Chemistry of the Earth*, 24(1): 31–35.

Lespinas F., Fortin V., Roy G., Rasmussen P. and Stadnyk T. (In Preparation) Performance evaluation of the Canadian Precipitation Analysis (CaPA). Manuscript in preparation for submission to Water Resources Research.

Lin, Y., K.E. Mitchell, E. Rogers, M.E. Baldwin, and G.I. DiMego, (1999). Test assimilations of the real-time, multi-sensor hourly precipitation analysis into the

Mahfouf, J.-F., Brasnett, B. and Gagnon, S. (2007). A Canadian precipitation analysis (CaPA) project: Description and preliminary results. *Atmosphere-Ocean*, 45: 1–17.

Mekis, É and Vincent L.A., 2011: An overview of the second generation adjusted daily precipitation dataset for trend analysis in Canada. Atmosphere-Ocean, 49 (2), 163-177.

Mo, K.C., Chelliah M., Carrera M.L., Higgins R.W., and W. Ebisuzaki, 2005: Atmospheric moisture transport over the United States and Mexico as evaluated in the NCEP Regional Reanalysis. *J. Hydrol.*, 6, 710-728.

Manitoba Water Stewardship. (2011). State of Winnipeg Lake 1999-2007. Retrieved 2013, September, from http://www.gov.mb.ca/ waterstewardship/water_quality/state_lk_winnipeg_report/. 222p.

Mesinger, F., DiMego G., Kalnay E., Mitchell K., ShafranP. C. ,Ebisuzaki W., Jovic D., Woollen J., Rogers E., Berbery E.H., Ek M.B., Fan Y., Grumbine R. , Higgins W., Li H, Lin Y., Manikin G., Parrish D., and Shi W. (2006). North American Regional Reanalysis *Bull. Amer. Meteor. Soc.,* 87: 343-360.

Miner, T. J., and Fritsch J. M. (1997). Lake-effect rain events. *Mon. Wea. Rev*., 125: 3231–3248.

Natural Resource Canada, Agriculture and Agri-Food Canada and Environment Canada, Ecosystem stratification Working Group (2009). Ecosystem of Canada, Retrieved 2013, September, from http://atlas.nrcan.gc.ca/site/english/maps/ forestry. html

Natural Resource Canada. (2013). October Mean Total Precipitation. In GeoGratis (API) v1.4. Retrieved September, 2013, from http://geogratis.gc.ca/api/en/nrcan-rncan/ess-sst/d8bb2bae-8893-11e0-9719-6cf049291510.html.

National Research Council Canada. (December, 2012). Green Kenue™: Software tool for hydrologic modellers. In National Research Council Canada. Retrieved September, 2013, from http://www.nrc-cnrc.gc.ca/eng/solutions/advisory-green_kenue_index .html.

NCEP Eta model. Preprints, 8th Conf. on Mesoscale Meteorology, Boulder, CO, *Amer. Meteor. Soc*., 341-344.

Newlands N.K., Davidson A., Howard A., Hill H. (2009). Validation and inter-comparison of three methodologies for interpolating daily precipitation and temperature across Canada. *Environmetrics*, 22(2):205-223.

NOAA (2012). The USHCN Version 2 Serial Monthly Datasets. NOAA. Retrieved 2013, Aug, from http://www.ncdc.noaa.gov/oa/climate/research/ushcn/.

Nieto, S., M. D. Frías, and C. Rodríguez-Puebla. (2004): Assessing two different climatic models and the NCEP–NCAR reanalysis data for the description of winter precipitation in the Iberian peninsula. *Int. J. Climatol.*, 24, 361–376.

Pechlivanidis I.G., Jackson B., McIntyre N., Wheater H.S. (2011). 'Catchment scale hydrological modelling: A review of model types, calibration approaches and uncertainty analysis methods in the context of recent developments in technology and applications'. *Global NEST Journal*, 13(3): 193-214.

Pietroniro A, Fortin V., Kouwen N., Neal C., Turcotte R., Davison B., Verseghy D., Soulis E. D., Caldwell R., Evora N., and Pellerin P. (2007): Development of the MESH modelling system for hydrological ensemble forecasting of the Laurentian Great Lakes at the regional scale, *Hydrol. Earth Syst. Sci.*, 11, 1279-1294

Pietroniro, A., Prowse T.D., Hamlin L., Kouwen N. and Soulis E.D. (1996). Application of a Grouped Response Unit Hydrologic Model to a Northern Wetland region. *Hydrological Processes*, 10: 1245-1261.

Province of Manitoba (2013). Portage La' Prairie Diversion. In *Province of Manitoba*. Retrieved 2013, September, from http://www.gov.mb.ca/flooding/fighting/portage_diversion.html.

Raddatz R. L. and Hanesiak J. M. (2008). Significant summer rainfall in the Canadian Prairie Provinces: modes and mechanisms 2000–2004, *International Journal of Climatology*, 28: 1607–1613

Raddatz , R.L. and Kern J. (1984). An Assessment of the Near Real-Time Rainfall Network on Canada's Eastern Prairies. *Atmosphere Ocean,* 22(4):474-483

Rasmussen, R., Baker B., Kochendorfer J., Meyers t., Landolt S., FischerA.P., Black J., Thériault J.M., Kucera P., Gochis D., Smith C., Nitu R., Hall M., Ikeda K., Gutmann E. (2012). How Well Are We Measuring Snow: The NOAA/FAA/NCAR Winter Precipitation Test Bed. *Bull. Amer. Meteor. Soc.*, 93: 811–829.

Ratto M., Young P.C., Romanowicz R., Pappenberger F., Saltelli A. and Pagano A. (2007). Uncertainty, sensitivity analysis and the role of data based mechanistic modelling in hydrology. *Hydrology and Earth System Sciences*, 11: 1249-1266.

Ruiz-Barradas, A., and Nigam, S. (2006). Great Plains hydroclimatic variability: The view from the North American regional reanalysis. *Journal of Climate,* 19 (12): 3004–3010.

Schellenberg G.J (2013). Evaluation of the Canadian precipitation analysis (CaPA) for hydrological modelling of the Churchill River basin. BSc Thesis, Department of Civil Engineering, University of Manitoba, Winnipeg MB. 79p.

Schertzer, W.M. (1997). Fresh water lakes, Chapter 6, p. 124-148.In W.G. Bailey, T.R. Oke and W.R. Rouse (ed.), *Surface climates of Canada*. McGill-Queens University Press. 369 p.

Shabbar, A. and Khandekar, M. (1996). The impact of El Niño-Southern Oscillation on the temperature field over Canada. *Atmosphere-Ocean* 34:401-416.

Shabbar, A., Bonsal, B. and Khandekar, M. (1997). Canadian precipitation patterns associated with the Southern Oscillation. *Journal of Climate*, 10: 3016-3027.

Spence C., Blanken P., Hedstrom N., Fortin, V., Wilson H. and Lenters J.D. (2011). Evaporation from Lake Superior: 1. Physical controls and processes. *Journal of Great Lakes Research*, 37(4): 707-716.

Stisen, S. and Sandholt, I. (2010). Evaluation of remote-sensing-based rainfall products through predictive capability in hydrological runoff modelling. *Hydrol. Process.*, 24: 879–891.

Stephenson G.R. and Freeze R.A. (1974). Mathematical simulation of subsurface flow contributions to snowmelt runoff, Reynolds Creek watershed, Idaho. *Water Resources Research*, 10: 284-294.

Stadnyk-Falcone, T.A. (2008). Mesoscale Hydrological Model Validation and Verification using Stable Water Isotopes: The isoWATFLOOD Model. PhD Thesis, Department of Civil and Environmental Engineering, University of Waterloo, Waterloo, ON. 385p. http://hdl.handle.net/10012/3970

Syewoon H., Graham W. D., Adams A., Geurink J. (2013). Assessment of the utility of dynamically-downscaled regional reanalysis data to predict stream flow in west central Florida using an integrated hydrologic model. *Regional Environmental Change*, 13(1):69-80.

Thiessen, A.H. (1911). Precipitation averages for large areas. *Monthly Weather Rev.*, 39: 1082–1084.

Tolika, K., Maheras, P., Flocas, H. A., and Imitriou, A. A-P. (2006). An evaluation of a General Circulation Model (GCM) and the NCEP-NCAR Reanalysis data for winter precipitation in Greece. *International Journal of Climatology*, 26: 935–955.

Uppala, S.M. , Kallberg, P.W. , Simmons, A.J. , Andrae, U., Costa Bechtold, V. Da , Fiorino, M. , Gibson, J.K. , Haseler, J. , Hernandez, A. , Kelly, G.A. , Li, X. , et al. (2005): The Era-40 Re-Analysis. In: Quarterly Journal of the Royal Meteorological Society 131, 2961-3012.

USGS (2012). The USGS Land Cover Institute (LCI). In *USGS*. Retrieved September, 2013, from http://landcover.usgs.gov/uslandcover.php.

Wheater H.S. (2002). Progress in and prospects for fluvial flood modeling. *Philosophical Transactions of the Royal Society of London, Series A-Mathematical Physical and Engineering Sciences*, 360: 1796.

Wheater H.S., Jakeman A.J., Beven K.J., Beck M.B. and McAleer M.J. (1993). Progress and directions in rainfall-runoff modelling. In Jakeman A.J. (Ed.), Beck M.B. (Ed.), McAllen M.J. (Ed.), *Modelling change in environmental systems*(pp 101-132), Chichester New York: Wiley.

Young P.C. (2003). Top-down and data-based mechanistic modelling of rainfall-flow dynamics at the catchment scale. *Hydrological Processes*, 17 (11): 2195-2217.

Young P.C., Jakeman A.J. and Post D.A. (1997). Recent advances in the data-based modelling and analysis of hydrological systems. *Water Science and Technology*, 36 (1): 99-116.

Appendices

Appendix A: Major Land Cover Types

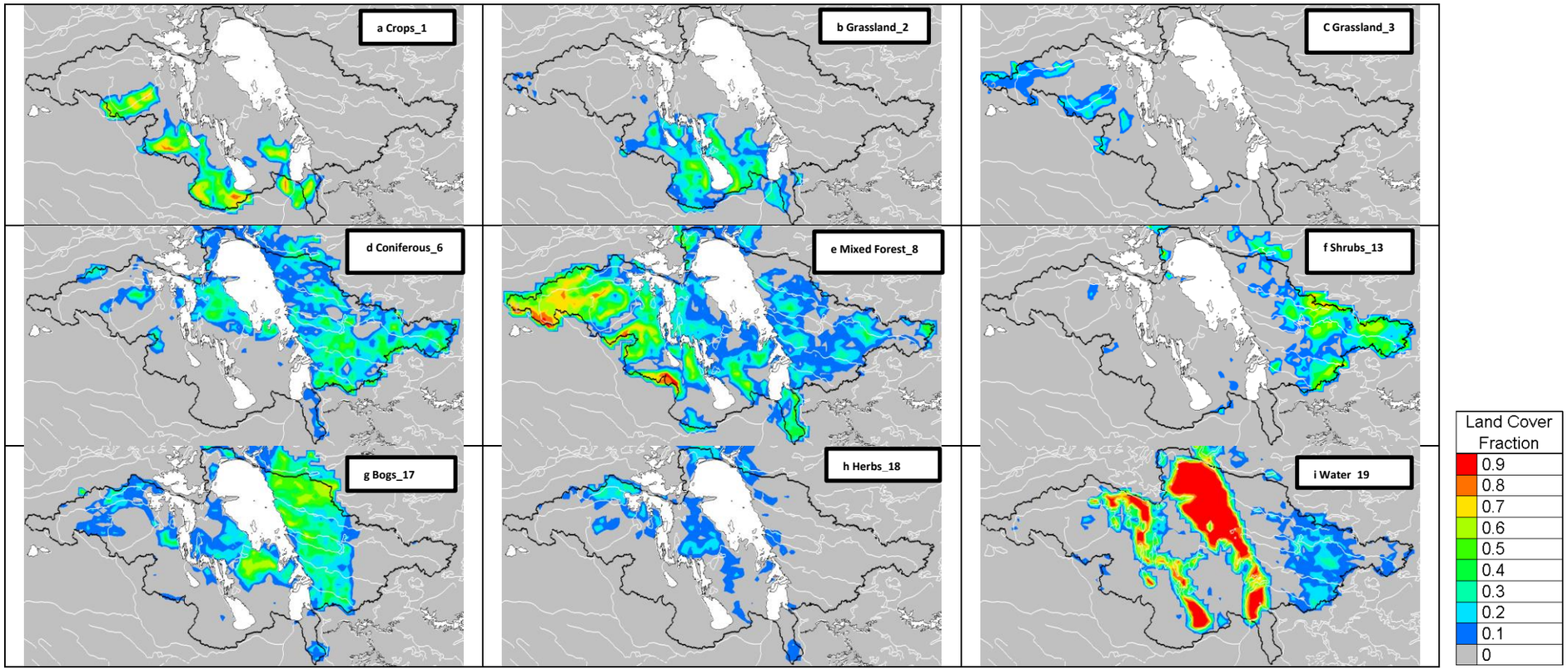

Figure A-1: Major Land covers at Lake Winnipeg Basin labeled from a to j and their corresponding land cover names

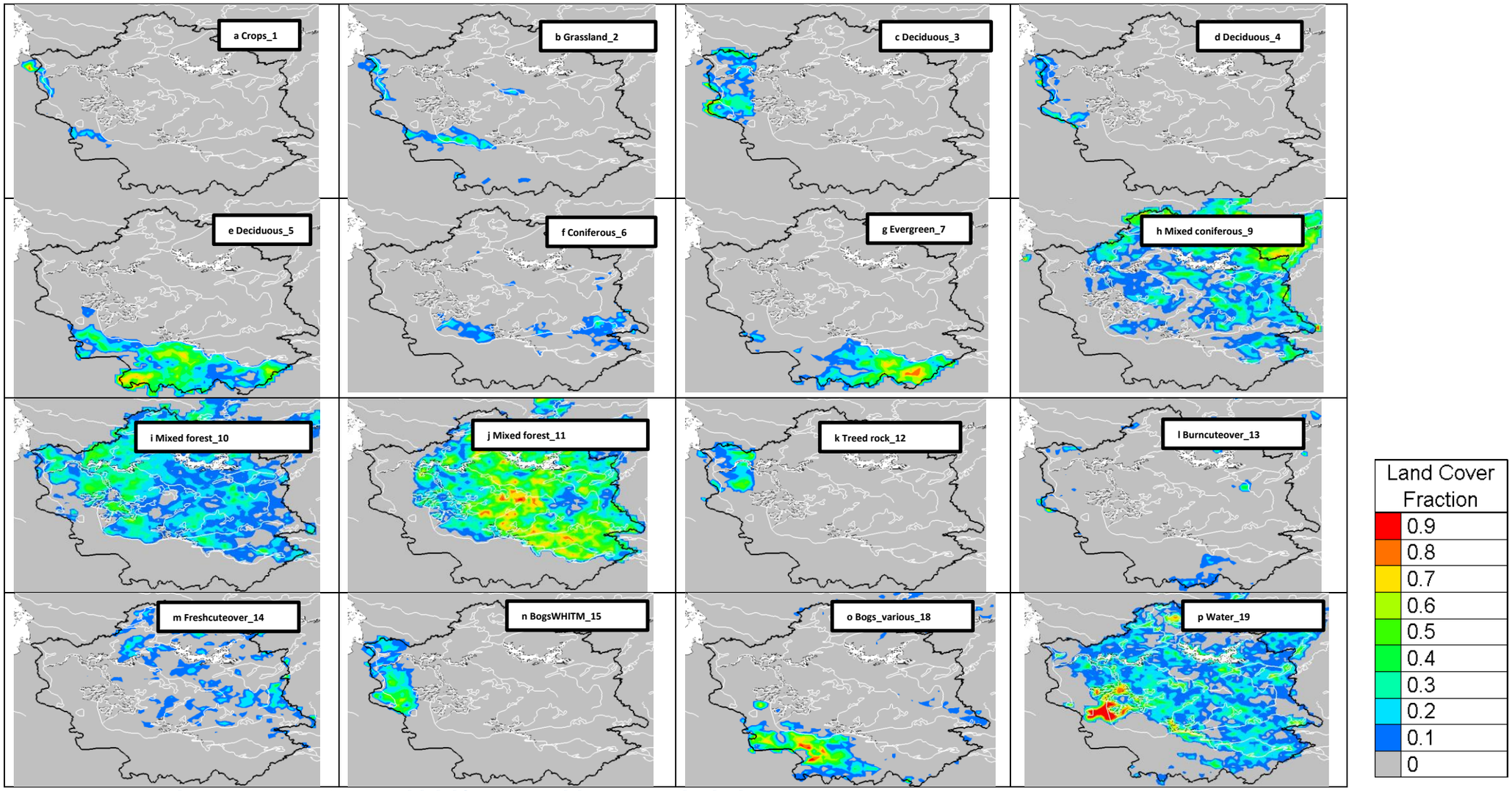

Figure A-2: Major Land covers at Winnipeg River Basin labeled from a to p and their corresponding land cover names.

Appendix B: Seasonal QQ Plots

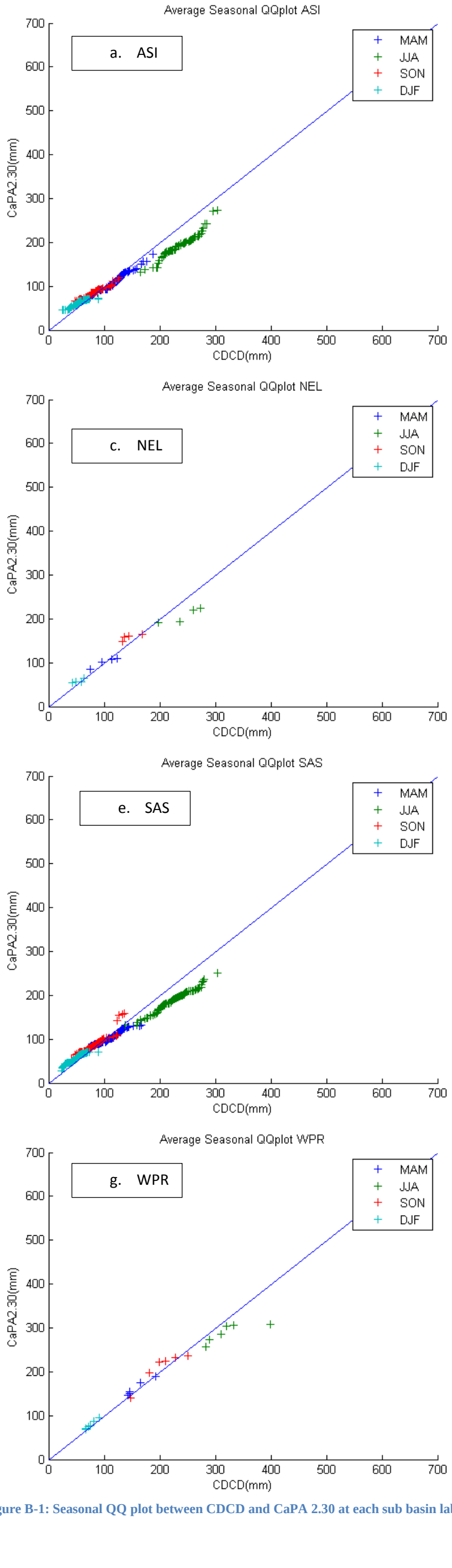

Figure B-1: Seasonal QQ plot between CDCD and CaPA 2.30 at each sub basin labeled from a to g, and their corresponding sub basin names

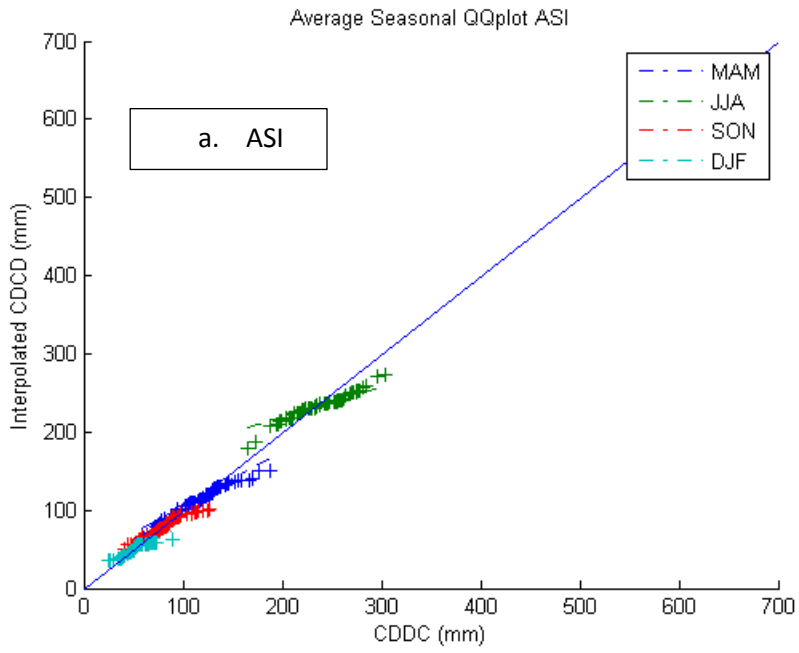

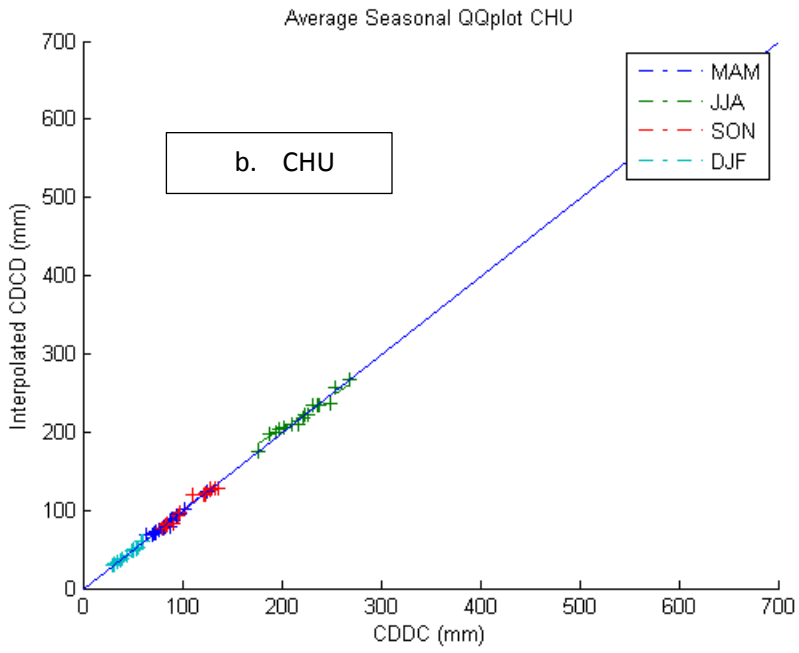

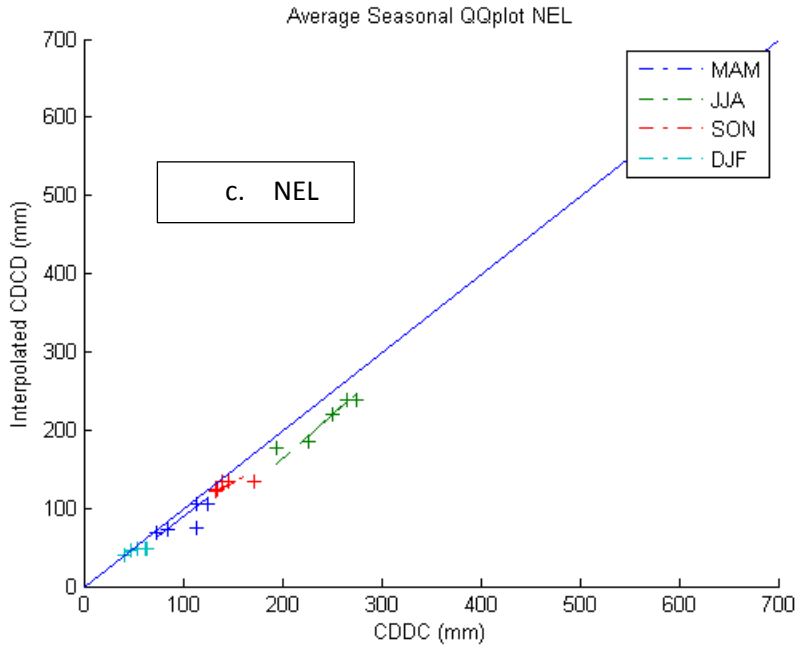

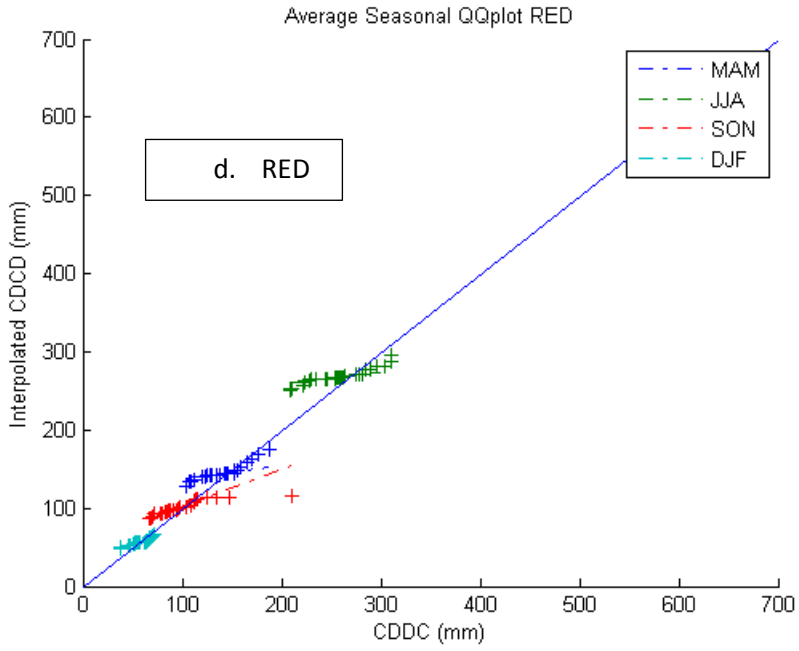

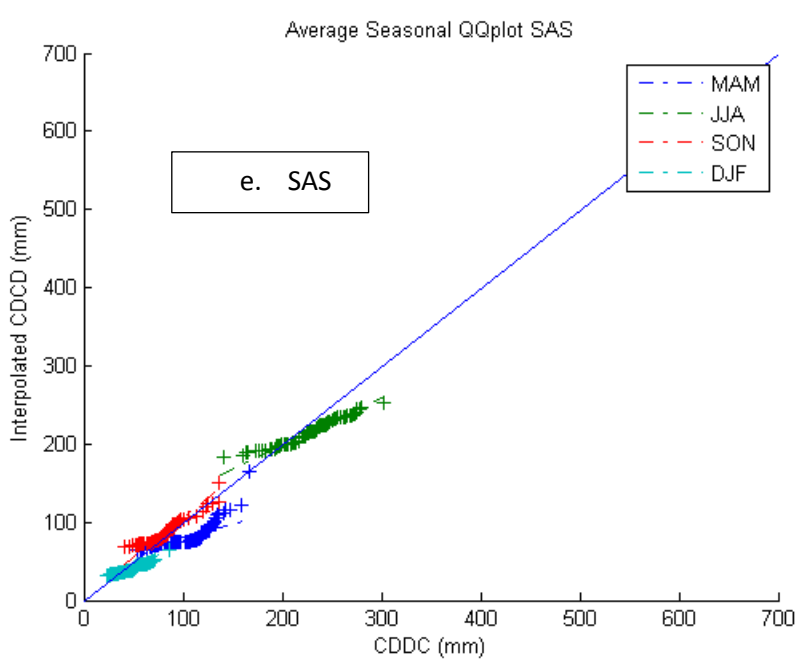

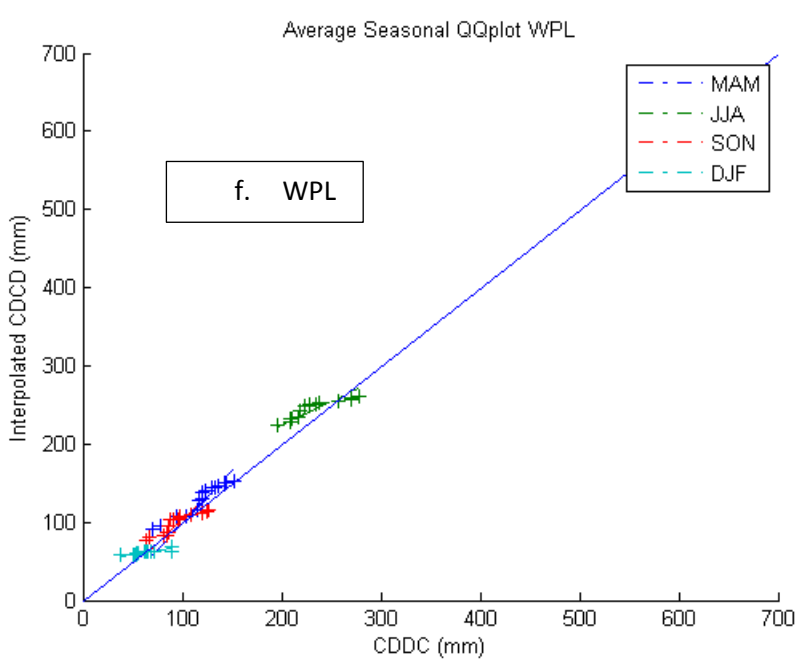

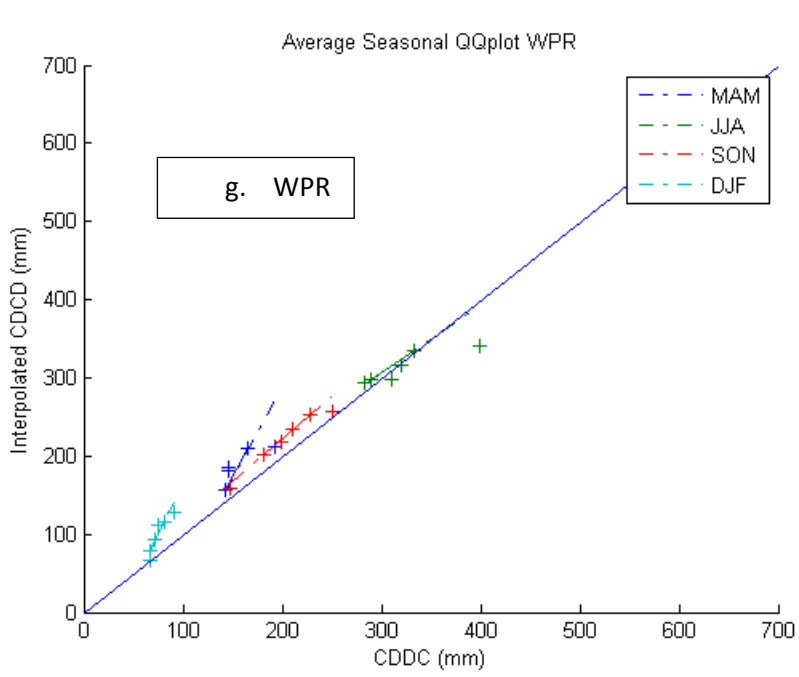

Figure B-2: Seasonal QQ plot between CDCD and CaPA 2.30 at each sub basin labeled from a to g, and their corresponding sub basin names

Appendix C: M2M results

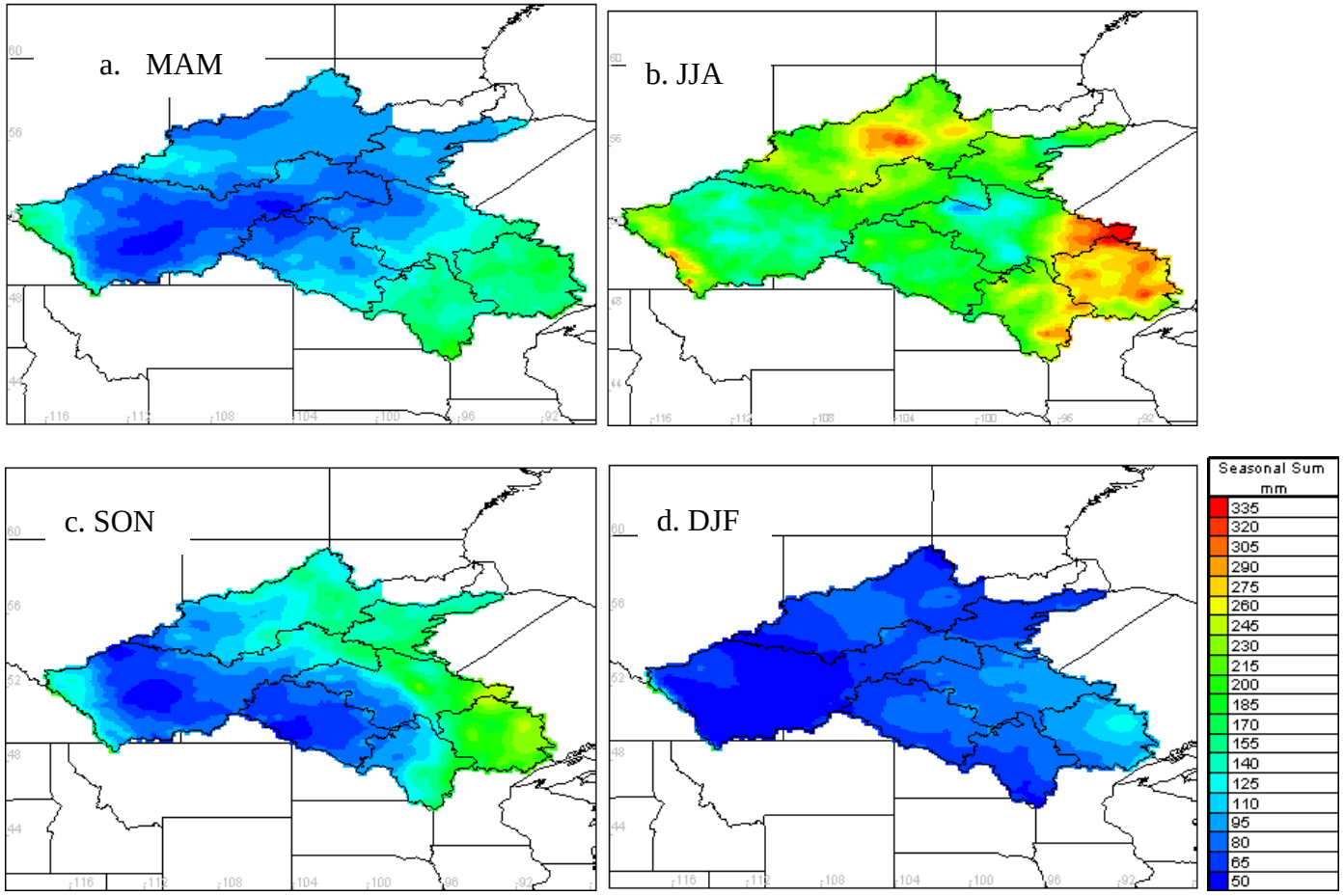

Figure C-1: CAPA seasonal Precipitation averaged over 2002 to 2005, label from a to d and their corresponding seasons

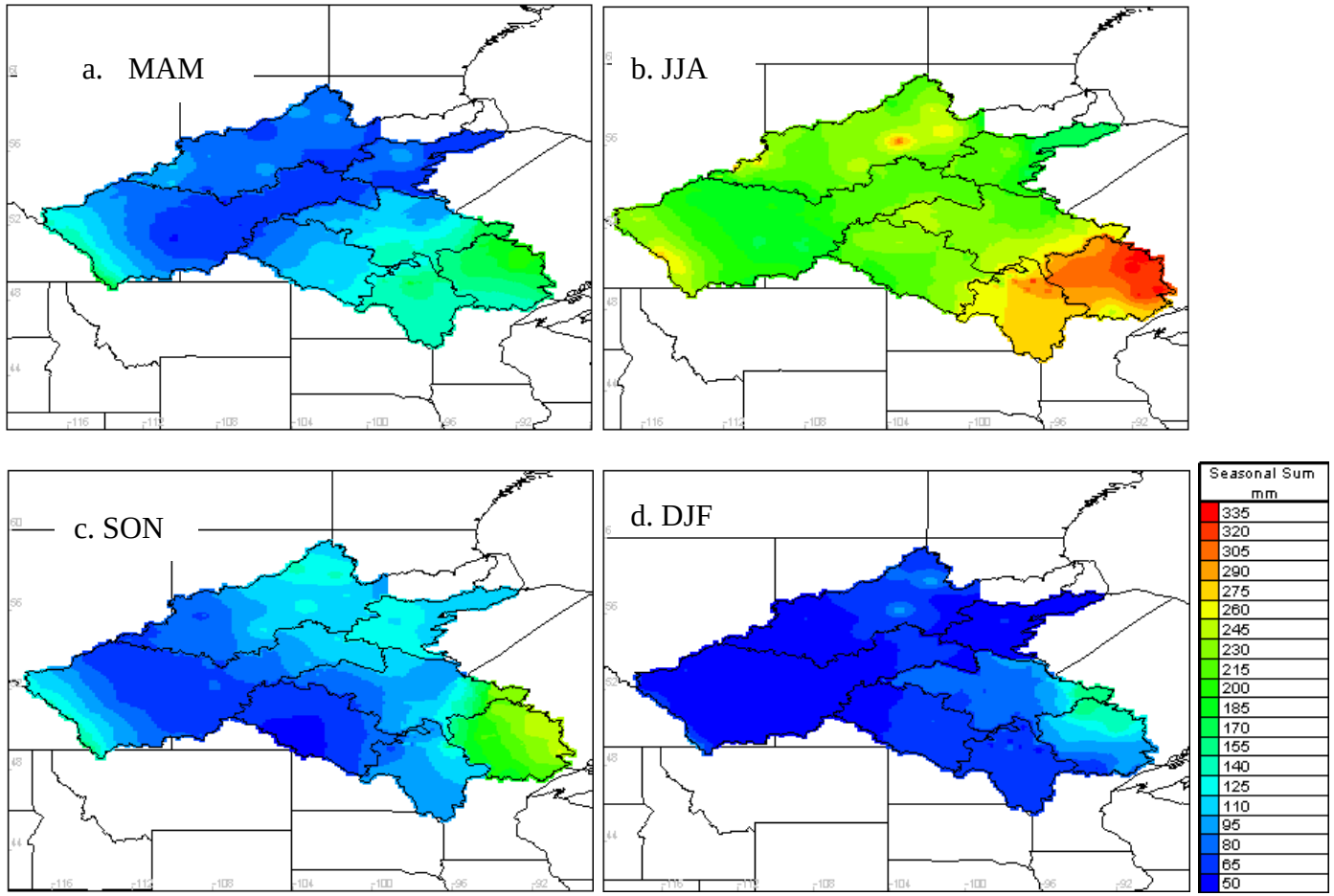

Figure C-2: CDCD seasonal Precipitation averaged over 2002 to 2005, label from a to d and their corresponding seasons

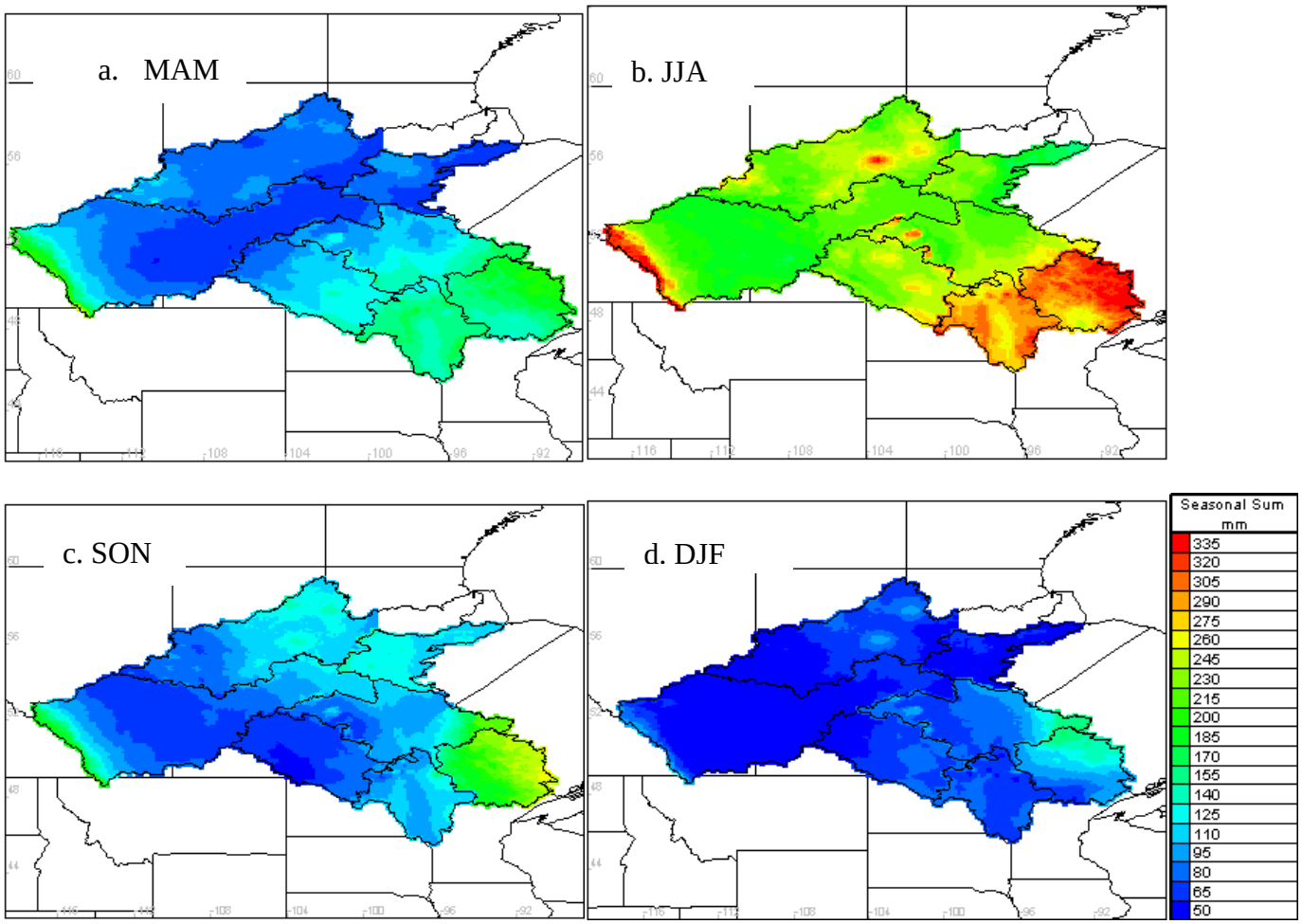

Figure C-3: ITCD seasonal Precipitation averaged over 2002 to 2005, label from a to d and their corresponding seasons

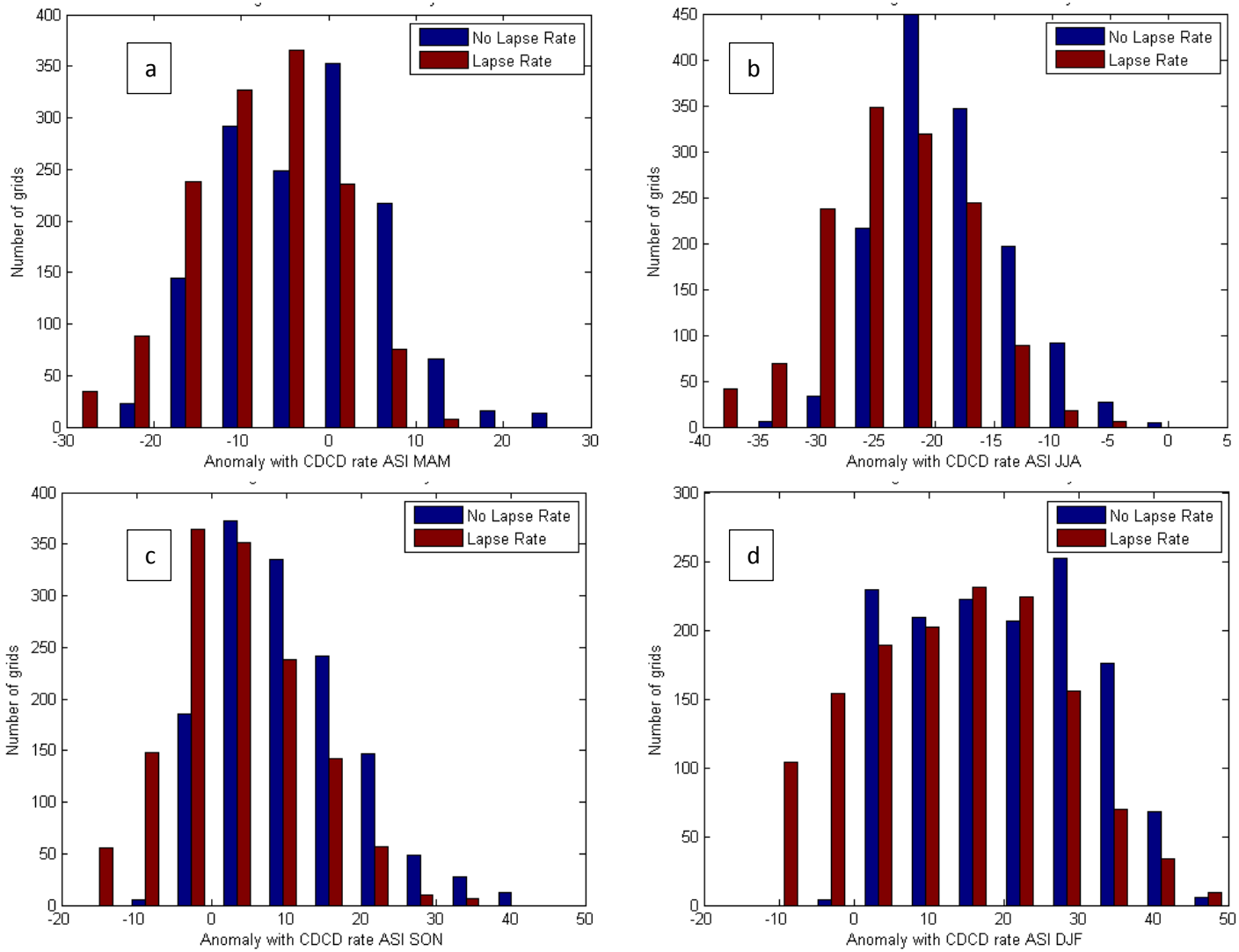

Figure C-4: Histogram of seasonal anomalies for the Assiniboine River Basin for (a) summer, (b) fall, (c) winter, and (d) spring

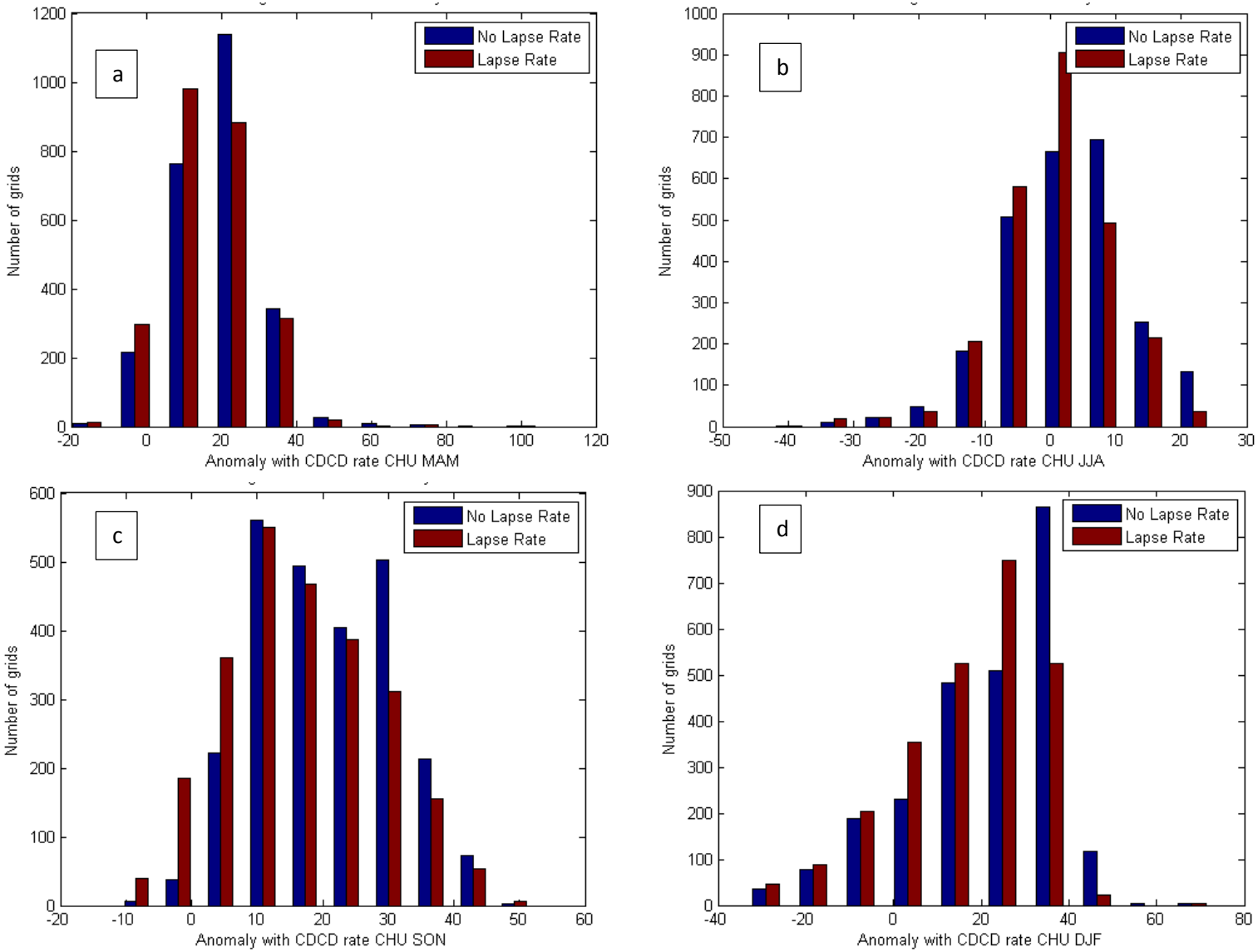

Figure C-5: Histogram of seasonal anomalies for the Churchill River Basin for (a) summer, (b) fall, (c) winter, and (d) spring

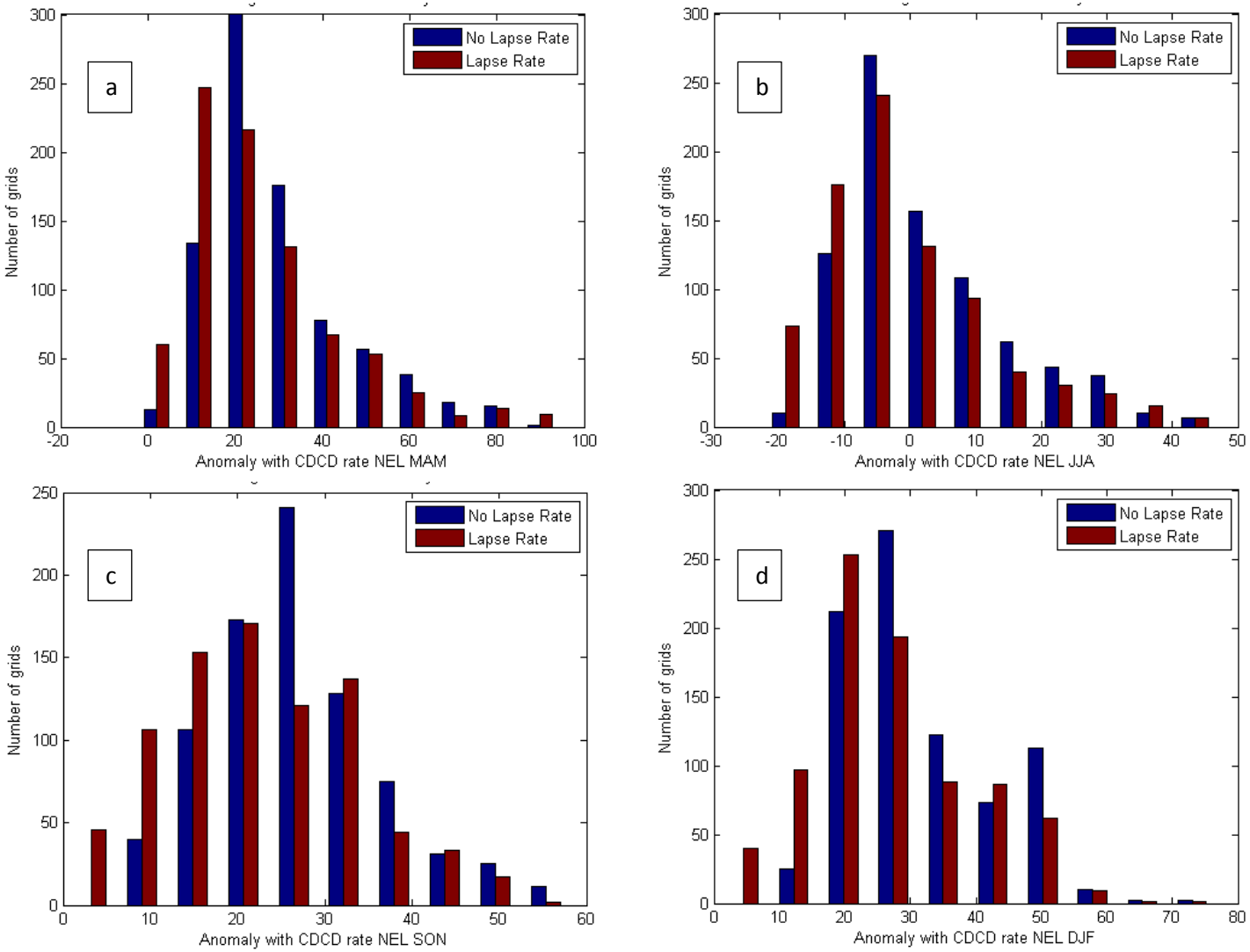

Figure C-6: Histogram of seasonal anomalies for the Nelson River Basin for (a) summer, (b) fall, (c) winter, and (d) spring

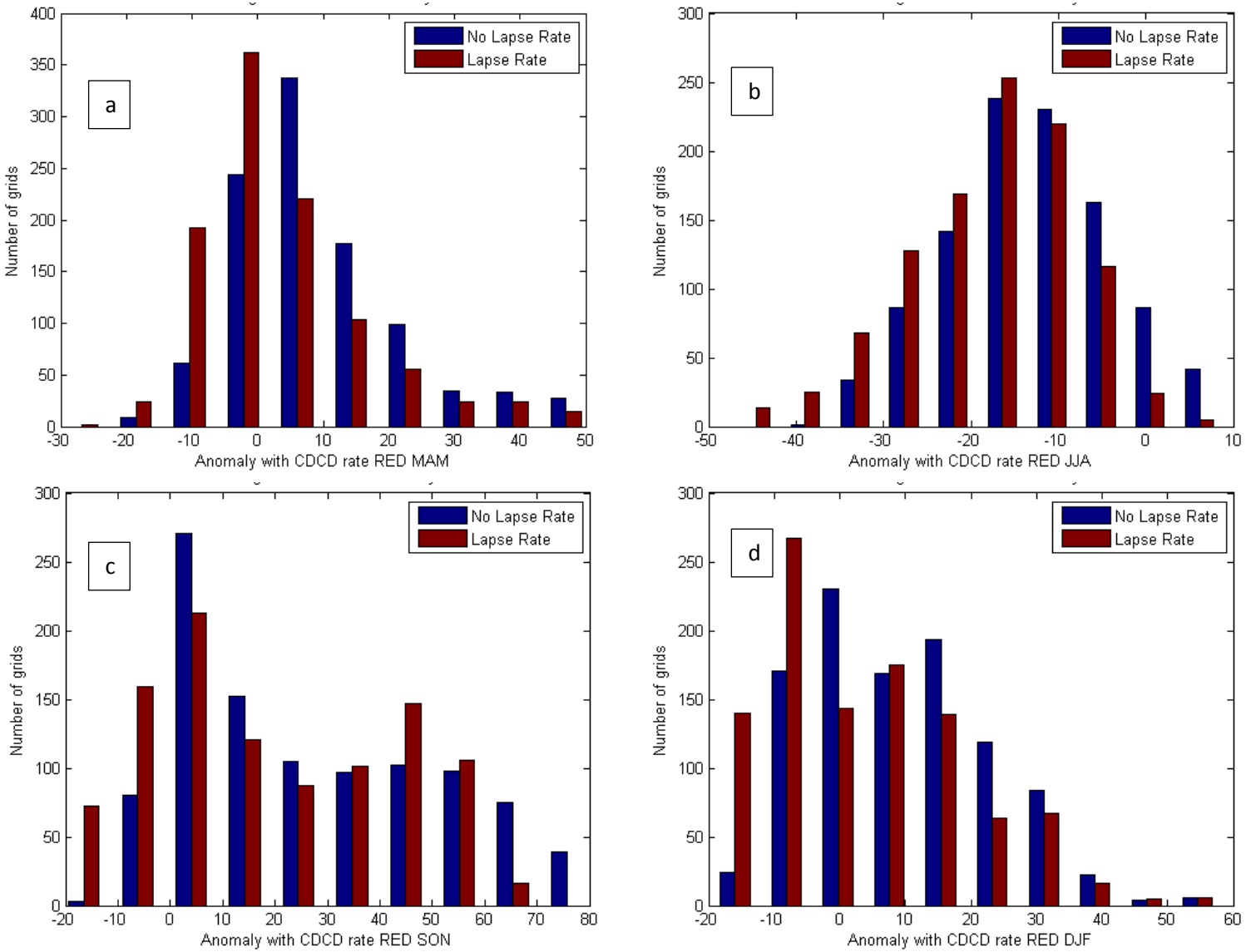

Figure C-7: Histogram of seasonal anomalies for the Red River Basin for (a) summer, (b) fall, (c) winter, and (d) spring

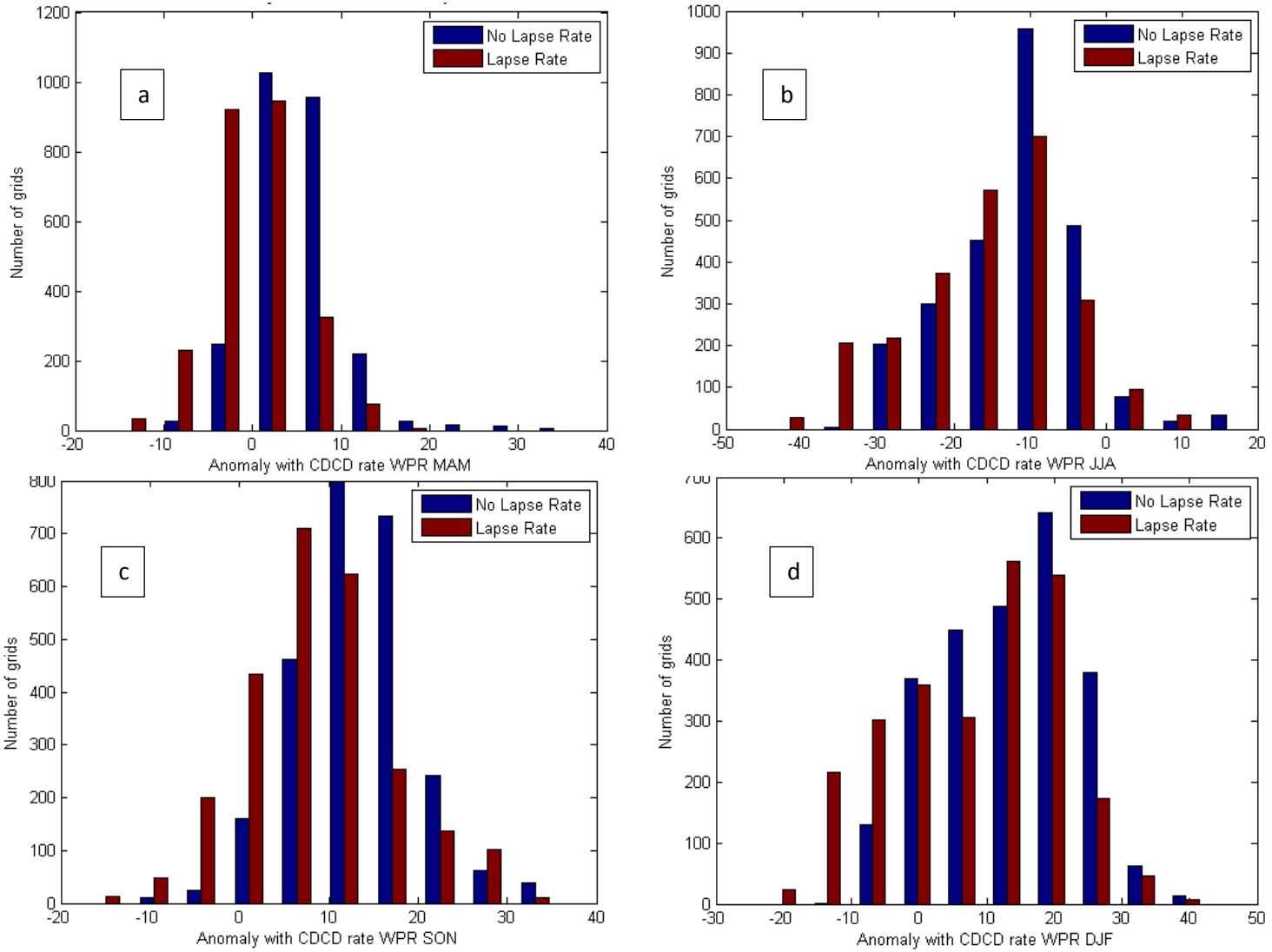

Figure C-8: Histogram of seasonal anomalies for the Saskatchewan River Basin for (a) summer, (b) fall, (c) winter, and (d) spring

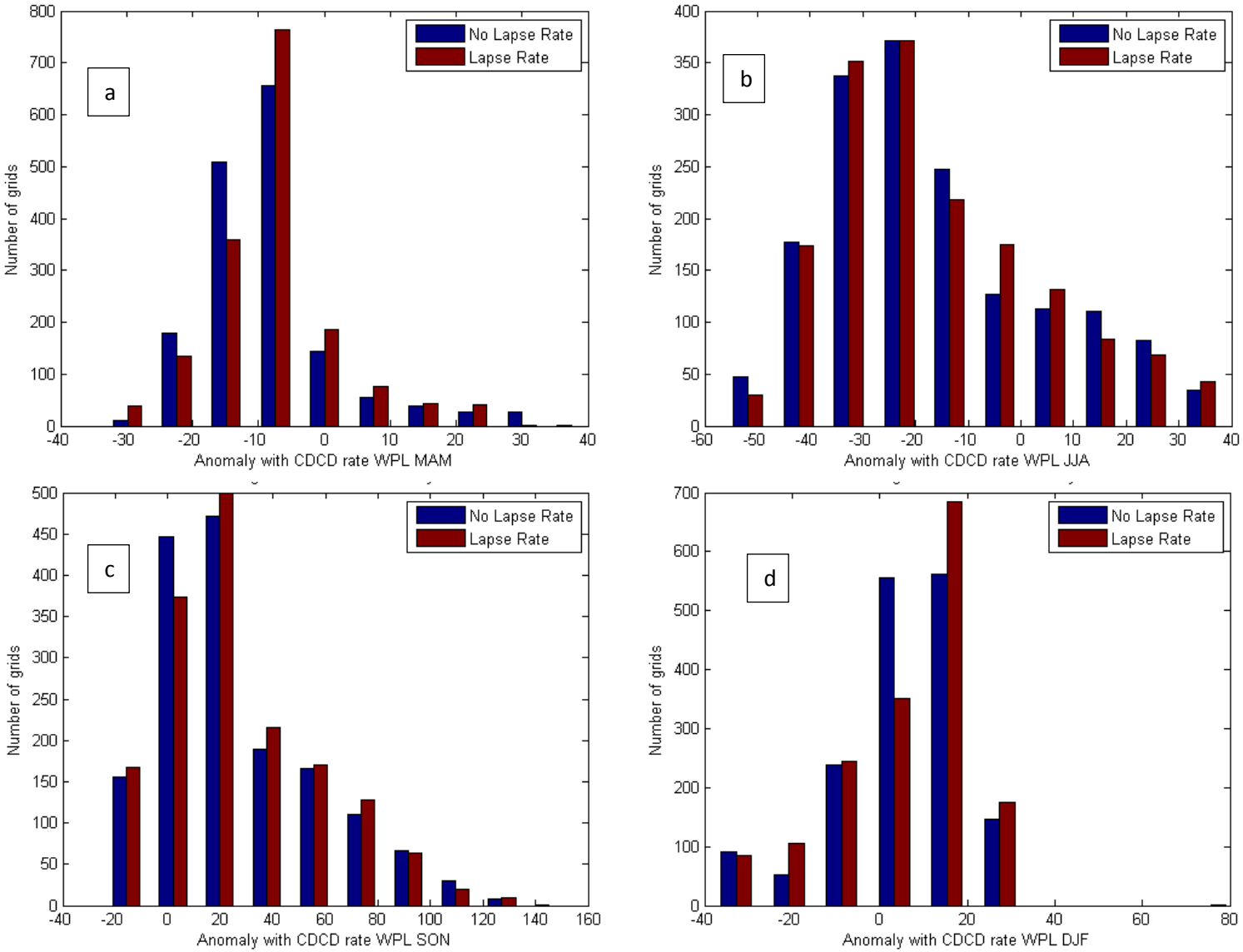

Figure C-9: Histogram of seasonal anomalies for the Lake Winnipeg Basin for (a) summer, (b) fall, (c) winter, and (d) spring

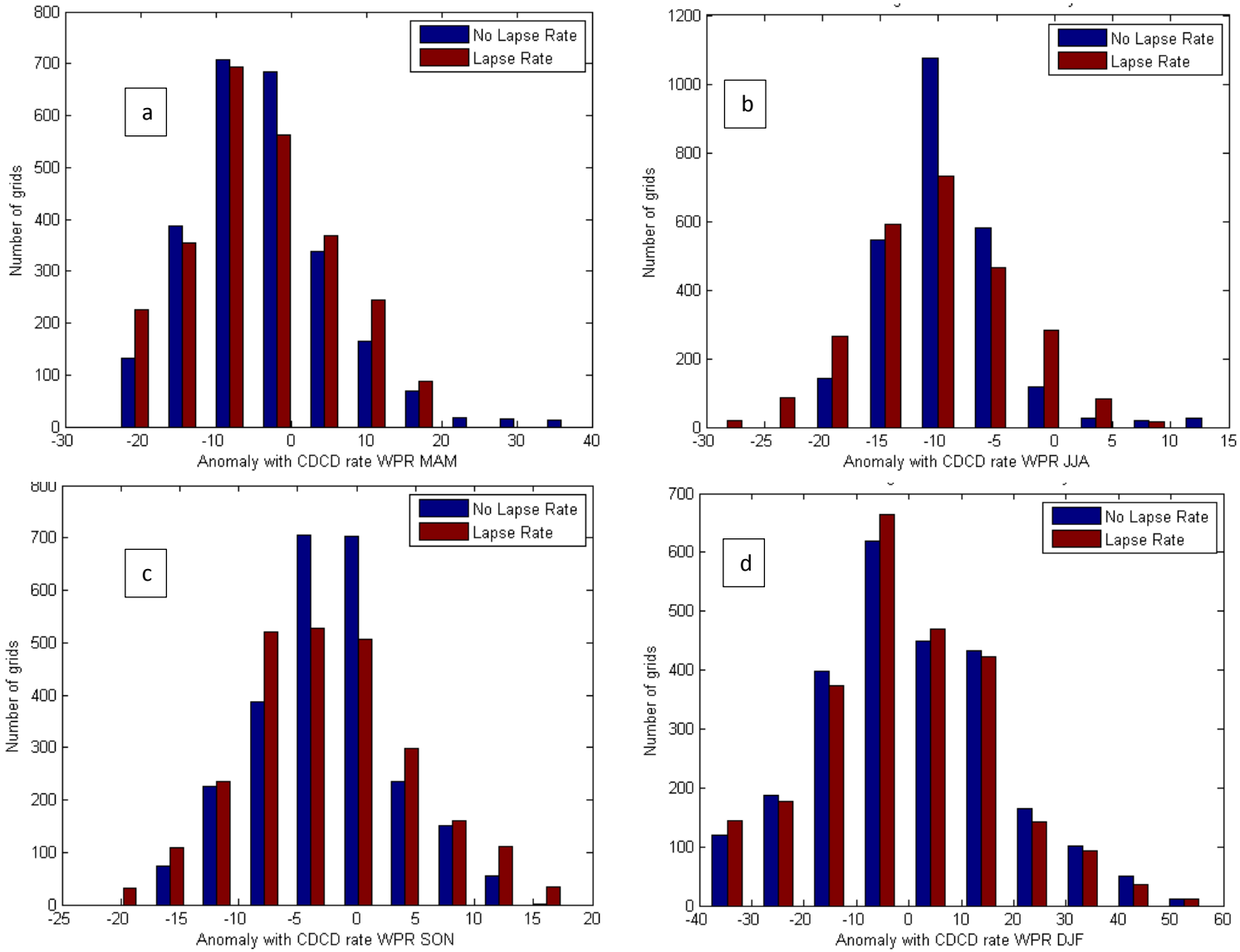

Figure C-10: Histogram of seasonal anomalies for the Winnipeg River Basin for (a) summer, (b) fall, (c) winter, and (d) spring

Appendix D: CaPA proxy validation hydrographs

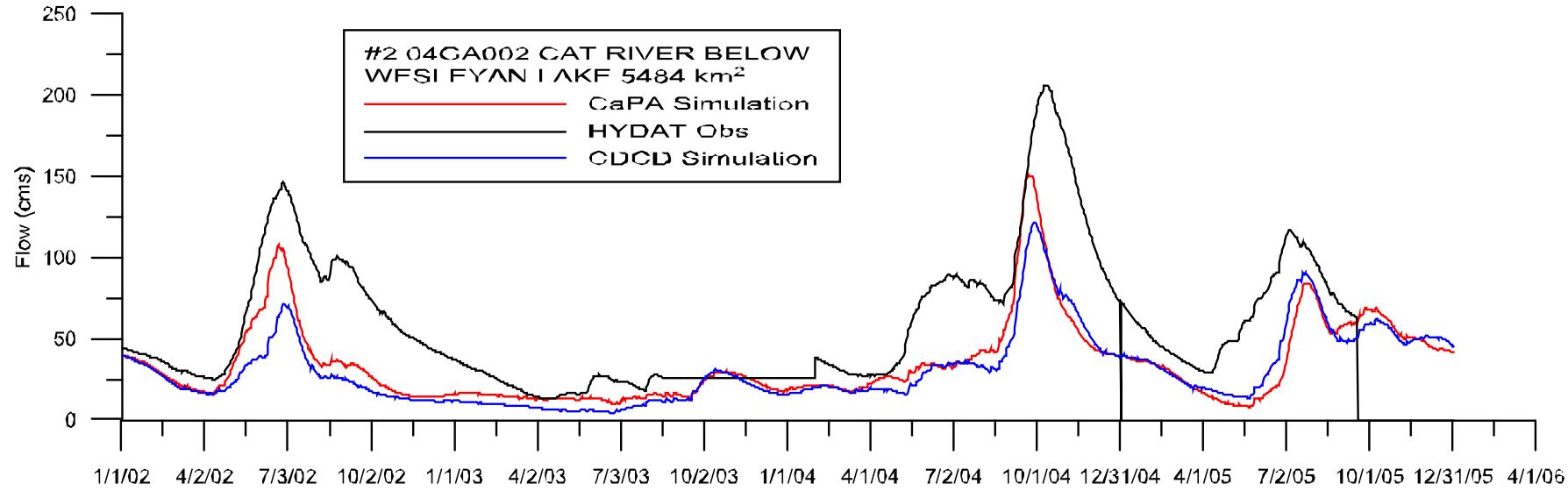

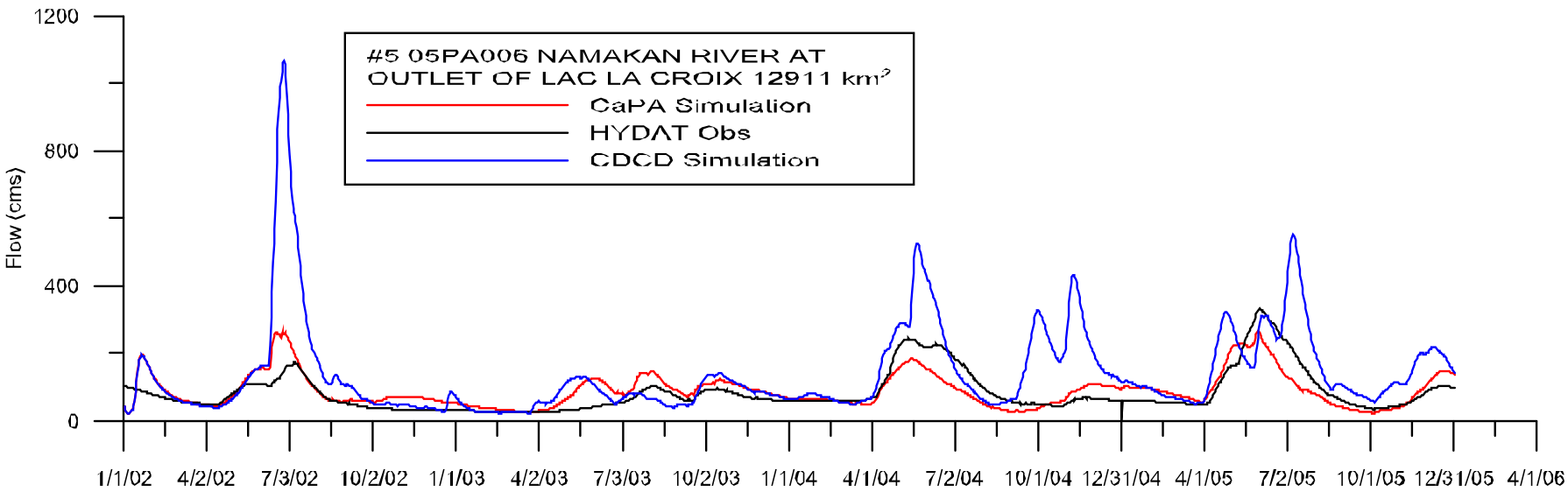

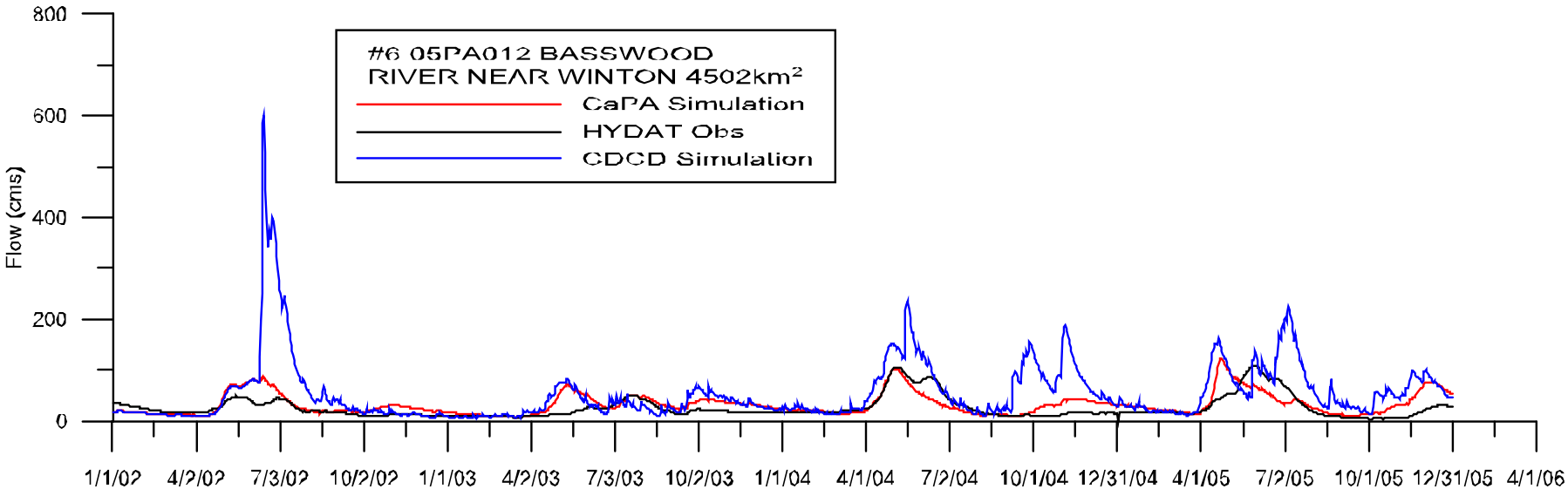

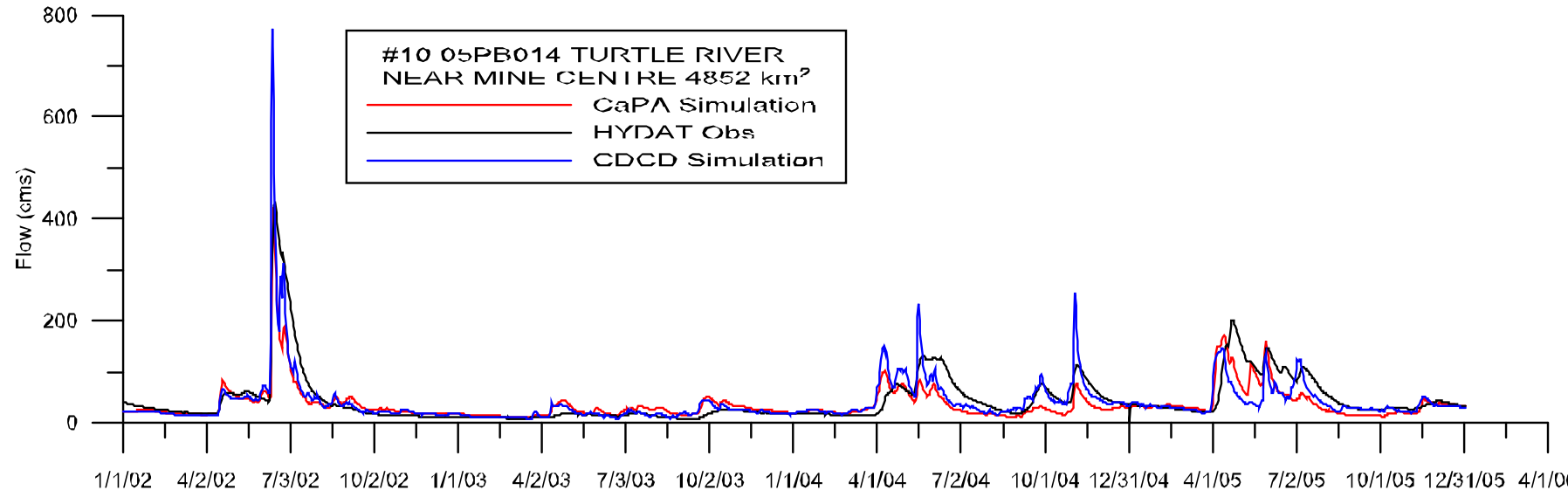

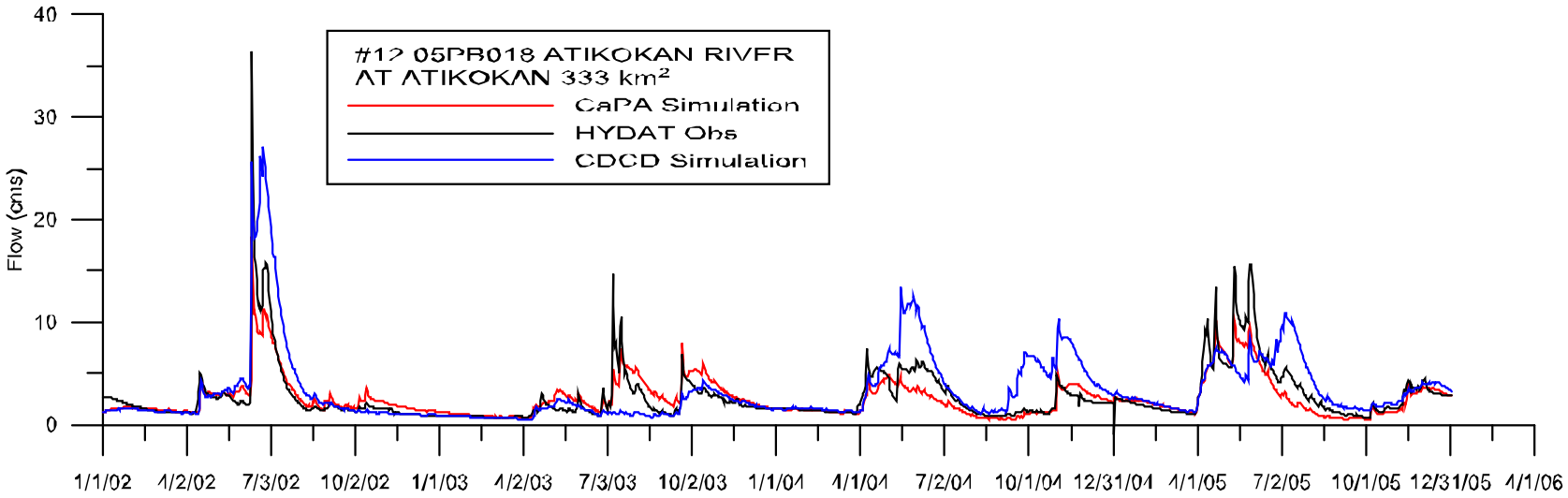
#12 05PB018 ATIKOKAN RIVER AT ATIKOKAN 333 km²
CaPA Simulation
HYDAT Obs
CDCD Simulation
Flow (cms)
0
10
20
30
40
1/1/02
4/2/02
7/3/02
10/2/02
1/1/03
4/2/03
7/3/03
10/2/03
1/1/04
4/1/04
7/2/04
10/1/04
12/31/04
4/1/05
7/2/05
10/1/05
12/31/05
4/1/06

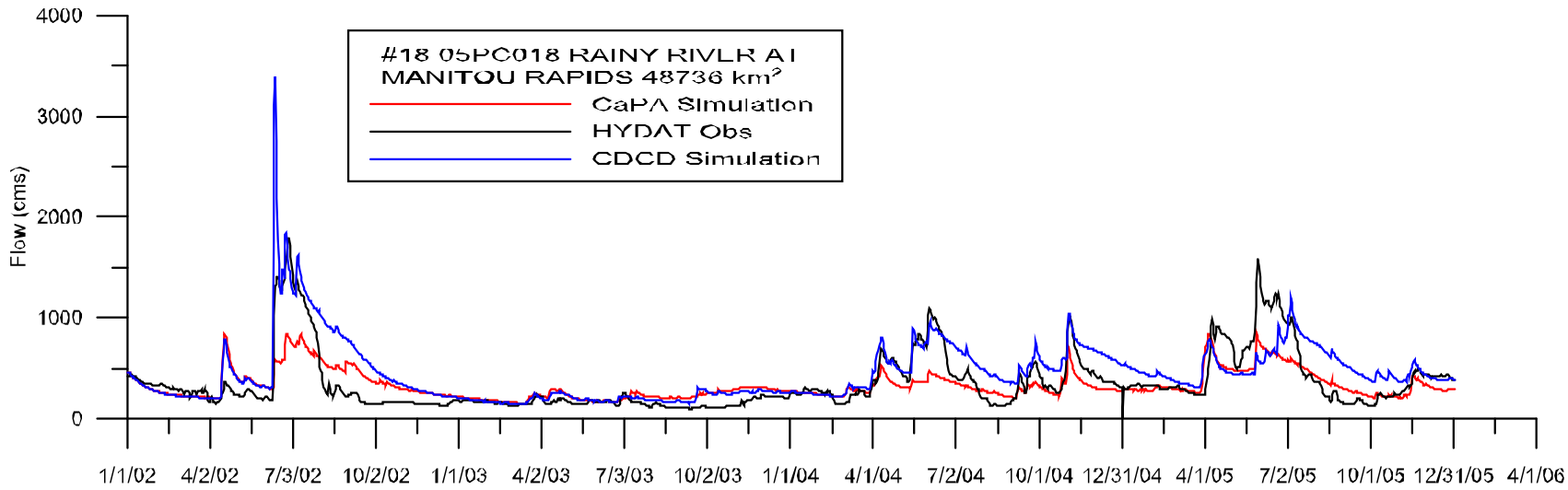
#18 05PC018 RAINY RIVER AT MANITOU RAPIDS 48736 km²
CaPA Simulation
HYDAT Obs
CDCD Simulation
Flow (cms)
0
1000
2000
3000
4000
1/1/02
4/2/02
7/3/02
10/2/02
1/1/03
4/2/03
7/3/03
10/2/03
1/1/04
4/1/04
7/2/04
10/1/04
12/31/04
4/1/05
7/2/05
10/1/05
12/31/05
4/1/06

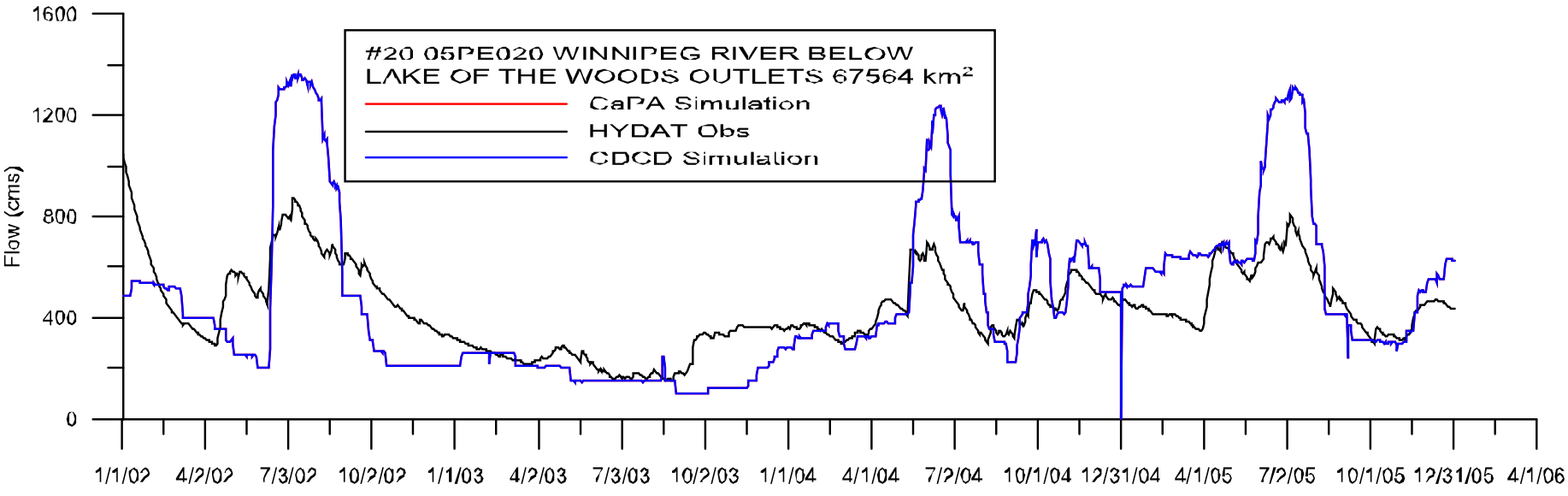
#20 05PE020 WINNIPEG RIVER BELOW LAKE OF THE WOODS OUTLETS 67564 km²
CaPA Simulation
HYDAT Obs
CDCD Simulation
Flow (cms)
0
400
800
1200
1600
1/1/02
4/2/02
7/3/02
10/2/02
1/1/03
4/2/03
7/3/03
10/2/03
1/1/04
4/1/04
7/2/04
10/1/04
12/31/04
4/1/05
7/2/05
10/1/05
12/31/05
4/1/06

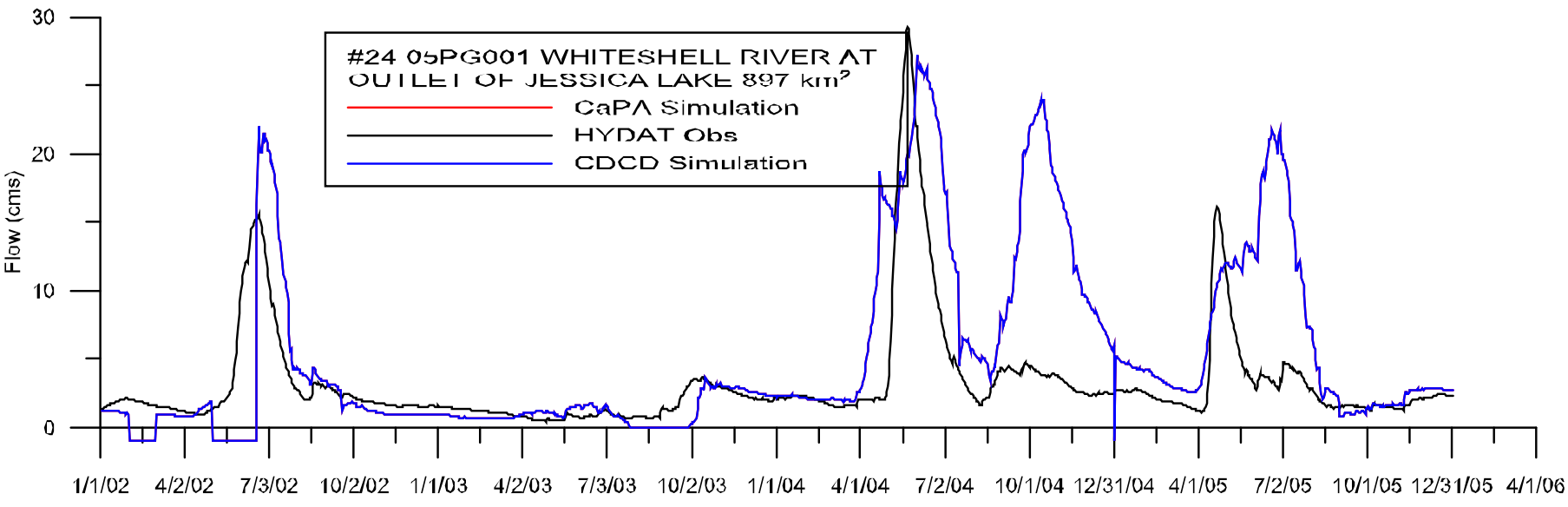
#24 05PG001 WHITESHELL RIVER AT OUTLET OF JESSICA LAKE 897 km²
CaPA Simulation
HYDAT Obs
CDCD Simulation
Flow (cms)
0
10
20
30
1/1/02
4/2/02
7/3/02
10/2/02
1/1/03
4/2/03
7/3/03
10/2/03
1/1/04
4/1/04
7/2/04
10/1/04
12/31/04
4/1/05
7/2/05
10/1/05
12/31/05
4/1/06

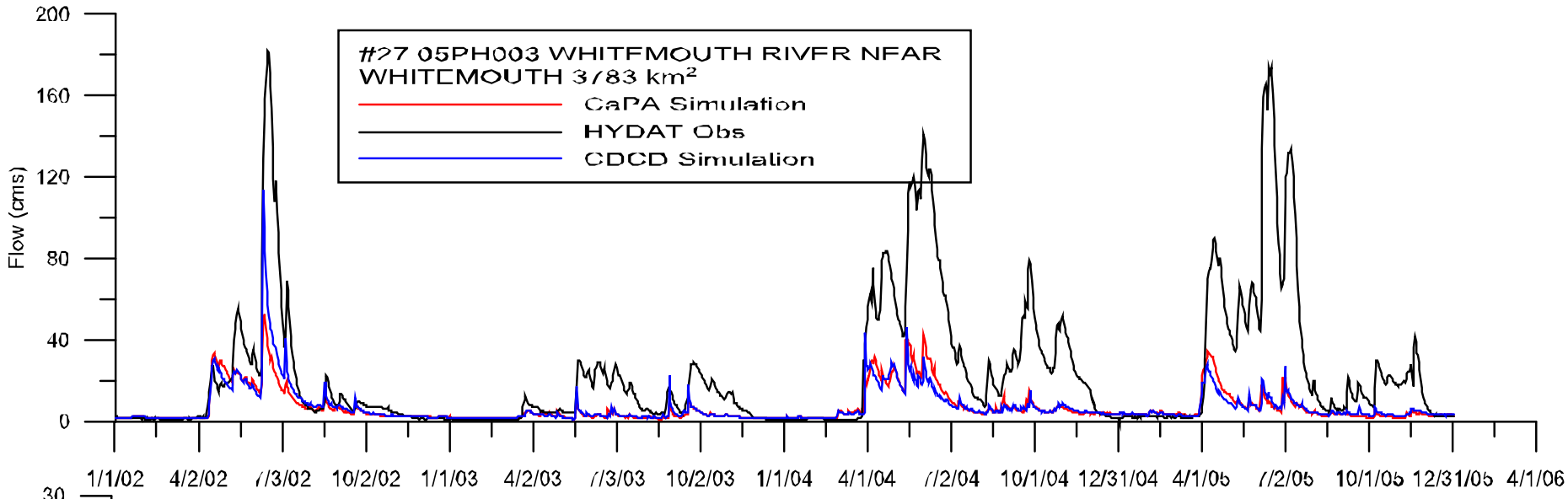
#27 05PH003 WHITEMOUTH RIVER NEAR WHITEMOUTH 3783 km²
CaPA Simulation
HYDAT Obs
CDCD Simulation
Flow (cms)
200
160
120
80
40
0
1/1/02 4/2/02 7/3/02 10/2/02 1/1/03 4/2/03 7/3/03 10/2/03 1/1/04 4/1/04 7/2/04 10/1/04 12/31/04 4/1/05 7/2/05 10/1/05 12/31/05 4/1/06

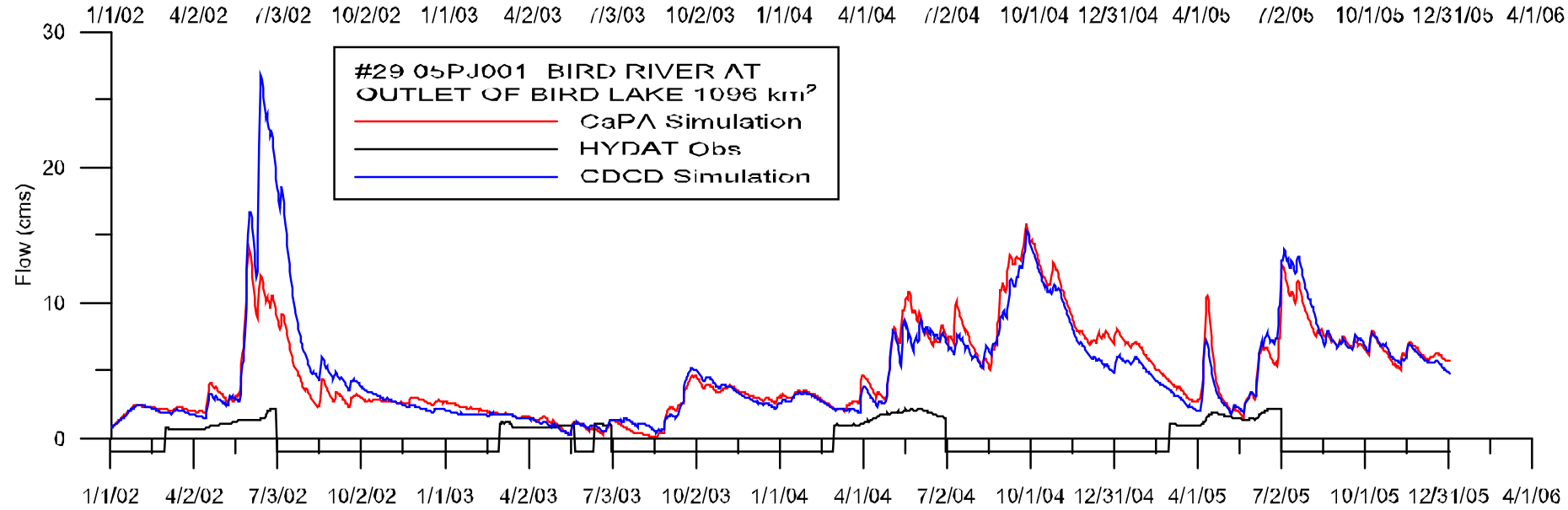
#29 05PJ001 BIRD RIVER AT OUTLET OF BIRD LAKE 1096 km²
CaPA Simulation
HYDAT Obs
CDCD Simulation
Flow (cms)
30
20
10
0
1/1/02 4/2/02 7/3/02 10/2/02 1/1/03 4/2/03 7/3/03 10/2/03 1/1/04 4/1/04 7/2/04 10/1/04 12/31/04 4/1/05 7/2/05 10/1/05 12/31/05 4/1/06

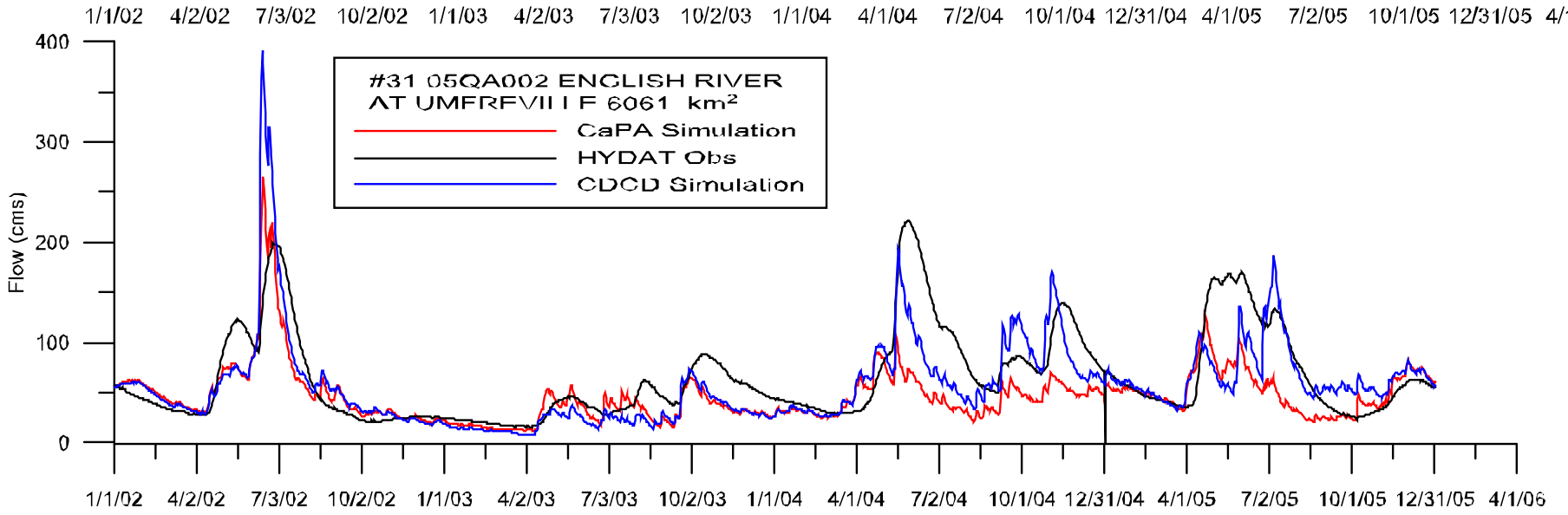
#31 05QA002 ENGLISH RIVER AT UMFRFVILLE 6061 km²
CaPA Simulation
HYDAT Obs
CDCD Simulation
Flow (cms)
400
300
200
100
0
1/1/02 4/2/02 7/3/02 10/2/02 1/1/03 4/2/03 7/3/03 10/2/03 1/1/04 4/1/04 7/2/04 10/1/04 12/31/04 4/1/05 7/2/05 10/1/05 12/31/05 4/1/06

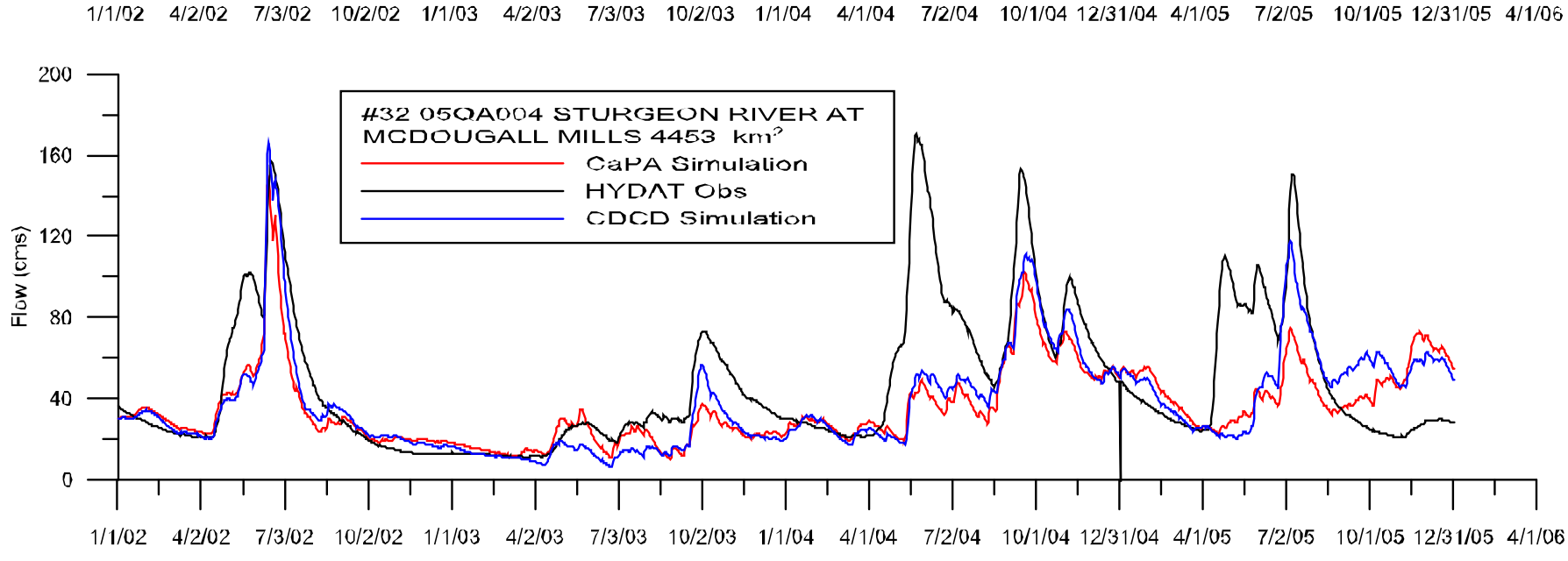
#32 05QA004 STURGEON RIVER AT MCDOUGALL MILLS 4453 km²
CaPA Simulation
HYDAT Obs
CDCD Simulation
Flow (cms)
200
160
120
80
40
0
1/1/02 4/2/02 7/3/02 10/2/02 1/1/03 4/2/03 7/3/03 10/2/03 1/1/04 4/1/04 7/2/04 10/1/04 12/31/04 4/1/05 7/2/05 10/1/05 12/31/05 4/1/06

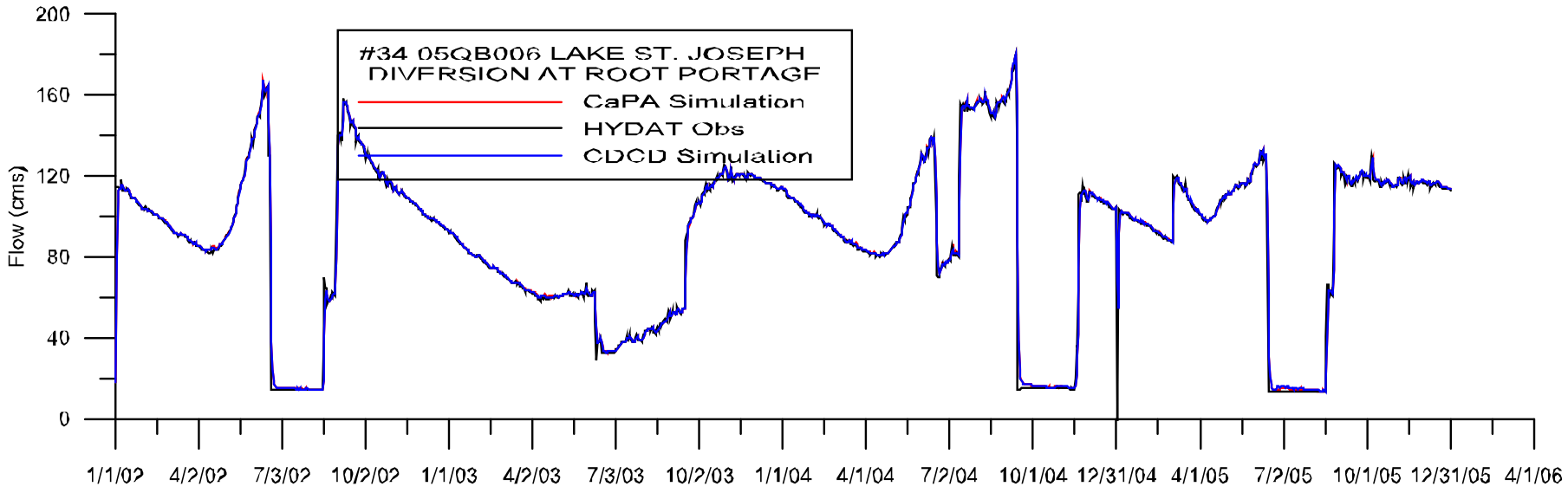
#34 05QB006 LAKE ST. JOSEPH
DIVERSION AT ROOT PORTAGE
CaPA Simulation
HYDAT Obs
CDCD Simulation
Flow (cms)
200
160
120
80
40
0
1/1/02
4/2/02
7/3/02
10/2/02
1/1/03
4/2/03
7/3/03
10/2/03
1/1/04
4/1/04
7/2/04
10/1/04
12/31/04
4/1/05
7/2/05
10/1/05
12/31/05
4/1/06

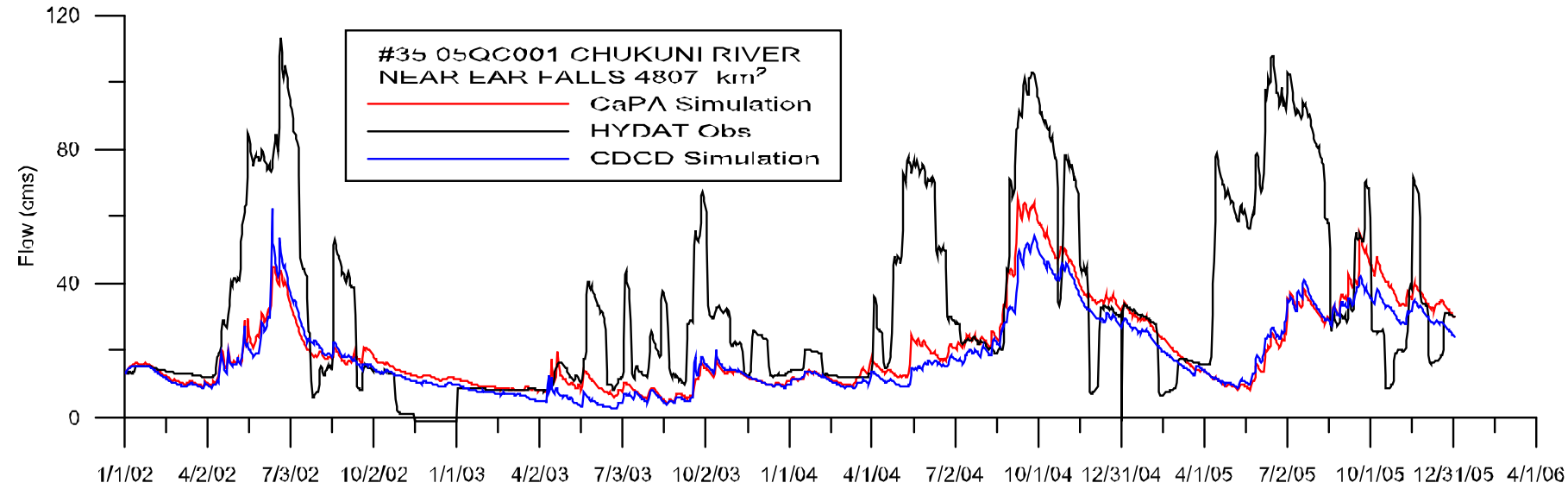
#35 05QC001 CHUKUNI RIVER
NEAR EAR FALLS 4807 km²
CaPA Simulation
HYDAT Obs
CDCD Simulation
Flow (cms)
120
80
40
0
1/1/02
4/2/02
7/3/02
10/2/02
1/1/03
4/2/03
7/3/03
10/2/03
1/1/04
4/1/04
7/2/04
10/1/04
12/31/04
4/1/05
7/2/05
10/1/05
12/31/05
4/1/06

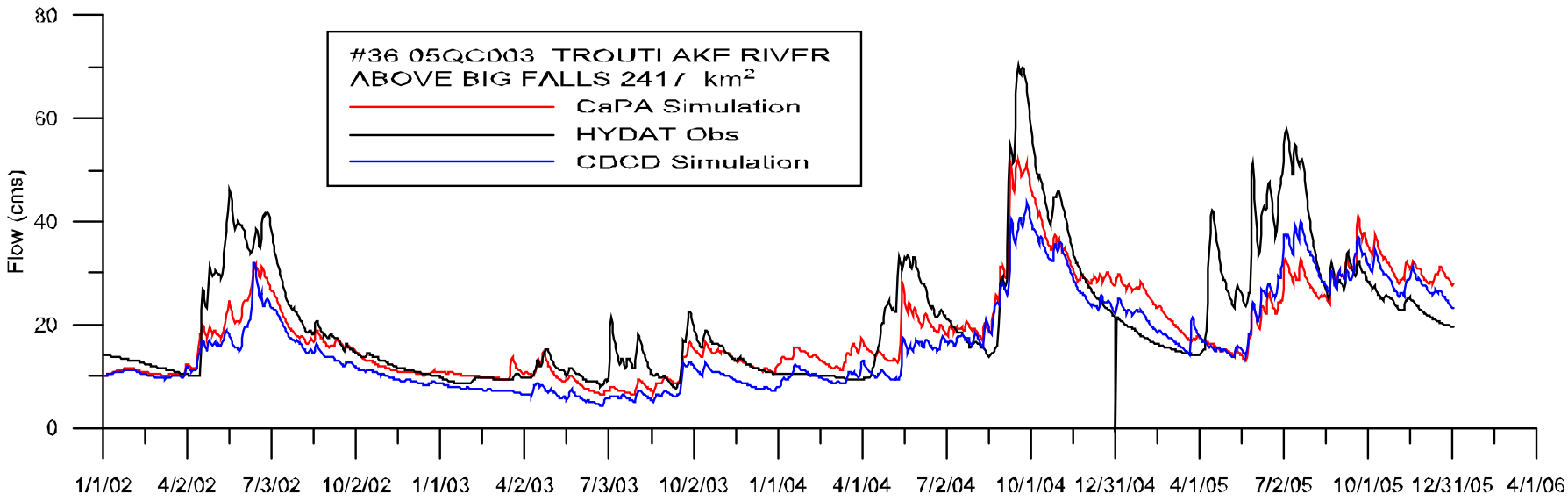
#36 05QC003 TROUTI AKE RIVER
ABOVE BIG FALLS 2417 km²
CaPA Simulation
HYDAT Obs
CDCD Simulation
Flow (cms)
80
60
40
20
0
1/1/02
4/2/02
7/3/02
10/2/02
1/1/03
4/2/03
7/3/03
10/2/03
1/1/04
4/1/04
7/2/04
10/1/04
12/31/04
4/1/05
7/2/05
10/1/05
12/31/05
4/1/06

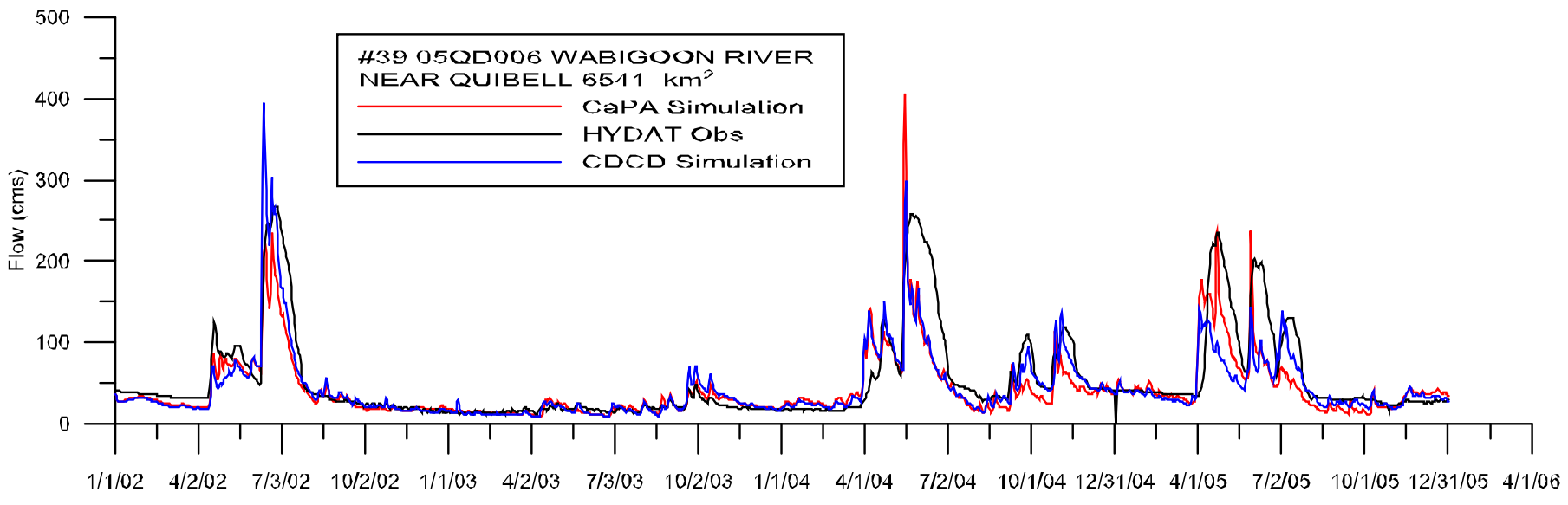
#39 05QD006 WABIGOON RIVER
NEAR QUIBELL 6541 km²
CaPA Simulation
HYDAT Obs
CDCD Simulation
Flow (cms)
500
400
300
200
100
0
1/1/02
4/2/02
7/3/02
10/2/02
1/1/03
4/2/03
7/3/03
10/2/03
1/1/04
4/1/04
7/2/04
10/1/04
12/31/04
4/1/05
7/2/05
10/1/05
12/31/05
4/1/06

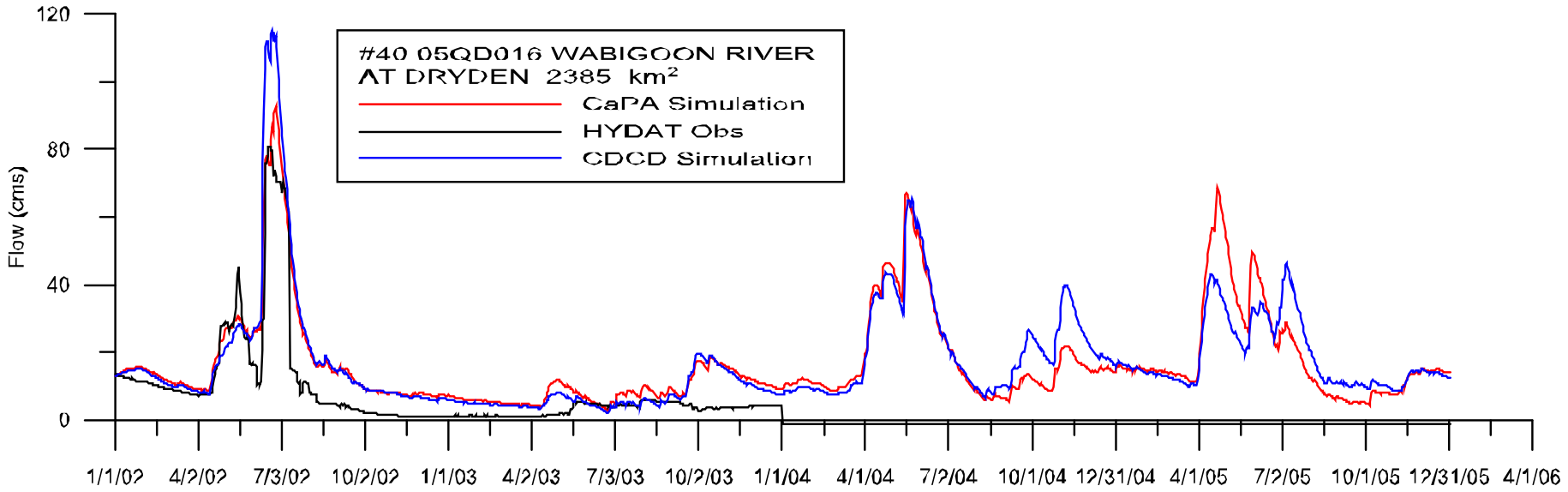
#40 05QD016 WABIGOON RIVER AT DRYDEN 2385 km²
CaPA Simulation
HYDAT Obs
CDCD Simulation
Flow (cms)
120
80
40
0
1/1/02 4/2/02 7/3/02 10/2/02 1/1/03 4/2/03 7/3/03 10/2/03 1/1/04 4/1/04 7/2/04 10/1/04 12/31/04 4/1/05 7/2/05 10/1/05 12/31/05 4/1/06

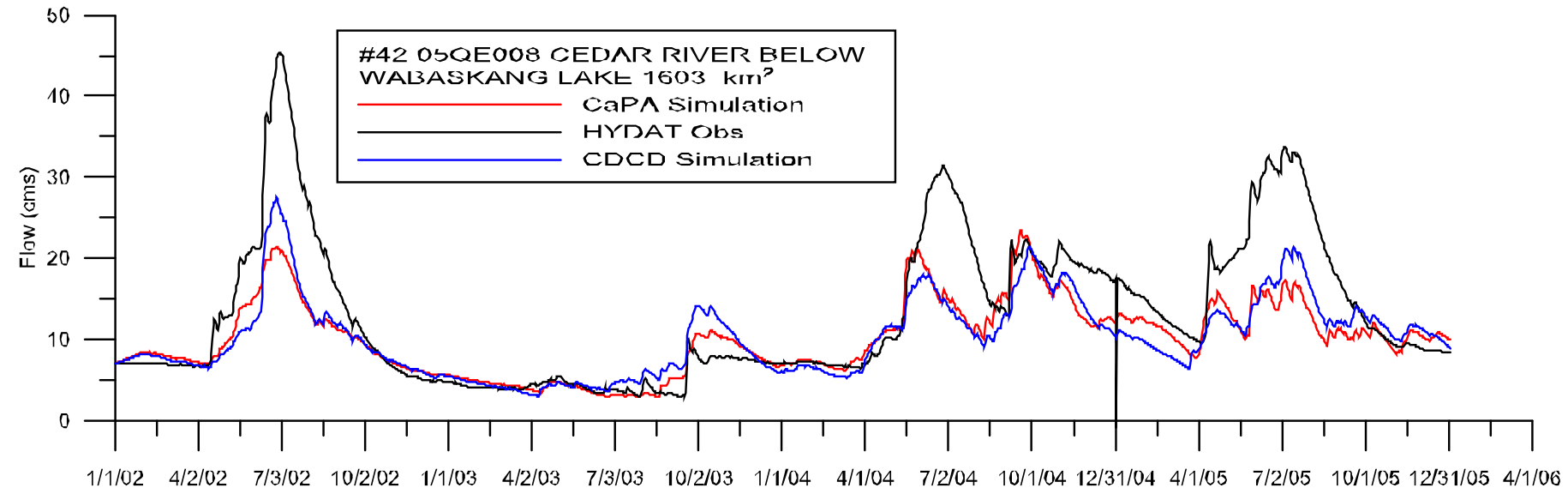
#42 05QE008 CEDAR RIVER BELOW WABASKANG LAKE 1603 km²
CaPA Simulation
HYDAT Obs
CDCD Simulation
Flow (cms)
50
40
30
20
10
0
1/1/02 4/2/02 7/3/02 10/2/02 1/1/03 4/2/03 7/3/03 10/2/03 1/1/04 4/1/04 7/2/04 10/1/04 12/31/04 4/1/05 7/2/05 10/1/05 12/31/05 4/1/06

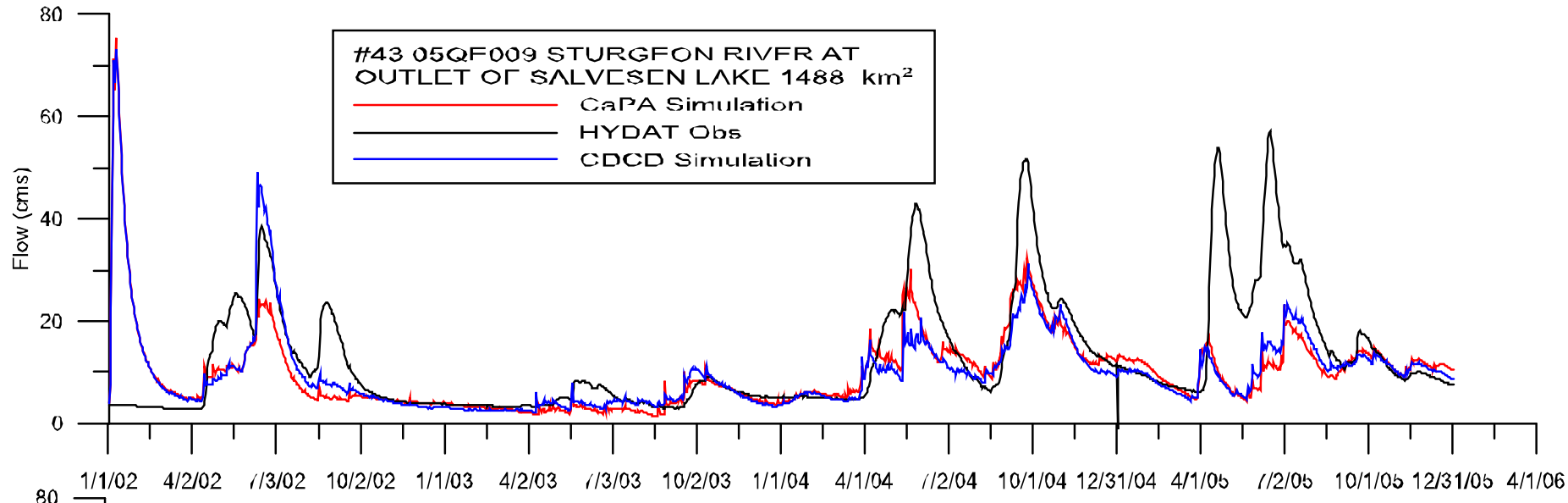
#43 05QF009 STURGEON RIVER AT OUTLET OF SALVESEN LAKE 1488 km²
CaPA Simulation
HYDAT Obs
CDCD Simulation
Flow (cms)
80
60
40
20
0
1/1/02 4/2/02 7/3/02 10/2/02 1/1/03 4/2/03 7/3/03 10/2/03 1/1/04 4/1/04 7/2/04 10/1/04 12/31/04 4/1/05 7/2/05 10/1/05 12/31/05 4/1/06

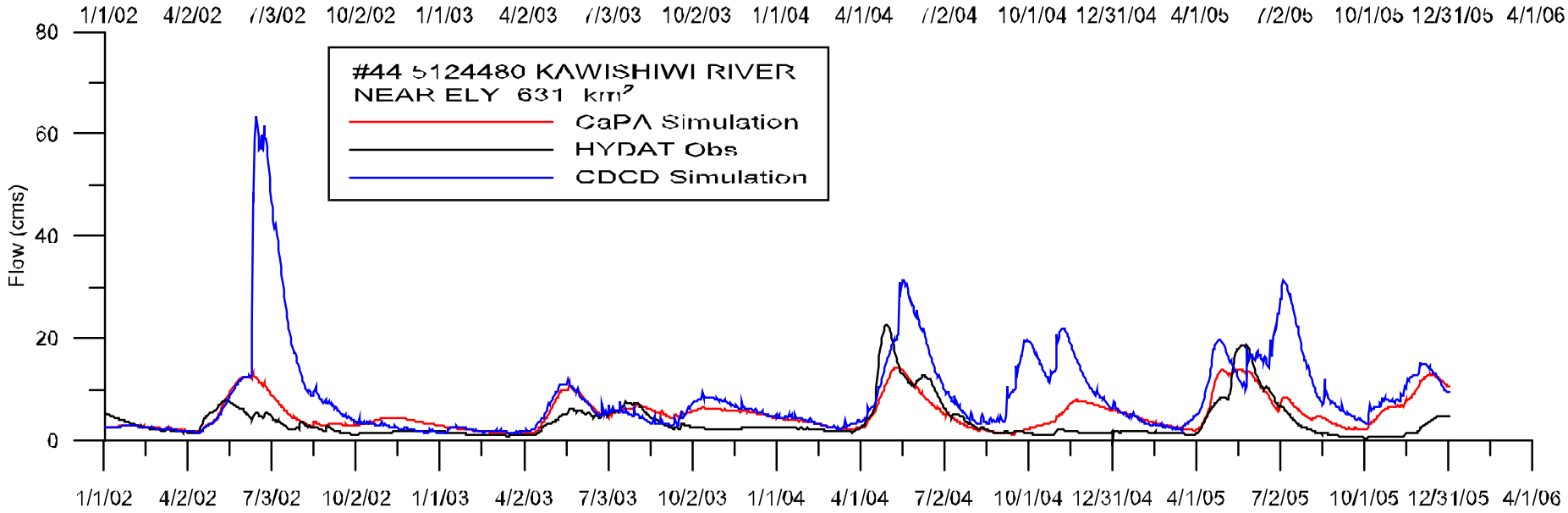
#44 5124480 KAWISHIWI RIVER NEAR ELY 631 km²
CaPA Simulation
HYDAT Obs
CDCD Simulation
Flow (cms)
80
60
40
20
0
1/1/02 4/2/02 7/3/02 10/2/02 1/1/03 4/2/03 7/3/03 10/2/03 1/1/04 4/1/04 7/2/04 10/1/04 12/31/04 4/1/05 7/2/05 10/1/05 12/31/05 4/1/06

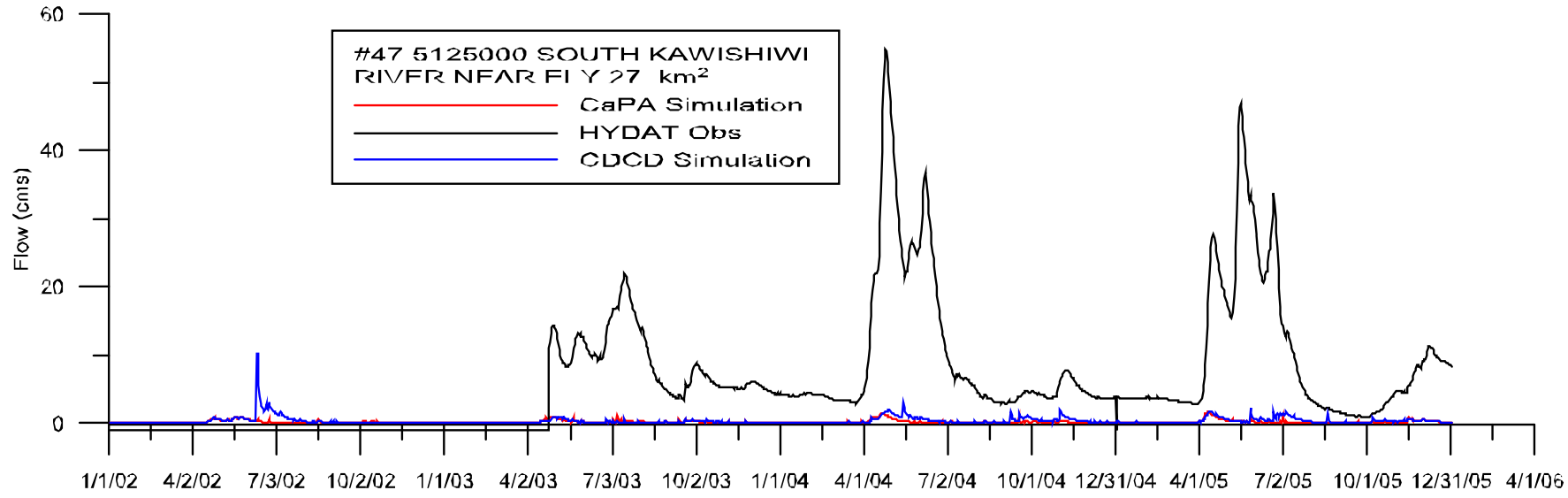
#47 5125000 SOUTH KAWISHIWI RIVER NEAR ELY 27 km²
CaPA Simulation
HYDAT Obs
CDCD Simulation
Flow (cms)
60
40
20
0
1/1/02
4/2/02
7/3/02
10/2/02
1/1/03
4/2/03
7/3/03
10/2/03
1/1/04
4/1/04
7/2/04
10/1/04
12/31/04
4/1/05
7/2/05
10/1/05
12/31/05
4/1/06

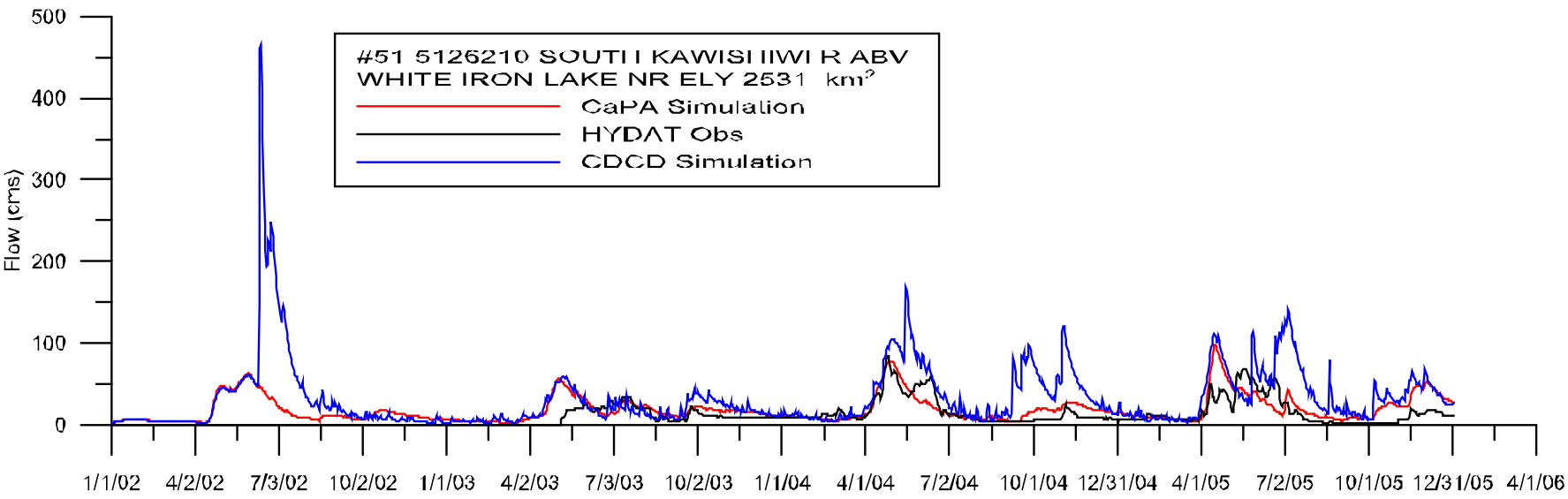
#51 5126210 SOUTH KAWISHIWI R ABV WHITE IRON LAKE NR ELY 2531 km²
CaPA Simulation
HYDAT Obs
CDCD Simulation
Flow (cms)
500
400
300
200
100
0
1/1/02
4/2/02
7/3/02
10/2/02
1/1/03
4/2/03
7/3/03
10/2/03
1/1/04
4/1/04
7/2/04
10/1/04
12/31/04
4/1/05
7/2/05
10/1/05
12/31/05
4/1/06

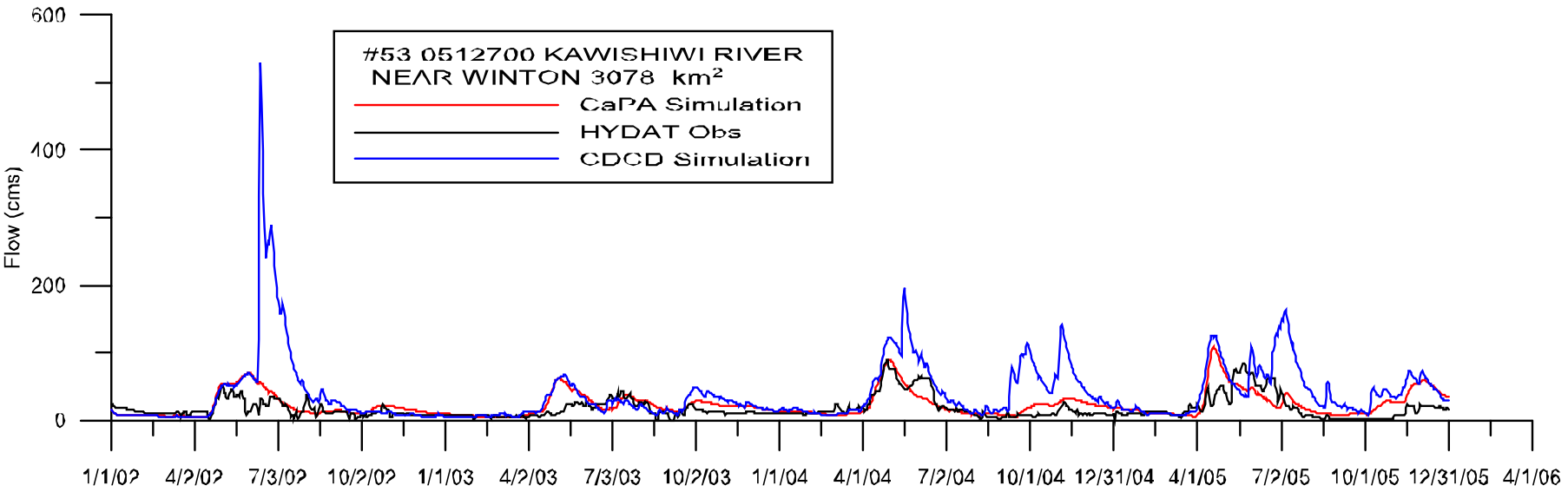
#53 0512700 KAWISHIWI RIVER NEAR WINTON 3078 km²
CaPA Simulation
HYDAT Obs
CDCD Simulation
Flow (cms)
600
400
200
0
1/1/02
4/2/02
7/3/02
10/2/02
1/1/03
4/2/03
7/3/03
10/2/03
1/1/04
4/1/04
7/2/04
10/1/04
12/31/04
4/1/05
7/2/05
10/1/05
12/31/05
4/1/06

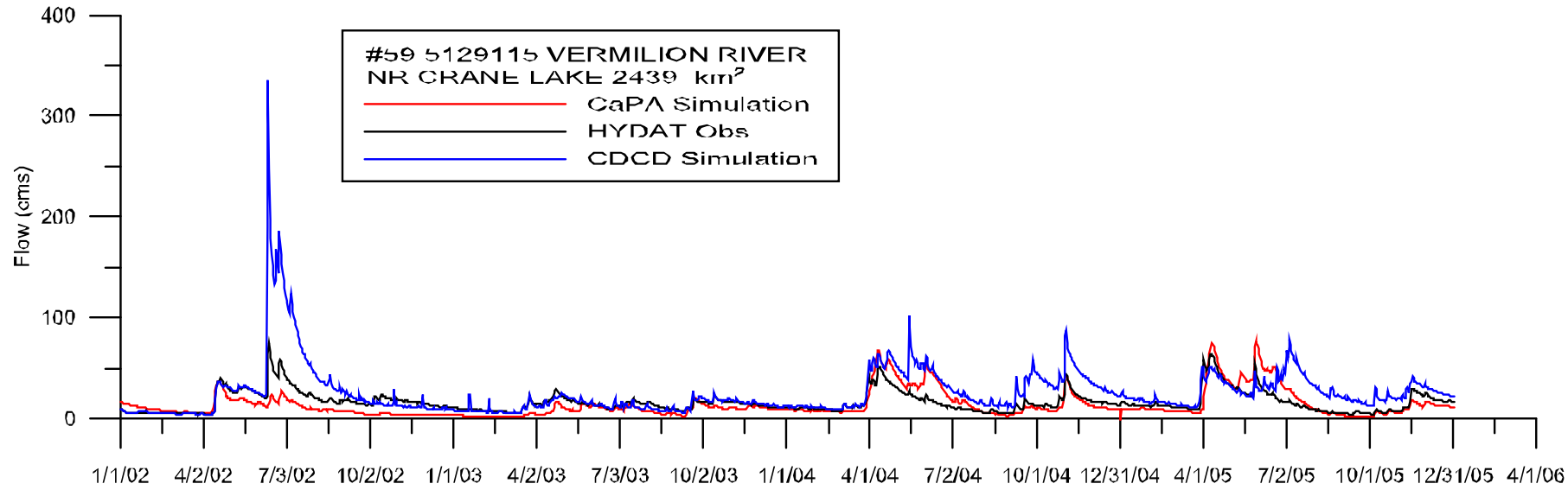
#59 5129115 VERMILION RIVER NR CRANE LAKE 2439 km²
CaPA Simulation
HYDAT Obs
CDCD Simulation
Flow (cms)
400
300
200
100
0
1/1/02
4/2/02
7/3/02
10/2/02
1/1/03
4/2/03
7/3/03
10/2/03
1/1/04
4/1/04
7/2/04
10/1/04
12/31/04
4/1/05
7/2/05
10/1/05
12/31/05
4/1/06

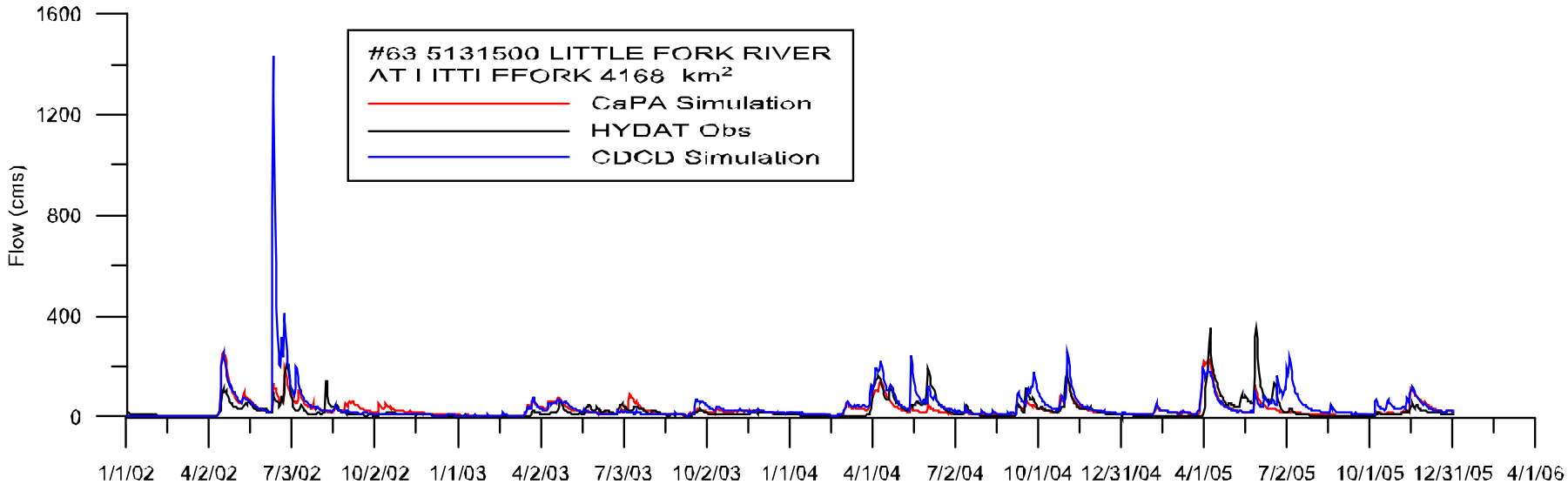
#63 5131500 LITTLE FORK RIVER
AT LITTLE FORK 4168 km²
CaPA Simulation
HYDAT Obs
CDCD Simulation
Flow (cms)
1600
1200
800
400
0
1/1/02 4/2/02 7/3/02 10/2/02 1/1/03 4/2/03 7/3/03 10/2/03 1/1/04 4/1/04 7/2/04 10/1/04 12/31/04 4/1/05 7/2/05 10/1/05 12/31/05 4/1/06

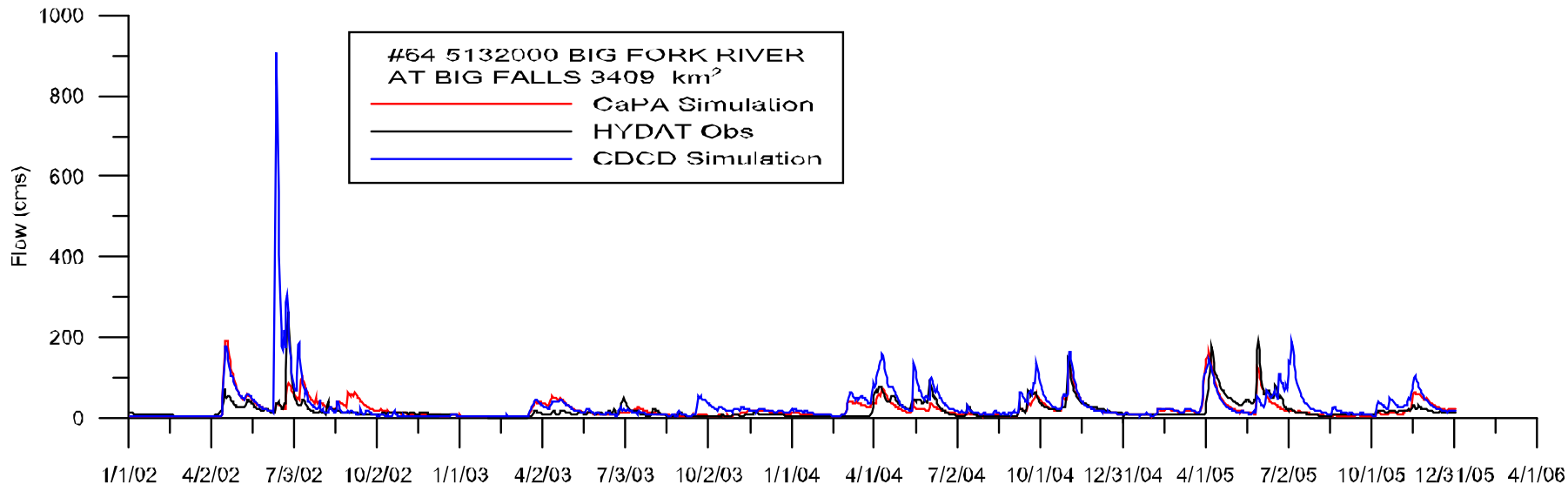
#64 5132000 BIG FORK RIVER
AT BIG FALLS 3409 km²
CaPA Simulation
HYDAT Obs
CDCD Simulation
Flow (cms)
1000
800
600
400
200
0
1/1/02 4/2/02 7/3/02 10/2/02 1/1/03 4/2/03 7/3/03 10/2/03 1/1/04 4/1/04 7/2/04 10/1/04 12/31/04 4/1/05 7/2/05 10/1/05 12/31/05 4/1/06

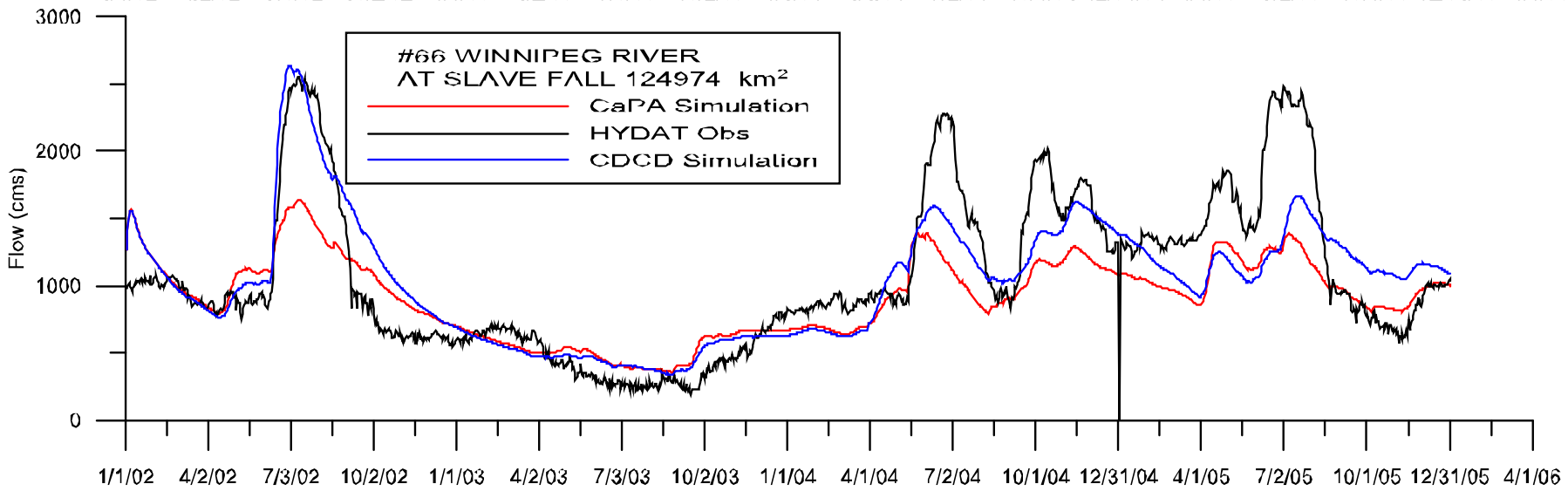
#66 WINNIPEG RIVER
AT SLAVE FALL 124974 km²
CaPA Simulation
HYDAT Obs
CDCD Simulation
Flow (cms)
3000
2000
1000
0
1/1/02 4/2/02 7/3/02 10/2/02 1/1/03 4/2/03 7/3/03 10/2/03 1/1/04 4/1/04 7/2/04 10/1/04 12/31/04 4/1/05 7/2/05 10/1/05 12/31/05 4/1/06

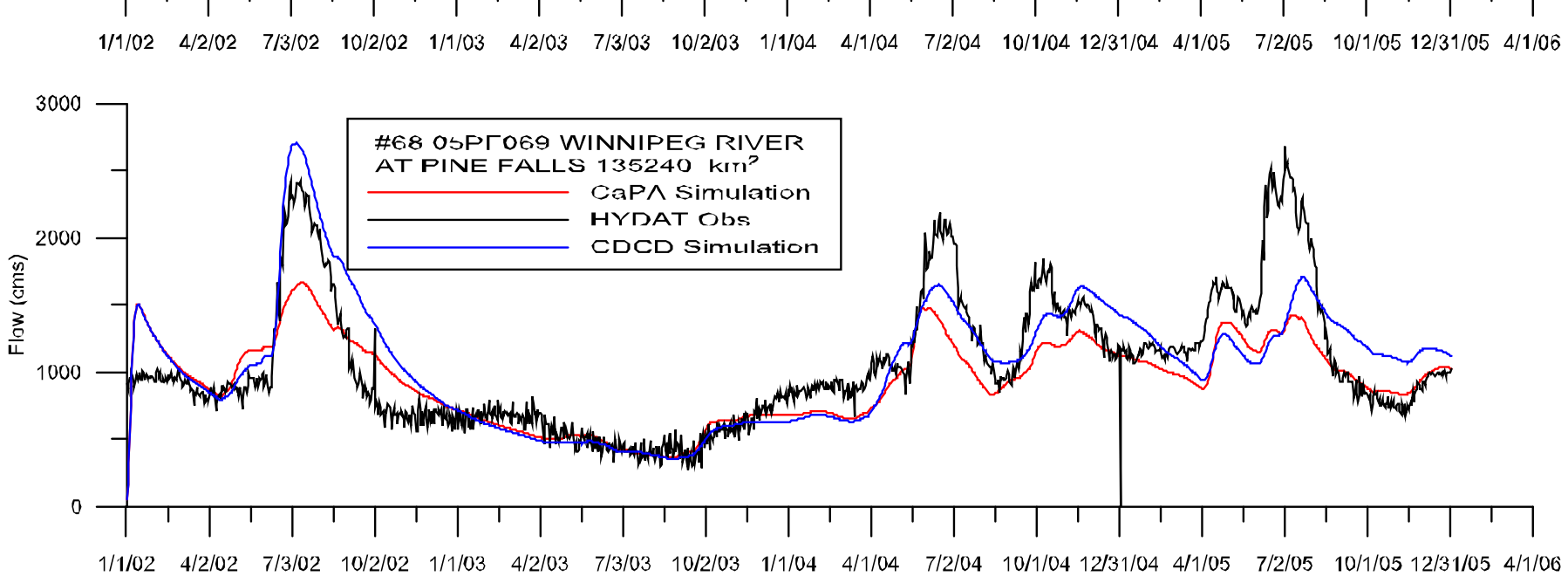
#68 05PF069 WINNIPEG RIVER
AT PINE FALLS 135240 km²
CaPA Simulation
HYDAT Obs
CDCD Simulation
Flow (cms)
3000
2000
1000
0
1/1/02 4/2/02 7/3/02 10/2/02 1/1/03 4/2/03 7/3/03 10/2/03 1/1/04 4/1/04 7/2/04 10/1/04 12/31/04 4/1/05 7/2/05 10/1/05 12/31/05 4/1/06

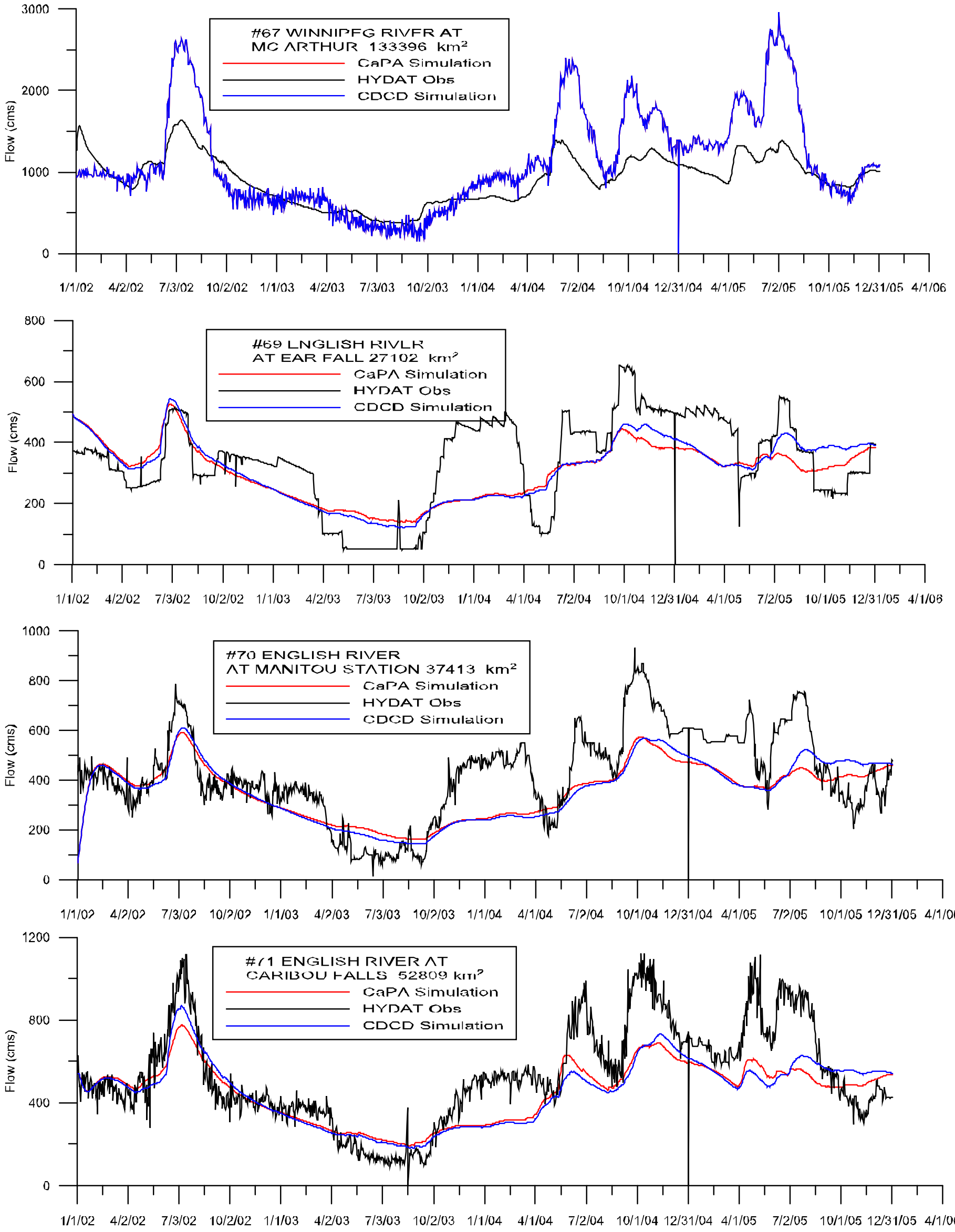

Figure D-1: Proxy validation hydrographs at the Winnipeg River basin, each hydrograph are labeled with its station number (#1 - #71) in WATFLOOD, station name, and drainage area.

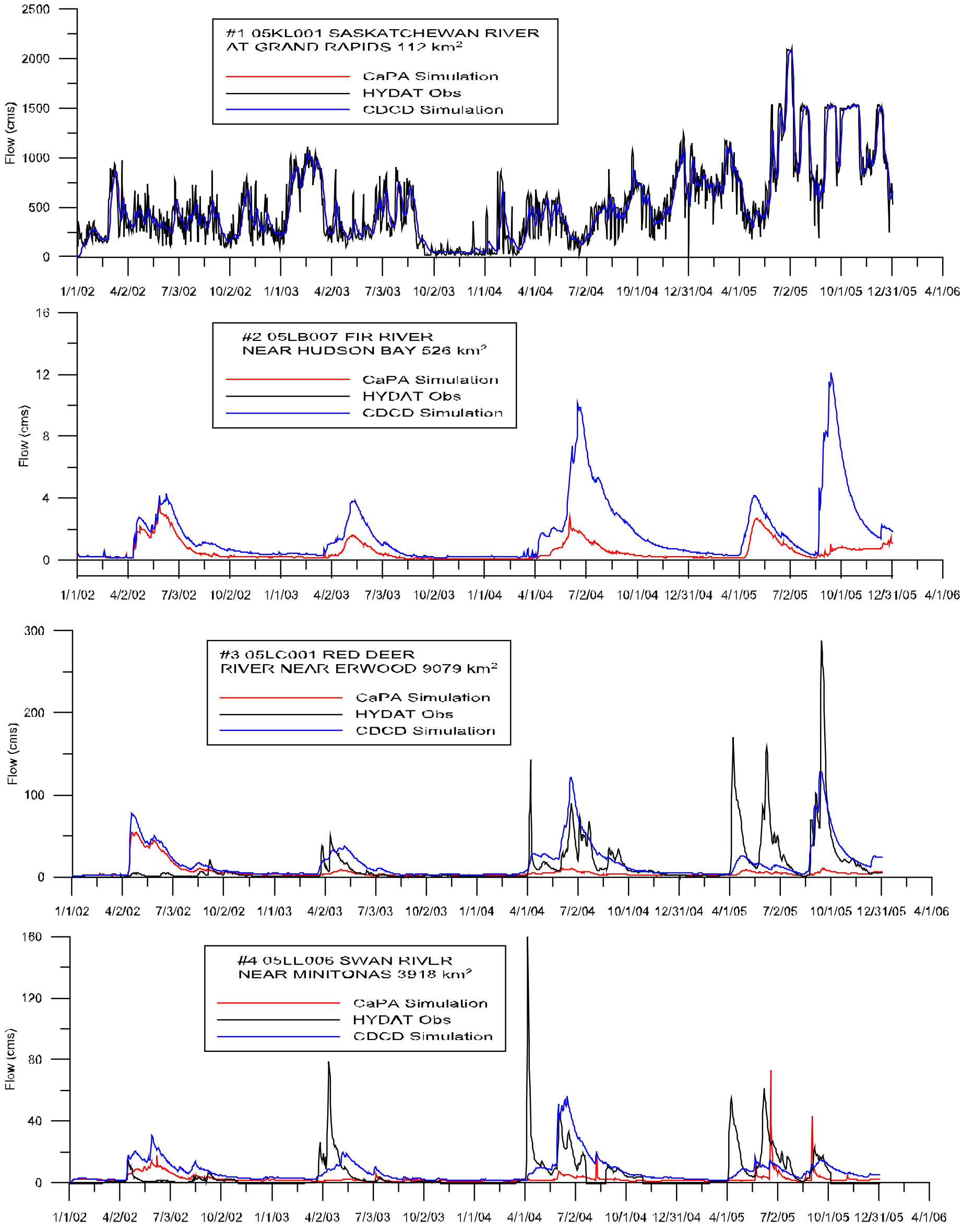
#1 05KL001 SASKATCHEWAN RIVER AT GRAND RAPIDS 112 km²
CaPA Simulation
HYDAT Obs
CDCD Simulation
Flow (cms)
2500
2000
1500
1000
500
0
#2 05LB007 FIR RIVER NEAR HUDSON BAY 526 km²
CaPA Simulation
HYDAT Obs
CDCD Simulation
Flow (cms)
16
12
8
4
0
#3 05LC001 RED DEER RIVER NEAR ERWOOD 9079 km²
CaPA Simulation
HYDAT Obs
CDCD Simulation
Flow (cms)
300
200
100
0
#4 05LL006 SWAN RIVLR NEAR MINITONAS 3918 km²
CaPA Simulation
HYDAT Obs
CDCD Simulation
Flow (cms)
160
120
80
40
0
1/1/02
4/2/02
7/3/02
10/2/02
1/1/03
4/2/03
7/3/03
10/2/03
1/1/04
4/1/04
7/2/04
10/1/04
12/31/04
4/1/05
7/2/05
10/1/05
12/31/05
4/1/06

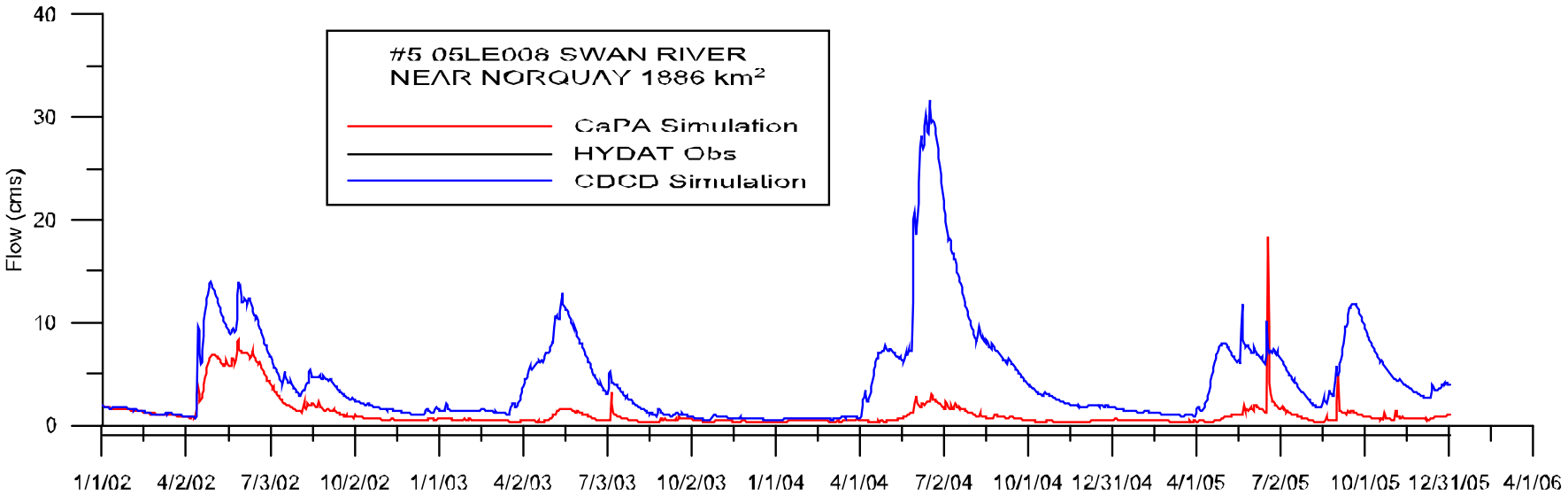
#5 05LE008 SWAN RIVER
NEAR NORQUAY 1886 km²
CaPA Simulation
HYDAT Obs
CDCD Simulation
Flow (cms)
40
30
20
10
0
1/1/02
4/2/02
7/3/02
10/2/02
1/1/03
4/2/03
7/3/03
10/2/03
1/1/04
4/1/04
7/2/04
10/1/04
12/31/04
4/1/05
7/2/05
10/1/05
12/31/05
4/1/06

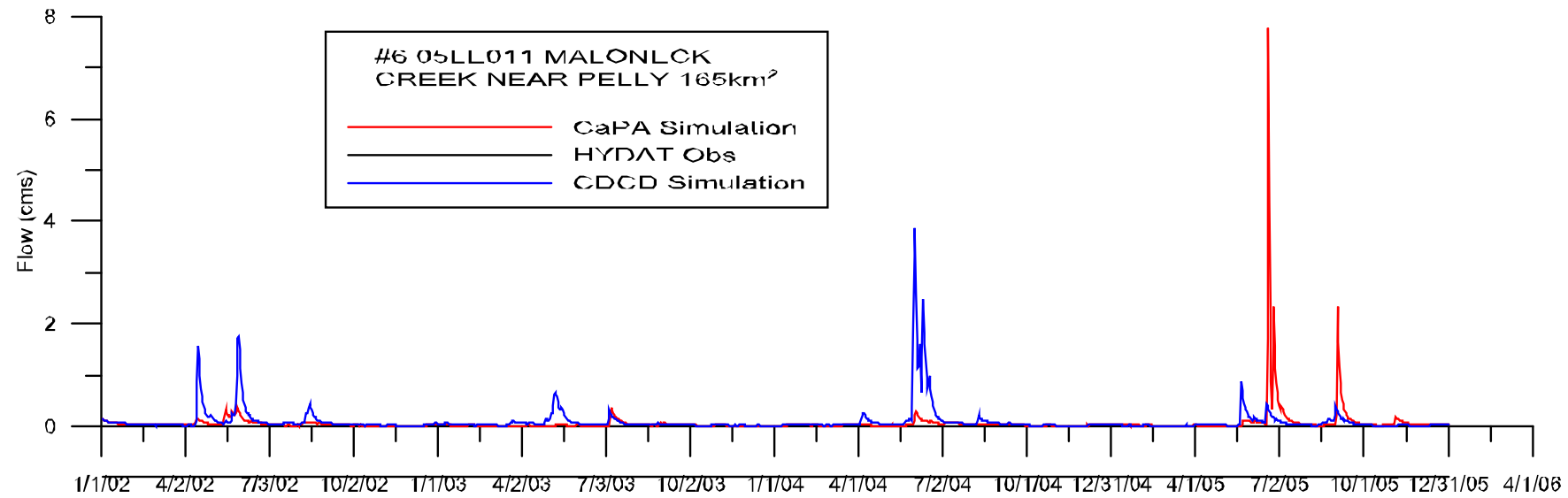
#6 05LL011 MALONLCK
CREEK NEAR PELLY 165km²
CaPA Simulation
HYDAT Obs
CDCD Simulation
Flow (cms)
8
6
4
2
0
1/1/02
4/2/02
7/3/02
10/2/02
1/1/03
4/2/03
7/3/03
10/2/03
1/1/04
4/1/04
7/2/04
10/1/04
12/31/04
4/1/05
7/2/05
10/1/05
12/31/05
4/1/06

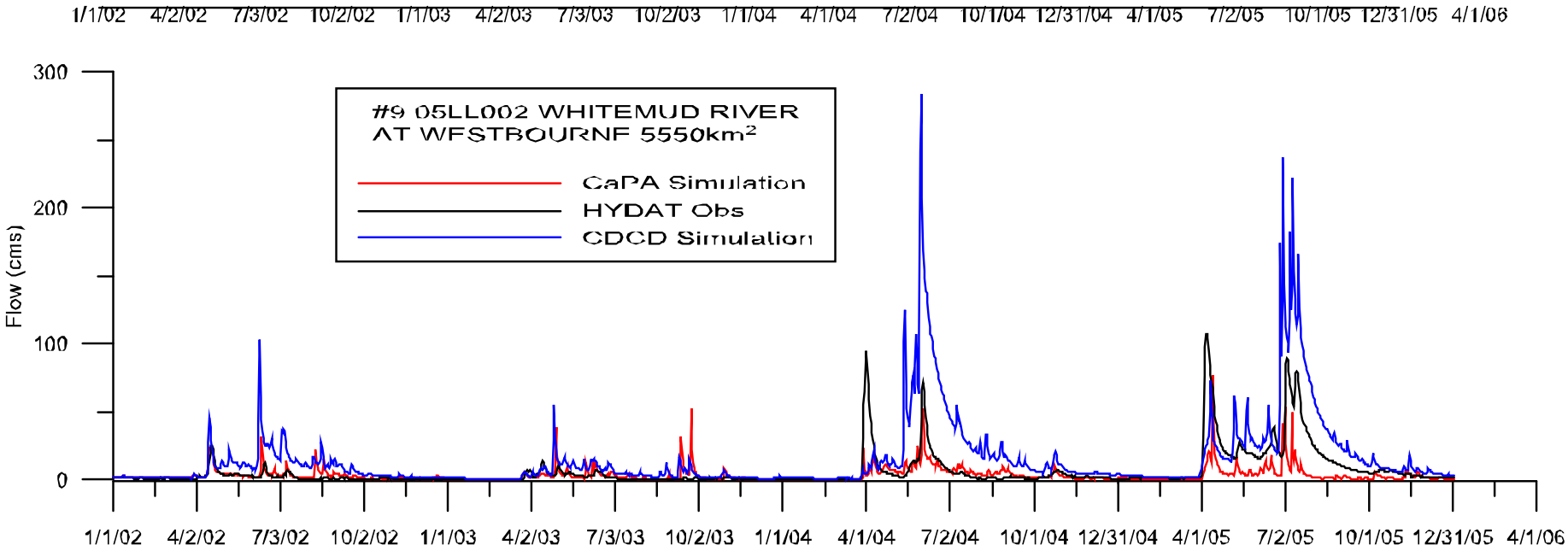
#9 05LL002 WHITEMUD RIVER
AT WESTBOURNE 5550km²
CaPA Simulation
HYDAT Obs
CDCD Simulation
Flow (cms)
300
200
100
0
1/1/02
4/2/02
7/3/02
10/2/02
1/1/03
4/2/03
7/3/03
10/2/03
1/1/04
4/1/04
7/2/04
10/1/04
12/31/04
4/1/05
7/2/05
10/1/05
12/31/05
4/1/06

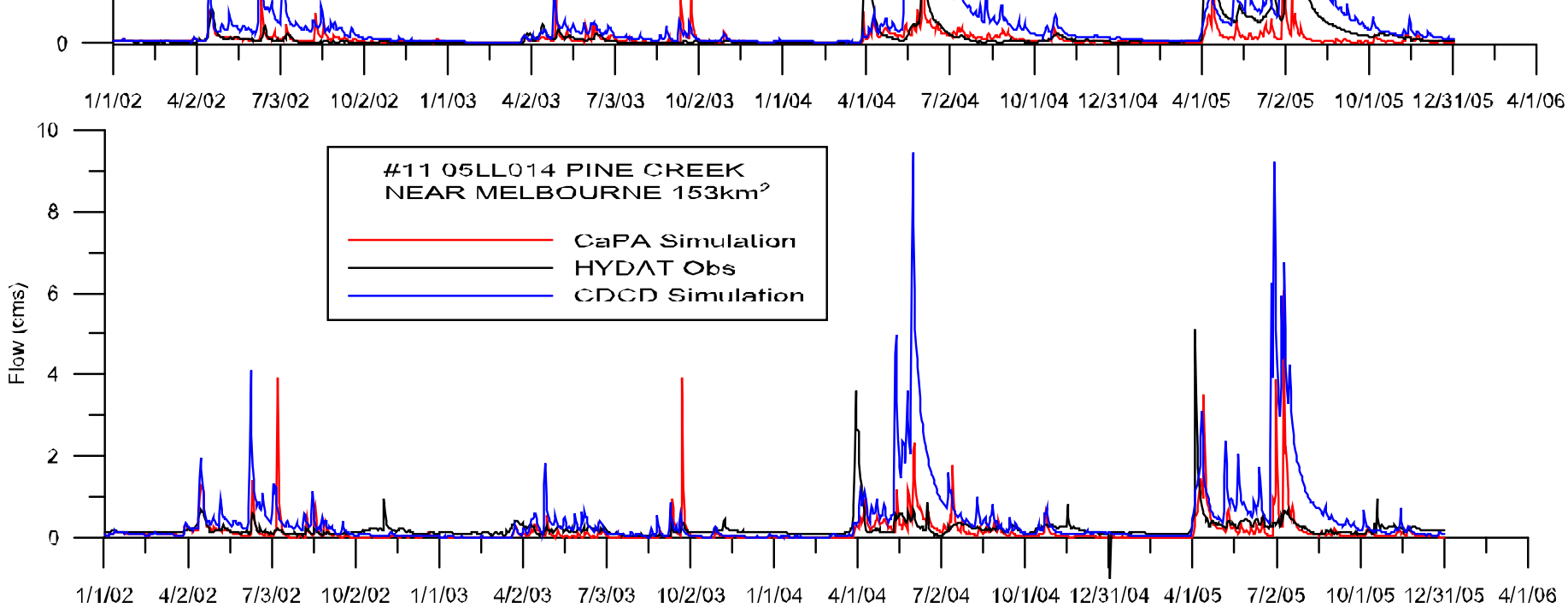
#11 05LL014 PINE CREEK
NEAR MELBOURNE 153km²
CaPA Simulation
HYDAT Obs
CDCD Simulation
Flow (cms)
10
8
6
4
2
0
1/1/02
4/2/02
7/3/02
10/2/02
1/1/03
4/2/03
7/3/03
10/2/03
1/1/04
4/1/04
7/2/04
10/1/04
12/31/04
4/1/05
7/2/05
10/1/05
12/31/05
4/1/06

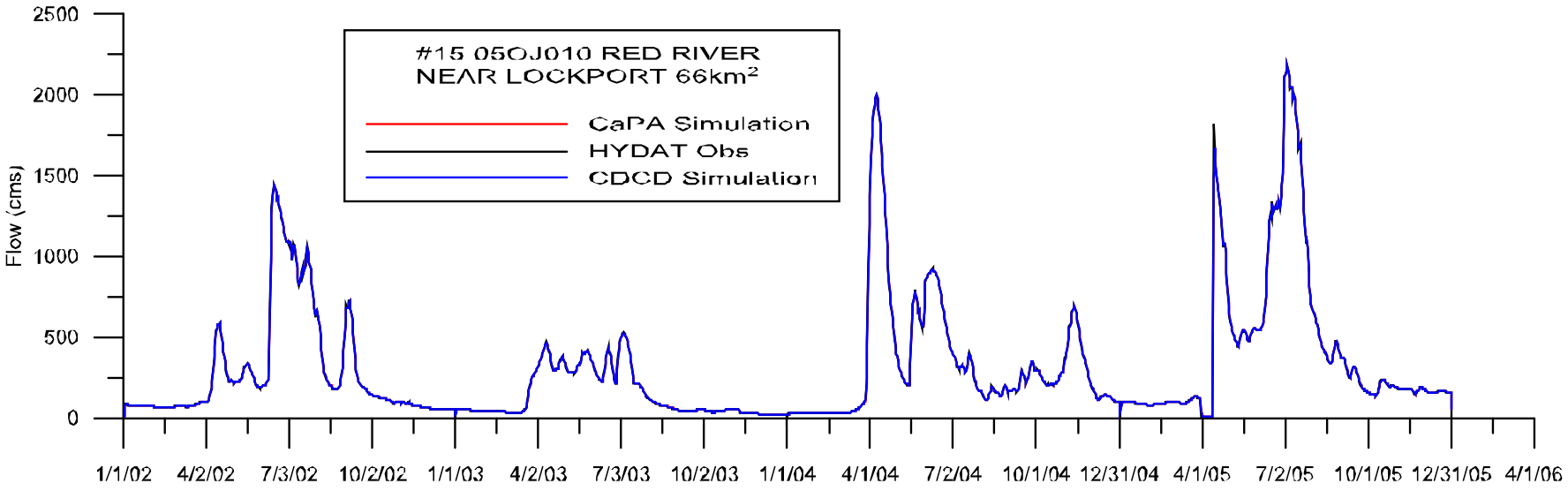
#15 05OJ010 RED RIVER
NEAR LOCKPORT 66km²
CaPA Simulation
HYDAT Obs
CDCD Simulation
Flow (cms)
2500
2000
1500
1000
500
0
1/1/02
4/2/02
7/3/02
10/2/02
1/1/03
4/2/03
7/3/03
10/2/03
1/1/04
4/1/04
7/2/04
10/1/04
12/31/04
4/1/05
7/2/05
10/1/05
12/31/05
4/1/06

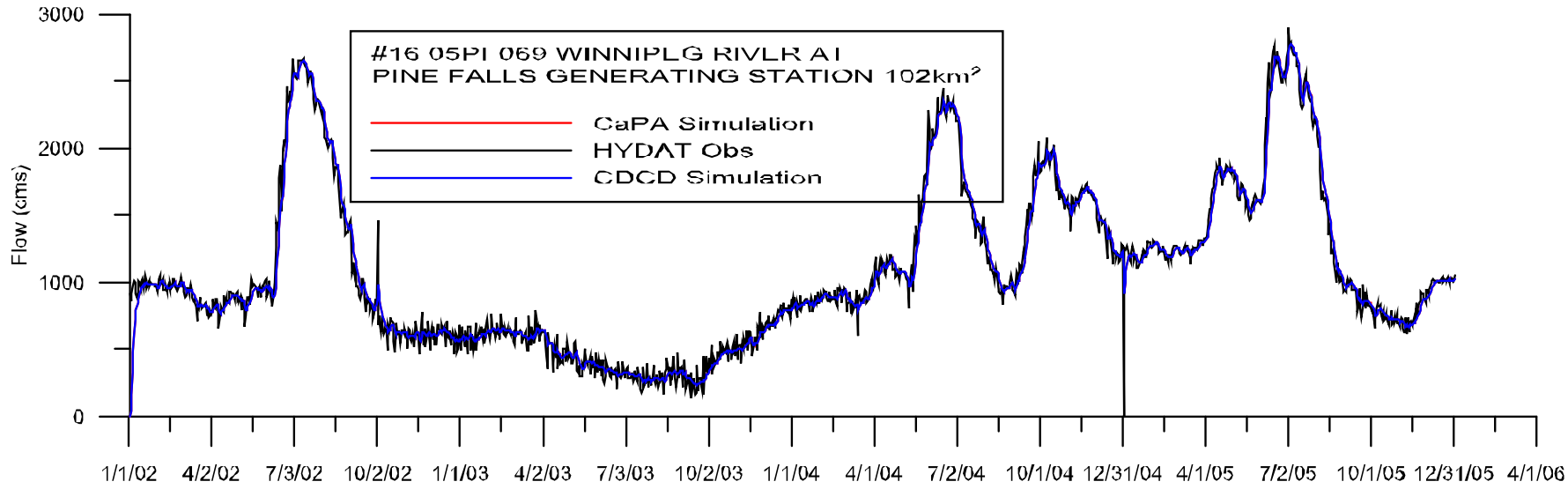
#16 05PI 069 WINNIPLG RIVLR AT
PINE FALLS GENERATING STATION 102km²
CaPA Simulation
HYDAT Obs
CDCD Simulation
Flow (cms)
3000
2000
1000
0
1/1/02
4/2/02
7/3/02
10/2/02
1/1/03
4/2/03
7/3/03
10/2/03
1/1/04
4/1/04
7/2/04
10/1/04
12/31/04
4/1/05
7/2/05
10/1/05
12/31/05
4/1/06

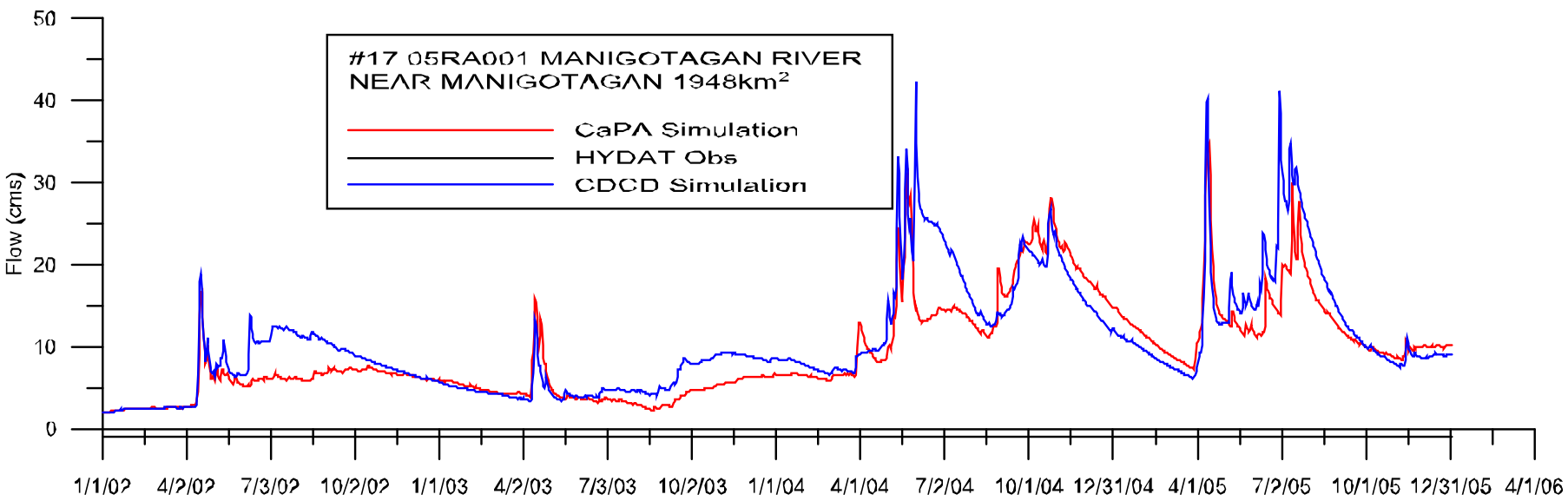
#17 05RA001 MANIGOTAGAN RIVER
NEAR MANIGOTAGAN 1948km²
CaPA Simulation
HYDAT Obs
CDCD Simulation
Flow (cms)
50
40
30
20
10
0
1/1/02
4/2/02
7/3/02
10/2/02
1/1/03
4/2/03
7/3/03
10/2/03
1/1/04
4/1/04
7/2/04
10/1/04
12/31/04
4/1/05
7/2/05
10/1/05
12/31/05
4/1/06

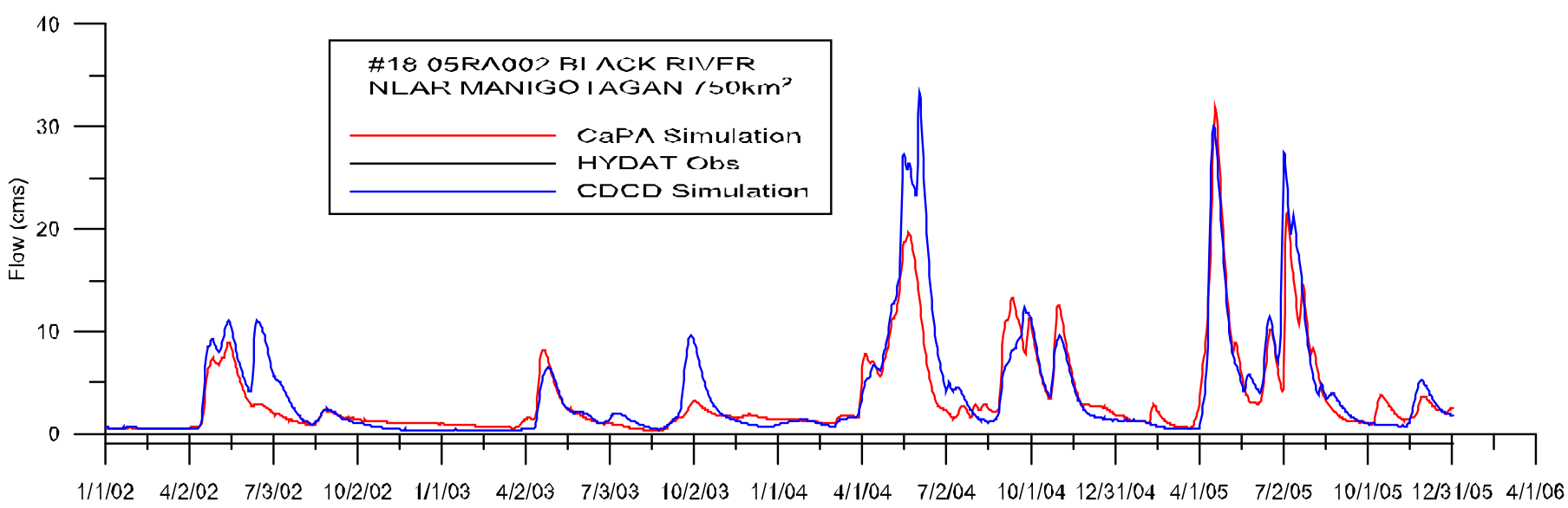
#18 05RA002 BLACK RIVER
NEAR MANIGOTAGAN 750km²
CaPA Simulation
HYDAT Obs
CDCD Simulation
Flow (cms)
40
30
20
10
0
1/1/02
4/2/02
7/3/02
10/2/02
1/1/03
4/2/03
7/3/03
10/2/03
1/1/04
4/1/04
7/2/04
10/1/04
12/31/04
4/1/05
7/2/05
10/1/05
12/31/05
4/1/06

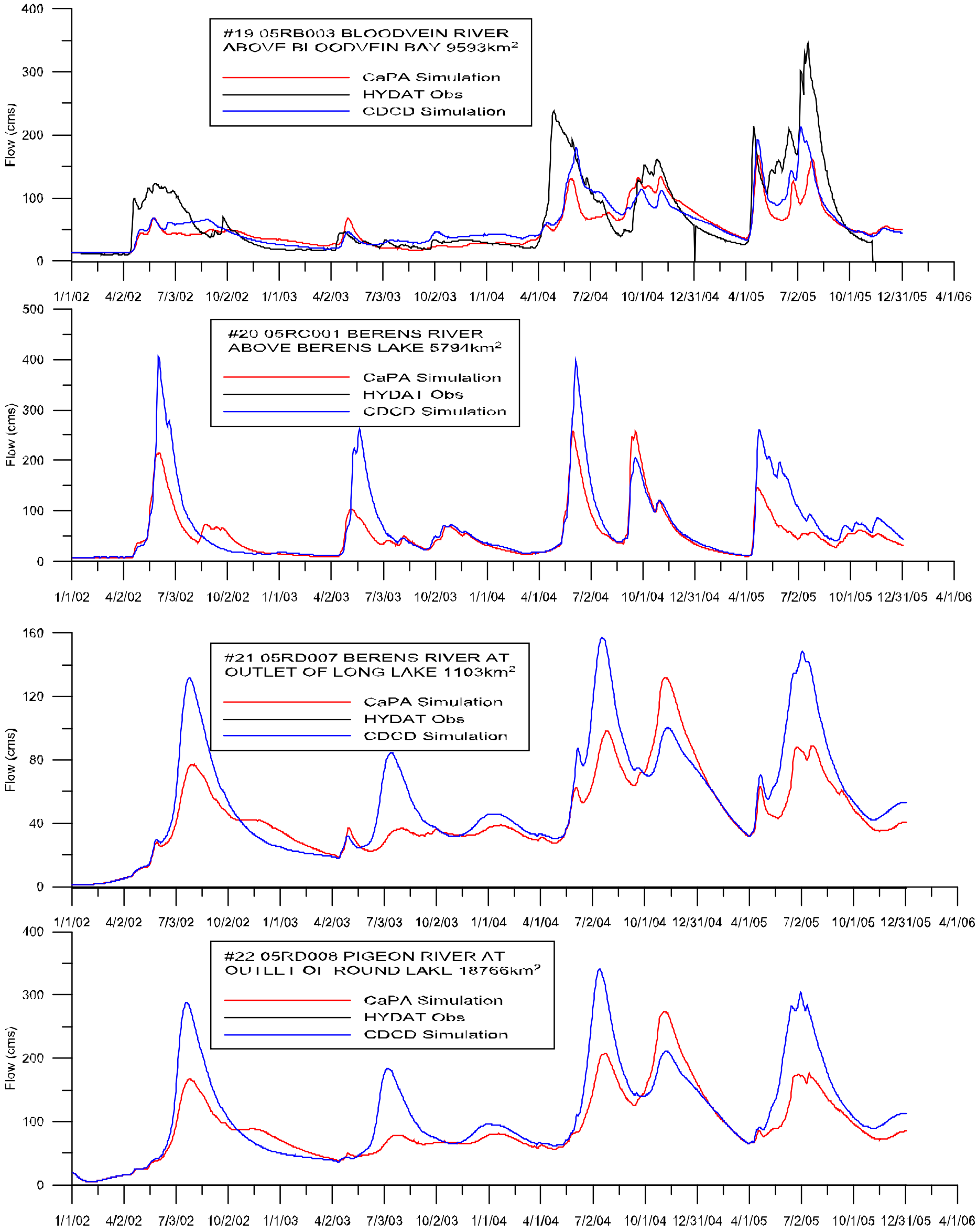
#19 05RB003 BLOODVEIN RIVER
ABOVE BLOODVEIN BAY 9593km²
CaPA Simulation
HYDAT Obs
CDCD Simulation
Flow (cms)
0
100
200
300
400
1/1/02
4/2/02
7/3/02
10/2/02
1/1/03
4/2/03
7/3/03
10/2/03
1/1/04
4/1/04
7/2/04
10/1/04
12/31/04
4/1/05
7/2/05
10/1/05
12/31/05
4/1/06
#20 05RC001 BERENS RIVER
ABOVE BERENS LAKE 5791km²
CaPA Simulation
HYDAT Obs
CDCD Simulation
Flow (cms)
0
100
200
300
400
500
#21 05RD007 BERENS RIVER AT
OUTLET OF LONG LAKE 1103km²
CaPA Simulation
HYDAT Obs
CDCD Simulation
Flow (cms)
0
40
80
120
160
#22 05RD008 PIGEON RIVER AT
OUTLET OF ROUND LAKE 18766km²
CaPA Simulation
HYDAT Obs
CDCD Simulation
Flow (cms)
0
100
200
300
400

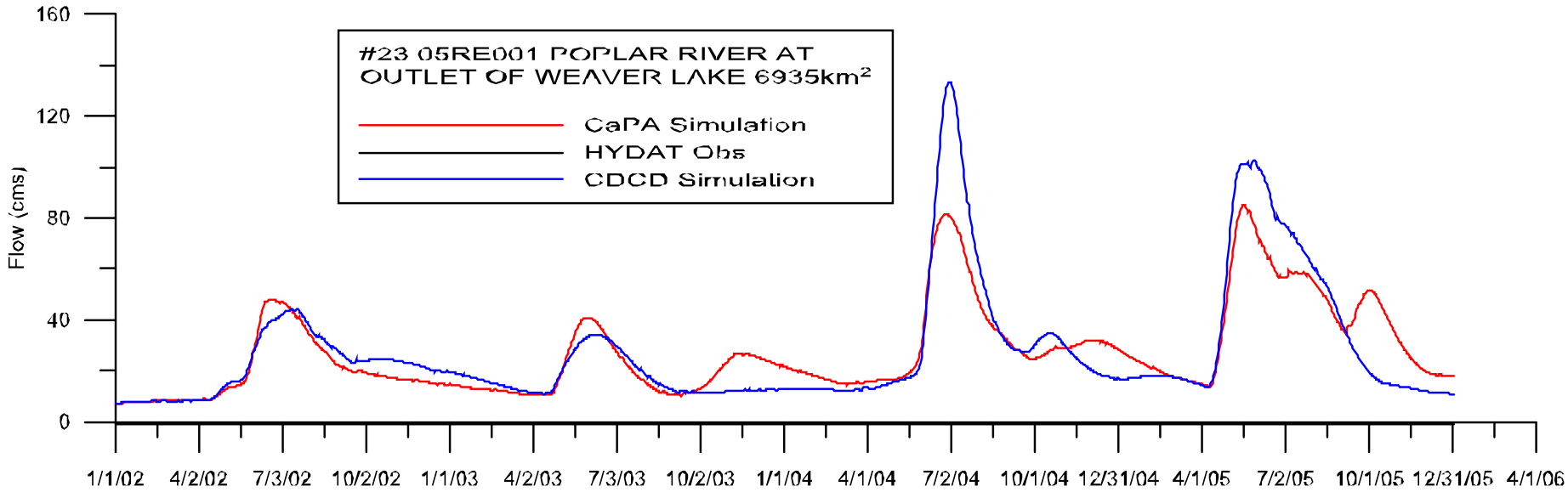
#23 05RE001 POPLAR RIVER AT OUTLET OF WEAVER LAKE 6935km²
CaPA Simulation
HYDAT Obs
CDCD Simulation
Flow (cms)
160
120
80
40
0
1/1/02
4/2/02
7/3/02
10/2/02
1/1/03
4/2/03
7/3/03
10/2/03
1/1/04
4/1/04
7/2/04
10/1/04
12/31/04
4/1/05
7/2/05
10/1/05
12/31/05
4/1/06

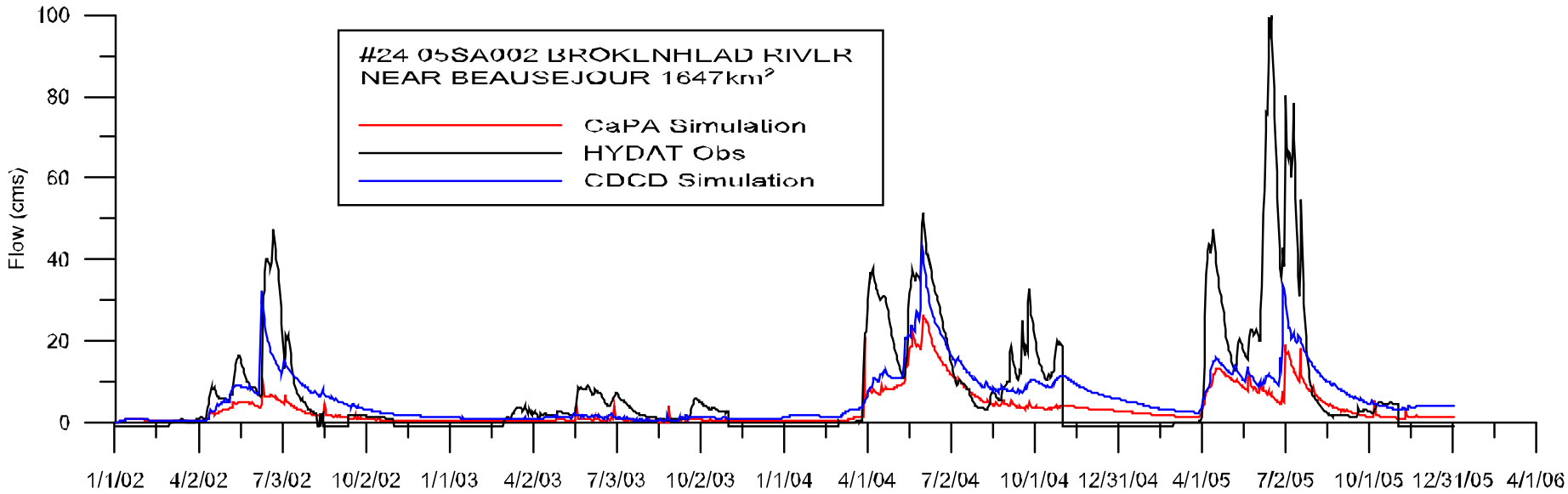
#24 05SA002 BROKLNHLAD RIVLR NEAR BEAUSEJOUR 1647km²
CaPA Simulation
HYDAT Obs
CDCD Simulation
Flow (cms)
100
80
60
40
20
0
1/1/02
4/2/02
7/3/02
10/2/02
1/1/03
4/2/03
7/3/03
10/2/03
1/1/04
4/1/04
7/2/04
10/1/04
12/31/04
4/1/05
7/2/05
10/1/05
12/31/05
4/1/06

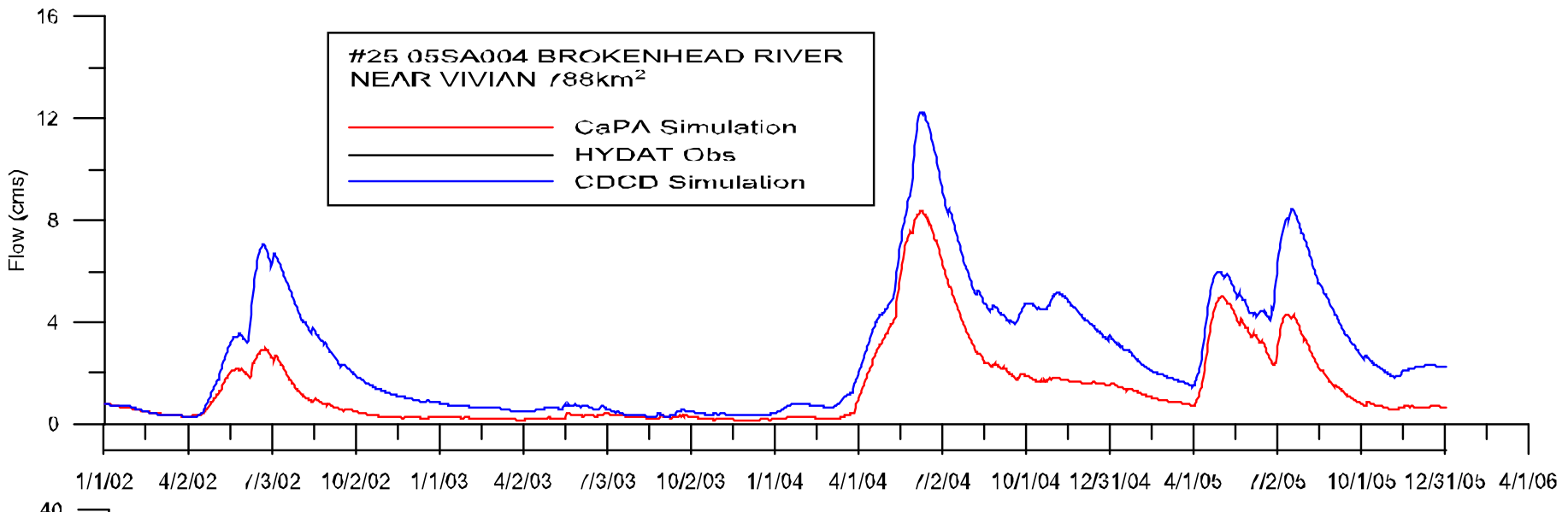
#25 05SA004 BROKENHEAD RIVER NEAR VIVIAN 788km²
CaPA Simulation
HYDAT Obs
CDCD Simulation
Flow (cms)
16
12
8
4
0
1/1/02
4/2/02
7/3/02
10/2/02
1/1/03
4/2/03
7/3/03
10/2/03
1/1/04
4/1/04
7/2/04
10/1/04
12/31/04
4/1/05
7/2/05
10/1/05
12/31/05
4/1/06

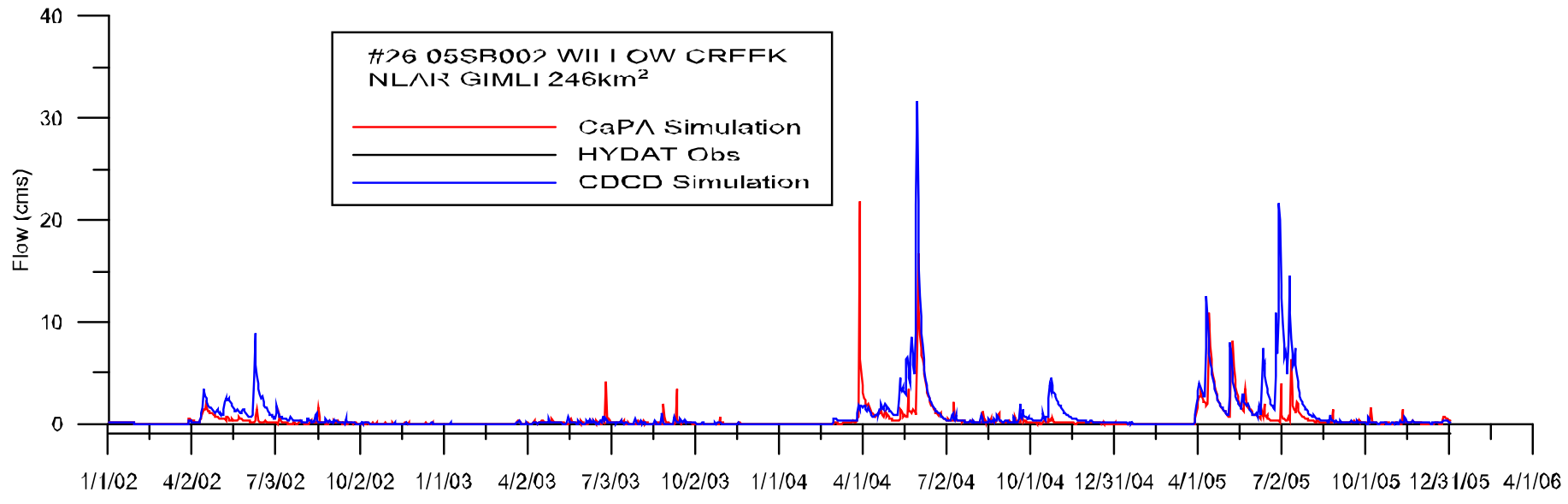
#26 05SB002 WILLOW CREEK NEAR GIMLI 246km²
CaPA Simulation
HYDAT Obs
CDCD Simulation
Flow (cms)
40
30
20
10
0
1/1/02
4/2/02
7/3/02
10/2/02
1/1/03
4/2/03
7/3/03
10/2/03
1/1/04
4/1/04
7/2/04
10/1/04
12/31/04
4/1/05
7/2/05
10/1/05
12/31/05
4/1/06

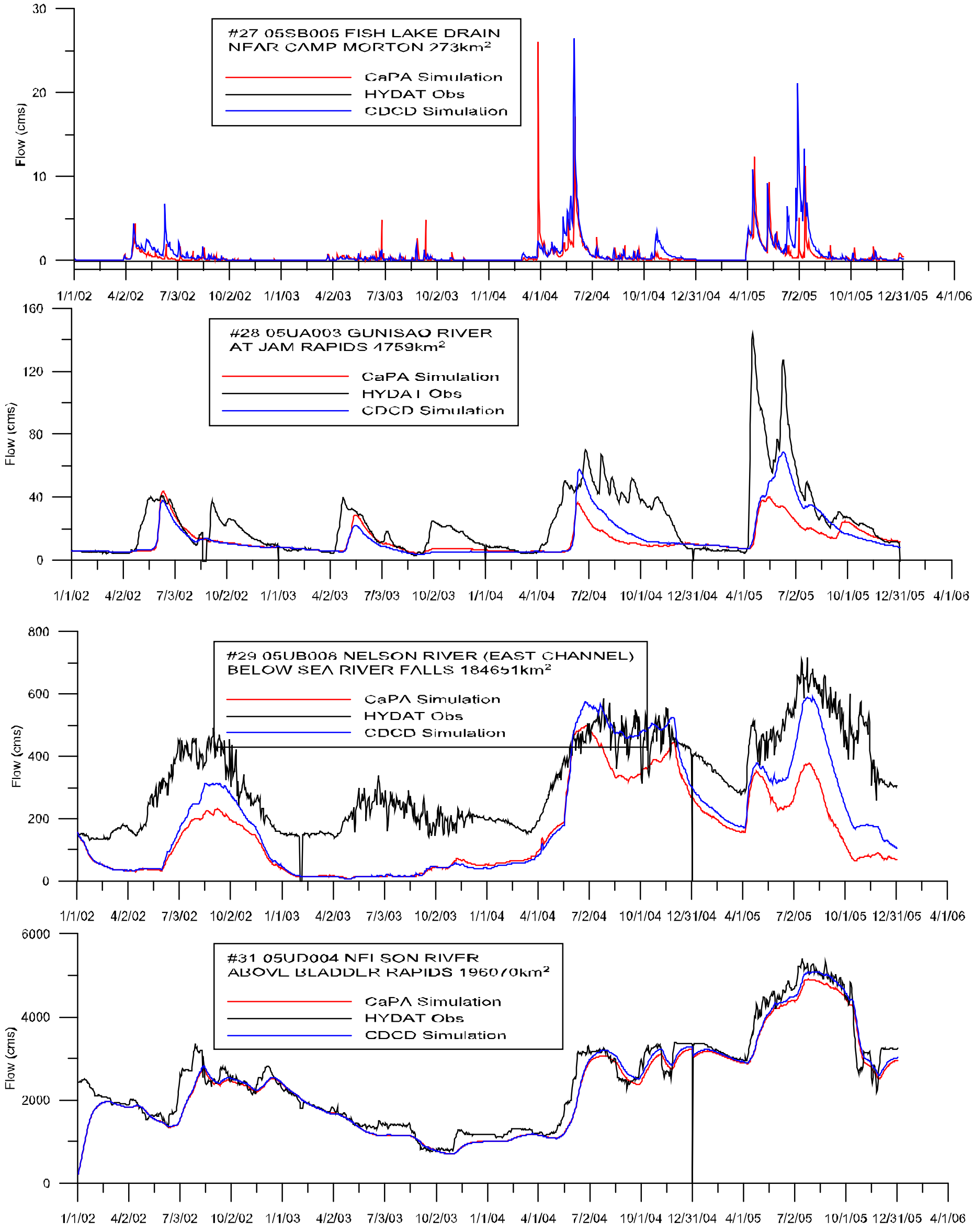

Figure D-2 Proxy validation hydrographs at the Lake Winnipeg basin, each hydrograph are labeled with its station numbers(#1-#31) in WATFLOOD, station name, and drainage area.

Appendix E: Enlarged view of basin setup

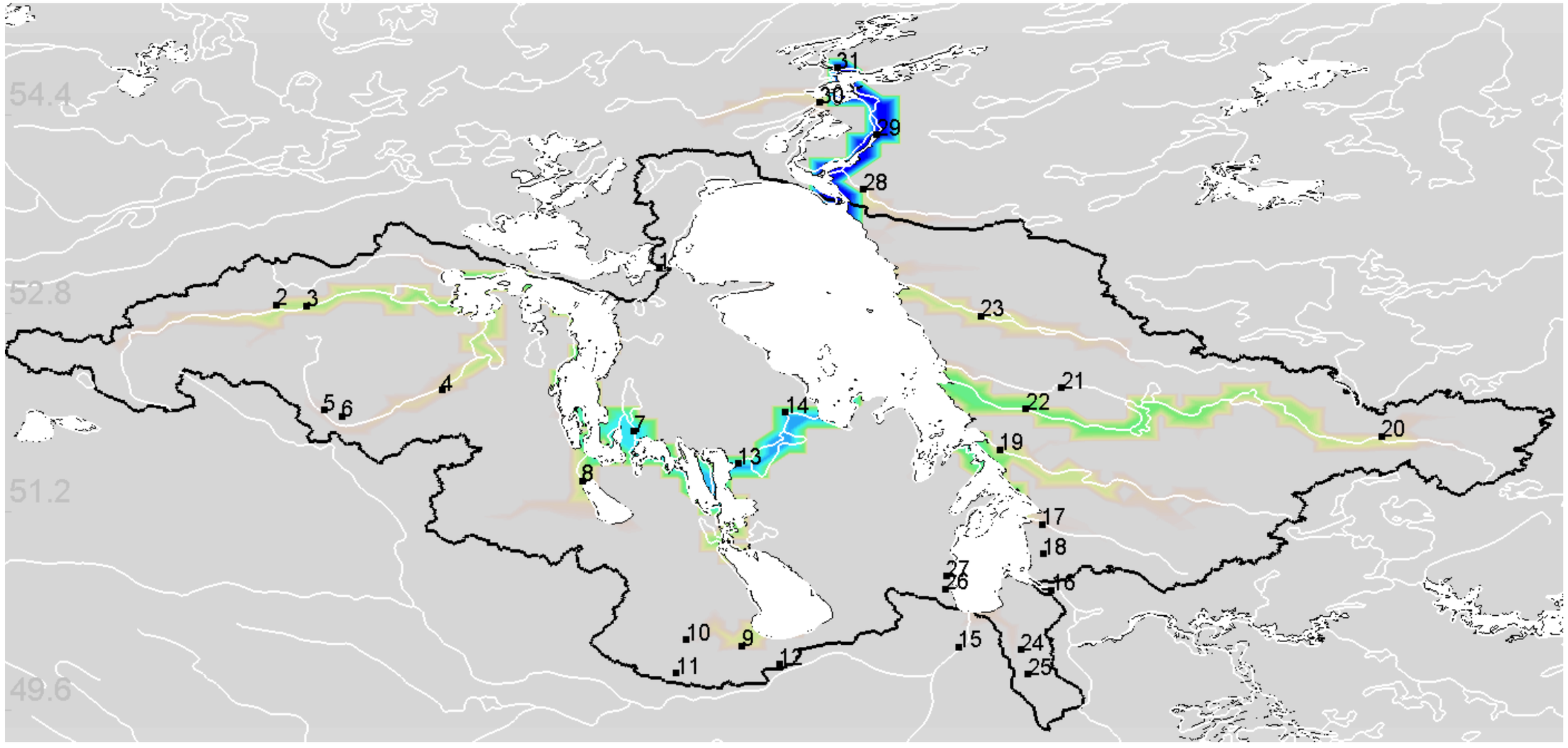

Figure E-1: Lake Winnipeg basin flow station numbers and major drainage systems.

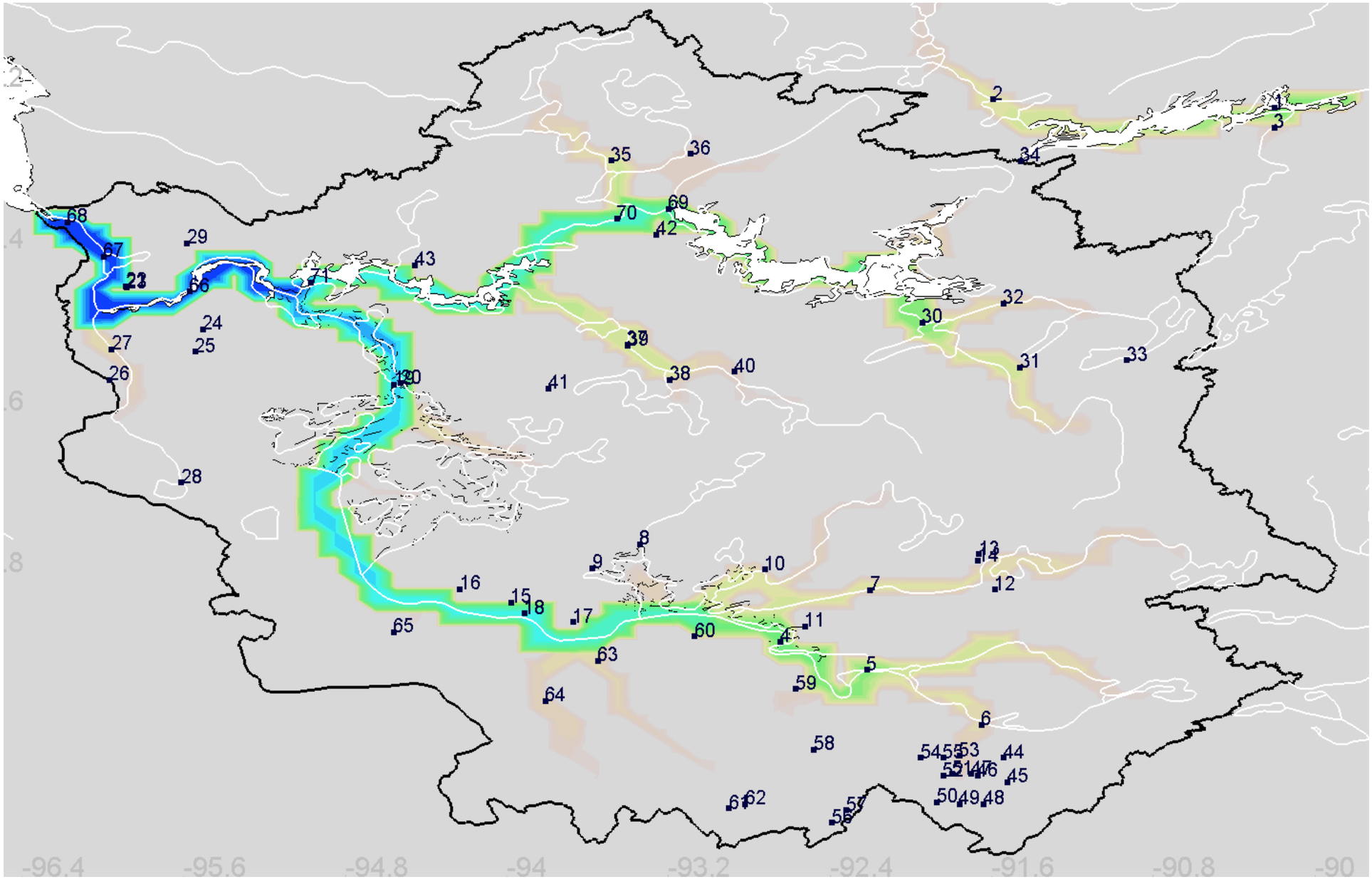

Figure E-2: Winnipeg River basin flow station numbers and major drainage systems.